*Thèse de Doctorat*

UNIVERSITE PIERRE & MARIE CURIE
LA SCIENCE A PARIS

# Integrabilité en AdS/CFT

Ansatz de Bethe et quantification de corde au delà du volume infini

---

# Integrability in AdS/CFT

Bethe ansatz and String quantization beyond infinite volume


Pedro Vieira

LPT, École Normale Supérieure
CFP, Universidade do Porto
**pedrogvieira@gmail.com**


| | | |
|---|---|---|
| **Juri:** | Miguel Sousa Costa | |
| | Romuald Janik | Raporteur |
| | Vladimir Kazakov | Directeur de Thèse |
| | Ivan Kostov | |
| | Joseph Minahan | Raporteur |
| | Fedor Smirnov | |
| | Jean-Bernard Zuber | |

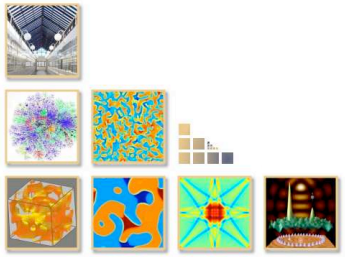

Para os meus pais Sérgio e Margarida

# Resumé

Dans cette thèse l'intégrabilité dans AdS / CFT est passée en revue. La technique de l'ansatz de Bethe est presentée et les équations de Bethe à toutes les boucles sont discutées. Du coté de la théorie des cordes, la méthode classique des bandes-finies est revisitée et une attention particulière est accordée à la quantification semi-classique de la supercorde. Les méthodes basées sur la courbe algébrique sont très générales et fournissent des contraintes fortes sur les équations quantiques. De telles contraintes sont explorées en detail pour la dualité $AdS_5/CFT_4$ bien qu'elles soient générales et valables, entre autres, pour le système $AdS_4/CFT_3$. Ces techniques permettent aussi d'étudier le système au delà de la limite de volume infini quand l'ansatz de Bethe asymptotique n'est plus valable.

# Abstract

In this thesis Integrability in AdS/CFT is reviewed. Bethe ansatz techniques are presented and the all loop Bethe equations are discussed. From the string side of the correspondence, the classical finite-gap method is revisited and special emphasis is given to the super-string semi-classical quantization. The algebraic curve methods are quite general and provide very important constraints on the full quantum equations. The formalism is extremely versatile and can be applied to the $AdS_5/CFT_4$ duality – the most studied case in this work – as well as to other integrable systems like e.g. the $AdS_4/CFT_3$ correspondence. Furthermore, these techniques yield valuable information about the spectrum of finite charge states when the asymptotic Bethe ansatz is no longer valid.

# (Outrageously incomplete) Acknowledgements

I met Volodya Kazakov, Kolya Gromov, Dadive Cassani and Pedro Ribeiro roughly four years ago in Paris and I acknowledge how lucky I have been for meeting these great new friends. Volodya Kazakov was my main PhD supervisor and I could hardly imagine a better one. His imagination and intuition are always mind blowing and his optimistic and energetic mood is completely contagious. Kolya was my main collaborator and working with him was always exciting and stimulating. Visiting him in Russia, apart from the mosquitos in the swamps, was something I loved and wish to repeat many times in the future. Davide was my office mate and my torture victim during these years. For some mysterious (and funny) reason he almost always turned out to be the target of my pranks and I will miss hiding his keys or mobile. Pedro was probably the colleague with whom I spent most of the time in Paris. We probably discussed everything there is to discuss and proposed solutions for all of the world's problems. I would also like to thank everyone in Paris for such wonderful years. This includes everyone at Ecole Normale Superieure, at the house of Portugal in CIUP and all the friends I met during this time. Merci beaucoup.

Miguel Costa was my co-advisor during these years but much more than that he was my first scientific mentor introducing me to high-energy physics. His advices are always of inestimable help and, even more so, he is a great friend. Miguel and João Penedones made my stay in Porto spectacular, scientifically and socially speaking. Along with everyone else at CFP, and in particular with João Viana Lopes who I must mention, they made my periods in Portugal superb.

I ought to thank Diana whose dedication and love are always infinite. She helped me enormously during these four years in Paris, specially during the first three (and highly painful) months of the DEA (master in theoretical physics). My humble success ought to be shared with her. Tiago, my brother, was always available to help me with proofreading papers and even the current thesis. He can spot "it"'s which should be "is"'s better than a bat[1] can find flies. Moreover he has the bizarre ability of performing such terribly boring task without ever loosing his great sense of humor. I owe him much. Finally my parents, the human beings I admire the most. I have never found their open mindedness elsewhere and this thesis is dedicated to them.

To conclude, I would like to thank everyone I had the luck and pleasure to discuss with and FCT who funded me by the grant SFRH/BD/17959/2004/0WA9.

Pedro Vieira, Paris 9 September, 2008

[1] microbats, the ones that eat flies

# Resumé detailé

## Resumé detailé

Cette thèse est consacrée à l'étude de intégralité et de son application à la dualité $AdS_5/CFT_4$ [1, 2, 3, 4, 5]. Cette dualité est une des nombreuses correspondances jauge/gravité entre les théories de la gravitation quantique et la physique des particules. Ils sont certainement parmi les plus fascinants sujets dans la science moderne. L'intégrabilité, pour resumer une longue histoire (au détriment de la rigueur), est la structure mathématique qui permet souvent de résoudre une théorie physique. Ainsi, lorsqu'on parle de l'intégrabilité dans AdS/CFT nous parlons de comprendre les caractéristiques de la gravité quantique et théories de jauge en les résoudrant. Il est de toute évidence un Saint Graal des physiciens théoriques.

### Theorie des cordes et AdS/CFT

La théorie des cordes n'est pas seulement l'approche la plus développée de la gravité quantique, mais un candidat pour une théorie du tout. Les correspondences jauge/cordes mentionnées ci-dessus s'incarnent dans la théorie des cordes comme des dualités cordes ouvertes/fermées. L'idée de base est que la somme sur les trous de la surface de l'univers de la corde peut être remplacées par un fond nontrivial sur lequel la corde se propage.

Nous allons nous déplacer lentement vers cette image mais on peut déjà dire qu'il n'y a rien d'extravagant dans ce sujet. Prenons la difusion d'un electron par un proton lourde en QED. À l'ordre dominant, l'electron jette un photon au proton (fig 1a) et cette échange virtuelle donne lieu à l'interaction de Coulomb. À l'ordre suivante on a les diagrammes de Bremsstrahlung (fig 1b), les corrections provues des photons virtuelles (fig 1c) et, le plus important, l'auto-energie du photon (fig 1d). Ce dernier effet polarise le vide renormalisant

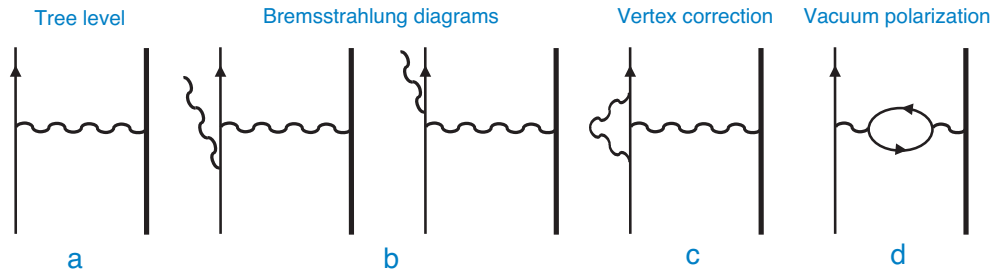


Figure 1: Processus virtuels qui contribuent pour la diffusion d'un electron par un photon lourd.

la charge du proton et corrige le potentiel de Coulomb en le potentiel de Uehling

$$V(r) = -\frac{\alpha}{r}\left(1 + \frac{\alpha}{4\sqrt{\pi}}\frac{e^{-2m_e r}}{(m_e r)^{3/2}} + \dots\right) . \tag{1}$$

En ajoutant de plus en plus de diagrammes de Feynman, on peut en principe améliorer (1) en n'importe quelle précision[2]. Ainsi on a deux descriptions alternatives pour le passage de l'électron par la région contenant le proton lourd. D'un côté on peut considérer l'électron et le proton comme étant dans un vide parfait et sommer sur les processus virtuelles (diagrammes de Feynman) qui deflectent la trajectoire de l'électron. De l'autre côté on peut oublier le proton et dire que l'électron se bouge dans une région non trivial où il y a un potentiel $V(r)$ donné par (1.1). Comme expliqué ci-dessous l'approche diagramatique de Feynman sera l'analogue de la somme sur les trous dans la surface d'univers de la corde tandis que le remplacement des trous par un fond nontrivial est précisément ce qu'on fait quand on remplace les diagrammes par le potentiel $V(r)$.

Dans la théorie des cordes les particules fondamentales ne sont pas des objects ponctuels mais des petites cordes vibrantes. En effet la caractéristique la plus attractive de la théorie des cordes est la proposition qui nous dit que *toutes* les particules sont en effet *la même* corde. L'excitations des diffèrents modes de la corde pourraient correspondre aux diffèrentes particules fondamentales observées dans la nature. Les cordes peuvent soit former des boucles fermés soit avoir ces extrémités attachées à des (hyper)-surfaces comme est representé dans la figure 2. Dans le premier cas, les cordes sont appelées de cordes fermées tandis que dans le dernier scénario elles sont appelées de cordes ouvertes et les planes dont elles finissent s'appellent branes.

Examinons maintenant une situation analogue à la dispersion de l'électron par un proton lourd mentionné ci-dessous, à savoir une corde fermée en passant par une D-brane. Comme d'habitude, la propagation quantique sera décrite par la somme sur les histoires et la surface d'univers d'une histoire typique sera une surface de Riemann avec $h$ poignés et $n$ trous (lorsque la cordes touche la brane ou les cordes ouvertes que l'y sont attachées)

[2]Comme anticipée ci-dessous on n'est pas concernée au rigueur mathématique sinon une note sure la nature asymptotique de l'expansion perturbative serait approprié à ce point-là.

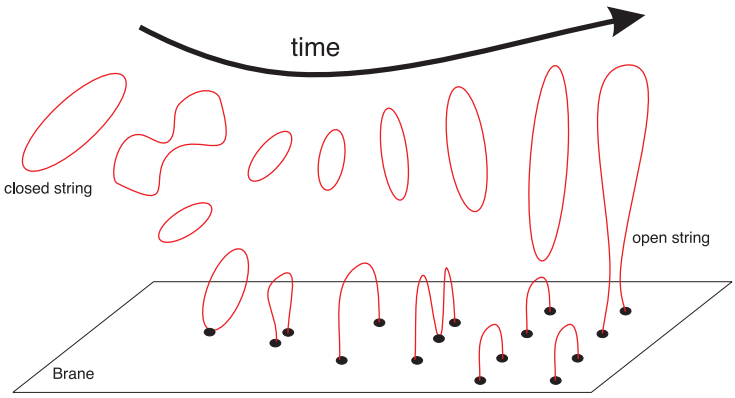


Figure 2: Dans la théorie des cordes on a des cordes fermées qui se bougent partout et des cordes ouvertes, attachées à des hyper-planes appelés branes. Dans cette figure, une corde fermée évolue vers deux cordes ouvertes dans la présence d'une brane. On peut aussi regarder ce processus dans la direction opposée comme décrivant la fusion de deux cordes ouvertes en une corde fermée. Quand deux points coincident dans l'espace-temps les cordes peuvent se fusionner ou séparer. Étant un processus local, on voit qu'une théorie des cordes fermées est possible mais une theorie des cordes ouvertes automatiquement requis la présence de cordes fermées.

intégrés dans l'espace-temps telle qu'elle est représentée dans la figure 3a. Si on somme sur tous les trous possibles il nous reste une propagation non triviale de la corde mais sans brane[6, 7, 8]. La description en des termes de la brane et de ses cordes ouvertes est échangée par un fond non-trivial sur lequel la corde fermée se propage comme l'illustre la figure 3b. C'est l'image derrière AdS/CFT.

L'exemple le plus connu de cette dualité se dégage lorsque l'on applique cette image à une configuration de $N$ $D3$ branes coincidents dans la theorie de cordes type IIB en espace plate a dix dimensions. Comme il est expliqué dans la section 1.2 ceci nous amène à une correspondance précise entre $\mathcal{N} = 4$ U(N) SYM et theorie des cordes type IIB en $AdS_5 \times S^5$.

## Contemplation, désespoir et intégrabilité

La conjecture entre $\mathcal{N} = 4$ U(N) SYM et théories de cordes type IIB en $AdS_5 \times S^5$ est absolument remarquable et il existe de nombreux angles différents à partir desquels nous pouvons la contempler:

- D'une part, nous pouvons dire que, plus d'une dualité entre une théorie de jauge quatre dimensionnelle et une théorie de la gravitation quantique, cette correspondance est une definition non-perturbative d'une théorie nontrivial de la gravitat. En effet la théorie des cordes est à ce jour seulement définie perturbativement et cette définition

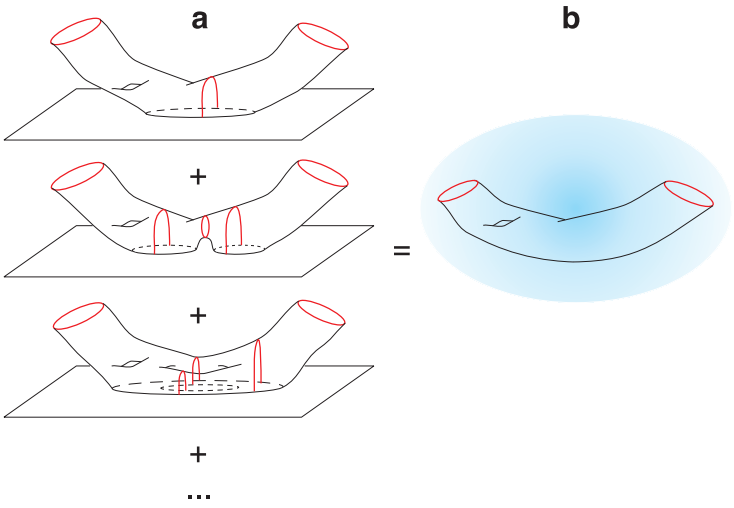


Figure 3: Quand une corde fermée se propage dans une région où il y a une brane, son évolution est décrite par une somme d'histoires qui comprend toutes les interactions possibles avec cet objet. Au contraire, nous pouvons remplacer toutes ces interactions avec la brane par un fond sur laquel la corde fermée se propage. C'est analogue de l'électron se déplaçant dans la présence du proton lourd - soit on somme tous les diagrammes de Feynman soit on considère son mouvement en présence d'un potentiel $V(r)$ non-trivial.

dual par moyen d'une théorie de jauge quantique unitaire et bien définie pourrait fournir la complétion non-perturbative de la théorie de la gravité. Ce point de vue a des conséquences immédiates. Par exemple, l'information ne peut pas être perdue si l'on considère des trous noirs dans $AdS$. En effet, en principe, nous pouvons préparer l'état qui permettra de créer le TN, on l'identifie dans la théorie dual, on l'évolue dans cette description explicitement unitaire et on l'identifie à nouveau dans le côté de gravité. Il ne s'agit que d'un exemple, parmi nombreux, de la grande puissance des dualités AdS / CFT comme des outils pour comprendre les mystères de la gravité quantique.

- Cette dualité est la plus aboutie réalisation du principe holographique. Gravité dans $AdS_{d+1}$ est encodée dans une théorie des champs vivant dans $\mathbb{M}_d$, la frontière de $AdS_{d+1}$! Il est remarquable qu'une théorie de jauge quatre dimensionnelle puisse encoder la dynamique d'une gravité dans un nombre de dimensions plus élevé. Plus remarquable encore, la dualité $AdS/CFT$ est une dualité entre la théorie de jauge sur la frontière et la gravité quantique dans son intérieure décrite par une somme de géométries qui sont simplement tenus d'être *asymptotiquement* anti-de Sitter.

- AdS / CFT est une dualité strictus sensus comme il relie des théories de jauge faiblement/fortement couplées et des théories des cordes fortement/faiblement couplées.

Cela signifie que nous pouvons accéder à des territoires précédemment inexpugnables de chaque théorie avec une relative facilité. Des cordes extrêmement quantiques avec une longueur beaucoup plus vaste que le radius de $AdS_5$ ont une description dual en termes de la théorie $\mathcal{N} = 4$ libre! Sur l'autre extrême, les effets dans théorie de jauge fortement couplés (et non-perturbative) peuvent être accessibles par des calculs classiques dans la théorie des cordes. La puissance de la dualité comme un outil de calcul peut difficilement être surestimée.

Toutes ces caractéristiques sont bien sur remarquables, mais il y a aussi un grand inconvénient dans tout cela relative au dernier point mentionné - sans le développement de quelques très puissantes techniques, le contrôle de n'importe quelle calcul devient une tache pratiquement impossible. Les calculs dans le régime perturbative dans la théorie de jauge correspondent aux calculs quantiques en interaction fort dans le côté des cordes tandis que des cordes classiques sont associées au régime non-perturbative fortement couplée de la théorie de jauge! Dans la limite de $N$ infinie, quand on considère la théorie de jauge planaire et des cordes libres - ces techniques puissantes apparaissent - l'intégrabilité [9, 10]. Il est maintenant largement reconnu que dans cette limite les deux théories sont complètement intégrables et, par conséquent, disposent de solution analytique! L' intégrabilité et, en particulier, des applications d'intégrabilité à AdS / CFT seront couvertes de manière approfondie dans tous les chapitres de cette thèse.

## Sur la thèse

Pendant les trois dernières années, la période de ma thèse, j'ai été plutôt a Paris avec des longues périodes à Porto. Ce pendant j'ai été co-auteur dans les articles [11, 12, 13, 14, 15, 16, 17, 18, 19, 20, 21] et procédures [22, 23]. Cette these ne couvrira pas [12, 23]. Les resultats en [11, 16, 19, 20, 22] sont utilisés mais ne sont pas à ce qu l'on donne le plus d'attention. De l'autre côté, la plupart des resultats presentés ici font partie des articles [13, 14, 15, 17, 18, 21]. Le texte principal est divisé en 2 parties. La partie II regarde plutôt l' ansatz de Bethe et le côté CFT de la correspondance. La partie III est dédié à l'étude du côté cordes de la correspondance. Cordes classiques sont étudiés dans le chapitre 4, le spectrum semi-classique est analisé dans le chapitre 5 et, finalement, dans le chapitre 6 on considère l'énergie du vide à une boucle au tour des solutions classiques génériques et on établisse le contact avec l'ansatz de Bethe étudié dans la partie II. Regardez l'appendix pour une description plus détaillé ou l'image 4 pour un plan moins detaille de la thèse.

On doit aussi inclure la note suivante. Due aux limitations d'espace, on a décidé de plutôt nous focaliser dans le limite d'échelle des équations de Bethe et dans les aspects de l'intégrabilité dans les cordes semi-classiques. En particulier, les développements les plus importants qui ont amené au très connu facteur scalaire de Beiser-Eden-Staudacher [24] ne seront pas développés en detail dans cette monographie. Par example, dans la section 3.7

on saute du traitment à une boucle des sections précédentes vers les conjectures à toutes les boucles laissant une grande bande de matérielle non couverte. Pour plus d'articles de révision sur le sujet de intégrabilité en AdS/CFT voir [25, 26, 27, 28, 29, 30, 31].

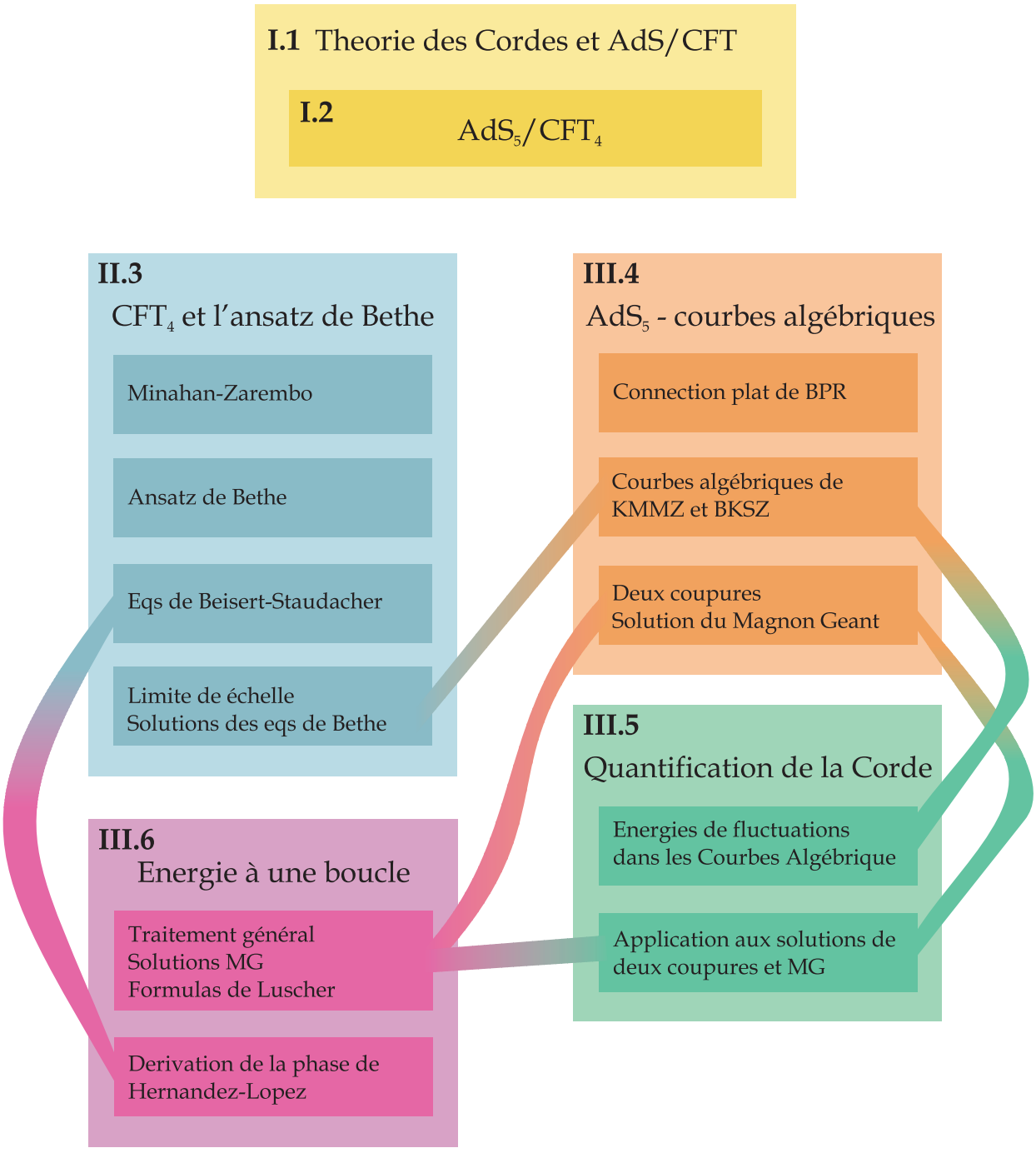


Figure 4: Plan générale de la thèse et organisation logique. Seuls les principaux sujets sont représentés, de nombreuses sections sont omises. Les parties II et III sont essentiellement indépendantes, sauf pour la dernière section du chapitre 6.4 qui exige les résultats de la section 3.7 dans la partie II

# Contents

# Part I

# Introduction and general setup

# Chapter 1

# Introduction

This thesis is devoted to the study of integrability and its application to Maldacena's $AdS_5/CFT_4$ duality [1, 2, 3, 4, 5]. This duality is one of many gauge/gravity correspondences between theories of quantum gravity and particle physics. They are certainly amongst the most fascinating topics in modern science. Integrability, to make a long story short (at the expense of rigor), is the mathematical structure which often allows one to solve a given physical theory. Thus, when speaking about integrability in AdS/CFT we speak about understanding features of quantum gravity and gauge theories by actually solving them. It is obviously a holy grail for theoretical physicists.

In this introduction we will constantly hand wave and rigor will never come along. Experts might consider completely jumping the first few sections.

## 1.1 String theory and AdS/CFT

String theory is not only the most developed approach to quantum gravity but a candidate for a theory of everything. The above mentioned gauge/gravity correspondences are incarnated in string theory as open/closed dualities. The basic idea is that the sum over the string worldsheet holes can be traded by a nontrivial background on which the string propagates.

We will move slowly towards this picture but we can already advance that there is nothing conceptually extravagant about it. Take the scattering of an electron by a heavy proton in QED. To leading order the electron throws a photon at the proton (fig 1.1a) and this virtual exchange leads to the Coulomb interaction. At next to leading order we have the Bremsstrahlung diagrams (fig 1.1b), the corrections from the virtual photons (fig 1.1c) and most importantly the photon self-energy (fig 1.1d). This latter effect screens the proton charge and corrects the Coulomb potential to the Uehling potential

$$V(r) = -\frac{\alpha}{r}\left(1 + \frac{\alpha}{4\sqrt{\pi}}\frac{e^{-2m_e r}}{(m_e r)^{3/2}} + \dots\right) . \tag{1.1}$$

By summing more and more Feynman diagrams we could in principle improve (1.1) to

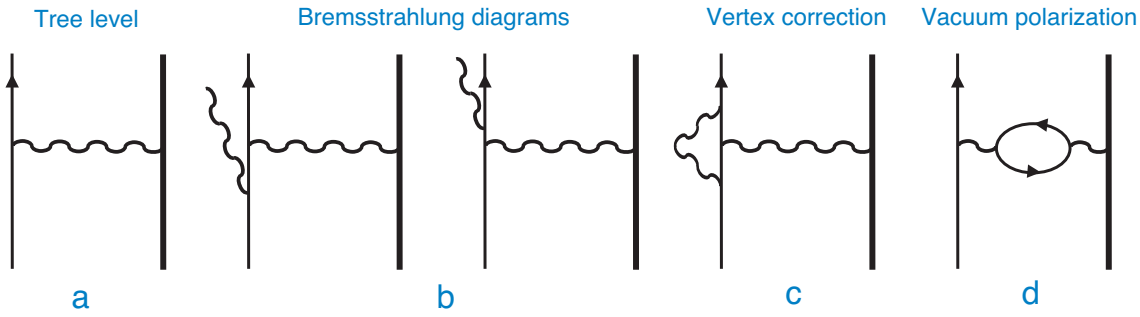


Figure 1.1: Virtual processes contributing to the scattering of an electron by an heavy proton.

any precision[1]. Thus we have two alternative descriptions for the passage of the electron by a region containing a heavy proton. On the one hand we can consider the electron and proton to be in a perfect vacuum and sum the virtual processes (Feynman diagrams) which will deflect the electron trajectory. On the other hand we can forget about the proton and say that the electron moves in a nontrivial region where there is a potential $V(r)$ given by (1.1). As explained bellow the Feynman diagramatic approach will be the analogous of summing over the worldsheet holes whereas the replacement of the holes by a nontrivial background is precisely what is done when we replace the Feynman diagrams by the potential $V(r)$.

In string theory fundamental particles are not point like objects but rather small vibrating strings. In fact the most attractive feature of string theory is the proposal that *all* particles are indeed the *very same* string. The excitation of different string modes would correspond to the several fundamental particles observed in nature. Strings can either form a closed loop or have its extremities attached to some (hyper)-surfaces as depicted in figure 1.2. In the former case the strings are denoted by closed strings while in the latter they are called open strings and the planes on which they end go by the name of branes[2]. When two points of the string overlap in space they can merge or split and thus open and closed strings can split and fuse between themselves as represented in the same figure 1.2. In particular by locality we see that, while we can have a theory of closed strings alone, a theory of open strings automatically contains closed strings.

Let us now consider a situation analogue to scattering of the electron by an heavy proton mentioned above, namely a closed string passing by a D-brane. The quantum propagation will be described by the usual sum over histories and the worldsheet of a typical history will be a Riemann surface with $h$ handles and $n$ holes (when the string meets the brane or the open strings attached to the brane) embedded in the spacetime as represented in

[1] As antecipated above we are not pretending to be rigorous, otherwise a note about the asymptotic nature of the perturbative expansion would be appropriate here.

[2] Today, String theory is actually the theory of strings and branes with a plethora of beautiful dualities between these objects.

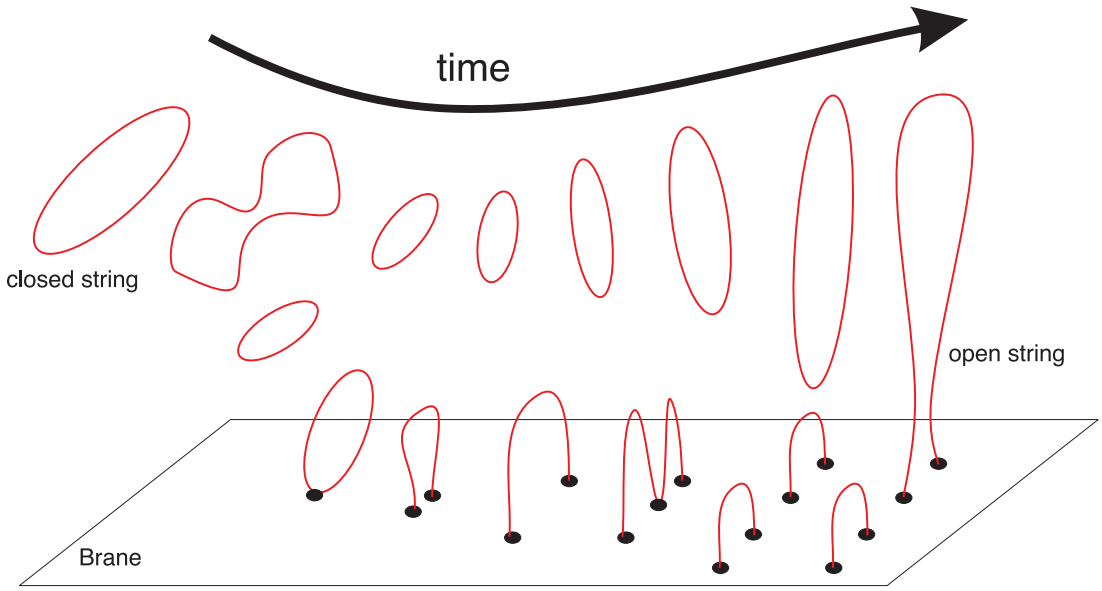


Figure 1.2: In String theory we have closed strings moving everywhere and open strings, attached to hyper-surfaces called branes. In this figure we depicted a possible evolution of a closed string into two open strings in the presence of a brane. We can also look at the process in the opposite direction as describing the fusion of two open strings into a single closed string. When two points are coincident in space-time the strings can merge or split. Since this is a local process, we see that a theory of closed string alone is possible but a theory of open strings automatically requires the presence of closed string.

figure 1.3a. If we sum over all the possible holes we are left with a non-trivial closed string propagation but without any brane [6, 7, 8]. The description in terms of the brane and its open strings is traded by a non-trivial background on which the closed string propagates as depicted in figure 1.3b. This is the picture behind AdS/CFT.

Technically what we do in figure 1.3a is to integrate over the moduli of such Riemann surfaces with $h$ handles and $n$ holes as represented in figure 1.4a. The crosses are the vertex operators representing the initial and final closed string states whereas the holes are described by boundary states. By the operator/state correspondence we can always replace these states by local operators and vice-versa. To replace a vertex operator by a boundary state we compute the path integral around the vertices up to some desired radius whereas to close a boundary state into a vertex operator we preform the path integral inside the hole. In this way we can close each of the $h$ holes and replace them by local operator insertions as represented in figure 1.4b. Schematically [8]

$$\int d\rho \rho^{L_0} |\mathcal{B}\rangle_k \leftrightarrow \mathcal{V}_k \,. \tag{1.2}$$

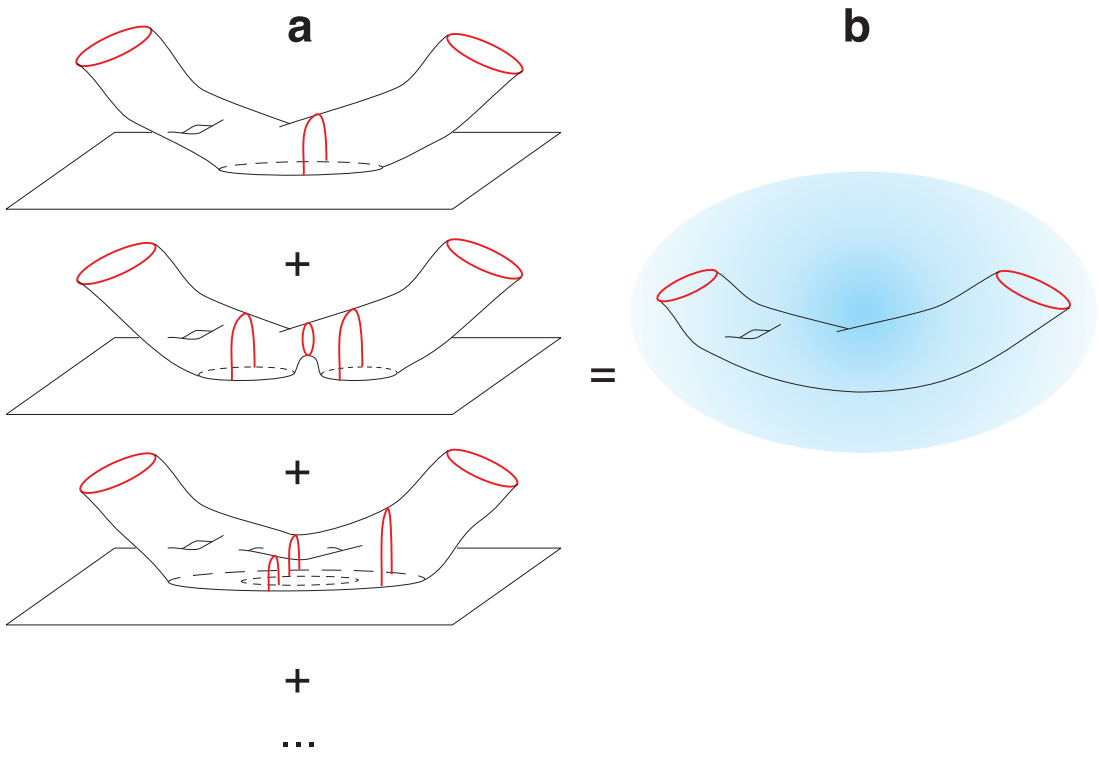


Figure 1.3: When a closed string propagates in a region where there is a brane its evolution is described by a sum of histories which comprises all possible interactions with this object. Instead we can sum over all this interactions and replace the brane by a non-trivial background on which the closed string propagates. This is the analogue of the electron moving in the presence of the heavy proton – either we sum all possible Feynman diagrams or we consider its movement in the presence of a non-trivial potential.

The Riemann surface with $h$ holes is replaced by a closed string with $h$ extra closed string insertions. This is precisely consistent with our pictures – branes are not only the basis for propagation of open strings but also (or rather alternatively) a source of closed strings. This sea of closed strings – which in particular contains gravitons – emitted by the brane can be interpreted as a deformation of the background on which the closed string propagates. Indeed since we should in principle sum over the position of the vertex operators we will obtain something like

$$\sum_{n=0}^{\infty} \frac{1}{n!} \int \prod_{i=1}^{n} d^2\sigma_i \mathcal{V}_i = \exp\left( \int d^2\sigma \mathcal{V} \right) \tag{1.3}$$

which will precisely deform the closed string action! This is schematized in figure 1.3c.

There are by now a few well understood examples where this picture was made rigorous and quite a lot of examples where this duality is a conjecture. We should add that these

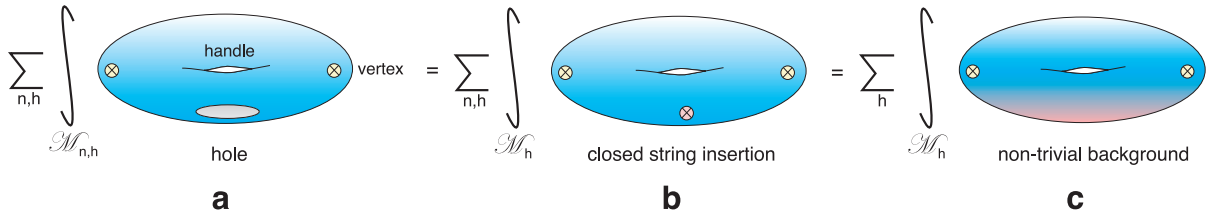


Figure 1.4: Technically the amplitude associated to the evolution of a closed string from one asymptotic state to another leaving as track a worlsheet with $h$ handle and $n$ holes is given by a path integral over the moduli space of Riemann surfaces of genus $h$ and $n$ holes with the insertion of two vertex operators accounting for the initial and final closed string states. The boundary states at the $n$ holes can be traded by the insertions of $n$ local operators by simply completing the path integral to the interior of the hole (this is the open-closed duality). These local operators are thought of as closed string vertices and we can replace the sum over all such vertices by a non-trivial background on which the path integral should be performed.

conjectures are most surely correct given the enormous quantity of highly nontrivial checks which have been preformed. The $AdS_5/CFT_4$ duality, which will be thoroughly analyzed in this thesis from the integrability point of view, is among such conjectured correspondences.

## 1.2 $AdS_5/CFT_4$

A particular fascinating duality emerges when we try to apply the pictures of the previous section to a configuration of $N$ coincident $D3$ branes in type IIB string theory in flat ten dimensional Minkowski space. The D3 branes extend along a (3+1) dimensional plane and their excitations are the open strings while the excitations of the empty (9+1) dimensional spacetime are the closed strings. Taking the low energy limit of this system only massless string modes survive and the complete effective action reduces to

$$S = S_{brane} + S_{bulk} + S_{interaction} \tag{1.4}$$

where $S_{brane}$ describes the massless string states – which organize into an $\mathcal{N} = 4$ supermultiplet in (3+1) dimensions – by an $\mathcal{N} = 4$ U(N) Super Yang-Mills Lagrangian plus higher derivative corrections and $S_{bulk}$ governs the closed massless states – which make a gravity ten dimensional supermultiplet – and is simply the type IIB supergravity effective action. $S_{interaction}$ couples both systems.

When we take the low energy limit by taking $\alpha' \to 0$ while keeping all dimensionless parameter fixed we see that the interaction lagrangian drops out and so do the higher derivative terms in the brane action. We obtain therefore a decoupled system of

$$\text{4D } \mathcal{N} = 4 \ U(N) \text{ SYM} \bigotimes \text{ free 10D } \mathcal{N} = 2 \text{ Chiral (IIB) supergravity} \tag{1.5}$$

This description corresponds to the *summing over holes* picture of the previous section. As the string tension $1/\alpha' \to \infty$ the holes will occupy almost all open string disk diagrams and we will recover t'Hooft fat graph for the $U(N)$ gauge theory. A thick line corresponds to the propagation of an open string. The two end-points of the string can end on either of the $N$ branes and thus this endows the thick line with the two color indices. This is the Chan Patton mechanism.

Let us now consider the background language where we sum over all holes – i.e., we compute the backreaction of the brane on the geometry – to generate a nontrivial background. To find this deformation at low energies we can consider ten dimensional type IIB supergravity. In this language the brane is an heavy charged hyper-plane deforming the geometry to

$$ds^2 = \frac{ds^2_{\mathbb{M}_4}}{\sqrt{1+\frac{l^4}{r^4}}} + \sqrt{1+\frac{l^4}{r^4}}\left(dr^2 + r^2 d\Omega^2_{S^5}\right) \quad , \quad l^4 = 4\pi g_s N \alpha'^2 \,. \tag{1.6}$$

From the point of view of the observer at infinity there are two kinds of low energy excitations: low energy massless excitations propagating away from the horizon at $r = 0$ and excitations of *arbitrary energy as measured by an observer close to the horizon* due to the huge red-shift typical of black hole horizons. Introducing $U = r/l^2$ we see that the near horizon geometry reduces to

$$ds^2 = l^2\left(\frac{dU^2}{U^2} + U^2 ds^2_{\mathbb{M}_4}\right) + l^2 d\Omega^2_{S^5} \tag{1.7}$$

which corresponds to the product space $AdS_5 \times S^5$, both with radius $l$. We stress again that when taking the low energy limit, all string excitations in the near horizon limit survive. Thus, we obtained again two decoupled systems,

$$\text{type IIB superstring in } AdS_5 \times S^5 \bigotimes \text{ free 10D } \mathcal{N}=2 \text{ Chiral (IIB) supergravity} \tag{1.8}$$

and therefore, comparing (1.8) and (1.5) we are lead to conjecture the equivalence between $\mathcal{N} = 4$ SYM and string theory in $AdS_5 \times S^5$. The precise mapping of parameters is summarized in table 1.1.

## 1.3 Contemplation, despair and integrability

The conjecture between $\mathcal{N} = 4$ U(N) SYM and type IIB superstring theory in $AdS_5 \times S^5$ is absolutely remarkable and there are many different angles from which we can contemplate it:

Table 1.1: $AdS_5/CFT_4$ map

| | $\mathcal{N}=4$ $U(N)$ SYM | type IIB superstrings in $AdS_5 \times S^5$ |
|---|---|---|
| | $\lambda = g_{YM}^2 N$ | $\lambda = \dfrac{R^4}{\alpha'^2}$ |
| $N$ | Number of colours | $g_s = \dfrac{R^4}{4\pi\alpha'^2}\dfrac{1}{N}$ |
| $N \to \infty$ with $\lambda$ fixed | planar theory | free strings |
| $N \to \infty$ and $\lambda \sim 0$ | perturbative regime | highly quantum free strings |
| $N \to \infty$ and $\lambda \gg 1$ | strongly coupled SYM | classical free strings |
| | Anomalous dimensions $\Delta$ | Energies of the string states $E$ |

- On the one hand we can say that, more than a duality between a 4D gauge theory and a nontrivial theory of quantum gravity, this correspondence is a *non-perturbative definition* of a nontrivial theory of quantum gravity. Indeed string theory is to date only defined perturbatively and this dual definition by means of a well defined unitary quantum gauge theory might provide the necessary non-perturbative completion of the theory. This point of view has immediate consequences. For example, information can not be lost if we consider black holes inside $AdS$. Indeed, in principle, we can prepare the state which will create the BH, relate it to the dual theory, evolve it in this *explicitly unitary* description and map it back to the gravity side. This is just an example, out of many, of the great power of the AdS/CFT dualities as tools to understand the mysteries of quantum gravity.

- This duality is the most successful realization of the holographic principle. Gravity in the $AdS_{d+1}$ bulk is encoded in a field theory living in $\mathbb{M}_d$, the boundary of $AdS_{d+1}$! It is remarkable that a four dimensional gauge theory might encode the dynamics of a higher dimensional gravity system. Even more remarkably, the $AdS/CFT$ duality is a duality between the gauge theory on the boundary and quantum gravity in the bulk described by a sum of geometries which are only required to be *asymptotically* anti de-Sitter.

- AdS/CFT is a duality strictus sensus as it maps weakly/strongly coupled gauge theory to strongly/weakly coupled string theory. This means that we can access previously impregnable territories of each theory with relative ease. Extremely quantum strings with string length much larger than the $AdS_5$ radius have a dual description as free $N = 4$! On the other extreme, strongly coupled (and non-perturbative) gauge

theory effects can be accessed by classical string computations. The power of the duality as a computational tool can hardly be overestimated.

All these features are of course remarkable but there is also a big drawback in all this related to the last item mentioned – without the development of some quite powerful techniques, checking any computation becomes a virtually impossible task. Perturbative CFT computations correspond to highly quantum interacting strings and classical strings are mapped to the non-perturbative strong coupled regime of the gauge theory!

In the limit of infinite $N$, when we consider planar gauge theory and free strings – such powerful techniques appear – integrability [9, 10]. It is now widely believed that in this limit both theories are fully integrable and thus amenable of analytic solution! In this introduction we will not dwell into this direction since integrability and in particular applications of integrability to AdS/CFT will be thoroughly covered in all the subsequent chapters of this thesis.

## 1.4 About the thesis

During the last three years, the period of my PhD, I was mostly localized in Paris with some large periods of time in Porto. During this period I was co-author in the papers [11, 12, 13, 14, 15, 16, 17, 18, 19, 20, 21] and proceedings [22, 23]. This thesis will not cover at all [12, 23]. The results in [11, 16, 19, 20, 22] are used but certainly not the main emphasis of this monograph. On the other hand, most of the results presented here are contained in the articles [13, 14, 15, 17, 18, 21].

The main text is split into two main parts. Part II deals mostly with Bethe Ansatz and with the $CFT$ side of the correspondence. Part III is devoted to the study of the string side of correspondence. Classical strings are studied in chapter 4, the semiclassical spectrum is analyzed is chapter 5 and in the last chapter 6 we consider the one-loop shift around generic classical solutions and make contact with the Bethe ansatz studied in part II. See the appendix for a fine grained description or figure 1.5 for a course grained plan of the thesis.

We should also include the following disclaimer. For the lack of space we chose to concentrate mostly on the scaling limit of Bethe equations and on aspects of semi-classical string integrability. In particular, most important developments leading to the famous Beiser-Eden-Staudacher dressing factor [24] are not properly covered in this monograph. For example, in section 3.7 we basically jump from the one-loop treatment of the previous sections to the all-loop conjectured equations leaving a huge pedagogical gap in between which would well deserve a monograph of its own. We refer the reader to [25, 26, 27, 28, 29, 30, 31] for more reviews on Integrability in AdS/CFT.

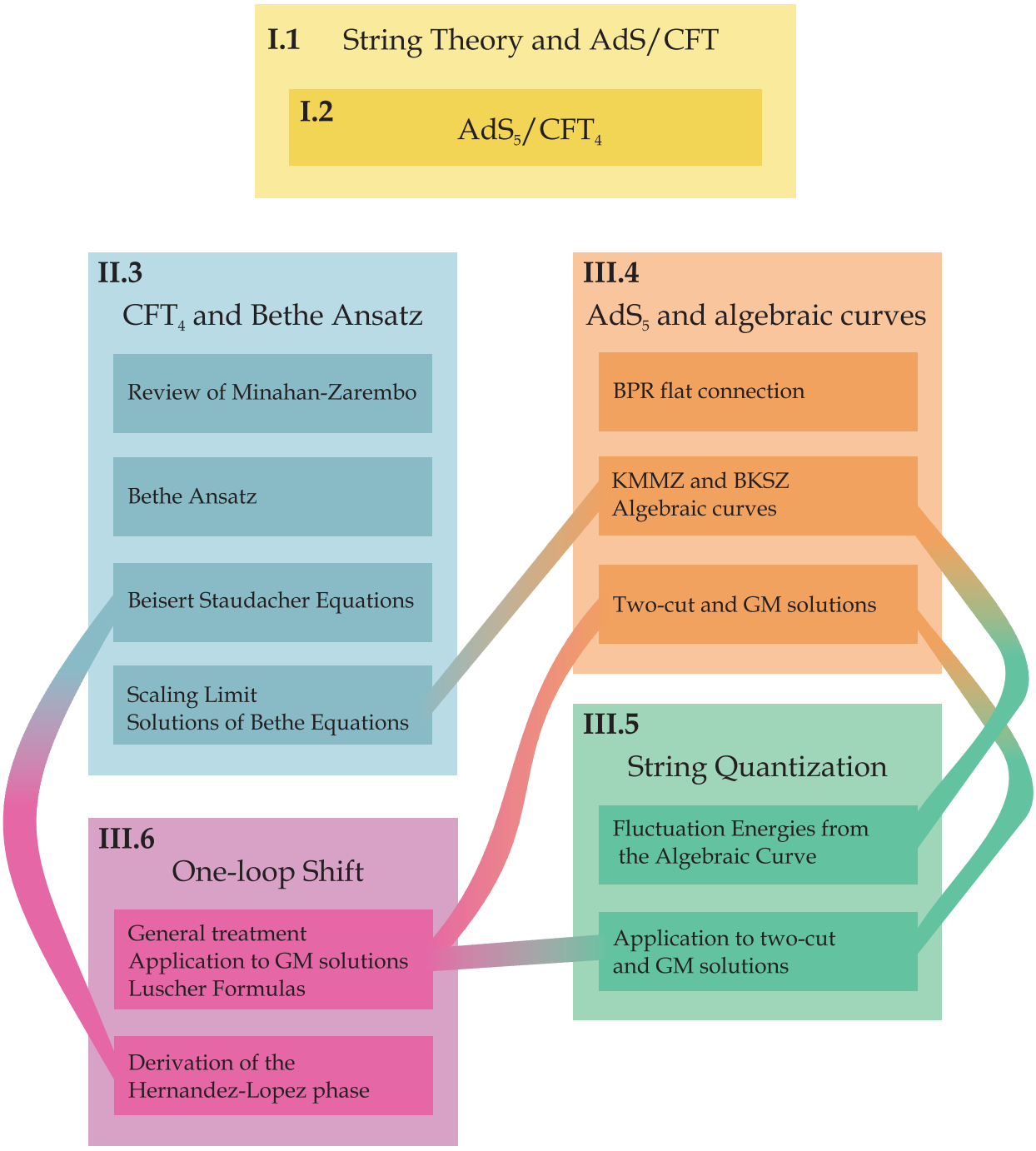


Figure 1.5: Course grained plan of the thesis and logical flow. Only main subjects are represented, many sections are omitted. Parts II and III are basically independent except for the last section in chapter 6.4 which requires the results of section 3.7 in part II

# Chapter 2

# Lagrangians of the AdS and CFT theories

In this section we will write down the Lagrangian of four dimensional $\mathcal{N} = 4$ $U(N)$ super symmetric Yang-Mills theory [32, 33] and the Metsaev-Tseytlin action for type IIB free strings in $AdS_5 \times S^5$ [34].

## 2.1 $\mathcal{N} = 4$ SYM

The fundamental fields in $\mathcal{N} = 4$ SYM are six real scalars, four dimensional gluons, and sixteen component Majorana spinors, all of them matrices of size $N \times N$,

$$\Phi_i = \Phi_i^a \, T^a \ , \ A_\mu = A_\mu^a \, T^a \ , \ \Psi = \Psi^a \, T^a \, , \tag{2.1}$$

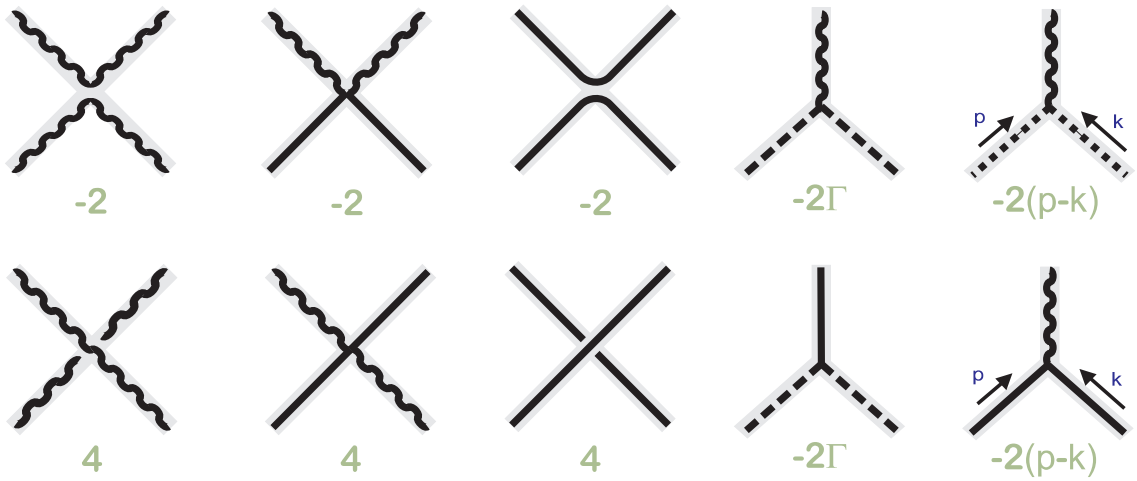


Figure 2.1: Component Feynman rules for $\mathcal{N} = 4$ super symmetric Yang-Mills theory. Solid, wavy, dashed and pointed lines represent scalars, gluons, fermions and ghosts respectively and their propagators are canonically normalized to $\frac{g_{YM}^2}{2}\frac{\delta^{ij}}{p^2}$, $\frac{g_{YM}^2}{2}\left(\frac{\eta^{\mu\nu}}{p^2} - (1-\zeta)\frac{p^\mu p^\nu}{p^4}\right)$, $\frac{g_{YM}^2}{2}\frac{\Gamma\cdot p}{p^2}$ and $\frac{g_{YM}^2}{2}\frac{1}{p^2}$. Obvious indices and delta functions are omitted and all vertices should be multiplied by $1/g^2$. For example the fourth vertex in the first row corresponds to $-\frac{2}{g_{YM}^2}\Gamma^\mu$, the last vertex in the second row yields $-\frac{2}{g_{YM}^2}(p^\mu - k^\mu)\delta_{ij}$, etc. The trivial $U(N)$ indices are omitted and fermionic loops should be accompanied by an extra factor of minus one.

where $T^a$ are the $N$ generators of $U(N)$ normalized as $\mathrm{Tr}\left(T^a T^b\right) = \frac{1}{2}\delta^{ab}$. The Lagrangian of $\mathcal{N} = 4$ SYM reads

$$L = \frac{1}{g_{YM}^2}\mathrm{Tr}\left[\frac{1}{2}[D_\mu, D_\nu]^2 + (D_\mu \Phi_i)^2 - \frac{1}{2}[\Phi_i, \Phi_j]^2 + i\bar{\Psi}\left(\Gamma^\mu D_\mu \Psi + \Gamma^i[\Phi_i, \Psi]\right) + \partial_\mu \bar{c} D_\mu c + \zeta\left(\partial_\mu A_\mu\right)^2\right]$$

where the covariant derivative is defined as usual

$$D_\mu \cdot = \partial_\mu \cdot - i\,[A_\mu, \cdot]$$

and $(\Gamma^\mu, \Gamma^i)$ are ten real $16 \times 16$ Dirac matrices normalized to $\mathrm{Tr}\left(\Gamma^A \Gamma^B\right) = 16\,\delta^{AB}$. Finally, $c$ and $\bar{c}$ are the Faddeev-Popov ghosts. The Feynman rules for this theory are summarized in figure 2.1. This is a superconformal field theory and its symmetry is $PSU(2,2|4)$ together with the gauge transformations.

This is quite a minimalistic description of this very rich field theory but it is actually more or less all we need for the moment. As we proceed we will introduce the several needed ingredients.

## 2.2 Superstring in $AdS_5 \times S^5$

We want to study superstrings moving in $AdS_5 \times S^5$. The isometry group of the $AdS_5$ part is

$$SO(4,2) \simeq SU(2,2)$$

while the symmetry of the five sphere is

$$SO(6) \simeq SU(4)\,.$$

Each of these spaces is the coset between the corresponding isometry groups and the symmetry group which leaves a fixed point (isotropy group) which is

$$SO(4,1) \simeq SP(2,2)$$

for anti de-Siter and

$$SO(5) \simeq SP(4)$$

for the $S^5$ factor. The bosonic part of the supercoset where the string moves is therefore

$$AdS_5 \times S^5 = \frac{SU(2,2) \times SU(4)}{SP(2,2) \times SP(4)}\,.$$

The full super space where the string moves has this bosonic part completed to the supercoset

$$\frac{PSU(2,2|4)}{SP(2,2) \times SP(4)}\,.$$

In order to write down the string action it is useful to recall a couple of facts about the several ingredients in this coset. The matrix superalgebra $su(2,2|4)$ is spanned by the $8\times 8$ supertraceless supermatrices

$$M = \left(\begin{array}{c|c} A & B \\ \hline C & D \end{array}\right)$$

where $A$ and $B$ belong to $u(2,2)$ and $u(4)$ respectively while the fermionic components are related by

$$C = B^\dagger \begin{pmatrix} \mathbb{I}_{2\times 2} & 0 \\ 0 & -\mathbb{I}_{2\times 2} \end{pmatrix} .$$

The supertraceless condition means

$$\mathrm{str}\, M \equiv \mathrm{Tr} A - \mathrm{Tr} D = 0 \,.$$

The $psu(2,2|4)$ superalgebra is the quotient of this algebra by the matrices proportional to the identity. Since the $su(2,2|4)$ algebra enjoys the automorphism[1]

$$\Omega \circ M = \begin{pmatrix} EA^TE & -EC^TE \\ EB^TE & ED^TE \end{pmatrix} \ , \ E = \begin{pmatrix} 0 & -1 & 0 & 0 \\ 1 & 0 & 0 & 0 \\ 0 & 0 & 0 & -1 \\ 0 & 0 & 1 & 0 \end{pmatrix} ,$$

with

$$\Omega^4 = 1 \,,$$

the algebra is endowed with a $\mathbb{Z}_4$ grading. This means that any algebra element can be decomposed into

$$M = \sum_{i=0}^{3} M^{(i)}$$

where $\Omega \circ M^{(n)} = i^n M^{(n)}$. Explicitly

$$M^{(0,2)} = \frac{1}{2}\begin{pmatrix} A \pm EA^TE & 0 \\ 0 & D \pm ED^TE \end{pmatrix}, M^{(1,3)} = \frac{1}{2}\begin{pmatrix} 0 & B \pm iEC^TE \\ C \mp iEB^TE & 0 \end{pmatrix} . \quad (2.2)$$

Elements of $M^{(0)}$ are invariant under the action of the automorphism meaning that $B = 0$, $C = 0$ and

$$A = EA^TE \ , \ \ D = ED^TD$$

which are precisely the defining relations for the denominator algebra $sp(2,2) \times sp(4)$ of the coset. Therefore the $M^{(0)}$ elements span this part of the coset which we want to gauge

[1] Meaning $\Omega \circ [M_1, M_2] = [\Omega \circ M_1, \Omega \circ M_2]$ as can be easily checked.

away. The remaining bosonic elements, $M^{(2)}$, orthogonal to the former, must generate the (orthogonal) complement of $sp(2,2) \times sp(4)$ in $su(2,2) \times su(4)$ which is precisely what we want to keep. $M^{(1)}$ and $M^{(3)}$ are the fermionic components of the current.

Finally, the Metsaev-Tseytlin action for the GS superstring in $AdS_5 \times S^5$ is then given in terms of the algebra current

$$J = -g^{-1}dg\,, \tag{2.3}$$

where $g(\sigma,\tau)$ is a group element of $PSU(2,2|4)$, by

$$S = \frac{\sqrt{\lambda}}{4\pi}\int \mathrm{str}\,\left(J^{(2)} \wedge *J^{(2)} - J^{(1)} \wedge J^{(3)}\right) + \Lambda \wedge \mathrm{str}\,J^{(2)}\,, \tag{2.4}$$

where the last term ensures that $J^{(2)}$ is supertraceless[2]. In section 4.2 where the emergence of classical integrability is studied, we will discuss this action further. Besides the obvious global $PSU(2,2|4)$ left multiplication symmetry the action (2.4) possesses a local gauge symmetry, $g \to gH$ with $H \in SP(2,2) \times SP(4)$, under which

$$J^{(i)} \;\;\to\;\; H^{-1}J^{(i)}H \quad , \quad i = 1,2,3 \tag{2.5}$$

while $J^{(0)}$ transforms as a connection,

$$J^{(0)} \;\;\to\;\; H^{-1}J^{(0)}H - H^{-1}dH\,. \tag{2.6}$$

The equations of motion following from (2.4) are equivalent to the conservation of the Noether current associated with the global left multiplication symmetry

$$d * k = 0 \tag{2.7}$$

where $k = gKg^{-1}$ and

$$K = J^{(2)} + \frac{1}{2} * J^{(1)} - \frac{1}{2} * J^{(3)} - \frac{1}{2} * \Lambda\,.$$

Just a few words on how to easily derive this equation just by looking at the action (2.4): The supertrace of a product of algebra components with different grading is not zero only if the total grading vanishes:

$$\mathrm{str}\,\left(M^{(m)}N^{(n)}\right) = 0 \quad , \quad \text{if } n+m \neq 0 \mod 4\,. \tag{2.8}$$

Thus suppose we make an infinitesimal left multiplication transformation under which $\delta J = g^{-1}dGg$ and want to see how the action changes. When varying each $J^{(n)}$ in (2.4)

[2]Obviously all components $J^{(i)}$ must be supertraceless since they are elements of $PSU(2,2|4)$. However, as manifest from (2.2), all other components are automatically supertraceless and thus require no Lagrange multipliers.

we can replace its variation by simply $\delta J = \sum \delta J^{(n)}$ since the superstrace will project back to the original component $\delta J^{(n)}$. Then we get $\delta S = \int \mathrm{str}\, g^{-1} dG g \wedge K$ and therefore, integrating by parts and using the cyclicity of the trace we obtain (2.7).

When we restrict ourselves to purely bosonic fields we should recover the usual sigma model action

$$S_b = \frac{\sqrt{\lambda}}{4\pi} \int_0^{2\pi} d\sigma \int d\tau \sqrt{h}\, \left( h^{\mu\nu}\, \partial_\mu u \cdot \partial_\nu u + \lambda_u \left( u \cdot u - 1 \right) - (u \to v) \right) , \tag{2.9}$$

where the lagrange multipliers constrain the embedding coordinates

$$\begin{aligned} 1 &= u \cdot u \equiv u_6^2 + u_5^2 + u_4^2 + u_3^3 + u_2^2 + u_1^2 \,, \\ 1 &= v \cdot v \equiv v_6^2 + v_5^2 - v_4^2 - v_3^2 - v_2^2 - v_1^2 \,. \end{aligned} \tag{2.10}$$

This restriction works as follows. For a purely bosonic representative $g$ we can write

$$g = \left( \begin{array}{c|c} \mathcal{Q} & 0 \\ \hline 0 & \mathcal{R} \end{array} \right) . \tag{2.11}$$

where $\mathcal{R} \in SU(4)$ and $\mathcal{Q} \in SU(2,2)$. Then we see that $\mathcal{R} E \mathcal{R}^T$ is a good parametrization of

$$SU(4)/SP(4) = S^5$$

because, by definition, it is invariant under $\mathcal{R} \to \mathcal{R} H$ with $H \in SP(4)$. In the same way $\mathcal{Q} E \mathcal{Q}^T$ describes the $AdS$ space. Then we can define the embedding coordinates $u$ and $v$ by the simple relations

$$u^j \Sigma_j^S = \mathcal{R} E \mathcal{R}^T \ , \ v^j \Sigma_j^A = \mathcal{Q} E \mathcal{Q}^T \tag{2.12}$$

where $\Sigma^S, \Sigma^A$ are the gamma matrices of $SO(6)$ and $SO(4,2)$. By construction these coordinates will automatically satisfy (2.10) and then the bosonic part of the action can be expressed in the usual non–linear $\sigma$ model form (2.9). For future convenience let us render the matrix form of the above relations explicit:

$$u_j \Sigma_j^S = \begin{pmatrix} 0 & -u_6 - i u_5 & -u_4 - i u_3 & -u_2 - i u_1 \\ u_6 + i u_5 & 0 & -u_2 - i u_1 & u_4 + i u_3 \\ u_4 + i u_3 & u_2 + i u_1 & 0 & -u_6 - i u_5 \\ u_2 + i u_1 & -u_4 - i u_3 & u_6 + i u_5 & 0 \end{pmatrix} \tag{2.13}$$

$$v_j \Sigma_j^A = \begin{pmatrix} 0 & -v_6 - i v_5 & v_4 + i v_3 & -v_2 - i v_1 \\ v_6 + i v_5 & 0 & v_2 + i v_1 & v_4 + i v_3 \\ -v_4 - i v_3 & -v_2 - i v_1 & 0 & -v_6 - i v_5 \\ v_2 + i v_1 & -v_4 - i v_3 & v_6 + i v_5 & 0 \end{pmatrix} \tag{2.14}$$

At this point we end our introduction. In the next chapter integrability comes onto stage.

# Part II

# Bethe ansatz

# Chapter 3

# Integrability in $\mathcal{N} = 4$ and Bethe ansatz

In this chapter we will start by reviewing the seminal work of Minahan and Zarembo [9] where integrability first appeared in $\mathcal{N} = 4$ SYM. We will then introduce the algebraic and coordinate Bethe ansatz formalism. In section 3.6 we will study the $SO(4)$ which shares many features with the $\mathcal{N} = 4$ Bethe equations proposed by Beisert and Staudacher (BS) [35] presented in section 3.7. In the remaining section we analyze the solutions to Bethe equations and in particular consider in detail the scaling limit of (nested) Bethe ansatz equations. We finish the chapter with a simple toy model as a curious application of the algebraic Bethe ansatz.

## 3.1 Spin chains

$\mathcal{N} = 4$ SYM is a superconformal field theory and therefore there is a basis of renormalized operators such that

$$\langle \mathcal{O}_A(x)\mathcal{O}_B(0)\rangle = \frac{\delta_{AB}}{|x|^{2\Delta_A}} \tag{3.1}$$

where $\Delta_A$ are the anomalous dimensions. The renormalized operators are related to the bare ones through

$$\mathcal{O}_A(x) = \left(e^{\hat{H}\log\Lambda}\right)_{AB}\mathcal{O}^0_B(x) \tag{3.2}$$

where $\hat{H}$ is the mixing matrix chosen in such a way that the correlation functions of $\mathcal{O}_A$ with arbitrary probes are finite.

Notice that to arrive at (3.1) we perform two non-trivial steps:

1. First we compute the mixing matrix $\hat{H}$ which acts on a family of bare operators yielding renormalized operators out of which we can construct (finite) correlation functions.

2. Next we find linear combinations of bare operators which are eigenvectors of the mixing matrix $\hat{H}$ with eigenvalues $\Delta_A$. These linear combinations of bare operators now renormalize trivially. Namely to render such operator finite we simply multiply it by $\Lambda^{\Delta_A}$. These renormalized operators are the ones entering in (3.1).

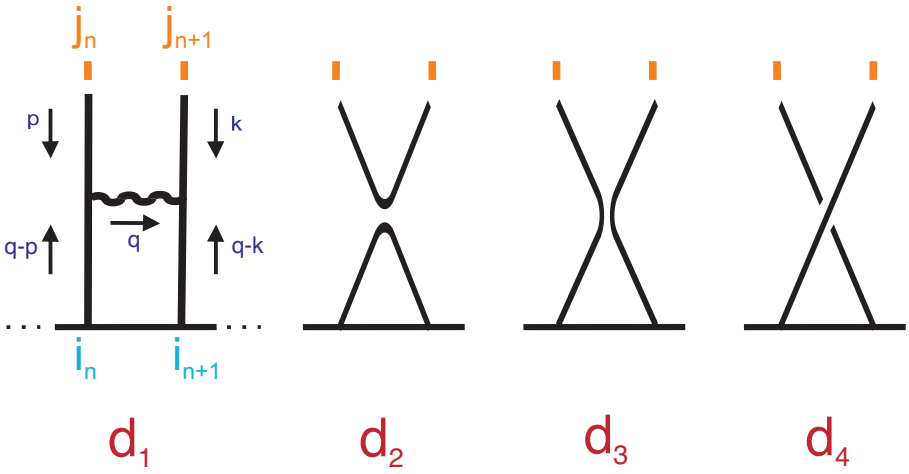


Figure 3.1: Non self-energy graphs contributing to the one loop mixing matrix for the $SO(6)$ scalars of planar $\mathcal{N} = 4$ SYM. The operator we renormalize is in the bottom and the trace is represented by the solid horizontal line. The probes, on the other hand, have free indices and are represented by the orange small tick marks on top.

Let us carefully review [9] how the computation of $\hat{H}$ goes for the $SO(6)$ sector of the theory where we consider operators of length $L$ made of the form

$$\mathcal{O}^0_A(x) = \mathrm{Tr}\left(\Phi_{i_1} \dots \Phi_{i_L}\right) . \tag{3.3}$$

In the planar limit we need to evaluate the diagrams listed in figures 3.1 and 3.2. The diagrams in figure 3.2 are of self-energy type and also renormalize the external legs so, to compute the total $\log \Lambda$ divergence, we must sum all diagrams in figure 3.1 plus half of the contribution of summing over the diagrams in figure 3.2. Since we only want to compute the $\Lambda$ diverging contributions, this computation is quite trivial. The first diagram $d_1$, for example, is given by

$$d_1 = \delta^{i_n}_{j_n}\delta^{i_{n+1}}_{j_{n+1}} \left(\frac{g^2_{YM}}{2}\right)^3 \left(\frac{1}{g^2_{YM}}\right)^2 N \int \frac{d^4q}{(2\pi)^4} \frac{[-2\,(2p^\mu - q^\mu)][-2\,(q_\nu - 2k_\nu)]}{(q-p)^2(q-k)^2q^2} \left(\eta_{\mu\nu} + (1-\zeta)\frac{q^\mu q^\nu}{q^2}\right)$$

where we used the Feynman rules of figure 2.1. This diagram diverges logarithmically with the cut-off and we can therefore expand the integrand at large $q$ to obtain

$$d_1 = \delta^{i_n}_{j_n}\delta^{i_{n+1}}_{j_{n+1}} \left(1 + (1-\zeta)\right) \frac{g^2_{YM}N}{16\pi^2} \log\Lambda + \text{finite} \tag{3.4}$$

Before computing the remaining diagrams let us introduce some notation which will make the forthcoming expressions much more eye friendly. First of all we introduce the t'Hooft coupling $\lambda \equiv g^2_{YM}N$ and $g$ as

$$g^2 \equiv \frac{\lambda}{16\pi^2} \equiv \frac{g^2_{YM}N}{16\pi^2} \tag{3.5}$$

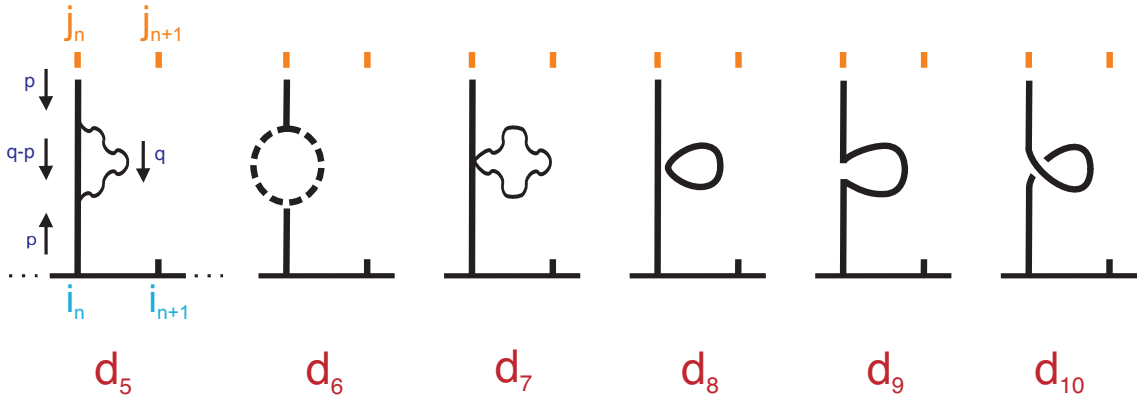


Figure 3.2: Self energy contribution to the dilatation operator.

Then we define the integrals

$$\mathcal{I}_1 \equiv g^2 \log\Lambda = \frac{\lambda}{2}\int \frac{d^4q}{(2\pi)^4}\frac{1}{(q^2)^2}\ ,\ \mathcal{I}_2 \equiv \frac{g^2}{2}\frac{\Lambda^2}{p^2} = \frac{\lambda}{2}\int \frac{d^4q}{(2\pi)^4}\frac{1}{q^2p^2} \tag{3.6}$$

and $\xi \equiv 1-\zeta$ in terms of which the previous result reads

$$d_1 = (1+\xi)\,\mathcal{I}_1\,\delta^{i_n}_{j_n}\delta^{i_{n+1}}_{j_{n+1}}\,. \tag{3.7}$$

In the same way we find

$$d_2 = -\,\mathcal{I}_1\,\delta^{j_n j_{n+1}}\delta_{i_l i_{l+1}}\ ,\ d_3 = -\,\mathcal{I}_1\,\delta^{j_n}_{i_n}\delta^{j_{n+1}}_{i_{n+1}}\ ,\ d_4 = 2\,\mathcal{I}_1\,\delta^{j_{n+1}}_{i_n}\delta^{j_n}_{i_{n+1}} \tag{3.8}$$

while the self energy type diagrams of figure 3.2 yield

$$\begin{aligned}
d_5 &= \delta^{j_n}_{i_n}\delta^{j_{n+1}}_{i_{n+1}}\,(2\,(1-\xi)\,\mathcal{I}_1 + (1+\xi)\,\mathcal{I}_2) \\
d_6 &= \delta^{j_n}_{i_n}\delta^{j_{n+1}}_{i_{n+1}}\,(\quad -4\,\mathcal{I}_1 + \quad 8\,\mathcal{I}_2) && (3.9)\\
d_7 &= \delta^{j_n}_{i_n}\delta^{j_{n+1}}_{i_{n+1}}\,(\quad -(4+\xi)\,\mathcal{I}_2) && (3.10)\\
d_8+d_9+d_{10} &= \delta^{j_n}_{i_n}\delta^{j_{n+1}}_{i_{n+1}}\,(\quad -5\,\mathcal{I}_2) && (3.11)
\end{aligned}$$

Now we must add up all divergencies. Notice that the external probes are also renormalized by $Z_\Phi$ so we should sum

$$d_1 + \cdots + d_4 + \frac{1}{2}\,(d_5 + \cdots + d_{10}) \tag{3.12}$$

which yields

$$+\,\frac{g^2N}{16\pi^2}\log(\Lambda)\left(2\,\delta^{j_n}_{i_n}\delta^{j_{n+1}}_{i_{n+1}} + \delta_{i_n i_{n+1}}\delta^{j_n j_{n+1}} - 2\,\delta^{j_{n+1}}_{i_n}\delta^{j_n}_{i_{n+1}}\right) \tag{3.13}$$

The fact that both the gauge dependence $\xi$ and the $\Lambda^2$ divergencies dropped out is a good indication that no mistake was done. From this result we see that we should take

$$\left(e^{\hat{H}\log\Lambda}\right)^{\ldots,i_n,i_{n+1},\ldots}_{\ldots,j_n,j_{n+1},\ldots} = 1 - \frac{g^2N}{16\pi^2}\log(\Lambda)\left(2\,\delta^{j_n}_{i_n}\delta^{j_{n+1}}_{i_{n+1}} + \delta_{i_ni_{n+1}}\delta^{j_nj_{n+1}} - 2\,\delta^{j_{n+1}}_{i_n}\delta^{j_n}_{i_{n+1}}\right) \quad (3.14)$$

for each pair of consecutive indices. To write this in a more compact form we regard the operators of the form (3.3) as spin chain states

$$|\uparrow_{i_1}\ldots\uparrow_{i_L}\rangle \quad (3.15)$$

with the only difference compared with the usual Heisenberg spin chain being that here one has six possible polarizations $\uparrow_1,\ldots,\uparrow_6$ for each individual spin. We can then write the full $SO(6)$ one-loop dilatation operator – now regarded as a spin chain Hamiltonian – as

$$\hat{H} = g^2\sum_{n=1}^{L}(2I_{n,n+1} + K_{n,n+1} - 2P_{n,n+1}) \quad (3.16)$$

where the identity, permutation and trace operators act on the correspondent two sites as

$$I|\ldots\uparrow_i\uparrow_j\ldots\rangle = |\ldots\uparrow_i\uparrow_j\ldots\rangle \quad (3.17)$$

$$P|\ldots\uparrow_i\uparrow_j\ldots\rangle = |\ldots\uparrow_j\uparrow_i\ldots\rangle \quad (3.18)$$

$$K|\ldots\uparrow_i\uparrow_j\ldots\rangle = \delta_{ij}\sum_{k=1}^{6}|\ldots\uparrow_k\uparrow_k\ldots\rangle \quad (3.19)$$

A particularly important (perturbatively) closed sector is obtained when considering operators made out of the two complex scalars

$$Z = \phi_1 + i\phi_2\ ,\ X = \phi_3 + i\phi_4 \quad (3.20)$$

which can be in this case mapped to usual $SU(2)$ spins

$$\mathrm{Tr}\,(ZZX\ldots) \leftrightarrow |\uparrow\uparrow\downarrow\ldots\rangle\,. \quad (3.21)$$

The Hamiltonian acting on this states reduces the usual Heisenberg Hamiltonian

$$\hat{H}_{xxx} = 2g^2\sum_{n=1}^{L}(I_{n,n+1} - P_{n,n+1}) \quad (3.22)$$

This spin chain is also known as $XXX$ spin chain, hence the subscript. We observe that the BPS protected state $\mathrm{Tr}(Z^L) \leftrightarrow |\uparrow\ldots\uparrow\rangle$, is an eigenvector of this Hamiltonian with zero eigenvalue. This again indicates that no mistake was done in the diagrammatics.

As explained in the beginning, by computing $\hat{H}$ we have done half of the job, namely we rendered the theory finite. That is the action of $e^{\hat{H}\log(\Lambda)}$ – which to this order in

perturbation theory reduces to $1+\hat{H}\log(\Lambda)$ – on any linear combination of bare operators such as

$$|\Psi\rangle_0 = |\uparrow_1\uparrow_1\uparrow_2\rangle + |\uparrow_1\uparrow_1\uparrow_2\rangle \tag{3.23}$$

yields a renormalized operator

$$|\Psi\rangle = \left(1+\hat{H}\log\Lambda\right)|\Psi\rangle_0\,. \tag{3.24}$$

Correlation functions between renormalized operators are finite and thus what we have done so far is already quite interesting. As mentioned in the beginning, to go further and compute the renormalized operators which *moreover* have a precise anomalous dimension we must diagonalize $\hat{H}$. For example we can check that

$$\hat{H}\left(\sum_{i=1}^{6}|\uparrow_i\uparrow_i\rangle\right) = 12g^2\left(\sum_{i=1}^{6}|\uparrow_i\uparrow_i\rangle\right) \tag{3.25}$$

and

$$\hat{H}\left(|ZXZX\rangle - |ZZXX\rangle\right) = 12g^2\left(|ZXZX\rangle\rangle - |ZZXX\rangle\right) \tag{3.26}$$

which is precisely the anomalous dimension of the Konishi operator. Moreover the operators $\sum_{i=1}^{6}\mathrm{Tr}\left(\Phi_i\Phi_i\right)$ and $\mathrm{Tr}\left[Z,X\right]^2$ belong to the same supermultiplet and therefore should have the same anomalous dimension, precisely as observed here.

It is when we try to go beyond these simple examples and compute the full spectrum of the one loop dilatation operator that integrability comes into play. Namely, it turns out that the Hamiltonian (3.16) is quite special.

## 3.2 Algebraic Bethe ansatz

In this section we will understand how to construct and automatically compute the spectrum of families of integrable Hamiltonians. Remarkably the hamiltonians (3.16) and (3.22) belong to such families.

For that purpose let us review the logic behind the Leningrad school algebraic Bethe ansatz formalism ( for nice reviews and references see e.g. [36, **?**]). We will try to describe this beautiful and general mathematical construction with some detail with the drawback of obliging us to hold our breath for quite a while before the connection with physics and the spin chain Hamiltonians which we found in the previous section appears.

We consider the Hilbert space $\mathcal{H}$ of some spin chain of length $L$ which will typically be given by a tensor product of $L$ copies of some fixed space $h$,

$$\mathcal{H} = h_1\otimes\cdots\otimes h_L\,. \tag{3.27}$$

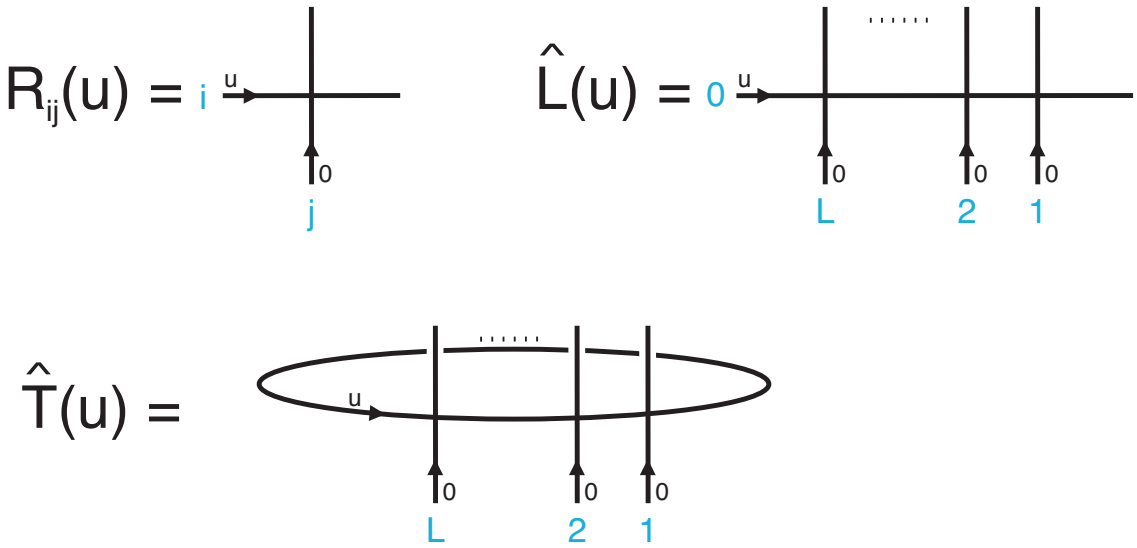


Figure 3.3: $R$-matrix, monodromy matrix $L(u)$ and transfer matrix, the fundamental building blocks of quantum integrability.

We assume (normally this is the case) that all sites are equal and thus all $h_j$ are isomorphic to the same vector space. For concreteness let us consider $SU(M)$ models for which $h_j \simeq \mathbb{C}^M$. We also consider an auxiliary space $h_0$, also isomorphic to $\mathbb{C}^M$.

Next there are three fundamental objects in the algebraic Bethe ansatz construction:

1. An $R$-matrix which acts in

$$R_{ij}(u) : h_i \otimes h_j \to h_i \otimes h_j \tag{3.28}$$

where in particular $h_i$ or $h_j$ can be the auxiliary space (if $i = 0$ or $j = 0$). This operator also depends on a complex number $u$ called the spectral parameter.

2. A monodromy matrix

$$\hat{L}(u) \equiv R_{0L}(u) \dots R_{02}(u) R_{01}(u) \tag{3.29}$$

which acts on the product of all spaces,

$$\hat{L}(u) : h_0 \otimes \mathcal{H} \to h_0 \otimes \mathcal{H} \,. \tag{3.30}$$

Notice that we can think of $\hat{L}(u)$ as being a $M \times M$ matrix in the auxiliary space with each entry being an operator acting on the physical Hilbert space $\mathcal{H}$.

3. A transfer matrix which is the trace of the monodromy matrix with respect to the auxiliary space,

$$\hat{T}(u) \equiv \mathrm{Tr}_0 \hat{L}(u) \,. \tag{3.31}$$

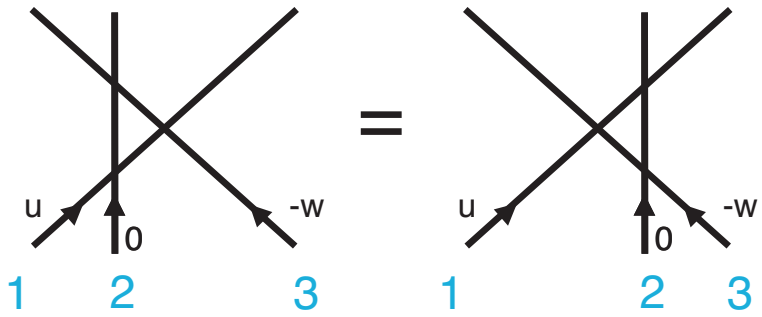


Figure 3.4: Yang Baxter relation.

Since the trace is taken over the auxiliary space we are left with an operator acting on the full spin chain Hilbert space,

$$\hat{T}(u) : \mathcal{H} \to \mathcal{H} \,. \tag{3.32}$$

These operators can be graphically represented as in figure 3.3.

For the construction that follows to go through the $R$-matrices must obey the triangular Yang-Baxter (YB) relation

$$R_{12}(u)R_{13}(u+w)R_{23}(w) = R_{23}(w)R_{13}(u+w)R_{12}(u)\,, \tag{3.33}$$

depicted in figure 3.4. This is basically the single restriction on the operators above but it is already quite constraining. For example, in $SU(M)$ we have only two invariant tensors acting on the product $h_1 \times h_2$, the identity

$$1 \;,\; (1)^{j_1,j_2}_{i_1,i_2} = \delta^{j_1}_{i_1}\delta^{j_2}_{i_2}\,, \tag{3.34}$$

and the permutation operator

$$P \;,\; (P)^{j_1,j_2}_{i_1,i_2} = \delta^{j_2}_{i_1}\delta^{j_1}_{i_2}\,. \tag{3.35}$$

Therefore, to construct an $SU(M)$ symmetric $R$-matrix we write

$$R(u) = h(u)1 + f(u)P\,. \tag{3.36}$$

Then plugging the $R$-matrix into (3.33) we obtain

$$\frac{h(u+w)}{f(u+w)} = \frac{h(u)}{f(v)} + \frac{h(w)}{f(w)} \tag{3.37}$$

which means that we can set $h(u)/f(u) = u/i$. Obviously, relation (3.33) does not fix the normalization of the $R$-matrix and we can chose $h(u)$ so that

$$R(u) = \frac{u1 + iP}{u+i}\,, \tag{3.38}$$

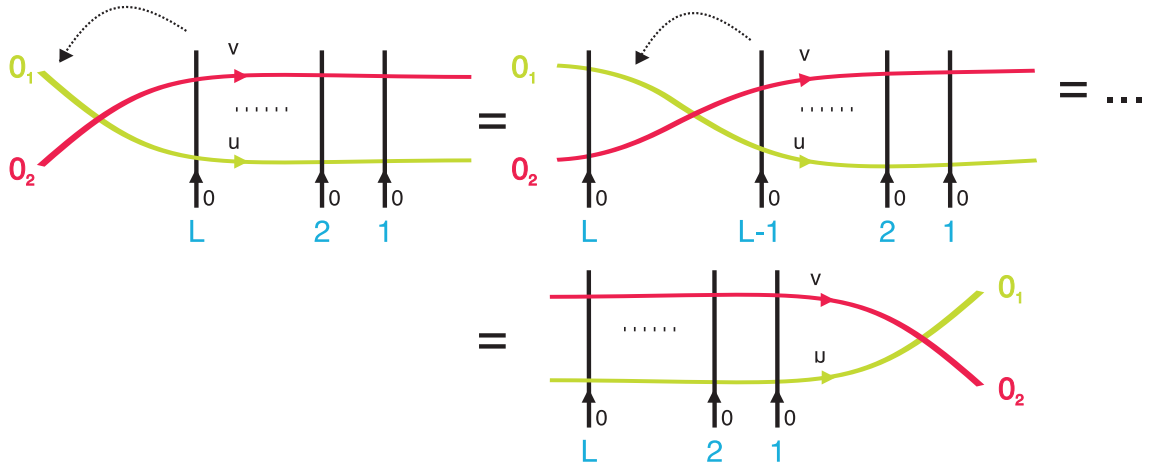


Figure 3.5: By successive application of the Yang Baxter relation we prove $R_{0_1 0_2}(u-v)\hat{L}_1(u)\hat{L}_2(v) = \hat{L}_2(v)\hat{L}_1(u)R_{0_1 0_2}(u-v)$ which trivially implies $\left[\hat{T}(u), \hat{T}(v)\right] = 0$. This commutation relation is of great importance and ensures quantum integrability of the Hamiltonians built out of the transfer matrix $\hat{T}(u)$.

which is the standard $SU(M)$ R-matrix.

So far we built a transfer matrix $\hat{T}(u)$ made out of $R$-matrices obeying the YB equation. Let us now continue our general considerations and understand why such transfer matrix is at all related with the Hamiltonians of the previous section or, more generically, to physical systems with integrable Hamiltonians. To do so we need to slightly enlarge our setup and include an extra auxiliary space. We denote the auxiliary spaces by $0_1$ and $0_2$ and add a subscript 1 or 2 to the monodromy matrix $L(u)$ to indicate which auxiliary space is being used. Then

$$R_{0_1 0_2}(u-v)\hat{L}_1(u)\hat{L}_2(v) = \hat{L}_2(v)\hat{L}_1(u)R_{0_1 0_2}(u-v)\,, \tag{3.39}$$

is a trivial consequence of the YB relation as explained in figure 3.5.

Multiplying this equation by $R^{-1}_{0_1 0_2}(u-v) = R_{0_1 0_2}(v-u)$ from the right we obtain

$$R_{0_1 0_2}(u-v)\hat{L}_1(u)\hat{L}_2(v)R_{0_1 0_2}(v-u) = \hat{L}_2(v)\hat{L}_1(u)\,, \tag{3.40}$$

so that taking the trace of this equality over both auxiliary spaces yields

$$\left[\hat{T}(u), \hat{T}(v)\right] = 0\,, \tag{3.41}$$

where we used the obvious relations

$$\mathrm{Tr}(RMR^{-1}) = \mathrm{Tr}(M)\ ,\ \ \mathrm{Tr}_{h_{0_1}\otimes h_{0_2}}(\hat{L}_1 \otimes \hat{L}_2) = \mathrm{Tr}_{h_{0_1}}(\hat{L}_1)\mathrm{Tr}_{h_{0_2}}(\hat{L}_2)\,. \tag{3.42}$$

Notice that since we take the trace over the auxiliary spaces the indices 1 and 2 can now be dropped. Obviously, for $\hat{T}(u)$ in (3.31) the choice of auxiliary space is irrelevant since we end up taking a trace over this space.

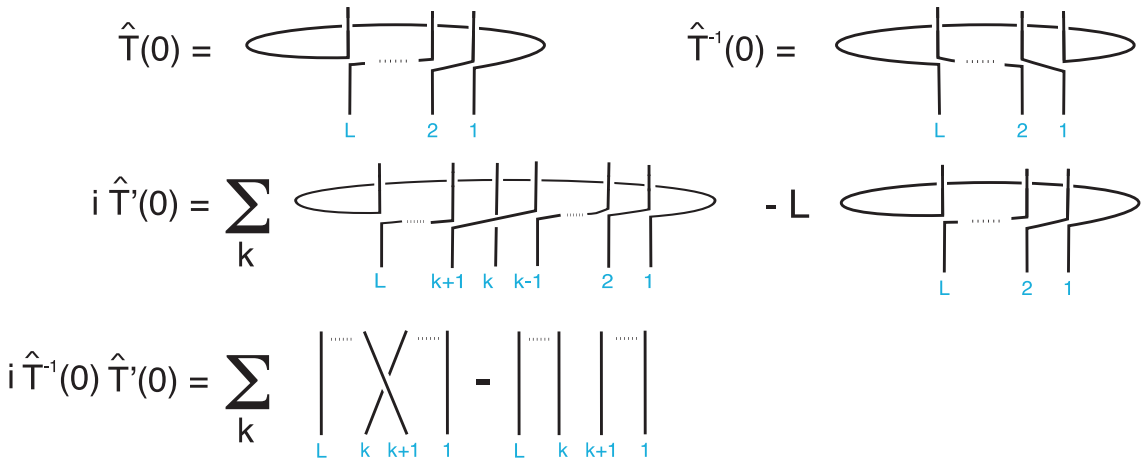


Figure 3.6: Transfer matrix and spin chain Hamiltonians.

Now, relation (3.41) tells us that the transfer matrices commute for different values of the spectral parameters which is most interesting. If we construct a spin chain Hamiltonian $H$ from the transfer matrix (usually by taking derivatives of its logarithm at a particular point $u^*$) then, by construction,

$$[H, \hat{T}(u)] = 0\,,$$

and we immediately obtain a huge number of conserved charges and hence quantum integrability!

Indeed, let us compute

$$\left(\frac{d}{du}\log\hat{T}(u)\right)_{u=0} = \hat{T}^{-1}(0)\,\hat{T}'(0) \tag{3.43}$$

At $u = 0$ the $R$-matrix (3.38) is nothing but the permutation operator and therefore

$$\hat{T}(0) = \mathrm{Tr}_0\left(P_{0L}\dots P_{01}\right) = P_{L,L-1}\dots P_{32}P_{21} \tag{3.44}$$

is the shift operator as clearly seen from figure 3.6 while

$$\hat{T}'(0) = \frac{1}{i}\sum_k \mathrm{Tr}_0\left(P_{0L}\dots\hat{P}_{0k}\dots P_{01}\right) - \frac{L}{i}\,\hat{T}(0)\,, \tag{3.45}$$

where the hatted permutation means this permutation is absent inside the trace. The first and second terms come respectively from the derivative acting on the numerator and denominator of one of the R-matrices (3.38) in the definition of the transfer matrix. As above, the first term shifts everything by one unit to the right while leaving $k$ untouched – see figure 3.6. Thus, when multiplying by $\hat{T}^{-1}(0)$ which shifts everything one unit to the left, we almost arrive to the starting configuration apart from a permutation of sites $k$ and

$k+1$. But a sum of such permutations is precisely the non-trivial part of the Hamiltonian (3.22)! Putting all the constants in the right place we conclude that the $\mathcal{N}=4$ SYM dilatation operator in the $SU(2)$ sector is described in this language as

$$H_{xxx} = 2g^2 \sum_{n=1}^{L} (1 - P_{n,n+1}) = \frac{2g^2}{i} \left( \frac{d}{du} \log \hat{T}(u) \right)_{u=0} . \tag{3.46}$$

Note that this Hamiltonian is actually slightly more general than (3.22) because here we are working in $SU(M)$ and $SU(2)$ is just a particular case.

We could repeat our analysis for $SO(M)$. The only difference would be that instead of (3.36) we would write

$$R(u) = h(u)1 + f(u)P + g(u)K \tag{3.47}$$

because for $SO(M)$ there are these three invariant tensors. Then we would impose the YB relation to fix these functions up to a normalization which we can freely chose. We would in this case find

$$R(u) \sim u1 - P + \frac{2u}{2u+2-M} K \tag{3.48}$$

and proceeding as before

$$\frac{1}{i} \left( \frac{d}{du} \log \hat{T}(u) \right)_{u=0} \sim \sum_{n=1}^{L} \left( K_{n,n+1} + \frac{M-2}{2} - \frac{M-2}{2} P_{n,n+1} \right) + \text{constant} . \tag{3.49}$$

The constant term depends on the normalization of $R(u)$ but is of course irrelevant for our discussion of integrable vs non-integrable Hamiltonians. On the other hand the relative coefficient between the trace and the permutation operators is fixed in our construction. What is absolutely remarkable and noticed by Minahan and Zarembo [9] is that the $SO(6)$ spin chain Hamiltonian (3.16) has precisely the correct relative factor for $M=6$! One dimensional integrability fits in this way in the four dimensional $\mathcal{N}=4$ super-symmetric gauge theory.

So far we explained how to construct integrable Hamiltonians and realized that those appearing in $\mathcal{N}=4$ SYM are precisely of this type. As it is, all this sounds like a mathematicians proof of the existence of the solution to the problem of computing the complete spectrum of these Hamiltonians. Of course our goal is to actually compute the spectrum. The diagonalization of these Hamiltonians will be the subject of the next section.

## 3.3 $SU(2)$ spin chain spectrum

The program of the algebraic Bethe ansatz is designed to diagonalize not only the Hamiltonian but also the transfer matrix $\hat{T}(u)$,

$$\hat{T}(u)|\Psi\rangle = T(u)|\Psi\rangle . \tag{3.50}$$

This is quite interesting because the spectrum of the Hamiltonian (3.46) is then simply obtained by taking the logarithmic derivative of this eigenvalue.

$$E_{xxx} = \frac{2g^2}{i}\left(\frac{d}{du}\log T(u)\right)_{u=0} . \tag{3.51}$$

However, we can immediately obtain the spectrum of many more Hamiltonians. For example, following the same reasoning as above, it is easy to see that

$$H_{\alpha,\beta} \equiv \left(\frac{\alpha}{i}\frac{d}{du}\log \hat{T}(u) + \frac{\beta}{2i}\frac{d^2}{du^2}\log \hat{T}(u)\right)_{u=0} = \sum_{n=1}^{L} \alpha\,(1 - P_{n,n+1}) + \beta\frac{i}{2}\,[P_{n-1,n}, P_{n,n+1}] \tag{3.52}$$

and therefore the spectrum of this Hamiltonian is trivially obtained replacing the operator $\hat{T}$ by the corresponding eigenvatue $T$,

$$E_{\alpha,\beta} = \left(\frac{\alpha}{i}\frac{d}{du}\log T(u) + \frac{\beta}{2i}\frac{d^2}{du^2}\log T(u)\right)_{u=0} . \tag{3.53}$$

By considering more and more derivatives we can obtain longer and longer ranged Hamiltonians together with their complete spectrum.

To compute $T(u)$ we will again follow a path where the physics might be a bit obscured. We will consider the symmetry group to be $SU(2)$ for simplicity.

The idea is to use the monodromy matrix $L(u)$ defined in (3.29) to build our *creation operators*. For that we recall that this object acts on $h_0 \otimes \mathcal{H}$ and thus can the thought of as being a $2 \times 2$ matrix in the auxiliary space where each entry is an operator in the full Hilbert space,

$$\hat{L}(u) \;=\; \begin{pmatrix} \hat{A}(u) & \hat{B}(u) \\ \hat{C}(u) & \hat{D}(u) \end{pmatrix} \tag{3.54}$$

Notice that with this notation

$$\hat{T}(u) = \hat{A}(u) + \hat{D}(u)\,.$$

The $R$-matrix $R_{0j}$ can also be written as a $2 \times 2$ matrix with entrances acting on $h_j$,

$$R_{0j} \;=\; \frac{1}{u+i}\begin{pmatrix} u + \frac{i}{2}\left(1+\sigma_j^z\right) & i\,\sigma_j^- \\ i\,\sigma_j^+ & u + \frac{i}{2}\left(1-\sigma_j^z\right) \end{pmatrix} \tag{3.55}$$

To obtain this expression from (3.38) we simply recall that the permutation operator can be written in terms of the Pauli matrices as

$$P = \begin{pmatrix} 1 & 0 & 0 & 0 \\ 0 & 0 & 1 & 0 \\ 0 & 1 & 0 & 0 \\ 0 & 0 & 0 & 1 \end{pmatrix} = \frac{1}{2}\left(1 + \vec{\sigma}\otimes\vec{\sigma}\right) .$$

Acting with a state with a ket $|\uparrow\rangle_j$ and a generic state in the auxiliary space we obtain

$$R_{0j}|\uparrow\rangle_j \otimes |\Phi\rangle = \begin{pmatrix} |\uparrow\rangle & \frac{i}{u+i}|\downarrow\rangle \\ 0 & \frac{u}{u+i}|\uparrow\rangle \end{pmatrix} |\Phi\rangle \tag{3.56}$$

and therefore the monodromy $\hat{L}(u)$ acts on the ferromagnetic vacuum

$$|\Omega\rangle = |\uparrow \dots \uparrow\rangle = |\uparrow\rangle_L \otimes \cdots \otimes |\uparrow\rangle_1 \tag{3.57}$$

as

$$\hat{L}(u)|\Omega\rangle \otimes |\Phi\rangle = \begin{pmatrix} |\uparrow\rangle_L & \frac{i}{u+i}|\downarrow\rangle_L \\ 0 & \frac{u}{u+i}|\uparrow\rangle_L \end{pmatrix} \otimes \cdots \otimes \begin{pmatrix} |\uparrow\rangle_1 & \frac{i}{u+i}|\downarrow\rangle_1 \\ 0 & \frac{u}{u+i}|\uparrow\rangle_1 \end{pmatrix} |\Phi\rangle \tag{3.58}$$

$$= \begin{pmatrix} |\Omega\rangle & |\text{non trivial}\rangle \\ 0 & \left(\frac{u}{u+i}\right)^L |\Omega\rangle \end{pmatrix} |\Phi\rangle \tag{3.59}$$

where the triangular nature of the matrix result (3.56) was crucial. Here $|\text{non trivial}\rangle$ represents some complicated (entangled) state whose explicit expression is not important. From this expression we read

$$\hat{A}(u)|\Omega\rangle = |\Omega\rangle \ , \ \hat{D}(u)|\Omega\rangle = \left(\frac{u}{u+i}\right)^L |\Omega\rangle \ , \ \hat{C}(u)|\Omega\rangle = 0 \ , \ \hat{B}(u)|\Omega\rangle = |\text{non trivial}\rangle \tag{3.60}$$

So in particular we found the action of $\hat{T}(u)$ on the ferromagnetic vacuum. The idea is now to use the $\hat{B}(u)$ operators as creation operators acting on this non-trivial vacuum. That is we propose the ansatz

$$|\Psi\rangle = \hat{B}(u_1) \dots \hat{B}(u_M)|\Omega\rangle \, . \tag{3.61}$$

Since we already know how $\hat{A}(u)$ and $\hat{D}(u)$ act on the vacuum, we only need to understand how they pass through the $\hat{B}(u_j)$ operators. To compute the algebra of the $\hat{A}, \hat{B}, \hat{C}, \hat{D}$ operators we simply need to evaluate (3.39). Recall that in this equation we have introduced two isomorphic auxiliary spaces $0_1$ and $0_2$ so that instead of (3.54)

$$\hat{L}(u) = \hat{A}(u) \otimes |\uparrow\rangle\langle\uparrow| + \hat{B}(u) \otimes |\uparrow\rangle\langle\downarrow| + \hat{C}(u) \otimes |\downarrow\rangle\langle\uparrow| + \hat{D}(u) \otimes |\downarrow\rangle\langle\downarrow|$$

we have two equivalent transfer matrices

$$\hat{L}_1(u) = \hat{A}(u) \otimes |\uparrow\rangle\langle\uparrow| \otimes 1 + \hat{B}(u) \otimes |\uparrow\rangle\langle\downarrow| \otimes 1 + \hat{C}(u) \otimes |\downarrow\rangle\langle\uparrow| \otimes 1 + \hat{D}(u) \otimes |\downarrow\rangle\langle\downarrow| \otimes 1$$
$$\hat{L}_2(v) = \hat{A}(v) \otimes 1 \otimes |\uparrow\rangle\langle\uparrow| + \hat{B}(v) \otimes 1 \otimes |\uparrow\rangle\langle\downarrow| + \hat{C}(v) \otimes 1 \otimes |\downarrow\rangle\langle\uparrow| + \hat{D}(v) \otimes 1 \otimes |\downarrow\rangle\langle\downarrow|$$

which can be written as $4 \times 4$ matrices with operators as entrances

$$\hat{L}_1(u) = \begin{pmatrix} \hat{A}(u) & \hat{B}(u) & 0 & 0 \\ \hat{C}(u) & \hat{D}(u) & 0 & 0 \\ 0 & 0 & \hat{A}(u) & \hat{B}(u) \\ 0 & 0 & \hat{C}(u) & \hat{D}(u) \end{pmatrix} , \; \hat{L}_2(v) = \begin{pmatrix} \hat{A}(v) & 0 & \hat{B}(v) & 0 \\ 0 & \hat{A}(v) & 0 & \hat{B}(v) \\ \hat{C}(v) & 0 & \hat{D}(v) & 0 \\ 0 & \hat{C}(v) & 0 & \hat{D}(v) \end{pmatrix} \quad (3.62)$$

The $R$-matrix appearing in (3.39) can also be explicitly written as a $4 \times 4$ matrix

$$R_{0_1 0_2}(u) = \frac{1}{u+i} \begin{pmatrix} u+i & 0 & 0 & 0 \\ 0 & u & i & 0 \\ 0 & i & u & 0 \\ 0 & 0 & 0 & u+i \end{pmatrix} \quad (3.63)$$

where of course each entry is a simple number and not an operator. Now we simply need to multiply these three matrices as in (3.39) and compare the sixteen entrances in the left and right hand sides to obtain the algebra of the monodromy matrix elements. We will only require the following relations among all those:

$$\hat{A}(u)\hat{B}(v) = \frac{u-v-i}{u-v}\hat{B}(v)\hat{A}(u) + \frac{i}{u-v}\hat{B}(u)\hat{A}(v) \quad (3.64)$$

$$\hat{D}(u)\hat{B}(v) = \frac{u-v+i}{u-v}\hat{B}(v)\hat{D}(u) - \frac{i}{u-v}\hat{B}(u)\hat{D}(v) \quad (3.65)$$

$$\hat{B}(u)\hat{B}(v) = \hat{B}(v)\hat{B}(u) \quad (3.66)$$

Thus when we act with $\hat{A}(u)$ on our ansatz (3.61) and consecutively use (3.64) this operator will arrive at the vacuum either with the same argument $u$ or with the argument of one of the parameters $u_j$ of the original $\hat{B}(u)$. That is

$$\hat{A}(u)|\Psi\rangle = A(u)|\Psi\rangle + \sum_{k=1}^{M} \alpha_k \hat{B}(u)\hat{B}(u_1)\dots\hat{B}(u_{k-1})\hat{B}(u_{k+1})\dots\hat{B}(u_M)|\Omega\rangle \quad (3.67)$$

To compute $A(u)$ is a trivial task. Namely it comes from always using the first term in (3.64) when passing through each of the $M$ $\hat{B}$'s and by then hitting the vacuum with $\hat{A}(u)$ using (3.60) so

$$A(u) = \prod_{j=1}^{M} \frac{u-u_j-i}{u-u_j} . \quad (3.68)$$

It is also trivial to find $\alpha_k$ by the following argument. We need to understand which terms in (3.64) were used when $\hat{A}(u)$ jumps through the $\hat{B}$ operators until it meets the vacuum. To find the coefficient $\alpha_k$ we first arrange all the $\hat{B}$'s in the product (3.61) so that the leftmost creation operator is $\hat{B}(u_k)$. We can clearly do so because the $\hat{B}$'s commute

between themselves. Then, since we want $\hat{A}(u)$ to exchange arguments with this first $\hat{B}(u_k)$ it is clear that in the first jump we use the second term in (3.64),

$$\hat{A}(u)\hat{B}(u_k)\prod_{j\neq k}\hat{B}(u_j)|\Omega\rangle = \frac{i}{u-u_k}\hat{B}(u)\hat{A}(u_k)\prod_{j\neq k}\hat{B}(u_j)|\Omega\rangle + \dots \tag{3.69}$$

but now we no longer want to swap arguments because we are already in the form (3.67)! Therefore we will continue to move $\hat{A}(u)$ until it hits $|\Omega\rangle$ using the first term in (3.64) in each step. Thus we find

$$\alpha_k = \frac{i}{u-u_k}\prod_{j\neq k}^{M}\frac{u_k-u_j-i}{u_k-u_j}\,. \tag{3.70}$$

In the same way we obtain

$$\hat{D}(u)|\Psi\rangle = D(u)|\Psi\rangle + \sum_{k=1}^{M}\delta_k\hat{B}(u)\hat{B}(u_1)\dots\hat{B}(u_{k-1})\hat{B}(u_{k+1})\dots\hat{B}(u_M)|\Omega\rangle \tag{3.71}$$

where

$$D(u) = \prod_{j=1}^{M}\frac{u-u_j+i}{u-u_j}\left(\frac{u}{u+i}\right)^L\,. \tag{3.72}$$

and

$$\delta_k = -\frac{i}{u-u_k}\prod_{j\neq k}^{M}\frac{u_k-u_j+i}{u_k-u_j}\left(\frac{u_k}{u_k+i}\right)^L\,. \tag{3.73}$$

We see that if we properly fix the Bethe roots $u_j$ it is possible to cancel the second term in (3.67) with the second term in (3.71) thus leaving us with a correct eigenvalue equation! More precisely, let us shift $u_j \to u_j - i/2$ so that our wave function reads

$$|\Psi\rangle = \hat{B}(u_1-i/2)\dots\hat{B}(u_M-i/2)|\Omega\rangle\,. \tag{3.74}$$

Then we found that

$$\hat{T}(u)|\Psi\rangle = T(u)|\Psi\rangle\,, \tag{3.75}$$

where $T(u)=A(u)+D(u)$ is given by

$$T(u) = \prod_{j=1}^{M}\frac{u-u_j-i/2}{u-u_j+i/2} + \left(\frac{u}{u+i}\right)^L\prod_{j=1}^{M}\frac{u-u_j+3i/2}{u-u_j+i/2}\,, \tag{3.76}$$

if we cancel $\alpha_k$ and $\delta_k$ which amounts to quantizing the Bethe roots $u_k$ according to the so called Bethe equations

$$\left(\frac{u_k+i/2}{u_k-i/2}\right)^L = \prod_{j\neq k}^{M}\frac{u_k-u_j+i}{u_k-u_j-i}\,. \tag{3.77}$$

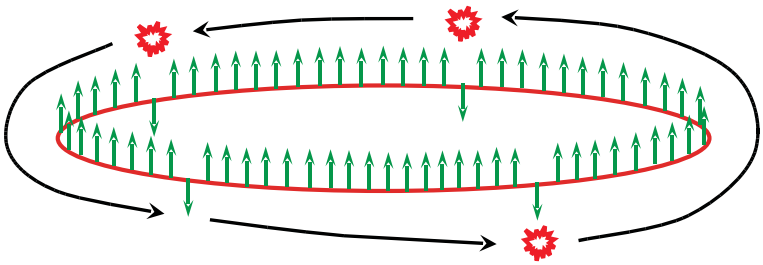

Figure 3.7: The Bethe ansatz equation quantized the momenta of the excitations by imposing that the phase $p_k L$ due to the free propagation plus the phase shifts due to the scattering with each of the other magnons is a multiple of $2\pi$.

This is the main result of this section.

In practice there is a shortcut to arrive at this result. We simply compute the eigenvalue $T(u) = A(u) + D(u)$ using the first terms in (3.64) and (3.65) to find (3.76). We know that the other terms in the algebra (3.64) and (3.65) will give something which will not be proportional to the original vector and which we will therefore want to cancel. We know that the cancelation of these terms will constrain the positions of the Bethe roots via some Bethe equations. To find these equations we make the following observation: Since the transfer matrix is obtained from the trace of a product of operators like (3.38) it can never have poles at $u = u_i$ but (3.76) seems to have such poles! The only way out is if the Bethe roots are such that the residues of the poles in (3.76) vanish. This condition yields precisely Bethe equations.

A remark: Notice that this reasoning also explains why we can not have coincident Bethe roots. If we set $u_1 = u_2$ then we still have $M$ conditions on the Bethe roots (from $M-2$ simple poles and 1 double pole) while having only $M-1$ positions $u_2, \ldots, u_M$ to fix.

It is easy to see from the $v \to \infty$ limit of (3.39) that $\left[\sum_j \sigma_j^z, \hat{B}(u)\right] = B(u)$ and therefore our ansatz corresponds to a state with $M$ spin flips in a ferromagnetic vacuum. Equation (3.77) has then a simple physical picture behind it. If we define

$$e^{ip} = \frac{u + i/2}{u - i/2} \quad , \quad u = \frac{1}{2}\cot\frac{p}{2} \tag{3.78}$$

then this equation can be written as

$$e^{ip_k L} \prod_{j \neq k}^{M} S(p_k, p_j) = 1 \,. \tag{3.79}$$

Thus, state (3.74) should be pictured as a collection of $M$ spin down excitations – called magnons – moving with momenta $p_k$ in the spin chain and scattering between themselves

as represented in figure 3.7. More precisely the Bethe equations tell us that if we pick one particle and carry it around the spin chain, the phase $p_k L$ due to the free propagation plus the phase shifts due to the scattering with each of the other magnons must give a trivial net result. From this description we clearly see the manifestation of integrability as factorized scattering. The fact that the scattering of one magnon with all the other magnons is given by a simple sequence of two-to-two scattering processes is not at all generic. In the next section we will explore this more physical approach to quantum integrability using the coordinate Bethe ansatz formalism.

Having quantized the momenta $\{p_k\}$ or alternatively the Bethe roots $\{u_k\}$ we compute the spectrum from (3.51) which yields

$$E_{xxx} = \sum_{j=1}^{M} \frac{2g^2}{u_j^2 + 1/4} \tag{3.80}$$

which is of the form $E_{xxx} = \sum_{j=1}^{M} \epsilon(p_j)$ with

$$\epsilon(p) = 8g^2 \sin^2 \frac{p}{2} \tag{3.81}$$

being the dispersion relation for each individual magnon. As mentioned in the beginning of this section one of the main advantages of the algebraic Bethe ansatz approach is that we can at once diagonalize large families of integrable Hamiltonians. For example, to find the spectrum of (3.52) we simply need to solve the *same* BAE (3.77) and then evaluate (3.53) using (3.76) to find

$$E_{\alpha,\beta} = \sum_{j=1}^{M} \frac{\alpha}{u_j^2 + \frac{1}{4}} + \frac{\beta}{\left(u_j^2 + \frac{1}{4}\right)^2}\,, \tag{3.82}$$

that is $E_{\alpha,\beta} = \sum_{j=1}^{M} \epsilon(p_j)$ with

$$\epsilon(p) = 4 \sin^2 \frac{p}{2} \left(\alpha + \beta \sin p\right)\,. \tag{3.83}$$

## 3.4 Quantum integrability and factorizable scattering

In $1+1$ dimensions, when two particles of equal mass scatter, momenta and energy conservation imply that the final set of individual momenta is equal to the original set,

$$\{p_1', p_2'\} = \{p_1, p_2\} \tag{3.84}$$

When we consider three or more particles the final set of momenta is in general *not* a simple rearrangement of the original one. On the other hand for systems with many conserved

charges this can be the case. For example, if we consider the scattering of three particles in a theory where not only the momenta and energy,

$$Q_1 = \sum_j p_j \ , \ Q_2 = \sum_j p_j^2 \, , \tag{3.85}$$

are conserved but where there is also an extra charge

$$Q_3 = \sum_j p_j^3 \, , \tag{3.86}$$

then the conservation of these three charges *does* imply that the final set of momenta is equal to the original set,

$$\{p_1', p_2', p_3'\} = \{p_1, p_2, p_3\} \, . \tag{3.87}$$

In the same way, the existence of $N$ relatively generic independent charges $Q_j$ would imply that the effect of a multiple particle scattering with original momenta $\{p_j\}$ would be to simply rearrange the individual momenta between the several particles. In this kind of theories, if we prepare the in-coming particles and collect them after the collision we would conclude that, since the momenta were simply interchanged, the scattering was *effectively* factorized into a sequence of many pairwise scattering processes.

Notice also that there is no solution to

$$p_1^n + p_2^n + p_3^n = {p'}_1^n + {p'}_2^n \ , \ \ n = 1, 2, 3 \, . \tag{3.88}$$

In integrable theories there is no particle creation or annihilation.

Let us review an argument due to Shankar and Witten [37] where factorizability is very clearly related to the existence of higher charges. Suppose we consider a superposition of plane waves

$$\psi(x,t) = e^{ip(x-x_0)+ip^2(t-t_0)} \tag{3.89}$$

into a wave packet of well definite momenta $p \simeq p_0$,

$$\Psi(x,t) = \int dp e^{-\alpha(p-p_0)^2} e^{ip(x-x_0)-i\frac{p^2}{2}(t-t_0)} \tag{3.90}$$

This wave packet is localized where the phase is stationary for $p \simeq p_0$ that is

$$x = x_0 + p_0(t-t_0) \, . \tag{3.91}$$

Now suppose the theory admits higher charges of the type mentioned above. If we act on this wave packet with a charge $e^{i\beta Q_n} = e^{i\beta p^n}$ we get

$$e^{i\beta Q_n} \, \Psi(x,t) = \int dp e^{-\alpha(p-p_0)^2} e^{ip(x-x_0)-i\frac{p^2}{2}(t-t_0)+i\beta p^n} \tag{3.92}$$

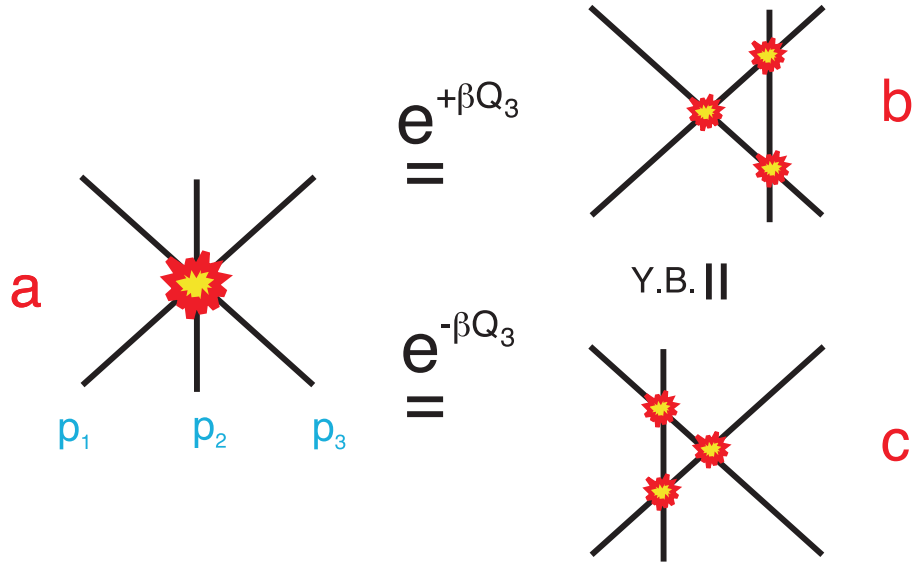


Figure 3.8: The action of Higher charges shifts each wave packet by a momentum dependent amount. This it implies factorized scattering and the Yang-Baxter relation $\hat{S}_{12}\hat{S}_{13}\hat{S}_{23} = \hat{S}_{23}\hat{S}_{13}\hat{S}_{12}$t.

and therefore the stationary phase condition telling us where the wave function is localized becomes now

$$x = x_0 + p_0(t - t_0) + \beta\, n\, p_0^{n-1}\,. \tag{3.93}$$

Now suppose we prepare three wave packets like (3.90) in such a way that they will scatter almost simultaneously in the future as in figure 3.8a. The probability amplitude for this process is the same as the probability amplitude for the process related to this one by application of the symmetry generated by any of the charges $Q_n$ – after all this is the definition of symmetry.

A symmetry transformation generated by the momenta or the energy corresponds to putting $n = 1, 2$ in (3.93). This simply means that we simply effectuate a global translation in space or time respectively.

Things are much more interesting for $n \geq 3$. When $n \geq 3$ each wave packet is shifted by an amount which depends on its momentum and thus the process in figure 3.8a can be transformed into that in figure 3.8b with the three wave packets scattering in a sequence of arbitrarily separated pairwise collisions. This shows that the existence of higher charges implies factorized scattering.

Furthermore since we could apply a symmetry transformation with a positive or negative deformation parameter $\beta$ we find out that not only the three-to-three scattering factorizes into a sequence of three chronologically ordered two-to-two scattering events but

also the order of these evens can be interchanged by applying the symmetry transformation generated by the higher charges as represented in figure 3.8c. Mathematically this means that for integrable theories

$$\hat{S}_{12}(p_1,p_2)\hat{S}_{13}(p_1,p_3)\hat{S}_{23}(p_2,p_3) = \hat{S}_{23}(p_2,p_3)\hat{S}_{13}(p_1,p_3)\hat{S}_{12}(p_1,p_2)\,. \tag{3.94}$$

If the S-matrix is a simple phase shift like in our previous example then of course this equation is empty. This is the case when we consider theories with a single type of particles without any internal degrees of freedom. On the other hand, in general particles have polarizations and/or spins which can change in a scattering process. In other words the S-matrices appearing in (3.94) are matrices. When this is the case equation (3.94) provides strong constraints on the form of the $S$-matrix.

The spectrum of integrable theories put in a large circle of perimeter $\mathcal{L}$ can easily be found. Let us consider particles without internal structure first. Since there is no particle creation we can consider a wave function with a precise number of particles. For simplicity let us consider three particles, the generalization will be obvious. Since the circle is large there is a region where $x_1 \ll x_2 \ll x_3$ which we denote by asymptotic region. In this region the wave function will be

$$\psi(x_1,x_2,x_3) \simeq \phi_{123} + \phi_{213}\,S_{12} + \phi_{132}\,S_{23} + \phi_{312}\,S_{13}\,S_{23} + \phi_{231}\,S_{13}\,S_{12} + \phi_{321}\,S_{23}\,S_{13}\,S_{12}\,, \tag{3.95}$$

where $S_{ij} \equiv S(p_i,p_j)$ and

$$\phi_{ijk} \equiv \exp\left(ip_ix_1 + ip_jx_2 + ip_kx_3\right)\,.$$

We are assuming the particles to be bosons so that the wave function in the other asymptotic regions such as $x_2 \ll x_1 \ll x_3$ can be trivially obtained from (3.95) from

$$\psi(x_1,x_2,x_3) = \psi(x_2,x_1,x_3)\,.$$

Obviously, when writing (3.95) we already used the factorizability property to decompose some three body S-matrices into products of two-to-two scattering processes.

Next we pick a particle and carry it around the circle. More rigorously, we impose the periodicity of the wave function

$$\psi(x_1+\mathcal{L},x_2,x_3) \;=\; \psi(x_1,x_2,x_3)$$

or, using the bosonic symmetry of the wave function,

$$\psi(x_2,x_3,x_1+\mathcal{L}) \;=\; \psi(x_1,x_2,x_3) \tag{3.96}$$

The advantage of this second expression is that the arguments are ordered so that we can use the wave function in (3.95). When comparing the several exponentials we find that this condition implies the quantization conditions

$$e^{ip_j\mathcal{L}} = \prod_{k\neq j}^{M} S(p_j, p_k) \tag{3.97}$$

with $M = 3$. Physically these equations translates the fact that the free phase acquired by a particle when carried around the ring plus the phase shifts due to the scattering with each of the other particles must be a trivial multiple of $2\pi$.

Having quantized the momenta of every individual particle by solving the Bethe equations we compute the spectrum of the theory from

$$E = \sum_{j=1}^{M} \epsilon(p_j) \tag{3.98}$$

where $\epsilon(p)$ is the dispersion relation.

Notice that in all this discussion it was crucial to have enough space for an asymptotic region to exist. Such asymptotic region was used in (3.96) to obtain Bethe equations. It was also implicitly used in (3.98) where we used the fact that there is a region where the wave function is given by a superposition of $M$ plane waves with precise individual momenta used to measure the energy of the state.

So far we studied Bethe equations of the form (3.97) which appear for example in the study of spin chains with $SU(2)$ symmetry. In this model the particles are down spins and hence have no internal structure. For the $SO(6)$ spin chain which we already described it is clear that we will have to find something more sophisticated.

In general, when particles transform under some nontrivial symmetry group with rank $r$ we must solve the diagonalization problem

$$|\psi\rangle = e^{iLp_k} \overleftarrow{\prod_{j=1}^{k-1}} \hat{S}\left(p_k, p_j\right) \overrightarrow{\prod_{j=M}^{k+1}} \hat{S}\left(p_k, p_j\right) |\psi\rangle \tag{3.99}$$

where $\hat{S}(p_k, p_j)$ is now a matrix and $|\psi\rangle$ is the multi-particle wave function. We will in general obtain not just one equation like (3.97) but rather a set of $r+1$ equations entangling the scattering of particles with momenta $p_k$ and $p_j$ in space-time with the scattering of spin waves in the isotopic space. These so called Nested Bethe ansatz equations will be of key importance throughout this monograph. In the next section they will appear for the first time in the study of the $SO(4)$ sigma model, an extremely instructive toy model for what follows.

Notice the striking mathematical similarity between equations (3.94) and (3.4). Thus often $S$-matrices and $R$-matrices will have exactly the same form (apart from normalizations). Obviously their physical meaning is completely different – $S$-matrices describe scattering of particles whereas $R$-matrices are used to construct integrable spin chain Hamiltonians (or integrable 2d statistical models).

## 3.5 Coordinate Bethe ansatz and higher loops.

In this section we will introduce the notion of perturbative integrability or more precisely perturbative asymptotic Bethe ansatz [38] and recognize the appearance of integrability in $\mathcal{N} = 4$ SYM from the factorized scattering perspective described in the previous section. For that purpose we will first review the coordinate Bethe ansatz description of integrable systems.

Let us consider again the diagonalization of the Heisenberg Hamiltonian

$$H_{xxx} = \sum_{n=1}^{L} 1 - P_{n,n+1} \tag{3.100}$$

and construct single, double and triple spin flip excitations moving on the ferromagnetic vacuum. To construct the single spin flip excitation, called magnon, we construct a plane

$$|k\rangle = \sum_{n=1}^{L} \psi(n)|n\rangle \ , \ \psi(n) = e^{ikn} \tag{3.101}$$

where $|n\rangle = \sigma_n^-|\uparrow \dots \uparrow\rangle$ is the state with all spins pointing up except for that in site $n$. Acting with the Hamiltonian on this state we find

$$H_{xxx}|k\rangle = \epsilon(k)|k\rangle \tag{3.102}$$

where

$$\epsilon(k) = 2 - 2\cos(k) = 4\sin^2\frac{k}{2} \tag{3.103}$$

which, apart from the normalization factor of $2g^2$ is precisely what we found in (3.81) from our general treatment in the algebraic Bethe ansatz formalism. Periodicity of the wave function quantizes $k = \frac{2\pi n}{L}$.

Next let us consider two excitations. This is of course more interesting because now the two magnons might scatter between themselves. Acting on the state

$$|\psi\rangle = \sum_{n<m} \psi(n,m)|n,m\rangle \ \ , \ \ |n,m\rangle = \sigma_n^-\sigma_m^-|\uparrow \dots \uparrow\rangle \tag{3.104}$$

with the Heisenberg Hamiltonian and imposing $\left(\hat{H}_{xxx} - E\right)|\psi\rangle = 0$ yields

$$E\,\psi(n,m) = 4\psi(n,m) - \psi(n+1,m) - \psi(n-1,m) - \psi(n,m+1) - \psi(n,m-1) \quad (3.105)$$

for $m > n+1$ and

$$E\,\psi(n,n+1) = 2\psi(n,n+1) - \psi(n-1,n+1) - \psi(n,n+2) \quad (3.106)$$

when the spin flips meet. Any superposition of plane waves

$$\psi(n,m) = e^{ikn+ipm} + S(k,p)e^{ipn+ikm} \quad (3.107)$$

solves the first equation describing the free propagation and gives

$$E = \epsilon(k) + \epsilon(p) \quad (3.108)$$

while the second condition governs the scattering between the magnons and fixes

$$S(p,k) = \frac{\frac{1}{2}\cot\frac{k}{2} - \frac{1}{2}\cot\frac{p}{2} - i}{\frac{1}{2}\cot\frac{k}{2} - \frac{1}{2}\cot\frac{p}{2} + i} \quad (3.109)$$

Periodicity of the wave function $\psi(n,m) = \psi(m,n+L)$ now yields

$$e^{ikL}S(p,k) = e^{ipL}S(k,p) = 1 \quad (3.110)$$

which under the transformation (3.78) reduce precisely to the Bethe equations (3.77) for $M=2$ found previously. Let us then consider three particle states where, as mentioned in the previous section, integrability can play a key role. Indeed, it is trivial to check (specially with Mathematica) that

$$|\psi\rangle = \sum_{n_1<n_2<n_2} \psi(n_1,n_2,n_3)|n_1,n_2,n_3\rangle\,,$$

with

$$\psi(n_1,n_2,n_3) = \phi_{123} + \phi_{213}\,S_{12} + \phi_{132}\,S_{23} + \phi_{312}\,S_{13}\,S_{23} + \phi_{231}\,S_{13}\,S_{12} + \phi_{321}\,S_{23}\,S_{13}\,S_{12}\,, \quad (3.111)$$

$S_{ij} \equiv S(p_i,p_j)$ and

$$\phi_{ijk} \equiv \exp\left(ik_in_1 + ik_jn_2 + ik_kn_3\right)\,, \quad (3.112)$$

is an eigenstate of $H_{xxx}$ with energy

$$E = \sum_{k=1}^{3} \epsilon(p_j)\,. \quad (3.113)$$

Periodicity of the wave function $\psi(n_1, n_2, n_3) = \psi(n_2, n_3, n_1 + L)$ then yields the Bethe equations (3.77),

$$e^{ip_j L} \prod_{k \neq j}^{3} S_{jk} = 1 \,,$$

Of course the fact that the ansatz worked is nontrivial but not surprising as we already solved this model explicitly by the algebraic Bethe ansatz.

The wave functions for many magnon states are obtained following the obvious pattern in (3.111). This ansatz for the wave function is of course far from obvious and was the key observation of Bethe in 1931 to realize it would work [39]. As we saw in the previous section such ansatz will generically work if there are a lot of extra conserved charges which is of course a priori not obvious when we look at a given Hamiltonian.

Let us now consider an $SU(2)$ Hamiltonian with also next to nearest neighbors local interactions. The most general ansatz for such Hamiltonian with zero energy for the ferromagnetic state is of the form

$$H_{\alpha,\beta,\gamma} = \alpha \sum_{n=1}^{L} (1 - P_{n,n+1}) + \beta \sum_{n=1}^{L} \frac{i}{2} \left[P_{n,n+1}, P_{n+1,n+2}\right] + \gamma \sum_{n=1}^{L} (1 - P_{n,n+2}) \,. \tag{3.114}$$

If $\gamma = 0$ we obtain an Hamiltonian which we already encountered in our algebraic Bethe ansatz treatment (3.52). In the algebraic Bethe ansatz approach we diagonalized the $SU(2)$ transfer matrix $\hat{T}(u)$. Since $\left[\hat{T}(u), \hat{T}(v)\right] = 0$, the eigenvector basis is independent of the spectral parameter $u$. The first and second terms in (3.114) are the first and second derivative of the logarithm of the transfer matrix at $u = 0$, see (3.52). Thus each of them – and therefore their sum – is diagonalized by the same set of eigenvectors which is of course not obvious at all from the coordinate Bethe ansatz perspective. For example, the ansatz (3.111) still diagonalizes $\hat{H}_{\alpha,\beta,0}$ with exactly the same $\alpha$ and $\beta$ independent $S$-matrix (3.109). Therefore the Bethe equations quantizing the magnon momenta are precisely the same since they follow from imposing periodicity for the wave function. The spectrum, on the other hand is trivially changed by the replacement of the dispersion relation by (3.83) which can be read from the single magnon wave function as before.

In the next subsection we will consider the last term to be present, $\gamma \neq 0$ and find out that there is a right structure to be studied in this case.

### 3.5.1 Two magnons in non-integrable models.

Let us now consider $\gamma \neq 0$ in (3.114). For simplicity we take $\beta = 0$ and, for the moment, we consider an infinite spin chain. Single particle states (3.101) are eigenstates with energy $E = \epsilon(k)$ where

$$\epsilon(p) = 4 \sin^2 \frac{p}{2} \left(\alpha + 4\gamma \cos^2 \frac{p}{2}\right) \,. \tag{3.115}$$


Figure 3.9: In a non integrable spin chain Hamiltonian the total energy and momenta conservation is not enough to ensure that the individual incoming momenta are simply interchanged. For example, in the model we consider we can create a pair of particles with the same total energy and momenta but different individual momenta as depicted by the red arrows. The wave function is then given by $\psi(n,m) = e^{ik_1 n + ik_2 m} + B e^{ik_2 n + ik_1 m} + D e^{ik_4 n + ik_3 m}$.

Two magnon states with wave function (3.107) are not eigenstates and therefore we must find a better ansatz for $\psi(n,m)$. For $m-n>2$ the free propagation equation (3.105) is simply replaced by the homogeneous equation

$$\begin{aligned}(E-4\alpha-4\gamma)\ \psi(n,m) = &-\alpha\left(\psi(n+1,m)+\psi(n-1,m)+\psi(n,m+1)+\psi(n,m-1)\right)\\ &-\gamma\left(\psi(n+2,m)+\psi(n-2,m)+\psi(n,m+2)+\psi(n,m-2)\right)\end{aligned} \tag{3.116}$$

The solution to this equation for fixed total momentum $P$ and energy $E$ is given by

$$\psi(n,m) = e^{iP\frac{n+m}{2}}\left(A\, e^{i\kappa\frac{n-m}{2}} + B\, e^{-i\kappa\frac{n-m}{2}} + C\, e^{i\kappa'\frac{n-m}{2}} + D\, e^{-i\kappa'\frac{n-m}{2}}\right) \tag{3.117}$$

where $k_{1,2} = \frac{1}{2}\left(P \pm \kappa\right)$ and $k_{3,4} = \frac{1}{2}\left(P \pm \kappa'\right)$ are the *four* solutions to

$$\epsilon(k_1)+\epsilon(k_2) = E \ \ , \ \ k_1+k_2 = P\,, \tag{3.118}$$

$$\epsilon(k_3)+\epsilon(k_4) = E \ \ , \ \ k_3+k_4 = P\,. \tag{3.119}$$

In particular we can easily see that

$$\cos\left(\frac{\kappa}{2}\right)+\cos\left(\frac{\kappa'}{2}\right) = -\frac{\alpha\cos\left(\frac{P}{2}\right)}{2\gamma\cos(P)}\,. \tag{3.120}$$

Notice that while before we could find an eigenstate with only $A, B \neq 0$ we now need to consider this more generic ansatz. Luckily this ansatz works not only for $m > n+2$ but also for $m = n+2$ and $m = n+1$. For these spin flip separations the Schrodinger equation gives

$$\begin{aligned}(E-2\gamma-4\alpha)\psi(n,n+2) = &\ \gamma\left(\psi(n-2,n+2)+\psi(n,n+4)\right)\\ &-\alpha\left(\psi(n+1,n+2)+\psi(n-1,n+2)+\psi(n,n+3)+\psi(n,n+1)\right)\end{aligned} \tag{3.121}$$

and

$$\begin{aligned}(E-2\alpha-4\gamma)\ \psi(n,n+1) = &-\alpha\left(\psi(n-1,n+1)+\psi(n,n+2)\right)\\ &-\gamma\left(\psi(n,n+3)+\psi(n-1,n)+\psi(n+1,n+2)+\psi(n-2,n+1)\right)\end{aligned} \tag{3.122}$$

which constrains the several coefficients of the wave function. Since the free propagation equation is solved by (3.117) for any $n$ and $m$ we can substract it for $m = n + 2$ and $m = n + 1$ from (3.121) and (3.122) to simplify these equations to

$$0 = 2\psi(n, n+2) - \psi(n+2, n+2) - \psi(n, n) \tag{3.123}$$

and

$$\begin{aligned} 0 &= \alpha\left(2\psi(n, n+1) - \psi(n+1, n+1) - \psi(n, n)\right) \\ &- \gamma\left(\psi(n+2, n+1) - \psi(n+1, n+2) + \psi(n, n-1) - \psi(n-1, n)\right) \end{aligned} \tag{3.124}$$

Physically what is happening depends on the reality of the relative momenta $\kappa$ and $\kappa'$.

If both have a positive imaginary part then we are describing a superposition of two bound states. In this case we must impose $B = D = 0$. Conditions (3.123) and (3.124) then describe a homogenous linear system for $A$ and $C$ whose characteristic determinant must vanish to be able to have $A, C \neq 0$. Thus for a fixed total momenta $P$ this characteristic equation plus (3.120) fixes completely $\kappa(P)$ and $\kappa'(P)$. This is probably the scenario which is most studied in the literature [40, 41] but it is the least interesting for our discussion.

Next, consider $\kappa$ and $\kappa'$ real. For a given total energy and momenta $A$ and $C$ are not fixed. There are therefore two natural choices for the wave function: $A = 0$ or $C = 0$. Let $C = 0$ and $A = 1$. Then the wave function is describing the scattering of two magnons with momenta $k_1$ and $k_2$ with normalized incoming flux. Upon collision, we obtain a reflected state with momenta $k_2$ and $k_1$ *plus* two magnons with momenta $k_3$ and $k_4$ with the same total energy and momenta as the original scattered magnons but with individual momenta which are *not* a permutation of the original ones. The reflection and creation coefficients associated to these processes are $B$ and $D$ as depicted in figure 3.9. They can easily be computed from (3.123) and (3.124).

There is a third scenario – which will actually be the most relevant for our discussion of the $\mathcal{N} = 4$ spin chain – where we have a coexistence of two real momenta $k_1$ and $k_2$ and a magnon bound state made out of $k_3$ and $k_4$. We will come back to it latter.

We will not consider the three magnon state for general $\alpha$ and $\gamma$ since this would be an ultra tedious and absolutely not enlightening exercise. The model is not integrable and therefore factorization does not hold and Bethe ansatz techniques can *not* be directly applied.

### 3.5.2 Perturbative integrability and higher orders in $SU(2)$

At the light of what we have just seen, it might seem like terrible news the fact that the dilatation operator for the $SU(2)$ sector in $\mathcal{N} = 4$ supersymmetric Yang-Mills theory is

precisely of the form of this non-integrable Hamiltonian! Namely it corresponds to [42]

$$\alpha = \left(\frac{g_{YM}^2 N}{8\pi^2}\right) - 4\left(\frac{g_{YM}^2 N}{8\pi^2}\right)^2 \quad , \quad \gamma = \left(\frac{g_{YM}^2 N}{8\pi^2}\right)^2 . \tag{3.125}$$

Notice that for finite $g_{YM}^2 N$ even the ground state might be quite nontrivial because the ferromagnetic nature of the chain can change to anti-ferromagnetic for large enough coupling. Single particle states are always easily found but two magnon states are already quite non-trivial. Three body factorization is not present so we have no Bethe ansatz to help us out.

The way out from this apparent dead end is the fact that we should always think perturbatively in $\lambda = g_{YM}^2 N$. Therefore the next to nearest neighbors interaction (as well as part of the contact term) is to be treated as a perturbation. More precisely at order $\lambda^n$ in perturbation theory we will have a range $n$ Hamiltonian and we will be able to make sense of the Bethe ansatz equations as a perturbative expansion provided the spin chain length is larger than $n$.

Let us then understand what happens when $\gamma/\alpha \ll 1$. In this limit the r.h.s of (3.120) is very large and thus if $\kappa$ is real the relative momenta $\kappa'$ must be complex. Thus the relevant wave functions in this regime are those describing the scattering of two particles in the presence of a bound state and therefore we should consider (3.117) with, say, $D = 0$. More precisely from (3.120) we obtain

$$e^{i\kappa'/2} = \left(-\cos P \sec\frac{P}{2}\right)\frac{\gamma}{\alpha} + \left(2\cos^2 P \sec^2\frac{P}{2}\cos\frac{\kappa}{2}\right)\left(\frac{\gamma}{\alpha}\right)^2 + \mathcal{O}\left(\left(\frac{\gamma}{\alpha}\right)^3\right) \tag{3.126}$$

Thus we conclude that perturbatively the effect of the magnon is solely to generate a fudge factor $(\gamma/\alpha)^{|n-m|}$ for small $|n-m|$. Since we work to leading order in $\gamma/\alpha$ this means that the effect of the magnon is to slightly renormalize the wavefunction $\psi(n, n+1)$. Therefore, inspired by this treatment, we try the ansatz

$$\psi(n,m) = \phi(n,m) + S(k,p)\phi(m,n) \tag{3.127}$$

where

$$S(k,p) = S^{(0)} + \frac{\gamma}{\alpha}S^{(1)} , \tag{3.128}$$

and

$$\phi(n,m) = e^{ikn+ipm}\left(1 + \frac{\gamma}{\alpha}f(k,p)\delta_{m,n+1}\right) \tag{3.129}$$

Here $S^{(0)}$ is the leading value (3.109) while $S^{(1)}$ corrects the magnon $S$-matrix. The function $f(k,p)$ is a local fudge factor or wave function renormalization which appears in the region

where the magnons are interacting. If we plug this wave function into (3.116), (3.123) and (3.124) and work always to order $(\gamma/\alpha)^2$ then we find that the ansatz does the job if we fix

$$S^{(1)}(k,p)/S^{(0)}(k,p) = \frac{32i\sin^2\frac{k}{2}\sin^2\frac{p}{2}\,(\sin p - \sin k)}{2\cos(k) + 2\cos(p) - \cos(k+p) - 3} \tag{3.130}$$

and

$$f(p,k) = -4\sin\frac{p}{2}\sin\frac{k}{2}\sec\frac{k+p}{2}\,. \tag{3.131}$$

In perturbation theory particle creation is suppressed and the two magnon problem becomes again more standard. The spectrum for the double magnon problem is then obtained from summing the two dispersion relations $\epsilon(p)$ and $\epsilon(k)$ where the momenta are to be quantized via the Bethe equations (3.110) with the $S$-matrix (3.128). All this should be done working always to leading $\gamma/\alpha$ order.

So far nothing that we did is especially remarkable since usually two body problems are solvable. Integrability, or rather perturbative integrability, arises in its full splendor when we consider the three magnon problem. It turns out that the ansatz (3.111) works if we use the corrected $S$-matrix (3.128) and replace the bare $\phi_{ijk}$ in (3.111) by

$$\begin{aligned}\phi_{ijk} \;=\; & \exp\left(ik_i n_1 + ik_j n_2 + ik_k n_3\right)\times \\ & \times\left(1 + f(k_i,k_j)\delta_{n_2,n_1+1} + f(k_j,k_k)\delta_{n_3,n_2+1} + g(k_1,k_2,k_3)\delta_{n_3=n_2+1}\delta_{n_2=n_1+1}\right)\,,\end{aligned} \tag{3.132}$$

where $g(k_1,k_2,k_3)$ is easily fixed by the action of the Hamiltonian and both $f$ and $g$ are defined as being completely symmetric with respect to permutations of their arguments, $f(p,k) = f(k,p)$, etc. Notice that (almost) all the needed ingredients are already contained in the two magnon problem, namely the $S$-matrix and the renormalization functions $f(k,p)$ are precisely as before. To write the complete wave function we merely need to compute a single triple contact term $g(p,k,q)$ which we can then use to build the four magnon scattering state. To find the four particle state we will again need to compute a single new contact term which we can then use to write an ansatz for the five particles state, etc.

On the other hand, let us stress, none of these contact terms actually need to be computed if we want to consider large enough chains! Having the ansatz (3.111) with a large enough spin chain, we simply need to impose the periodicity condition $\psi(n,m,r) = \psi(m,r,n+L)$ to find the Bethe equations

$$e^{ip_j L} = \prod_{k\neq j}^{3} S_{jk}\,,$$

where the S-matrix is given by (3.128), and the momenta should be computed in small $\gamma/\alpha$ perturbation theory. The energy is then computed in perturbation theory from the

sum dispersion relation (3.115)

$$E = \sum_{k=1}^{3} \epsilon(p_j)\,. \tag{3.133}$$

To summarize, the setup to study the anomalous dimensions of large single trace operators in $N = 4$ super symmetric Yang-Mills theory is as follows. At order $g^{2n}$ we first consider the single magnon state which will tell us what the dispersion relation $\epsilon(p)$ is to this order. Then we solve the two magnon problem from which we compute the $S$-matrix also up to order $g^{2n}$. Finally, to compute any $M$-magnon state we simply solve Bethe equations

$$1 = e^{ip_k L} \prod_{j\neq k}^{M} S(p_k, p_j)$$

and read the spectrum from

$$E = \sum_{k=1}^{M} \epsilon(p_k)\,. \tag{3.134}$$

In all intermediate steps we should work perturbatively up to order $g^{2n}$. These formulas work for $n < L$ otherwise the range of the spin chain Hamiltonian will be as large as the spin chain length and there will be no asymptotic region for the magnons.

For example up to three loops the SYM spectrum can be found from the Beisert-Dippel-Staudacher equations [43] which read

$$\left(\frac{x_k^+}{x_k^-}\right)^L = \prod_{j\neq k}^{M} \frac{u_k - u_j + i/2}{u_k - u_j - i/2}\,,\ E = 2gi \sum_{k=1}^{M} \left(x_k^+ - x_k^- - \frac{1}{x_k^+} + \frac{1}{x_k^-}\right)\,, \tag{3.135}$$

where

$$x_k^{\pm} = \frac{u_k \pm i/2 + \sqrt{(u_k \pm i/2)^2 - 4g^2}}{2g}\,. \tag{3.136}$$

Starting at four loops these equations fail to reproduce the correct spectrum and must be replaced by the all-loop Beisert-Staudacher equations [35] described below. These equations are seven Nested Bethe ansatz equations (the $PSU(2,2|4)$ symmetry group is of rank 7) but before introducing them it is instructive to make a small detour and consider first a much simpler toy model which is what we will do in the next section.

## 3.6 $SO(4)$ sigma model – Nested Algebraic Bethe Ansatz

In this section we review in great detail a particularly simple example of a relativistic theory described by a set of asymptotic Nested Bethe equations: the $SO(4)$ non-linear sigma model or $SU(2)$ principal chiral field.

We introduce the rapidities $\theta$ in terms of which we parametrize the energy and momentum of the mass $m$ particles

$$p = m \sinh \pi\theta \ , \ \ E = m \cosh \pi\theta \, . \tag{3.137}$$

Next we consider the two-to-two S-matrix. By relativistic invariance it must depend only on the Mandelstam variables

$$s = (p_1 + p_2)^2 = 4m^2 \cosh^2 \frac{\pi\theta}{2} \ , \ \ u = (p_1 - p_2)^2 = -4m^2 \sinh^2 \frac{\pi\theta}{2} \ , \ \ t = 0 \tag{3.138}$$

where we used the fact the initial and final momenta are only at most permuted to define the Mandelstam variables using $p'_j = p_j$ for $j = 1, 2$ and $\theta = \theta_1 - \theta_2$. Therefore the $S$-matrix depends only of this difference of rapidities. It must be of the form

$$S_{ik}^{j\,l}(\theta) = S_2(\theta) \left[ \delta_{ik}\delta_{jl}\, g^{-1}(\theta) + \delta_{ij}\delta_{lk} + \delta_{il}\delta_{jk}\, h^{-1}(\theta) \right] \tag{3.139}$$

because there are no more tensors we could build. Moreover since the model is integrable this S-matrix must obey the YB equations (3.94) and thus the relative coefficients should be as in (3.48) for $M = 4$

$$h(\theta) = g(i\lambda - \theta) = \frac{i\theta}{\lambda} \, . \tag{3.140}$$

because mathematically the YB relations (3.94) also appeared for the R-matrices in (3.33).

Changing $i \leftrightarrow j$ and the channel $s = 4m_0^2 \cosh^2(\pi\theta/2) \leftrightarrow u$ (i.e. $\theta \to i - \theta$) should leave the S-matrix invariant. This is crossing–symmetry. It implies

$$S_2(\theta) = S_2(i - \theta) \tag{3.141}$$

and $h(\theta) = g(i - \theta)$, or $\lambda = 1$.

Finally we impose the most natural requirement, namely, unitarity. Setting

$$S_{mn}^{j\,l}(-\theta) S_{ik}^{mn}(\theta) = \delta_{ij}\delta_{kl}\, S_2(-\theta) S_2(\theta) \left(1 + h^{-1}(-\theta) h^{-1}(\theta)\right) + \delta_{ik}\delta_{jl}\,(\ldots) + \delta_{il}\delta_{kj}\,(\ldots)$$

to be equal to $\delta_{ij}\delta_{kl}$ one obtains 3 equations. The exact expressions inside the parentheses are not relevant for our discussion. It suffices to say that, for the $g$ and $h$ we found (3.140), (3.140), they vanish identically. Thus one is left with

$$S_2(-\theta) S_2(\theta) = \frac{\theta^2}{\theta^2 + 1} \, . \tag{3.142}$$

From (3.141) and (3.142) it follows that $S_2(\theta)$ is given by

$$\frac{\theta}{\theta - i}\, S_0^2(\theta) \ , \ \ S_0(\theta) = i\, \frac{\Gamma\left(-\frac{\theta}{2i}\right) \Gamma\left(\frac{1}{2} + \frac{\theta}{2i}\right)}{\Gamma\left(\frac{\theta}{2i}\right) \Gamma\left(\frac{1}{2} - \frac{\theta}{2i}\right)} \tag{3.143}$$

times a Castillejo-Dalitz-Dyson factor

$$f(\theta)=\prod_{k=1}^{L}\frac{\sinh\pi\theta+i\sin\alpha_k}{\sinh\pi\theta-i\sin\alpha_k} \tag{3.144}$$

where $\alpha_k$ are arbitrary real numbers. The form (3.143) is needed to have the right pole and zero structure according to (3.141) and (3.142) while the ambiguity (3.144) is unfixed since $f(\theta)/f(i-\theta)=f(\theta)\,f(-\theta)=1$. Absence of additional bound states forces one not only to exclude this factor but also to introduce the $i$ in $S_0(\theta)$ [44, 45]. For the non-linear sigma model the correct S-matrix is indeed given by the minimal choice (3.143). To verify this claim some convincing cross checks are done [46, 47].

The power of integrability and symmetry is incredible. We did not even write the Lagrangian of the theory! Of course this is also a drawback since many checks need to be done to ensure we solved the correct theory.

Since $SO(4)=SU(2)\times SU(2)$ we can replace $i,k,j,l$ by $(\alpha,\dot\alpha),(\beta,\dot\beta),(\alpha',\dot\alpha'),(\beta',\dot\beta')$ and write (3.139) as

$$\begin{aligned}&\frac{S_0^2(\theta)}{(\theta-i)^2}\left(i\theta\,\epsilon_{\alpha\beta}\epsilon_{\dot\alpha\dot\beta}\epsilon^{\alpha'\beta'}\epsilon^{\dot\alpha'\dot\beta'}+\theta(\theta-i)\,\delta_\alpha^{\alpha'}\delta_{\dot\alpha}^{\dot\alpha'}\delta_\beta^{\beta'}\delta_{\dot\beta}^{\dot\beta'}-i(\theta-i)\,\delta_\alpha^{\beta'}\delta_{\dot\alpha}^{\dot\beta'}\delta_\beta^{\alpha'}\delta_{\dot\beta}^{\dot\alpha'}\right)\\ =\;&\frac{S_0^2(\theta)}{(\theta-i)^2}\left(\theta\,\delta_\alpha^{\alpha'}\delta_\beta^{\beta'}-i\delta_\alpha^{\beta'}\delta_\beta^{\alpha'}\right)\left(\theta\,\delta_{\dot\alpha}^{\dot\alpha'}\delta_{\dot\beta}^{\dot\beta'}-i\delta_{\dot\alpha}^{\dot\beta'}\delta_{\dot\beta}^{\dot\alpha'}\right).\end{aligned}$$

or

$$\hat S(\theta)=\hat S_R(\theta)\times\hat S_L(\theta)\;\;,\;\;\hat S_{L,R}(\theta)=S_0(\theta)\,\hat{\mathcal{R}}(\theta)\;\;,\;\;\hat{\mathcal{R}}=\frac{\theta\hat I-i\hat P}{\theta-i} \tag{3.145}$$

where $\hat P$ is the permutation operator in $\mathbb{C}^2\times\mathbb{C}^2$. Notice that, since $SO(4)=SU(2)\times SU(2)$, we could have started with this ansatz where

$$\hat S_{L,R}(\theta)=\hat S_0(\theta)\,\frac{\theta}{\theta-i}\left(\hat I-h^{-1}(\theta)\,\hat P\right).$$

instead of starting with (3.139). The absence of the channel where two particles annihilate is obvious since the particles are charged with left/right charge. The YB relation would then fix both $\hat S_L$ and $\hat S_R$ to be proportional to the $SU(2)$ R-matrix already encountered in (3.38).

Let us now start from the obtained S-matrix (3.145) and carry out the algebraic Bethe ansatz program [48]. We introduce a ghost particle in the auxiliary space 0 and scatter it through the other particles. We want to diagonalize

$$\hat T(\theta)\,|\Psi\rangle=\Lambda(\theta)|\Psi\rangle\,, \tag{3.146}$$

where the transfer matrix is given by

$$\hat{T}(\theta) = \mathrm{Tr}_0 \prod_{k=1}^{L} \hat{S}_{0k}(\theta - \theta_k)\,,$$

with the trace being over the auxiliary space. This is a relevant problem because, once solved for any $\theta$, one can set $\theta = \theta_k$ so that the ghost particle will exchange its quantum numbers with particle $k$ as $\hat{S}_{0k}(0) = -P_{0k} \times P_{0k}$. In other words,

$$-\,\mathrm{Tr}\,\hat{T}(\theta_k) = \hat{S}_{k,k-1}(\theta_k - \theta_{k-1}) \ldots \hat{S}_{k,1}(\theta_k - \theta_1)\hat{S}_{k,N}(\theta_k - \theta_N) \ldots \hat{S}_{k,k+1}(\theta_k - \theta_{k+1})$$

so that the periodicity condition on the wave function reads

$$-\; e^{im_0 \mathcal{L} \sinh(\pi\theta_k)}\,\mathrm{Tr}\,\hat{T}(\theta_k)\,|\Psi\rangle = |\Psi\rangle\,. \tag{3.147}$$

Let us then consider (3.146). Notice that mathematically this is absolutely identical to (3.50) appearing in the study of the Heisenberg spin chain and we can therefore easily adapt all the steps in section 3.3 to the current problem. There are only two minor differences. First here we have a tensor product of two identical $S$-matrices (right and left). Second, the argument of the $S$-matrices is $\theta - \theta_j$ whereas in (3.50) this was always the same argument $u$ for all $R$-matrices. Thus, technically, (3.146) is identical to the study of in-homogeneous spin chains with $SU(2) \times SU(2)$ symmetry.

We consider

$$|\Psi\rangle = \prod_{i=1}^{J_u} \hat{B}_L(u_i) \prod_{j=1}^{J_v} \hat{B}_R(v_j)|\,\Omega(\theta_1, \ldots, \theta_L)\rangle \tag{3.148}$$

where $\Omega$ is the state with $L$ particles, where the right and left spin of every particle is pointing in the up direction, and

$$\hat{L}_R(\theta) = \prod_{k=1}^{L} \hat{S}_{R,\,0k}(\theta - \theta_k) = \begin{pmatrix} \hat{A}_R(\theta) & \hat{B}_R(\theta) \\ \hat{C}_R(\theta) & \hat{D}_R(\theta) \end{pmatrix} \tag{3.149}$$

with a similar definition for the left sector. Acting on $|\Omega\rangle$ one has

$$\mathcal{R}_{0k}(\theta)|\,\Omega\rangle = \frac{1}{\theta - i} \begin{pmatrix} \theta - \frac{i}{2}(\tau^3 + 1) & -i\tau^- \\ -i\tau^+ & \theta + \frac{i}{2}(\tau^3 - 1) \end{pmatrix} |\,\Omega\rangle = \frac{1}{\theta - i} \begin{pmatrix} (\theta - i)\,|\,\Omega\rangle & * \\ 0 & \theta|\,\Omega\rangle \end{pmatrix}$$

The upper most right element is not important for our discussion. However the zero in the left down corner is important. It implies that $|\,\Omega\rangle$ is eigenvalue of both $A$ and $D$ with eigenvalues

$$\begin{aligned} \hat{A}(\theta)|\,\Omega\rangle &= \prod_{\alpha=1}^{L} S_0(\theta - \theta_\alpha)\,|\,\Omega\rangle\,, \\ \hat{D}(\theta)|\,\Omega\rangle &= \prod_{\alpha=1}^{L} S_0(\theta - \theta_\alpha)\frac{\theta - \theta_a}{\theta - \theta_a - i}\,|\,\Omega\rangle\,. \end{aligned}$$

So now we only have to understand how $A$ and $D$ pass through the $B$'s. As in section 3.3, the YB relations imply

$$\hat{L}^{a}_{R,L}(\theta)\,\hat{L}^{a'}_{R,L}(\theta')\,\mathcal{S}_{aa'}(\theta'-\theta)=\mathcal{S}_{aa'}(\theta'-\theta)\,\hat{L}^{a'}_{R,L}(\theta')\,\hat{L}^{a}_{R,L}(\theta)\,,$$

where $a$ and $a'$ are two $\mathbb{C}^2$ auxiliary spaces. This gives us the commutation relations between the elements of the transfer matrix (3.149). In particular

$$\begin{aligned}
[B(\theta),B(\theta')] &= 0\\
A(\theta)\,B(\theta') &= \frac{\theta'-\theta-i}{\theta'-\theta}\,B(\theta')\,A(\theta)+\frac{i}{\theta'-\theta}\,B(\theta)\,A(\theta') \qquad (3.150)\\
D(\theta)\,B(\theta') &= \frac{\theta'-\theta+i}{\theta'-\theta}\,B(\theta')\,D(\theta)-\frac{i}{\theta'-\theta}\,B(\theta)\,D(\theta') \qquad (3.151)
\end{aligned}$$

for symbols in the same right or left sector. Symbols in different sectors commute to zero of course. Then, acting on (3.148), one has

$$\begin{aligned}
-\operatorname{Tr}\hat{T}(\theta)\,|\Psi\rangle &= (\hat{A}_R(\theta)+\hat{D}_R(\theta))\times(\hat{A}_L(\theta)+\hat{D}_L(\theta))\prod_{i=1}^{J_u}\hat{B}_L(u_i)\times\prod_{j=1}^{J_v}\hat{B}_R(v_j)|\,\Omega(\theta_1,\dots,\theta_L)\rangle\\
&= \prod_{\alpha=1}^{L}S_0^2(\theta-\theta_a)\left(\prod_{i=1}^{J_u}\frac{u_i-\theta-i}{u_i-\theta}+\prod_{i=1}^{J_u}\frac{u_i-\theta+i}{u_i-\theta}\prod_{\alpha=1}^{L}\frac{\theta-\theta_a}{\theta-\theta_\alpha-i}\right)\\
&\times\left(\prod_{i=1}^{J_v}\frac{v_i-\theta-i}{v_i-\theta}+\prod_{i=1}^{J_v}\frac{v_i-\theta+i}{v_i-\theta}\prod_{\alpha=1}^{L}\frac{\theta-\theta_a}{\theta-\theta_\alpha-i}\right)|\,\Psi\rangle+\dots
\end{aligned}$$

where dots stand for *undesirable* terms which would make $|\Psi\rangle$ not to be an eigenvector of $\operatorname{Tr}\hat{T}$ while the displayed terms are the one we obtain ignoring the second term in the rhs of both (3.150) and (3.151). The condition that these *undesirable* terms vanish gives us a set of equations for $u_i$ and $v_j$. There is however a shortcut to arrive at these equations provided we know that these terms can indeed be killed. The argument is the following – each of the two last terms inside the big parentheses came from the diagonalization of a product of $\mathcal{Q}=\theta-iP$. The diagonalization of such a product of operators must yield a polynomial in $\theta$ therefore the residues of the apparent poles which seem to be part of the eigenvalue for $\theta=u_i$ (or $v_j$) must vanish. This implies

$$\begin{aligned}
1 &= \prod_{i\neq j}^{J_u}\frac{u_j-u_i-i}{u_j-u_i+i}\prod_{\alpha=1}^{L}\frac{u_j-\theta_a}{u_j-\theta_a-i}\,, \qquad (3.152)\\
1 &= \prod_{i\neq j}^{J_v}\frac{v_j-v_i-i}{v_j-v_i+i}\prod_{\alpha=1}^{L}\frac{v_j-\theta_a}{u_j-\theta_a-i}\,. \qquad (3.153)
\end{aligned}$$

Furthermore (3.147) reads

$$e^{im_0\mathcal{L}\sinh\pi\theta_\beta}\prod_{\alpha\neq\beta}^{L}S_0^2(\theta_\beta-\theta_a)\prod_{i=1}^{J_u}\frac{\theta_\beta-u_i+i}{\theta_\beta-u_i}\prod_{i=1}^{J_v}\frac{\theta_\beta-v_i+i}{\theta_\beta-v_i}=1\,. \tag{3.154}$$

After the trivial shift $(u,v)\to(u+i/2,v+i/2)$ we finally find the complete set of Bethe equations

$$e^{-i\mu\sinh\pi\theta_\alpha} = \prod_{\beta\neq\alpha}S_0^2\left(\theta_\alpha-\theta_\beta\right)\prod_j\frac{\theta_\alpha-u_j+i/2}{\theta_\alpha-u_j-i/2}\prod_k\frac{\theta_\alpha-v_k+i/2}{\theta_\alpha-v_k-i/2}\,, \tag{3.155}$$

$$1 = \prod_\beta\frac{u_j-\theta_\beta-i/2}{u_j-\theta_\beta+i/2}\prod_{i\neq j}\frac{u_j-u_i+i}{u_j-u_i-i}\,,\,, \tag{3.156}$$

$$1 = \prod_\beta\frac{v_k-\theta_\beta-i/2}{v_k-\theta_\beta+i/2}\prod_{l\neq k}\frac{v_k-v_l+i}{v_k-v_l-i}\,. \tag{3.157}$$

They have a clear physical meaning. $u$'s and $v$'s are the Bethe roots appearing from the diagonalization of (3.146) and characterize each quantum state. A quantum state with no such roots corresponds to the highest weight ferromagnetic state where all spins of both kinds are up. In this case we can drop the last two equations and the first one is of the form (3.97). Adding a $u$ ($v$) root corresponds to flipping one of the right (left) $SU(2)$ spins, thus creating a magnon. This is particularly clear from equations (3.156,3.157) which in the limit $\lambda\to 0$, when $\theta_\alpha\simeq 0$, are precisely the usual Bethe equations for the diagonalization of an Heisenberg hamiltonian for the periodic chain of length $L$, originally solved by Hans Bethe [39], provided we identify the momentum of magnons with

$$e^{ip}=\frac{u+i/2}{u-i/2}\,. \tag{3.158}$$

The left and right charges of the wave function, associated with the two $SU(2)$ spins are given by

$$Q_L=L-2J_u\,,\qquad Q_R=L-2J_v\,. \tag{3.159}$$

Thus, in sum, equations (3.155)-(3.156) describe the entangled scattering of physical particles and the corresponding isotopic spin waves.

## 3.7 Back to $\mathcal{N}=4$ and Nested Bethe Ansatz

In the previous sections we encountered what are probably the two most important quantities in quantum integrability – the R-matrix and the S-matrix. They are mathematically very similar (if not equivalent) as they are both defined as operators acting on a product of

two vector spaces and obeying the Yang-Baxter triangular relations (3.33) and (3.94). The main difference is that for the $S$-matrix we often impose additional physical constraints such as crossing symmetry with no (obvious) counterpart in the $R$-matrix construction.

As explained in the previous section the $R$-matrix can be used to build integrable spin chain Hamiltonians. In particular, by taking $n$ derivatives of the logarithm of the transfer matrix we generate Hamiltonians of range $n$.

The $S$-matrix, on the other hand, describes the two body scattering of integrable theories which, due to the factorizability property arising from a large number of conserved charges, defines the scattering between any number of external particles. When $M$ particles are put in a big circle of perimeter $L$ the quantization of the momentum of these particles is given by (3.99) which can be reduced to a diagonalization problem absolutely equivalent to the diagonalization of an inhomogenous spin chain as described in the previous section.

The obvious question:

How do these objects appear in the study of $\mathcal{N}=4$ SYM at higher loops and for the full set of $PSU(2,2|4)$ operators?

### 3.7.1 $R$-matrix

The product of two $SU(2)$ spin 1/2's yields

$$\frac{1}{2}\otimes\frac{1}{2}=0\oplus 1\,, \tag{3.160}$$

while the product of two vector representations in $SO(M)$ gives

$$M\otimes M=1\oplus\frac{M^2-M}{2}\oplus\frac{M^2-1}{2}\,. \tag{3.161}$$

From (3.160) we conclude that if we want to construct an operator with $SU(2)$ symmetry acting on a product of two spin $\frac{1}{2}$'s it must be built out of the projectors

$$\frac{1}{2}\left(1-P\right)\ ,\ \frac{1}{2}\left(1+P\right)\,, \tag{3.162}$$

into the anti-symmetric (spin 0) and symmetric (spin 1) spaces. Indeed the $SU(2)$ Heisenberg spin chain Hamiltonian (3.22) and the corresponding $R$-matrix (3.38) are constructed precisely out of this two invariant tensors.

Similarly, the decomposition (3.161) implies the existence of three invariant tensors,

$$\frac{1}{M}K\ ,\ \frac{1}{2}\left(1-P\right)\ ,\ \frac{1}{2}\left(1+P\right)-\frac{1}{M}K \tag{3.163}$$

projecting into the trace, anti-symmetric and symmetric traceless spaces obtained from the product of two vector representations. Once again the Minahan-Zarembo $SO(6)$ Hamiltonian (3.16) and the corresponding $R$-matrix (3.48) are build out of these structures.

The tensor structures available for the $PSU(2,2|4)$ spin chain appearing in $\mathcal{N}=4$ SYM are in infinite number because the symmetry group is non-compact and the representation is infinite dimensional. The product of two fields in the field strength multiplet decomposes into an infinite sum of irreducible modules

$$\mathcal{V}_F \otimes \mathcal{V}_F = \bigoplus_{j=0}^{\infty} \mathcal{V}_j \tag{3.164}$$

so that the 1-loop spin chain Hamiltonian and the corresponding $R$-matrix ought to be built from the projectors $\mathcal{P}_j$ into these modules. Indeed the full one-loop Dilatation operator was found to be given as [49]

$$H = \sum_{n=1}^{L} \left( \sum_{k=1}^{j} \frac{1}{k} \right) \mathcal{P}^{j}_{n,n+1} \,, \tag{3.165}$$

and the $R$-matrix

$$R(u) = \sum_{j=0}^{\infty} (-1)^j \frac{\Gamma(-j-iu)\Gamma(1+iu)}{\Gamma(-j+iu)\Gamma(1-iu)} \mathcal{P}_j \tag{3.166}$$

obeys the Yang-Baxter relation (3.33) and reproduces – by a transfer matrix construction as described in section 3.2 – the $\mathcal{N}=4$ 1-loop Dilatation operator.

There are four type of $R$-matrices in the literature. Those of the type we have seen so far where the ratios between the pre-factors of the several invariant tensors are rational functions of the spectral parameter $u$ are called rational R-matrices. Then we have the trigonometric and elliptic R-matrices where these rations are expressed in terms of trigonometric or elliptic functions. They will play no role whatsoever in our discussion. Then there are all the other $R$-matrices which we group together and call *exotic*. The Shastry's Hubbard R-matrix [50] and Beisert S-matrix [51, 52] based on the extended $SU(2|2)$ symmetry are examples of such exotic matrices (actually they can be closely related so they are rather a *single example* of such matrices). To analyze the one-loop spectrum of $\mathcal{N}=4$ and to study most spin chains models in condensed matter, the rational $R$-matrices are enough and in this subsection we will stick to them.

Let us then consider with great generality the diagonalization of the transfer matrix

$$\hat{T}(u) = \mathrm{Tr}_0 R_{0L}(u) \dots R_{01}(u) \tag{3.167}$$

for rational $R$-matrices symmetric with respect to some Lie (super) group of rank $r$ with Cartan matrix $M_{ab}$. The physical space at each site $1, \dots L$ can be either the space where the fundamental representation acts (as seen in the previous sections) or some other space where a representation with Dynkin labels $V_a$ lives. Then each quantum state is parameterized by a set $\{u_{a,j}\}$ of Bethe roots where $a = 1, \dots, r$ refers to the Dynkin node and

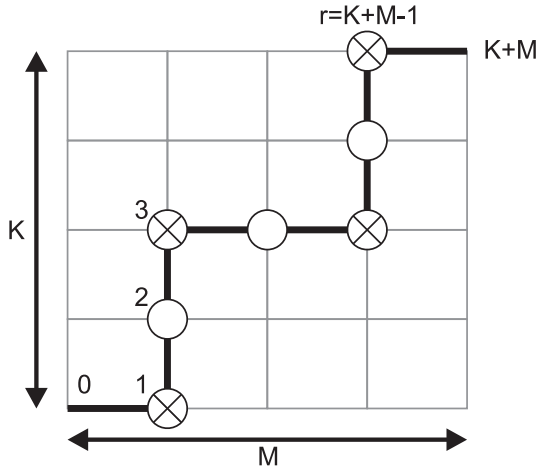


Figure 3.10: For $su(K|M)$ super algebras the Dynkin diagram is not unique. The several possible choices can be represented as the paths going from the up right corner $(M, K)$ to the origin always approaching this point with each step. The turns are the fermionic nodes whereas the straight lines correspond to the usual bosonic nodes. Different paths will correspond to different sets of Bethe equations which are related by fermionic dualities which flip a *left–down* fermionic turn into *down–left* turn or vice-versa [53].

$j = 1, \ldots, K_a$ where $K_a$ is the excitation number of *magnons* of type $a$. The Bethe equations from which we find the position of these roots are then given by

$$\left(\frac{u_{a,j} + \frac{i}{2}V_a}{u_{a,j} - \frac{i}{2}V_a}\right)^L = -\prod_{b=1}^{r} \frac{Q_b\left(u_{a,j} + \frac{i}{2}M_{ab}\right)}{Q_b\left(u_{a,j} - \frac{i}{2}M_{ab}\right)} \tag{3.168}$$

where

$$Q_a(u) = \prod_{j=1}^{K_a} (u - u_{a,j})$$

are the Baxter polynomials. In fact, contrary to what happens for the usual Lie algebras, for super algebras the Dynkin diagram (and thus the Cartan matrix) is not unique. Take for example the $su(K|M)$ super algebra. The different possible Dynkin diagrams can be identified [53] as the different paths starting from $(M, K)$ and finishing at $(0, 0)$ (always approaching this point with each step) in a rectangular lattice of size $M \times K$ as in figure 3.10. The turns in this path represent the fermionic nodes whereas the bosonic nodes are those which are crossed by a straight line – see figure 3.10 (the index $a$ goes along the path as indicated). The Cartan matrix $M_{ab}$ is then given by

$$M_{ab} = (p_a + p_{a+1})\,\delta_{ab} - p_{a+1}\delta_{a+1,b} - p_a\delta_{a,b+1}$$

where $p_a$ is associated with the link between the node $a$ and $a+1$ and is equal to $+1$ $(-1)$ if this link is vertical (horizontal). The Bethe equations corresponding to the different

choices of Cartan matrices are equivalent and related by the well known fermionic dualities [54, 55, 53].

For example, for an $SU(2)$ spin $s$ chain we have a single Dynkin node with $M_{11}=2$ and the spin $s$ representation corresponds to the Dynkin labels $V_p=2s$. Thus we get

$$\left(\frac{u_j+is}{u_j-is}\right)^L=\prod_{k\neq j}^{M}\frac{u_j-u_k+i}{u_j-u_k-i}\ ,\ \ j=1,\ldots,M \tag{3.169}$$

and the equations we found in (3.77) are those where the physical space is in the fundamental representation for which $s=1/2$.

Another example, the $SO(6)$ spin chain with spins in the vector representation **6**, is obtained from

$$M_{ab}=\begin{pmatrix}2&-1&0\\-1&2&-1\\0&-1&2\end{pmatrix}\ ,\ V_a=\begin{pmatrix}0\\1\\0\end{pmatrix} \tag{3.170}$$

so that

$$1 = \prod_{k\neq j}^{K_1}\frac{u_{1,j}-u_{1,k}+i}{u_{1,j}-u_{1,k}-i}\prod_{k=1}^{K_2}\frac{u_{1,j}-u_{2,k}-\frac{i}{2}}{u_{1,j}-u_{2,k}+\frac{i}{2}} \tag{3.171}$$

$$\left(\frac{u_{2,j}+\frac{i}{2}}{u_{2,j}-\frac{i}{2}}\right)^L = \prod_{k=1}^{K_1}\frac{u_{2,j}-u_{1,k}-\frac{i}{2}}{u_{2,j}-u_{1,k}+\frac{i}{2}}\prod_{k\neq j}^{K_2}\frac{u_{2,j}-u_{2,k}+i}{u_{2,j}-u_{2,k}-i}\prod_{k=1}^{K_3}\frac{u_{2,j}-u_{3,k}-\frac{i}{2}}{u_{2,j}-u_{3,k}+\frac{i}{2}} \tag{3.172}$$

$$1 = \prod_{k=1}^{K_2}\frac{u_{3,j}-u_{2,k}-\frac{i}{2}}{u_{3,j}-u_{2,k}+\frac{i}{2}}\prod_{k\neq j}^{K_3}\frac{u_{3,j}-u_{3,k}+i}{u_{3,j}-u_{3,k}-i} \tag{3.173}$$

which are indeed precisely the Bethe equations diagonalizing the Minahan-Zarembo spin chain Hamilonian (3.16) [56, 57, 9].

Finally, the seven (the rank of $PSU(2,2|4)$) one-loop $\mathcal{N}=4$ Bethe equations which particular diagonalize (3.165) follow from the Cartan matrix and Dynkin labels

$$M_{ab}=\begin{pmatrix}0&1&&&&&\\1&-2&1&&&&\\&1&0&-1&&&\\&&-1&2&-1&&\\&&&-1&0&1&\\&&&&1&-2&1\\&&&&&1&0\end{pmatrix}\ ,\ V_a=\delta_{a,4}\,, \tag{3.174}$$

and therefore read [58]

$$1 = \prod_{j=1}^{K_2} \frac{u_{1,k}-u_{2,j}+\frac{i}{2}}{u_{1,k}-u_{2,j}-\frac{i}{2}} \tag{3.175}$$

$$1 = \prod_{j\neq k}^{K_2} \frac{u_{2,k}-u_{2,j}-i}{u_{2,k}-u_{2,j}+i} \prod_{j=1}^{K_3} \frac{u_{2,k}-u_{3,j}+\frac{i}{2}}{u_{2,k}-u_{3,j}-\frac{i}{2}} \prod_{j=1}^{K_1} \frac{u_{2,k}-u_{1,j}+\frac{i}{2}}{u_{2,k}-u_{1,j}-\frac{i}{2}}\,, \tag{3.176}$$

$$1 = \prod_{j=1}^{K_2} \frac{u_{3,k}-u_{2,j}+\frac{i}{2}}{u_{3,k}-u_{2,j}-\frac{i}{2}} \prod_{j=1}^{K_4} \frac{u_{3,k}-u_{4,j}-\frac{i}{2}}{u_{3,k}-u_{4,j}+\frac{i}{2}}\,, \tag{3.177}$$

$$\left(\frac{u_{4,k}+\frac{i}{2}}{u_{4,k}-\frac{i}{2}}\right)^L = \prod_{j\neq k}^{K_4} \frac{u_{4,k}-u_{4,j}+i}{u_{4,k}-u_{4,j}-i} \prod_{j=1}^{K_3} \frac{u_{4,k}-u_{3,j}-\frac{i}{2}}{u_{4,k}-x_{3,j}+\frac{i}{2}} \prod_{j=1}^{K_5} \frac{u_{4,k}-u_{5,j}-\frac{i}{2}}{u_{4,k}-x_{5,j}+\frac{i}{2}} \tag{3.178}$$

$$1 = \prod_{j=1}^{K_6} \frac{u_{5,k}-u_{6,j}+\frac{i}{2}}{u_{5,k}-u_{6,j}-\frac{i}{2}} \prod_{j=1}^{K_4} \frac{u_{5,k}-u_{4,j}-\frac{i}{2}}{u_{5,k}-u_{4,j}+\frac{i}{2}}\,, \tag{3.179}$$

$$1 = \prod_{j\neq k}^{K_6} \frac{u_{6,k}-u_{6,j}-i}{u_{6,k}-u_{6,j}+i} \prod_{j=1}^{K_5} \frac{u_{6,k}-u_{5,j}+\frac{i}{2}}{u_{6,k}-u_{5,j}-\frac{i}{2}} \prod_{j=1}^{K_7} \frac{u_{6,k}-u_{7,j}+\frac{i}{2}}{u_{6,k}-u_{7,j}-\frac{i}{2}}\,, \tag{3.180}$$

$$1 = \prod_{j=1}^{K_6} \frac{u_{7,k}-u_{6,j}+\frac{i}{2}}{u_{7,k}-u_{6,j}-\frac{i}{2}}\,, \tag{3.181}$$

from which the spectrum is obtained though

$$E = \sum_{j=1}^{K_4} \frac{2g^2}{u_{4,j}^2+1/4}\,. \tag{3.182}$$

Of course, since this is a supergroup there are many possible choices of Dynkin diagram (i.e. Cartan Matrix) which would give equivalent set of Bethe equations, related by the so called fermionic dualities as described above.

Despite their apparent complexity we should keep in mind that by solving these equations we are obtaining the full 1-loop spectrum of $\mathcal{N}=4$ supersymmetric Yang-Mills theory avoiding the task of computing dozens of Feynman graphs which, even at 1-loop, is quite an involved and painful task.

What about more loops? When we consider higher orders in perturbation theory we obtain a next-to-nearest neighbors Hamiltonian. It would be excellent if such long range would simply come from considering more derivatives of the log of the transfer matrix like in (3.52). This optimistic scenario was not yet realized, certainly not for the full supergroup, and not even for any of its smaller subsectors. So far, integrability is to be thought perturbatively as explained in section 3.5.2.

Actually, the Dilatation operator itself is only known to a few loops, not many at all. For the $SU(2)$ sector it is known up to four loops [59] but this is absolutely exceptional

compared to the remaining sectors. See [60, 61] for some very interesting works concerning larger subsectors.

We could imagine that a fundamental $R$-matrix exists but it is not directly related to the long-ranged Hamiltonian. A particularly appealing possibility would be that some extra hidden local degrees of freedom exist and the long range interactions we perceive would rather be the effect of integrating out these fundamental degrees of freedom. This scenario finds compelling evidence at strong coupling in [62, 11, 63, 14], at weak coupling in [64] and for general coupling in [65]. In [62, 11, 63, 14] quantum sigma models describing the $S^n$ subsector of $AdS_5 \times S^5$ type IIB superstring were seen to reproduce the long range conjectured AFS string Bethe equations [66] at strong coupling when the rapidities ($\theta$'s) of the relativistic particles were integrated out thus leaving an effective Hamiltonian for the isospin degrees of freedom. In [64] the BDS equations (3.135) [43], which are known to describe the $SU(2)$ sector of the supersymmetric gauge theory spectrum up to three loops, were shown to be equivalent to the Hubbard model at half filling where again integrating out the momenta ($q$'s) of the electrons yields an effective long range Hamiltonian with $SU(2)$ symmetry for the spins of the electrons. No definite success was achieved so far for the full $PSU(2,2|4)$ group.

### 3.7.2 S-matrix

Let us now consider the diagonalization of

$$\hat{T}(u, \{\theta_i\}) = \mathrm{Tr}_0 S_{0L}(u - \theta_i) \dots S_{01}(u - \theta_i) \tag{3.183}$$

Since, as explained before, the $R$-matrix and the $S$-matrix are basically the same object from the mathematical point of view, the periodicity equations (3.183) are equivalent to the study of inhomogeneous spin chains where the inhomogeneities are the $\theta_i$.

When we analyze this problem we also find some equations for the diagonalization of the transfer matrix – they are the same as in (3.167) except for the present of the inhomogeneities – but what we do with the eigenvalue of the transfer matrix is completely different. In (3.167) we typically take the logarithm of the eigenvalue of the transfer matrix to read of the spectrum of a spin chain. In (3.183) we evaluate it at $u = \theta_i$ and equal this expression to $e^{ip(\theta_i)\mathcal{L}}$ to quantize in this way the momenta of the physical particles. Obviously the length of the circle $\mathcal{L}$ and the number of physical particles $L$ should not be confused. The spectrum is then given by a sum of dispersion relations $\epsilon(\theta_i)$.

Notice that there are two types of Bethe equations here: The *genuine* Bethe equations which diagonalize the inhomogeneous transfer matrix and a last equation – called *middle node equation* – obtained by equating the eigenvalue of the transfer matrix at $u = \theta_j$ to $e^{ip(\theta_j)\mathcal{L}}$. The genuine Bethe equations differ from the usual spin chain Bethe equations (3.168) only by the fact that there are inhomogeneities which will appear in the potential

terms. These Bethe equations are given by

$$\prod_{n=1}^{L}\frac{u_{a,j}-\theta_n+\frac{i}{2}V_a}{u_{a,j}-\theta_n-\frac{i}{2}V_a}=-\prod_{b=1}^{r}\frac{Q_b\left(u_{a,j}+\frac{i}{2}M_{ab}\right)}{Q_b\left(u_{a,j}-\frac{i}{2}M_{ab}\right)}\,. \tag{3.184}$$

The *middle node equation* is less universal and is not completely fixed by symmetry. It reads

$$e^{i\mathcal{L}p(\theta_n)}=\prod_{m\neq n}^{L}S_0(\theta_n,\theta_m)\prod_{b=1}^{r}\frac{Q_b\left(\theta_n+\frac{i}{2}V_b\right)}{Q_b\left(\theta_n-\frac{i}{2}V_b\right)}\,. \tag{3.185}$$

For example in the $SO(6)$ sigma model we have particles in the vector representation and, using again (3.170) we trivially generalize the $SO(6)$ spin chain equations to the asymptotic Bethe ansatz equations for the relativistic particles of the sigma model:

$$1 = \prod_{k\neq j}^{K_1}\frac{u_{1,j}-u_{1,k}+i}{u_{1,j}-u_{1,k}-i}\prod_{k=1}^{K_2}\frac{u_{1,j}-u_{2,k}-\frac{i}{2}}{u_{1,j}-u_{2,k}+\frac{i}{2}} \tag{3.186}$$

$$\prod_{n=1}^{L}\frac{u_{2,j}-\theta_n+\frac{i}{2}}{u_{2,j}-\theta_n-\frac{i}{2}} = \prod_{k=1}^{K_1}\frac{u_{2,j}-u_{1,k}-\frac{i}{2}}{u_{2,j}-u_{1,k}+\frac{i}{2}}\prod_{k\neq j}^{K_2}\frac{u_{2,j}-u_{2,k}+i}{u_{2,j}-u_{2,k}-i}\prod_{k=1}^{K_3}\frac{u_{2,j}-u_{3,k}-\frac{i}{2}}{u_{2,j}-u_{3,k}+\frac{i}{2}} \tag{3.187}$$

$$1 = \prod_{k=1}^{K_2}\frac{u_{3,j}-u_{2,k}-\frac{i}{2}}{u_{3,j}-u_{2,k}+\frac{i}{2}}\prod_{k\neq j}^{K_3}\frac{u_{3,j}-u_{3,k}+i}{u_{3,j}-u_{3,k}-i} \tag{3.188}$$

$$e^{im\mathcal{L}\sinh\theta_n} = \prod_{m\neq n}^{L}S_0(\theta_m,\theta_n)\prod_{j=1}^{K_2}\frac{\theta_n-u_{2,j}+\frac{i}{2}}{\theta_n-u_{2,j}-\frac{i}{2}} \tag{3.189}$$

Yet another example, the $SO(4)=SU(2)\times SU(2)$ sigma model described in section 3.6 is given precisely by two $SU(2)$ inhomogeneous Bethe equations (3.155) and (3.156) plus a middle node equation (3.157).

We will shortly see that this last example is highly instructive as it carries many resemblances with what we find in $\mathcal{N}=4$ SYM. Let us recall the spectacular successes which arose from the $S$-matrix approach in $\mathcal{N}=4$ SYM. The key idea is to look at operators like

$$\mathrm{tr}\,(ZZ\ldots ZXZ\ldots ZXZ\ldots ZZ)\;\longleftrightarrow\;|\uparrow\uparrow\ldots\uparrow\downarrow\uparrow\ldots\uparrow\downarrow\uparrow\ldots\uparrow\uparrow\rangle \tag{3.190}$$

as a vacuum (the $Z$ fields) on top of which particles (in this example the $X$ fields) propagate [38]. The symmetry of the $S$-matrix scattering these particles, also known as magnons, is the subgroup of the full $PSU(2,2|4)$ symmetry which leave the vacuum invariant. Actually the symmetry of $\mathcal{N}=4$ is the semi-direct product of $PSU(2,2|4)$ with the several gauge transformations. When we precisely keep track of these gauge transformations we arrive at the symmetry group for the $S$-matrix as being $SU(2|2)^2$ extended by two central charges [51, 52, 67, 68].

At 1-loop the central extension is irrelevant and therefore, before continuing, let us take a second look at (3.175-3.181) and make the following observation. We can think of these seven equations as two $SU(2|2)$ wings plus a middle node equation – the first three Bethe equations (3.175-3.177) and the last three (3.179-3.181) are the two $SU(2|2)$ inhomogeneous spin chain equations and the middle node equation (3.178) is the analogue of (3.185). To compare (3.184) and (3.185) with (3.175-3.181) we identify

$$L \leftrightarrow K_4\,, \tag{3.191}$$

$$\mathcal{L} \leftrightarrow L\,, \tag{3.192}$$

$$\theta_n \leftrightarrow u_{4,j}\,, \tag{3.193}$$

$$S_0(\theta_n,\theta_m) \leftrightarrow \frac{u_{4,k}-u_{4,j}+i}{u_{4,k}-u_{4,j}-i}\,. \tag{3.194}$$

On the other hand, at one loop we were also able to understand the seven $\mathcal{N}=4$ Bethe equations as stemming from the diagonalization a spin chain Hamiltonian with symmetry group $PSU(2,2,|4)$ of rank seven. Obviously

$$7 = 1 + 2 \times 3\,.$$

As already anticipated in the previous subsection we are able to understand the all loop equations in the $SU(2|2)$ language but to date no satisfactory all loop $PSU(2,2|4)$ $R$-matrix was found.

Let us continue our general discussion of the all loop S-matrix. To find this S-matrix we would proceed like in the previous section – first we would start to write the most general ansatz compatible with the index structure of the scattered states. This is the analogue of (3.139). A proper contraction of all the indices involved can be translated into the fancier statement that

$$[J,S]=0 \tag{3.195}$$

where $J$ are the residual bosonic generators (Lorentz and R-symmetry transformations) of $SU(2|2)$. Next we could try to constrain the several elements in the expression of the S-matrix – the analogue of $h$ and $g$ in (3.139) – by imposing the same symmetry equation (3.195) for the several fermionic generators. It turns out that this fixes (up to an overall function) the $(4^4)^2$ entries of this matrix [51, 52, 68]! This $S$-matrix was directly computed from worldsheet Feynmann diagrams at tree level in [69] and up to two loops in [70, 71] in a particular scaling limit [72] with perfect agreement with the S-matrix guessed by the bootstrap method based on the symmetries of the problem.

The next step in the study of the $SO(4)$ sigma model in section 3.6 was to impose the Yang-Baxter triangle relation on the S-matrix in order to constrain it even further. Notice that here everything is fixed before the analogue step! The only thing we can do is to check whether the $SU(2|2)$ extended S-matrix obeys or not the YB equation. There are two possible scenarios:

1. If it does not, it would mean that there are no $SU(2|2)$ extended integrable models because YB is a necessary (although not sufficient) condition.

2. If we are lucky enough and the $S$-matrix does obey YB, then this means we have a chance that the model is integrable. Notice that we have *not* proven in any way that the many body scattering factorizes in a product of two body S-matrices and thus we have not ensured the model to be integrable but rather we have checked an important necessary condition for this to be the case. (See [73] for an explicit check of factorizability of the $S$-matrix at strong coupling.)

Of course it is the second scenario which turns out to be realized [51, 52, 68].

The following step in the study of the $SO(4)$ sigma model was to fix the overall dressing factor multiplying the S-matrix. This is quite a subtle point from the $\mathcal{N} = 4$ point of view. For example the existence of crossing symmetry for a spin chain model seems hard to justify. On the other hand we have $AdS/CFT$. From this duality large spin chains with $L$ sites are dual to string states with angular momentum $L$. Such states are described in the light cone gauge by a two dimensional field theory living in a large circle of length proportional to $L$. This two dimensional theory is not relativistic and therefore crossing symmetry, if it exists, will not be as simple as (3.141). The analogue of this relation was found by Janik in [74]. The idea was to translate crossing relations like (3.141) into solid Hopf-algebraic relations using the anti-pode. Then, when studying the light-cone gauged string theory we realize that, although there is no obvious relativistic symmetry as for $SO(4)$ sigma model, the mathematical Hopf structure is still there and thus we can write the analogous of the crossing relation for this theory.

To solve it is not at all a trivial business since, as for the $SO(4)$ sigma model, there are infinitely many solutions [75] and one of them must be singled out. A proposal for such solution was made in [24][1].

Furthermore, the Dilatation operator is part of the symmetry algebra and it turns out that symmetry alone fixes the dispersion relation to

$$\epsilon_\infty(p) = \sqrt{1 + f(g) \sin^2 \frac{p}{2}}\,, \tag{3.196}$$

and there is convincing evidence that

$$f(g) = 16g^2 \tag{3.197}$$

for all values of the t'Hooft coupling.

Knowing the S-matrix and the dispersion relation of the several magnons we simply need to diagonalize (3.99) and read of the spectrum from (3.134). This was what we did to

[1] At this point we must again again refer to the disclaimer at the end of section 1.3.

arrive at (3.155)-(3.157). The same procedure applied to the Beisert S-matrix yields the Beisert-Staudacher equations [35] yielding the full asymptotic spectrum of $AdS_5/CFT_4$.

These Bethe equations are a deformation of the one-loop Bethe equations through the introduction of the map

$$x+\frac{1}{x}=\frac{u}{g}\ \ ,\ \ x^{\pm}+\frac{1}{x^{\pm}}=\frac{1}{g}\left(u\pm\frac{i}{2}\right)\,.$$

The BS equations then read

$$\begin{aligned}
1 &= \prod_{j=1}^{K_2}\frac{u_{1,k}-u_{2,j}+\frac{i}{2}}{u_{1,k}-u_{2,j}-\frac{i}{2}}\prod_{j=1}^{K_4}\frac{1-1/x_{1,k}x^{+}_{4,j}}{1-1/x_{1,k}x^{-}_{4,j}}\,,\\
1 &= \prod_{j\neq k}^{K_2}\frac{u_{2,k}-u_{2,j}-i}{u_{2,k}-u_{2,j}+i}\prod_{j=1}^{K_3}\frac{u_{2,k}-u_{3,j}+\frac{i}{2}}{u_{2,k}-u_{3,j}-\frac{i}{2}}\prod_{j=1}^{K_1}\frac{u_{2,k}-u_{1,j}+\frac{i}{2}}{u_{2,k}-u_{1,j}-\frac{i}{2}}\,,\\
1 &= \prod_{j=1}^{K_2}\frac{u_{3,k}-u_{2,j}+\frac{i}{2}}{u_{3,k}-u_{2,j}-\frac{i}{2}}\prod_{j=1}^{K_4}\frac{x_{3,k}-x^{+}_{4,j}}{x_{3,k}-x^{-}_{4,j}}\,,\\
\left(\frac{x^{+}_{4,k}}{x^{-}_{4,k}}\right)^{L} &= \prod_{j\neq k}^{K_4}\frac{u_{4,k}-u_{4,j}+i}{u_{4,k}-u_{4,j}-i}\,\sigma^2(x_{4,k},x_{4,j})\\
&\times \prod_{j=1}^{K_1}\frac{1-1/x^{-}_{4,k}x_{1,j}}{1-1/x^{+}_{4,k}x_{1,j}}\prod_{j=1}^{K_3}\frac{x^{-}_{4,k}-x_{3,j}}{x^{+}_{4,k}-x_{3,j}}\prod_{j=1}^{K_5}\frac{x^{-}_{4,k}-x_{5,j}}{x^{+}_{4,k}-x_{5,j}}\prod_{j=1}^{K_7}\frac{1-1/x^{-}_{4,k}x_{7,j}}{1-1/x^{+}_{4,k}x_{7,j}}\,,\\
1 &= \prod_{j=1}^{K_6}\frac{u_{5,k}-u_{6,j}+\frac{i}{2}}{u_{5,k}-u_{6,j}-\frac{i}{2}}\prod_{j=1}^{K_4}\frac{x_{5,k}-x^{+}_{4,j}}{x_{5,k}-x^{-}_{4,j}}\,,\\
1 &= \prod_{j\neq k}^{K_6}\frac{u_{6,k}-u_{6,j}-i}{u_{6,k}-u_{6,j}+i}\prod_{j=1}^{K_5}\frac{u_{6,k}-u_{5,j}+\frac{i}{2}}{u_{6,k}-u_{5,j}-\frac{i}{2}}\prod_{j=1}^{K_7}\frac{u_{6,k}-u_{7,j}+\frac{i}{2}}{u_{6,k}-u_{7,j}-\frac{i}{2}}\,,\\
1 &= \prod_{j=1}^{K_6}\frac{u_{7,k}-u_{6,j}+\frac{i}{2}}{u_{7,k}-u_{6,j}-\frac{i}{2}}\prod_{j=1}^{K_4}\frac{1-1/x_{7,k}x^{+}_{4,j}}{1-1/x_{7,k}x^{-}_{4,j}}\,.
\end{aligned}\tag{3.198}$$

The spectrum of all conserved charges is then given by the momentum carrying roots $u_4$ alone from

$$\mathcal{Q}_n=\sum_{j=1}^{K_4}\mathbf{q}_n(u_{4,j})\ \ ,\ \ \mathbf{q}_n=\frac{i}{n-1}\left(\frac{1}{(x^{+})^{n-1}}-\frac{1}{(x^{-})^{n-1}}\right)\tag{3.199}$$

and the spectrum of anomalous dimensions (or string states energies) follows from

$$E=2g\mathcal{Q}_2\,.\tag{3.200}$$

The BES dressing kernel [24] can be written in a simple integral form as [76]

$$\sigma_{\rm BES}(u_j,u_k)=e^{i\theta_{jk}}\ \ ,\ \ \theta_{jk}=\chi(x^{+}_j,x^{+}_k)+\chi(x^{-}_j,x^{-}_k)-\chi(x^{+}_j,x^{-}_k)-\chi(x^{-}_j,x^{+}_k)-(k\leftrightarrow j)\tag{3.201}$$

with

$$\chi(x,y) = -i \oint \frac{dz_1}{2\pi} \oint \frac{dz_2}{2\pi} \frac{1}{(x-z_1)(y-z_2)} \log \Gamma(1 + ig(z_1 + 1/z_1 - z_2 - 1/z_2)) \quad (3.202)$$

integrated over the contours $|z_1| = |z_2| = 1$. This kernel interpolates between

$$\sigma_{\rm BES}(u,v) \stackrel{\lambda\to 0}{\to} 1\,, \quad (3.203)$$

at weak coupling and

$$\sigma_{\rm BES}(u_j,u_k) \stackrel{\lambda\to\infty}{\to} \frac{1-1/x_k^+ x_j^-}{1-1/x_k^- x_j^+} \left( \frac{x_k^- x_j^- - 1}{x_k^- x_j^+ - 1} \frac{x_k^+ x_j^+ - 1}{x_k^+ x_j^- - 1} \right)^{i(u_k-u_j)} \equiv \sigma_{\rm AFS}(u_j,u_k)\,, \quad (3.204)$$

for large values of the t'Hooft coupling. $\sigma_{\rm AFS}$ is the AFS dressing kernel proposed in [66] in the study of the quantum string Bethe equations for the $AdS_5 \times S^5$ string. The BES kernel can be written in several ways. Above we used the integral representation of Dorey, Hofman and Maldacena [76]. Another useful writing of the BES kernel in terms of the charges introduced above (3.199) is

$$\sigma(u_j,u_k) = e^{i\theta_{jk}} \;\;,\;\; \theta_{jk} = \sum_{r=2,s=r+1} c_{r,s} \left[ \mathbf{q}_r(x_j)\mathbf{q}_s(x_k) - \mathbf{q}_r(x_k)\mathbf{q}_s(x_j) \right] \quad (3.205)$$

where the coefficients $c_{r,s}$ are given in [75, 24]

$$c_{r,s} = g\delta_{r+1,s} + \frac{1+(-1)^{r+s}}{\pi} \frac{(r-1)(s-1)}{(r+s-2)(s-r)} + \mathcal{O}\left(1/g\right)\,. \quad (3.206)$$

The leading order yields the AFS phase [66] and the next to leading order produces the HL factor [77]. Notice furthermore that the product of the BES kernel in (3.198) can be written as [66]

$$\prod_{j=1}^{K_4} \sigma_{\rm BES}(u_{4,k},u_{4,j}) = \exp\left( \sum_{r=2,s=r+1} i\, c_{r,s}\, \left( \mathbf{q}_r(x_{4,k})\mathcal{Q}_s - \mathbf{q}_s(x_{4,k})\mathcal{Q}_r \right) \right)\,, \quad (3.207)$$

Despite the fact that the $S$-matrix is known to all loops in the t'Hooft coupling we should always keep in mind that these equations are asymptotic and do not capture wrapping effects which start at order $g^{2L}$.

In the next section we will study an important limit of Nested Bethe ansatz equations and analyze some important dualities.

## 3.8 Solutions of Nested Bethe ansatz equations

The goal of this section is to provide us with some intuition about what are the configurations of Bethe roots emerging from systems of nested Bethe equations. We will see that there is an interesting regime where the Bethe roots organize into single roots, stacks, cuts and cuts of stacks. We shall consider two simple spin chain models which already capture all the non-trivial features found in more complex equations such as the Beisert-Staudacher Bethe ansatz.

### 3.8.1 $SU(2)_s$ spin chain. Scaling limit and condensates.

In this section we will consider the solutions to an $SU(2)$ spin $s$ whose Bethe equations are given in (3.169). The $s = \pm 1/2$ cases appear in the study of $\mathcal{N} = 4$ SYM at one loop. The choice $s = 1/2$ appears in the study of the $SU(2)$ sector in the computation of the anomalous dimensions of operators of the form (3.190) while for $s = -1/2$ we obtain an $SL(2)$ non-compact spin chain relevant for the diagonalization of operators made out of a complex scalar $Z$ and covariant derivatives $D$ in some chosen light-cone direction.

To study the solutions to (3.169) we take the log of these equations. Obviously

$$e^{ix} = e^{iy} \;\Rightarrow\; x = y + 2\pi n \tag{3.208}$$

so that for each $j = 1, \ldots, M$ we have a possible choice of the branch log parameterized by an integer $n_j$. We can thus write the Bethe equations as

$$F(u_j) - 2\pi n_j + \sum_{k \neq j} f(u_j - u_k) = 0 \tag{3.209}$$

where

$$F(u) = \frac{L}{i} \log \frac{u - is}{u + is} \;,\; f(u) = \frac{1}{i} \log \frac{u + i}{u - i} \,. \tag{3.210}$$

In the definitions of $f$ and $F$ we chose the branch of the log in such a way that these functions decay for large real arguments. For example, $f(u)$ is plotted in fig. 3.11a as a solid line. The dashed line in this figure corresponds to the curve $2/u$ which can be clearly seen to approximate $f(u)$ for large $|u|$.

We can now use our physical intuition to understand where the Bethe roots will organize themselves in the complex plane. To do so we think of (3.209) as the static equilibrium condition for the positions $u_j$ of $M$ particles. In this language $F(u_j)$ is an external force felt by each particle located at $u_j$ and $-2\pi n_j$ is a constant force exerted on particle $j$. Finally $f(u_i - u_k)$ is an interaction force by particle $k$ on particle $j$.

We first consider all mode numbers $n_j$ to be the same, $n_j = n > 0$, and take $s$ to be negative. We also ignore the self-interactions $f(u_j - u_k)$ in a first approach to the problem.

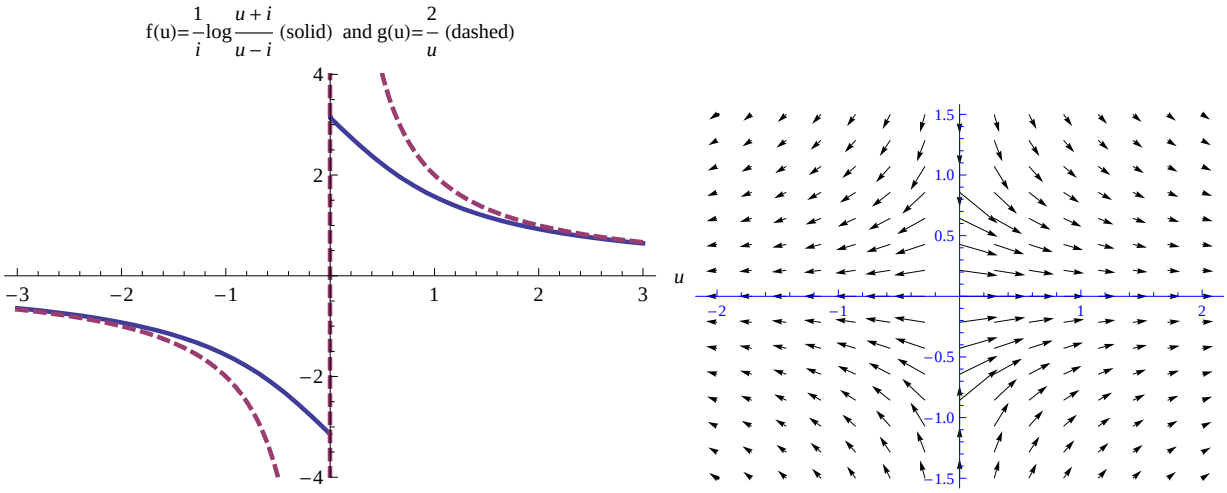


Figure 3.11: a) Left: Plot of $f(u) = \frac{1}{i}\log\frac{u+i}{u-i}$ for real values of $u$. If we think of $f(u)$ as a force then it is repulsive and falls of at log distances as $2/u$ typical of 2d coulomb interactions. b) Right: Vector plot of $(\Re(f(u)), \Im(f(u)))$ in the complex plane. We see that $f(u)$ repels in the horizontal direction and attracts in the vertical direction. Thus blobs of particles are squeezed vertically and stretched horizontally leading to real cuts as described in the text. See figure 3.14 for an example of such cut distribution. If the force is instead $-f(u)$ then it will create cuts oriented vertically because all arrows in this figure are reversed. See figure 3.13 for some typical configurations.

For negative $s$ the plot of the external force $F(u)$ will look exactly like a rescaled version of the plot of $f(u)$ since $F(u) = Lf(u/|s|)$ in this case. Thus, if we *sprinkle* some particles in a region of positive $u$, say at $u \sim 1$, the external force $F(u_j)$ will tend to push these particles and send them to $u = +\infty$. However each particle feels an additional force $-2\pi n$ pushing it towards the origin and therefore an equilibrium is reached. In figure 3.12 we plot the effective potential for $n = 1$ and $L = 10$. If there was no self interaction the particles would simply move towards the solid point in figure 3.12. Notice that they would stay in the real axis because the external force has negative/positive imaginary part in the upper/lower half-planes as seen in the vector plot in figure 3.11. This force compresses in the vertical direction while stretching in the horizontal one.

Now we turn on the self-interactions $f(u_j - u_k)$. The particles will start to repel each others with a force depicted in figure 3.11. This will spread the particles close to the equilibrium point marked in figure 3.12. By the same line of reasoning as before, the interaction between the several particles will distribute them along the real axis and constrain them to have zero imaginary part. In figure 3.14a an example of such configuration is plotted.

After this analysis it is clear what happens in the generic situation with several mode numbers. Let us group the $M$ mode numbers $\{n_j\}$ into $K$ large groups of identical integers $n^A$ with $A = 1, \ldots, K$. Then, particles belonging to the same group with the same integer

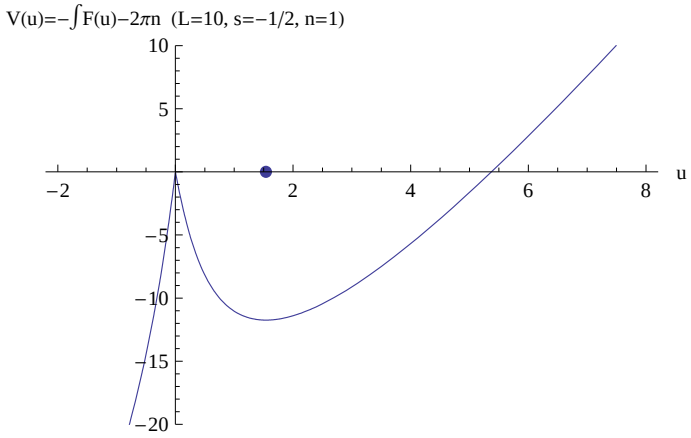


Figure 3.12: The external coulomb force pushing the particles to infinity is balanced by the constant force $-2\pi n$ coming from the mode numbers. In the figure we plot the effective potential and the corresponding equilibrium point as a solid dot for $L = 10$ and $n = 1$.

$n^A$ will feel the same external potential and therefore lie close the the same equilibrium point. The self-interaction between them will simply stretch the Bethe roots in the real direction close to this point. Thus, we will have $K$ groups of Bethe roots distributed along disjoint straight line segments in the real axis. As described below, when $K$ is large, the particles condense into $K$ real cuts.

Let us now turn to the $SU(2)$ case where $s = 1/2$ is positive. In this case we write the equilibrium condition as

$$\frac{L}{i}\log\frac{u_j + i/2}{u_j - i/2} - 2\pi n_j + \sum_{k\neq j}\frac{-1}{i}\log\frac{u_j - u_k - i}{u_j - u_k + i} = 0 \tag{3.211}$$

from which we see that the external force is the same as before. Therefore, in a first approximation, before considering the particle self-interactions everything is as above. Roots with the same mode number will position themselves at a minimum like the solid dot in figure 3.12.

However, when we bring the self-interaction between the roots $u_j$ and $u_k$ onto stage, the situation is quite different compared to what we had in the $SL(2)$ chain. Now, due to the minus sign in the last term in (3.211), this force is obtained from the vector plot in figure 3.11b by flipping the direction of all arrows. It is now attractive in the real direction and repulsive in the imaginary one. Thus a blob of roots close to the solid point in figure 3.12 will be squeezed horizontally and stretched vertically – we will therefore obtain a cut crossing the real axis perpendicular to it.

This cut will then bend and form an umbrella like shape as depicted in figure 3.13a [78]. This is again clear from the static equilibrium picture: the roots close to the real axis

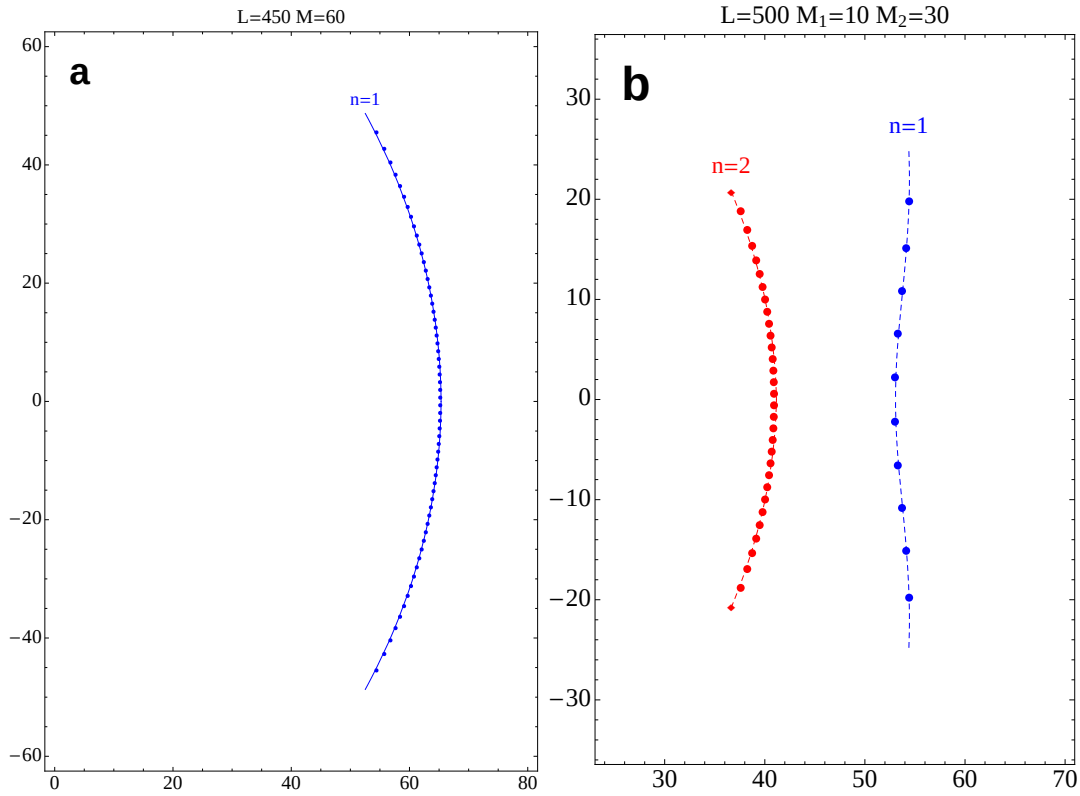


Figure 3.13: In the $SU(2)$ electrostatic pictures the particle attract in the horizontal direction and repel in the vertical direction. They also feel an external force with opposite behavior. Therefore the cuts will orient themselves vertically. When there is a single cut we find the umbrella shaped cuts as depicted in the left. This is because the roots close to the real axis *feel* the horizontal repulsive external force more strongly than the roots in the tails. For two cuts we obtain the picture in the right. The roots attract one another horizontally and therefore the middle of both cuts *want* to approach each other leading to the observed deformation of the cut to the right.

are closer to the origin and therefore feel a larger repulsive external force. Thus they will be pushed to the right more that the endpoints of the cut.

For the generic situation where the Bethe roots are grouped into $K$ sets of roots sharing the same mode numbers, we obtain $K$ umbrella cuts in the complex plane as represented in figure 3.13b for $K = 2$.

A natural question one might pose is *how bent are these umbrellas*? It depends dramatically on where we are trying to put these cuts. Recall that the position $u$ (interception with the real axis) of the cut is given in a first approximation by

$$\frac{L}{i}\log\frac{u+i/2}{u-i/2} = 2\pi n, \tag{3.212}$$

i.e. it is dictated by the choice of the mode number $n$. If $L$ is large there are two natural

choices for $n$:

$$n \sim L \ , \ \text{Choice A} \, ,$$
$$n \sim 1 \ , \ \text{Choice B} \, .$$

Choice A is the most common in the condensed matter literature. When $n \sim L$ the equilibrium position marked by the solid dot in fig. 3.12 is given by $u^* \sim 1$ and the umbrellas are almost absolutely straight vertical lines with Bethe roots separated by $i$. To see this consider a configuration with two Bethe roots in the general spin $s$ SU(2) system,

$$\left(\frac{u_1 + is}{u_1 - is}\right)^L = \frac{u_1 - u_2 + i}{u_1 - u_2 - i} \ , \ \left(\frac{u_2 + is}{u_2 - is}\right)^L = \frac{u_2 - u_1 + i}{u_2 - u_1 - i} \tag{3.213}$$

Let us write $u_{1,2} = u \pm vi$ where $u, v > 0$. Then it is clear that

$$\left|\left(\frac{u_1 + is}{u_1 - is}\right)^L\right| \ \begin{array}{l} \gg \ 1 \ , \ \text{for } s > 0 \\ \ll \ 1 \ , \ \text{for } s < 0 \end{array} \tag{3.214}$$

where by $\gg 1$ ($\ll 1$) we mean exponentially divergent (suppressed) in the parameter $L$. This means that the roots $u_1$ and $u_2$ must be such that the r.h.s of the first equation in (3.213) is also exponentially large (small) if $s > 0$ ($s < 0$). Thus we must have

$$|u_1 - u_2 - i| \ \ll \ 1 \ , \ \text{for } s > 0 \, , \tag{3.215}$$

or

$$|u_1 - u_2 + i| \ \ll \ 1 \ , \ \text{for } s < 0 \, . \tag{3.216}$$

Equation (3.215) means that the two Bethe roots in the $SU(2)$ chain are very rigidly bound and their separation is precisely $u_1 - u_2 = i$ with exponential precision. The same analysis could be carried for more than two roots and the conclusion would be that we can have bound states of $M$ particles separated by $i$ up to exponentially suppressed corrections:

$$u_j = u + ij \ , \ j = -\frac{M}{2}, \ldots, \frac{M}{2} \, . \tag{3.217}$$

Thus we see that the $SU(2)$ umbrellas in case $A$ are not bent at all.

On the other hand, equation (3.216) is impossible to satisfy because our starting hypothesis was that $u_1 - u_2 = 2vi$ with $v > 0$. This is precisely as predicted since for non-compact spin chains we expect the solutions to be real as explained above.

Next we consider case $B$. The mere existence of another scenario might seem odd at first since the argument leading to the conclusion that the roots must be separated by $i$

seems spotless. It is not so. The key difference between case $A$ and $B$ is that in the former the equilibrium position following from (3.212) is $u \sim 1$ whereas in the latter we have $u \sim L$. In case $B$ equation (3.214) does not follow and we have instead

$$\left(\frac{u_1+is}{u_1-is}\right)^L \simeq \exp\left(i\frac{2sL}{u}\right) = \mathcal{O}(1)\,. \tag{3.218}$$

Therefore the r.h.s of the first equation in (3.213) no longer needs to explode and we can have complex roots which are not rigidly separated by $i$.

These configurations are characterized by the fact that the Bethe roots scale with the size of the chain,

$$u_j \sim L\,. \tag{3.219}$$

Moreover, for the particles to condense into cuts, we also need large number Bethe roots. If $M_a$, with $a = 1, \ldots, K$, is the number of roots on each cut, the scaling limit is characterized by (3.219) together with

$$K_a/L \text{ fixed}\,. \tag{3.220}$$

This scaling limit was first introduced by Sutherland [79] and rediscovered in the context of the AdS/CFT correspondence in [78]. In this regime the momenta of the magnons is very small

$$\frac{1}{i}\log\frac{u_j+is}{u_j-is} \simeq \frac{2s}{u_j} = \mathcal{O}(1/L) \tag{3.221}$$

and so is the total energy of the state

$$E \simeq \sum_{j=1}^{M}\frac{1}{u_j^2+1/4} \sim \sum\sum_{j=1}^{M}\frac{1}{u_j^2} = \mathcal{O}(1/L) \tag{3.222}$$

which means that we are studying some semi-classical limit of low-lying long wave length fluctuations around the ferromagnetic vacuum with $E=0$. Indeed, in this limit, the theory is well described by a Landau-Lifshistz model with coupling $1/L$ [80, 81, 82].

In the rest of this section we will consider a simple configuration of Bethe roots corresponding to a single $SL(2)$ cut in the scaling limit. We will solve this problem by several different means, each of which will teach us something different, useful for the discussions that will follow. In the scaling limit the Bethe equations (3.209) become

$$\frac{1}{z_j} + \frac{2}{L}\sum_{k\neq j}\frac{1}{z_j - z_k} = 2\pi n_j \tag{3.223}$$

where $z_j = u_j/L$ and we consider $n_j = n$ for all $j$ so that

$$\frac{1}{z_j} + \frac{2}{L}\sum_{k\neq j}\frac{1}{z_j - z_k} = 2\pi n \tag{3.224}$$

and we will therefore obtain a single real cut as described above. Finally, the energy of the corresponding state is read from

$$E = \frac{2g^2}{L^2} \sum_{j=1}^{M} \frac{1}{z_j^2} \tag{3.225}$$

### Laguerre Polynomials

A very elegant way to find the exact position of the Bethe roots $\{z_j\}$ solution of (3.224) uses the baxter polynomial

$$Q(z) = \prod_{j=1}^{M} (z - z_j)\,.$$

By virtue of (3.223), this function obeys

$$\frac{1}{L}\frac{Q''(z_j)}{Q'(z_j)} = \frac{1}{L}\sum_{k\neq j}^{M} \frac{2}{z_j - z_k} = 2\pi n - \frac{1}{z_j} \tag{3.226}$$

which means that

$$R(z) = z\,Q''(z) - L\,Q'(z)\,(2\pi n z - 1) \tag{3.227}$$

is zero at $z = z_j$ for $j = 1, \ldots, M$. Since it is clearly an $M$-th order polynomial it must be equal to $Q(z)$ up to a multiplicative constant which can be easily fixed from the large $z$ asymptotics,

$$R(z) = -2\pi n L M Q(z)\,. \tag{3.228}$$

and therefore, combining these two equations we obtain

$$zQ''(z) - L\,Q'(z)\,(2\pi n z - 1) + 2\pi n L M Q(z) = 0 \tag{3.229}$$

which is nothing but the defining differential equation for the generalized Laguerre polynomials. Thus we obtain $Q(z) = L_M^{L-1}(2\pi n L z)$ so that the *exact* positions of the Bethe roots following from (3.224) are the zeros of the Laguerre polynomials,

$$L_M^{L-1}(2\pi n L z_j) = 0\,. \tag{3.230}$$

### Quadratic equation I

In this and the next subsections we will approach the solution of the electrostatic problem (3.224) using the resolvent

$$G(z) \equiv \frac{1}{L}\sum_{j=1}^{M} \frac{1}{z - z_j} \tag{3.231}$$

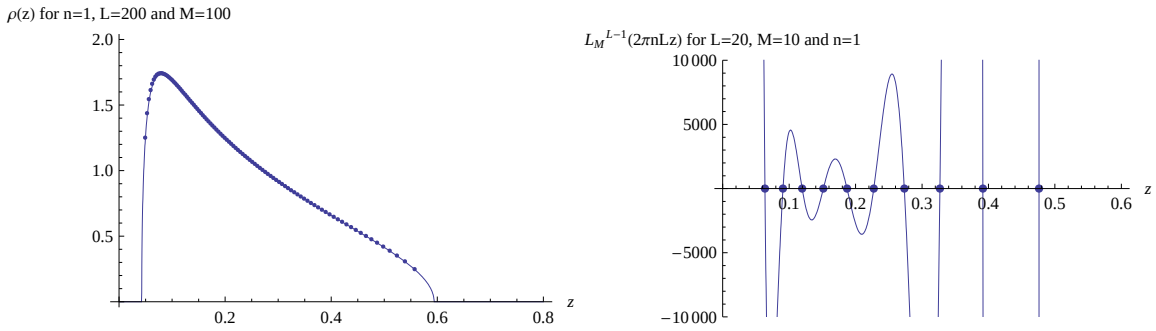


Figure 3.14: a) Left: Condensation of an $SL(2)$ cut into a dense cut. The solid line is the analytical prediction for the density of Bethe roots in the continuous limit whereas the dots are the numerical values. b) Right: The exact positions of the Bethe roots obeying $\frac{1}{z_j}+\frac{2}{L}\sum_{k\neq j}\frac{1}{z_j-z_k}=2\pi n$ are the zeros of the generalized Laguerre polynomials, $L_M^{L-1}(2\pi nLz_j)=0$.

instead of the Baxter polynomial $Q(z)$, the reason being that this quantity turns out to have a nicer large $M, L$ limit. Notice that the Bethe roots which were encoded in the zeros of $Q(z)$ are now located at the poles of $G(z)$. It is trivial to obtain a differential equation for $G(z)$. For example we can use the fact that

$$G(z)=\frac{1}{L}\frac{Q'(z)}{Q(z)} \tag{3.232}$$

together with the differential equation (3.229) for $Q(z)$ to obtain

$$G(z)^2-\left(2\pi n-\frac{1}{z}\right)G(z)+\frac{2\pi nM}{Lz}=-\frac{1}{L}G'(z) \tag{3.233}$$

In the large $L$ limit we can simply drop the r.h.s. and solve the quadractic equation to get

$$G(z)=\frac{1}{2}\left(2\pi n-\frac{1}{z}-\frac{1}{z}\sqrt{(2\pi nz-1)^2-\frac{8\pi nM}{L}z}\right) \tag{3.234}$$

Notice that in the continuous limit the poles in (3.231) condensed into the square root in this expression. Indeed, we can easily obtain the density of Bethe roots. Since

$$\frac{1}{x\pm i0}=P\frac{1}{x}\mp i\pi\delta(x) \tag{3.235}$$

we have

$$\rho(z)=-\frac{G(z+i0)-G(z-i0)}{2\pi i} \tag{3.236}$$

where

$$\rho(z)\equiv\frac{1}{L}\sum_{j=1}^{M}\delta(z-z_j)\,. \tag{3.237}$$

The resolvent (3.234) is discontinuous between the two branch-points of the square root and the discontinuity is

$$\rho(z) = \frac{1}{2\pi z}\sqrt{-(2\pi n z - 1)^2 + \frac{8\pi n M}{L} z}\,. \tag{3.238}$$

This density is plotted in figure (3.14) and seen to fit perfectly the corresponding numerics. Notice also that the energy (3.222) is simply given by

$$E = -\frac{2g^2}{L} G'(0) \tag{3.239}$$

so that using (3.234),

$$E = \frac{8g^2 n^2 \pi^2 M(M+L)}{L^2}\,. \tag{3.240}$$

Before moving to the next subsection let us mention a lateral comment concerning the square root in (3.234). It is always a delicate business to properly choose the square root branches. We have a cut uniting the two branch points as in figure 3.14a. At $z = +\infty$ we have

$$\frac{1}{z}\sqrt{(2\pi n z - 1)^2 - \frac{8\pi n M}{L} z} = 2\pi n - \frac{1}{z}\left(\frac{M}{L} + 1\right) + \mathcal{O}(1/z^2) \tag{3.241}$$

so that

$$G(z) = \frac{1}{z}\frac{M}{L} + \mathcal{O}(1/z^2) \tag{3.242}$$

which is precisely what we should get from the definition (3.231). On the other hand, in order to reach $z = 0$, we cross the cut in figure 3.14a and thus

$$\frac{1}{z}\sqrt{(2\pi n z - 1)^2 - 4G(0) z} = -\frac{1}{z} + (2\pi n - 2G(0)) + \mathcal{O}(z) \tag{3.243}$$

so that $1/z$ singularitiy does cancel in (3.234). Notice also that if we continue moving to the left until $z = -\infty$ we find

$$\frac{1}{z}\sqrt{(2\pi n z - 1)^2 - 4G(0) z} = 2\pi n - \frac{1}{z}\left(\frac{M}{L} + 1\right) + \mathcal{O}(1/z^2) \tag{3.244}$$

precisely like as (3.241) which is what we expect since there should be no singularity at $z = \infty$ and therefore $G(z)$ should be analytic for large $z$.

### Quadratic equation II

In this section we will consider a slightly different derivation of the quadractic equation (3.233) which does not rely on the differential equation (3.229) for $Q(z)$. The idea is to compute

$$G(z)^2 = \frac{1}{L^2}\sum_{j,k}^{M} \frac{1}{(z - z_j)(z - z_k)}\,. \tag{3.245}$$

Using the identity

$$\frac{1}{(z-y)(z-x)}+\frac{1}{(x-y)(z-y)}+\frac{1}{(y-x)(z-x)}=0 \tag{3.246}$$

and decomposing the sum in (3.245) into the diagonal $j=k$ part and the rest we obtain

$$G(z)^2=\frac{1}{L^2}\sum_{j=1}^{M}\frac{1}{(z-z_j)^2}+\frac{1}{L}\sum_{j=1}^{M}\frac{1}{z-z_j}\frac{1}{L}\sum_{k\neq j}^{M}\frac{2}{z_j-z_k} \tag{3.247}$$

The first term is precisely $-\frac{1}{L}G'(z)$ and in the second term we can replace the last sum by $2\pi n-\frac{1}{z_j}$ using Bethe equations (3.224)

$$G(z)^2=-\frac{1}{L}G'(z)+\frac{1}{L}\sum_{j=1}^{M}\frac{1}{z-z_j}\left(2\pi n-\frac{1}{z_j}\right) \tag{3.248}$$

and using again (3.246) to massage the last term we find

$$G(z)^2-\left(2\pi n-\frac{1}{z}\right)G(z)+\frac{G(0)}{z}=-\frac{1}{L}G'(z) \tag{3.249}$$

where $G(0)$ must be found by self-consistency. For example, plugging the large $z$ asymptotics (3.242) into this expression and collecting the $1/z$ leading powers in this expression we obtain

$$G(0)=2\pi nM/L\,, \tag{3.250}$$

and therefore (3.233) follows.

### Hilbert problem

The Bethe equations (3.224) in the scaling limit can be written as

$$2\int_{\mathcal{C}}P\frac{\rho(y)}{z-y}=V(z)\equiv 2\pi n-\frac{1}{z}\ ,\ z\in\mathcal{C} \tag{3.251}$$

with $\mathcal{C}$ begin the cut from $z=(a,b)$ where the Bethe roots condensed. Notice that the fact that in (3.224) we should not sum over $k=j$ translates into the principal part prescription in the scaling limit. Notice moreover that, in terms of the resolvent,

$$G(z)=\int_{\mathcal{C}}\frac{\rho(y)}{z-y} \tag{3.252}$$

the above equation is simply

$$2\not{G}(z)=V(z)\ ,\ z\in\mathcal{C} \tag{3.253}$$

where the slash stands for average above and below the cut. This is obviously a consequence of (3.235).

Before moving on let us point out that (3.234) clearly satisfies this equation because when we average $G(z)$ on the cut the square root cancels and we are left with $2\pi n - \frac{1}{z}$ which is precisely $V(z)$.

Equations of the form (3.251) are easily solved for a general $V(z)$ in the r.h.s. The solution is given by

$$G(z) = \int_a^b \frac{dy}{2\pi} \sqrt{\frac{(z-a)(z-b)}{(a-y)(y-b)}} \frac{V(y)}{z-y} \tag{3.254}$$

First let us check that this indeed solves (3.253). We compute $G(z+i0) + G(z-i0)$ so we use (3.235) applied to the $1/(z-y)$ factor in (3.254). Notice that since there is a square root multiplying this factor, for $G(z-i0)$ we obtain an extra minus sign and therefore it is the delta function part in (3.235) that survives and not the principal part! More precisely,

$$G(z+i0) + G(z+i0) = \int_a^b \frac{dy}{2\pi} \sqrt{\frac{(z-a)(z-b)}{(a-y)(y-b)}} V(y)(-2\pi i)\delta(z-y) = V(z)$$

and thus (3.254) is indeed the solution we seek.

Finally to find $a$ and $b$ we impose the asymptotics (3.242) on our solution to get

$$0 = \int_a^b \frac{dy}{2\pi} \frac{V(y)}{\sqrt{(a-y)(y-b)}} \ , \ \frac{M}{L} = \int_a^b \frac{dy}{4\pi} \frac{(2y-a-b)V(y)}{\sqrt{(a-y)(y-b)}} \tag{3.255}$$

Since our potential is an extremely simple analytic function all integrals in this section are trivially computed by first transforming the integral from $a$ to $b$ into a contour integral around the cut and then deforming this contour and computing the integral by residues. For example the last integral becomes

$$\frac{M}{L} = \frac{1}{2} \oint_{\mathcal{C}_0 \cup \mathcal{C}_\infty} \frac{dy}{4\pi} \frac{(2y-a-b)V(y)}{\sqrt{(a-y)(y-b)}} \tag{3.256}$$

where $\mathcal{C}_0$ and $\mathcal{C}_\infty$ are clockwise loops around $z=0$ and $z=\infty$. Thus we find

$$\frac{4M}{L} = \frac{a+b}{\sqrt{ab}} - 2\,, \tag{3.257}$$

while the first integral in (3.255) gives

$$0 = 2\pi n - \frac{1}{\sqrt{ab}}\,. \tag{3.258}$$

These relations yield

$$a,b=\frac{1}{2\pi n}\left(1+\frac{2M}{L}\mp 2\sqrt{\frac{M}{L}\left(1+\frac{M}{L}\right)}\right) \tag{3.259}$$

which are indeed precisely the branch points for the resolvent (3.234). Finally the integral (3.254) can be computed in the same way (there is simply an extra pole at $y=z$) yielding

$$G(z)=\frac{1}{2}\left(2\pi n-\frac{1}{z}-\frac{1}{z}\sqrt{\frac{(z-a)(z-b)}{ab}}\right) \tag{3.260}$$

which for the branchpoints given by (3.259) is precisely (3.234) found in the previous subsection.

### Finite Gap

In this subsection we consider a last approach to the problem (3.224), based on the finite gap method which was applied to the $SU(2)$ spin chain in the KMMZ paper [83]. The idea is to define a quasi-momenta

$$p(z)=G(z)+\frac{1}{2z} \tag{3.261}$$

and realize that in the scaling limit $e^{ip(z)}$ and $e^{-ip(z)}$ form a Riemann surface described by an hyper-elliptic algebraic curve. This is true not only for the single cut problem we are now interested in but also for a general $K$ cut solution so let us consider for a moment this more general scenario. For each cut $\mathcal{C}^A$ we have an integer mode number $n^A$ and

$$2\not{G}(z)=2\pi n^A-\frac{1}{z}\ ,\ z\in\mathcal{C}^A \tag{3.262}$$

or

$$p(z+i0)+p(z-i0)=2\pi n^A\ ,\ z\in\mathcal{C}^A\,. \tag{3.263}$$

This condition implies

$$e^{ip(z-i0)}=e^{-p(z+i0)}\ ,\ z\in\mathcal{C}^A\,, \tag{3.264}$$

which means that when we cross a cut $e^{\pm ip(z)}$ becomes $e^{\mp ip(z)}$ so that $e^{ip(z)}$ and $e^{-ip(z)}$ are indeed the two branches of a single analytic function taking values in a two-sheeted Riemann surface.

Notice also that another way to get rid of the mode numbers in (3.263) is to consider the derivative of the quasimomenta,

$$p'(z-i0)-(-p'(z+i0))=0\ ,\ z\in\mathcal{C}^A\,. \tag{3.265}$$

and thus $\pm p'(z)$ also define a two sheeted Riemann surface.

Before continuing the general discussion let us notice that (3.234) gives

$$p(z) = \frac{1}{2}\left(2\pi n - \frac{1}{z}\sqrt{(2\pi n z+1)^2 + \frac{8\pi n M}{L}z}\right) \tag{3.266}$$

so that when computing $p'(z)$ we kill the constant term outside the square root and therefore obtain an expression which simply changes sign when we cross the cut, exactly as required.

In the general $K$ cut scenario, $p'(z)$ is a meromorphic function in the Riemann surface with a double pole at $z = 0$ (by definition) which behaves as $1/\sqrt{z - x_k}$ close to each of the $2K$ branch points (because $p(z) \sim \sqrt{z - x_k}$). This means

$$p'(z) = \frac{g(z)}{z^2\sqrt{f(z)}} \tag{3.267}$$

where $f(z) = \prod_{j=1}^{2K}(z - x_k)$ and $g(z) = \sum_{j=0}^{N} c_j z^N$. Since at infinity, again by definition, we have $p'(z) \simeq \frac{1/2 - L/M}{z^2}$,

$$N = K\,.$$

In section 4.5.1 we will consider a very similar problem when studying the KMMZ string finite gap treatment [83]. Here let us go back to the problem we are interested in which corresponds to $K = 1$,

$$p'(z) = \frac{c_0 + c_1 z}{z^2\sqrt{(z-a)(z-b)}}\,. \tag{3.268}$$

This expression can be easily integrated and the several analytical properties following from the definition of the quasi-momenta fix the values of the four unknown constants [83].

Actually, for such elementary one-cut solutions it is simpler to guess the solution (3.254) without any computation, merely from the knowledge of the analytical properties of the quasi-momentum $p(z)$. Later in this thesis we will study the superstring algebraic curve and its semi-classical quantization. By then, such reasonings which rely heavily on the analytical properties of the quantities we aim at computing will be explained in detail.

### 3.8.2 $SU(2,1)$ spin chain. Bosonic duality and cuts of stacks.

In the previous section we analyzed the solutions to the Bethe equations (3.169) and saw that the Bethe roots can organize themselves into cuts and condensates. This qualitative picture remains valid for most simple Bethe ansatz equations of the form

$$e^{ip_j\mathcal{L}}\prod_{k\neq j}^{M} S(p_j, p_k) = 1\,. \tag{3.269}$$

However, as explained before, in general we need to deal with several entangled equations following from the diagonalization of (3.167) or (3.183). In particular the BS equations (3.198) are a set of seven equations whose complexity clearly exceeds (3.269).

To understand the scaling limit for Nested Bethe equations we consider a $SU(1,2)$ spin chain in the fundamental representation described by the following system of NBA equations[2]

$$e^{i\phi_1-i\phi_2} = -\frac{Q_1\left(u_{1,j}+i\right)}{Q_1\left(u_{1,j}-i\right)}\frac{Q_2\left(u_{1,j}-i/2\right)}{Q_2\left(u_{1,j}+i/2\right)} \ , \ j=1\dots K_1 \tag{3.270}$$

$$e^{i\phi_2-i\phi_3}\left(\frac{u_{2,j}-\frac{i}{2}}{u_{2,j}+\frac{i}{2}}\right)^L = -\frac{Q_2\left(u_{2,j}+i\right)}{Q_2\left(u_{2,j}-i\right)}\frac{Q_1\left(u_{2,j}-i/2\right)}{Q_1\left(u_{2,j}+i/2\right)} \ , \ j=1\dots K_2 \tag{3.271}$$

Here we are considering twisted (quasi-periodic) boundary conditions. From an algebraic Bethe ansatz point of view this corresponds to the diagonalization of a transfer matrix with the insertion, inside the trace, of an additional diagonal matrix [84] parameterized by

$$g=\text{diag}\left(e^{i\phi_1},e^{i\phi_2},e^{i\phi_3}\right)\in SU(1,2)\,. \tag{3.272}$$

The eigenvalues of the local conserved charges depend on $u_{2,j}$ only,

$$\mathcal{Q}_r=\sum_{j=1}^{K_a}\frac{i}{r-1}\left(\frac{1}{(u_{2,j}+i/2)^{r-1}}-\frac{1}{(u_{2,j}-i/2)^{r-1}}\right)\,. \tag{3.273}$$

We denote the $u_2$ roots by *middle node* roots and the $u_1$ roots by auxiliary roots.

First, consider only middle node excitations, $K_1=0\neq K_2$ in the scaling limit where $u\sim K_2\sim L\gg 1$. We use $x_{a,j}=u_{a,j}/L$ to denote the rescaled Bethe roots. In the absence of $x_{1,j}$ roots, the Bethe equations for the roots $x_{2,j}$ are precisely the same we discussed in the previous section for the $SL(2)$ spin chain apart from the presence of the extra twists. The Bethe roots organize themselves into $K$ cuts which we denote $\mathcal{C}_{23}^A$ with $A=1,\dots,K$ and on each of these cuts we have

$$2\pi n_{23}^A=\not{p}_2-\not{p}_3\ ,\ x\in\mathcal{C}_{23}^A\,. \tag{3.274}$$

where we introduced the quasi-momenta

$$\begin{aligned} p_1 &= -\frac{1}{2x}+G_1 \qquad -\phi_1\,,\\ p_2 &= -\frac{1}{2x}-G_1+G_2-\phi_2\,,\\ p_3 &= -\frac{3}{2x} \qquad -G_2-\phi_3\,, \end{aligned} \tag{3.275}$$

[2]These equations are exactly the same as for the $su(3)$ spin chain except for the sign of the Dynkin labels which makes the system simpler because the Bethe roots are in general real.

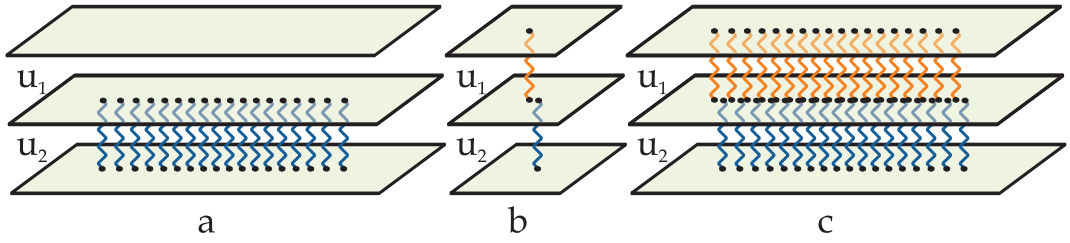


Figure 3.15: The *middle node* Bethe roots $u_2$ can condense into a line as depicted in figure 3.15a (The spins in this spin chain transform in a non-compact representation and thus the cuts are tipically real. For the $su(2)$ Heisenberg magnet the solutions are distributed in the complex plane as some *umbrella* shaped curves [78] as described in the previous section.). Roots of different types can form bound states, called stacks [49], as shown in figure 3.15b. The stacks behave as fundamental excitations and can also form cuts of stacks as represented in figure 3.15c.

and the resolvents are defined as before,

$$G_a(x) \int \frac{\rho_a(y)}{x-y} \quad , \quad \rho_a(y) = \frac{1}{L} \sum_{j=1}^{K_a} \delta(x - x_{a,j}) \, . \tag{3.276}$$

Of course, since we are considering no roots $x_{1,j}$ we have $G_1 = 0$ but for latter use we already introduced the appropriate general definition (3.275).

Next let us consider a state with only two roots $u_{2,1} \equiv u$ and $u_{1,1} \equiv v$ with different flavors, that is $K_1 = K_2 = 1$. Bethe equations then yield

$$u = \frac{1}{2} \cot \frac{\phi_1 - \phi_3 + 2\pi n}{2L} \ , \ v = u + \frac{1}{2} \cot \frac{\phi_1 - \phi_2}{2} \tag{3.277}$$

which tell us that if $n \sim 1$ we are in the scaling limit where $v \sim u \sim L$ and $v = u + \mathcal{O}(1)$ – the two Bethe roots form a bound state, called stack [49], and can be thought of as a fundamental excitation – see figure 3.15*b*. On the other hand we notice that, strictly speaking, for the usual untwisted Bethe ansatz with $\phi_a = 0$ the stack no longer exists.

Since the stack in figure 3.15*b* seems to behave as a fundamental excitation one might wonder whether there exists a cut with $K_1 = K_2$ roots of type $u_1$ and $u_2$, like in figure 3.15*c*, *dual* to the configuration plotted in figure 3.15*a*. To answer affirmatively to this question let us introduce a novel kind of duality in the Bethe ansatz techniques which we shall call *bosonic duality*.

Indeed, as we explain in detail in Appendix A, given a configuration of $K_1$ roots of type $u_1$ and $K_2$ roots of type $u_2$, we can write

$$2i \sin(\tau/2) \, Q_2(u) = e^{i\tau/2} Q_1(u - i/2) \tilde{Q}_1(u + i/2) - e^{-\tau/2} Q_1(u + i/2) \tilde{Q}_1(u - i/2) \, , \tag{3.278}$$

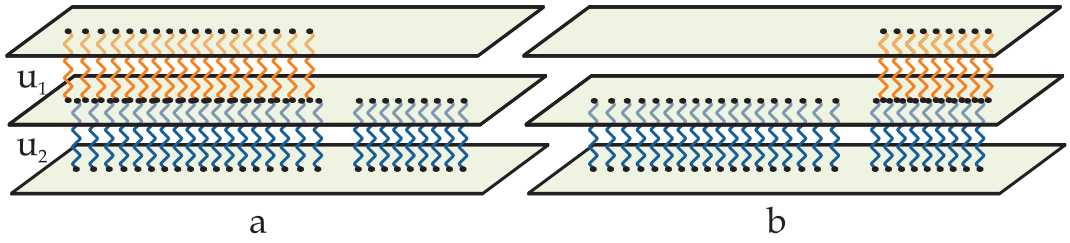


Figure 3.16: In the scaling limit, to the leading order, the bosonic duality reads $Q_2 \simeq Q_1\tilde{Q}_1$ with $Q_a = \prod_{k=1}^{K_a}(u - u_a)$. Thus, suppose we start with the configuration in figure 3.16a. Here the $K_1$ roots $u_1$ form a cut of stacks together with $K_1$ out of the $K_2$ middle node roots $u_2$. If we apply the bosonic duality to this configuration, the $K_2 - K_1$ new roots $\tilde{u}_1$ must be close to the roots $u_2$ which were previously *single* while the cut of stacks in figure 3.16a will become, after the duality, a cut of simple roots as depicted in figure 3.16b.

where

$$\tilde{Q}_1(u) = \prod_{j=1}^{\tilde{K}_1}(u - \tilde{u}_{1,j}) \ , \ \tilde{K}_1 = K_2 - K_1 \, ,$$

and $\tau = \phi_1 - \phi_2$. Moreover this decomposition is unique and thus defines unambiguously the position of the new set of roots $\tilde{u}_1$. Then, as we explain in Appendix A, the new set of roots $\{\tilde{u}_1, u_2\}$ is a solution of the same set of Bethe equations (3.168) with

$$\phi_1 \leftrightarrow \phi_2 \, .$$

Let us then apply this duality to a configuration like the one in figure 3.15*a* where the roots $u_2 \sim L$ are in the scaling limit and where there are no roots of type $u_1$, $K_1 = 0$. To the leading order, we see that the $\tilde{u}_1$ in (3.278) will scale like $L$ so that the $\pm i/2$ inside the Baxter polynomials can be dropped and we find $Q_2 \simeq \tilde{Q}_1$, that is

$$\tilde{u}_{1,j} = u_{2,j} + \mathcal{O}(1)$$

and therefore we will indeed obtain a configuration like the one depicted in figure 3.15*c*. Moreover the local charges (3.273) of this dual cut are exactly the same as those of the original cut 3.15*a* since they are carried by the *middle node* roots $u_2$ which are untouched during the duality transformation.

Finally, if we apply the duality transformation to some configuration in the scaling limit as represented in figure 3.16*a*, we find, by the same reasoning as above, $Q_2(u) \simeq Q_1(u)\tilde{Q}_1(u)$. Thus the dual roots $\tilde{u}_1$ will be close to the roots $u_2$ which were not yet part of a stack (the ones making the cut in the right in figure 3.16*a*). Hence, after the duality, we will obtain a configuration like the one in figure 3.16*b*.

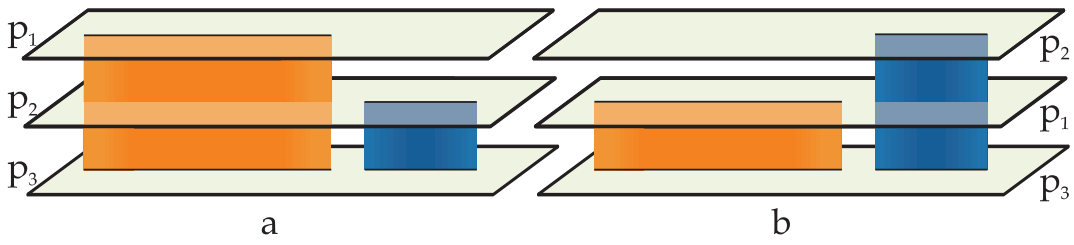


Figure 3.17: In the scaling limit the configurations in figure 3.16 condense into some disjoint segments, cuts, and we obtain a Riemann surface whose sheets are the quasi-momenta. In this continuous limit the duality corresponds to the exchange of the Riemann sheets.

We conclude that, in the scaling limit with a large number of roots, the distributions of Bethe roots condense into cuts in such a way that the quasi-momenta $p_{\rm i}$ introduced above become the three sheets of a Riemann surface, see figure 4$a$, obeying

$$2\pi n^A_{\rm ij} = p_{\rm i}(x+i0) - p_{\rm j}(x-i0)\ ,\ x \in \mathcal{C}^A_{\rm ij}\,. \tag{3.279}$$

when $x$ belongs to a cut joining sheets $i$ and $j$ with mode number $n^A_{\rm ij}$. The duality transformation amount to a reshuffling of sheets 1 and 2 of this Riemann surface[3] so that a surface like the one plotted in figure 3.17$a$ transforms into the one indicated in figure 3.17$b$.

## 3.9 BS equations in the scaling limit

In this section we will consider the scaling limit of the full Beisert-Staudacher equations. Stacks will be again the fundamental excitations and therefore we will also have cuts made out of stacks as in the previous section. Each stack corresponds to a different YM field or, in the dual theory language, to a string polarization. We represent the sixteen (physical) momentum carrying excitations in figure 3.18. In figure 3.19 we depict a possible configuration where the Bethe roots condensed into two square root cuts.

To make this pictures solid we should construct eight quasi-momenta such that the seven BS Bethe equations follow simply from

$$p_i(x+i0) - p_j(x-i0) = 2\pi n^A_{ij}\ ,\ x \in \mathcal{C}^A_{ij} \tag{3.280}$$

As described in the previous sections, if we find such quasi-momenta then $\{p'_i\}$ or $\{e^{ip_i}\}$ will define an eight-sheeted algebraic curve.

At weak coupling the definition of such quasi-momenta is absolutely obvious as it mimics the one in the previous section without any conceptual modification. We will

[3]This interpretation needs not be restricted to the scaling limit and can be made exact [15].

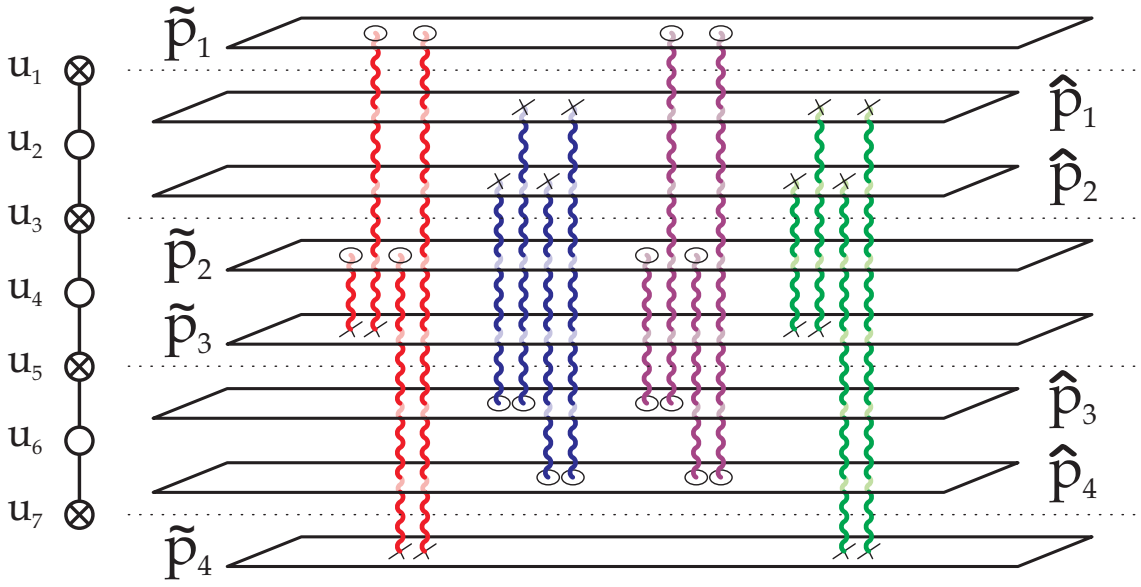


Figure 3.18: The several physical fluctuations in the string Bethe ansatz. The 16 elementary physical excitations are the stacks (they strictly speaking not bound states but, as discussed in the previous section, they behave like so in most aspects) containing the middle node root. From the left to the right we have four $S^5$ fluctuations (scalars in $\mathcal{N}=4$), four $AdS_5$ modes (covariant derivatives in $\mathcal{N}=4$) and eight fermionic excitations (fermions in $\mathcal{N}=4$). The bosonic (fermionic) stacks contain an even (odd) number of fermionic roots represented by a cross in the $psu(2,2|4)$ Dynkin diagram in the left.

instead consider the appropriate strong coupling scaling limit

$$\sqrt{\lambda} \sim u \sim K_a \sim L \gg 1\,.$$

which, as we will see latter, corresponds to the semi-classical string regime. In this limit we have

$$x^{\pm} = x \pm \frac{i}{2}\,\alpha(x) + \mathcal{O}\left(\frac{1}{\lambda}\right)$$

where

$$\alpha(x) \equiv \frac{4\pi}{\sqrt{\lambda}}\frac{x^2}{x^2-1}\,.$$

Thus, if we define the resolvents $G_a$ and $H_a$ for each type of roots

$$G_a(x) = \sum_{j=1}^{K_a} \frac{\alpha(y_{a,j})}{x-y_{a,j}}\,,\quad H_a(x) = \sum_{j=1}^{K_a} \frac{\alpha(x)}{x-y_{a,j}}\,, \tag{3.281}$$

and denote $\bar{H}_a(x) = H_a(1/x)$ and $\mathcal{J} = L/\sqrt{\lambda}$, we have the eight quasi-momenta we were

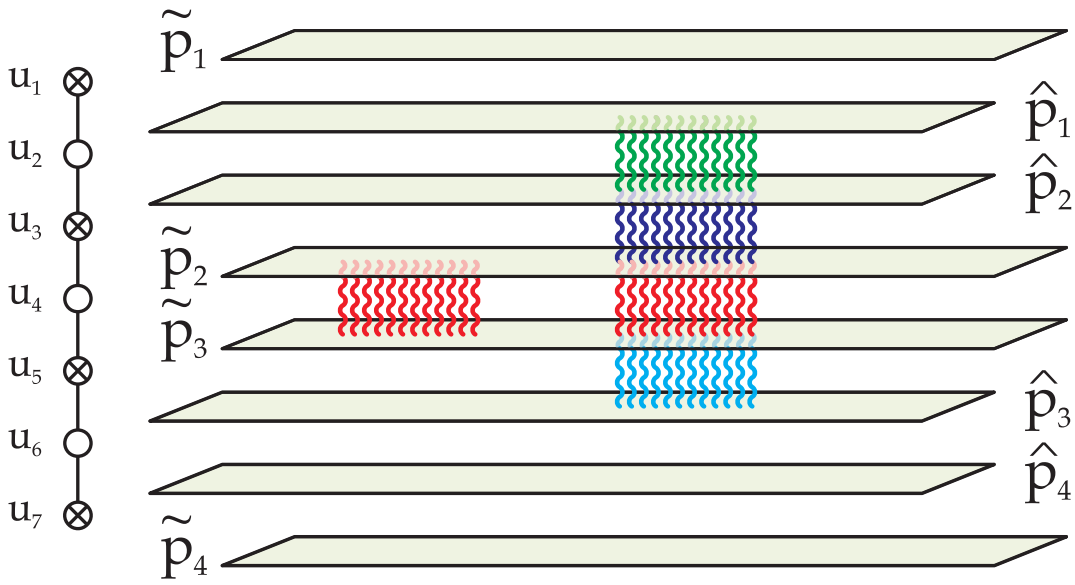


Figure 3.19: Cuts of stacks in the BS equations.

looking for as:

$$\begin{array}{l|l}
\hat{p}_1 = +\dfrac{2\pi\mathcal{J}x - G_4'(0)x}{x^2-1} - H_1 + H_2 + \bar{H}_2 - \bar{H}_3 & \tilde{p}_1 = +\dfrac{2\pi\mathcal{J}x + G_4(0)}{x^2-1} - H_1 - \bar{H}_3 + \bar{H}_4 \\
\hat{p}_2 = +\dfrac{2\pi\mathcal{J}x - G_4'(0)x}{x^2-1} - H_2 + H_3 + \bar{H}_1 - \bar{H}_2 & \tilde{p}_2 = +\dfrac{2\pi\mathcal{J}x + G_4(0)}{x^2-1} + H_3 - H_4 + \bar{H}_1 \\
\hat{p}_3 = -\dfrac{2\pi\mathcal{J}x - G_4'(0)x}{x^2-1} - H_5 + H_6 + \bar{H}_6 - \bar{H}_7 & \tilde{p}_3 = -\dfrac{2\pi\mathcal{J}x + G_4(0)}{x^2-1} - H_5 + H_4 - \bar{H}_7 \\
\hat{p}_4 = -\dfrac{2\pi\mathcal{J}x - G_4'(0)x}{x^2-1} - H_6 + H_7 + \bar{H}_5 - \bar{H}_6 & \tilde{p}_4 = -\dfrac{2\pi\mathcal{J}x + G_4(0)}{x^2-1} + H_7 + \bar{H}_5 - \bar{H}_4
\end{array} \tag{3.282}$$

The charges (3.199) in the scaling limit are then obtained from

$$G_4(x) = -\sum_{n=0}^{\infty} \mathcal{Q}_{n+1} x^n \,.$$

We can also write

$$\frac{2\pi}{\sqrt{\lambda}}\,\delta\mathcal{D} = \mathcal{Q}_2 \,.$$

For example let us consider $\tilde{p}_1(x+i0) - \hat{p}_1(x-i0)$ on a cut of roots $u_1$. We have

$$\tilde{p}_1(x+i0) - \hat{p}_1(x-i0) = \frac{G_4(0) + G_4'(0)x}{x^2-1} - H_2 - \bar{H}_2 + \bar{H}_4 \ , \tag{3.283}$$

which is precisely the expansion of the first equation in (3.198). Indeed

$$\frac{1}{i}\sum_{k=1}^{K_2}\log\frac{u_{1,j}-u_{2,k}+i/2}{u_{1,j}-u_{2,k}-i/2}\simeq\sum_{k=1}^{K_2}\frac{1}{u_{1,j}-u_{2,k}}=H_2(x_{1,j})+\bar{H}_2(x_{1,j}) \tag{3.284}$$

where in the last line we used the identity

$$\frac{1}{u-v}=\frac{\alpha(x(u))}{x(u)-x(v)}+\frac{\alpha(1/x(u))}{1/x(u)-x(v)}\,. \tag{3.285}$$

This explains the combination $H_2+\bar{H}_2$ in (3.283). Then we have

$$\frac{1}{i}\sum_{k=1}^{K_4}\log\frac{1-1/x_{1,j}x^+_{4,k}}{1-1/x_{1,j}x^-_{4,k}}\simeq\sum_{k=1}^{K_4}\frac{\alpha(x_{4,k})}{x_{4,k}(x_{1,j}x_{4,k}-1)}=-\frac{G_4(0)+G_4'(0)x_{1,j}}{x_{1,j}^2-1}-\bar{H}_4(x_{1,j}) \tag{3.286}$$

which matches the remaining terms in (3.283). In the same way we could check that the remaining six equations follow from the pairs of quasimomenta $(\hat{p}_1,\hat{p}_2),(\hat{p}_2,\tilde{p}_1),\dots$ as represented in figures 3.18, 3.19. In particular to obtain the expansion of the middle node equation in (3.198) the strong coupling AFS asymptotics (3.204) is used.

These quasi-momenta, built from the BS equations, have some very precise analytical properties which can be read from their definitions. For example, the large $x$ asymptotics of each quasi-momenta are easily obtained, e.g.

$$\hat{p}_1\simeq\frac{2\pi J+\mathcal{Q}_2-K_1+K_2}{x}+\mathcal{O}(1/x^2)\,. \tag{3.287}$$

There are other properties which are less trivial to realize. For example, from the definition of the quasi-momenta we see that these functions are swapped among themselves when $x\to 1/x$. We have

$$\hat{p}_2(1/x)=-\hat{p}_1(x)\,, \tag{3.288}$$

with similar expressions relating $\hat{p}_4(1/x)$ with $\hat{p}_3(x)$, $\tilde{p}_1(1/x)$ with $\tilde{p}_2(x)$ and $\tilde{p}_4(1/x)$ with $\tilde{p}_3(x)$.

It is also obvious that the quasi-momenta have simple poles at $x=\pm1$ because each individual term in (3.282) has such poles. What is much less trivial but can be again checked in a straightforward way is that the residues of the several quasi-momenta are synchronized as

$$\{\hat{p}_1,\hat{p}_2,\hat{p}_3,\hat{p}_4|\tilde{p}_1,\tilde{p}_2,\tilde{p}_3,\tilde{p}_4\}\simeq\frac{\{\alpha_\pm,\alpha_\pm,\beta_\pm,\beta_\pm|\alpha_\pm,\alpha_\pm,\beta_\pm,\beta_\pm\}}{x\pm1}\,. \tag{3.289}$$

We will find all these analytical properties from a completely different starting point, namely they will appear in the finite gap discussion of the superstring classical motion.

The fact that they follow from the strong coupling limit of the $\mathcal{N}=4$ SYM Bethe equations is a spectacular indication of the validity of the $AdS/CFT$ conjecture[4].

To end this section let us mention a particular solution of the BS equations in the scaling limit. We consider only roots $u_4$ to be excited. Thus we set to zero all resolvents except $H_4$ and $\bar{H}_4$ so that, from (3.282), we automatically find that the $AdS$ quasi-momenta $\hat{p}_i$ are given by

$$\begin{pmatrix} \hat{p}_1 \\ \hat{p}_2 \\ \hat{p}_3 \\ \hat{p}_4 \end{pmatrix} = \frac{2\pi\kappa x}{x^2-1} \begin{pmatrix} +1 \\ +1 \\ -1 \\ -1 \end{pmatrix} \tag{3.290}$$

where $\kappa = \Delta/\sqrt{\lambda}$ with $\Delta = J + \delta\mathcal{D}$ being the total anomalous dimension (or energy of the string state). To compute $H_4(x)$ for a general choice of mode numbers is of course unfeasible. However if we consider a simple scenario with for example a single mode number this can be easily done using the techniques explained in section 3.8.1. In this case, the Bethe equation we need to solve can be found from $\tilde{p}_2(x-i0) - \tilde{p}_3(x-i0)$ and reads

$$\frac{4\pi\mathcal{J}x + 2G(0)}{x^2-1} - 2H_4(x) = 2\pi n \;\Leftrightarrow\; \frac{4\pi\mathcal{J}x_j + 2G(0)}{x_j^2-1} - 2\sum_{k\neq j}\frac{\alpha(x_j)}{x_j - x_k} = 2\pi n\,. \tag{3.291}$$

This can be solved by the methods used in the previous section. In the process of computation it becomes clear that, if $G(0) = 2\pi m$, the choice $n = 2m$ greatly simplifies the final expressions. Thus, let us consider $n = 2m$ in what follows. Computing $H_4$ and plugging it into the definitions of the sphere quasi-momenta we obtain:

$$\begin{pmatrix} \tilde{p}_1 \\ \tilde{p}_2 \\ \tilde{p}_3 \\ \tilde{p}_4 \end{pmatrix} = 2\pi \begin{pmatrix} +\frac{x}{x^2-1}K(1/x) \\ +\frac{x}{x^2-1}K(x) - m \\ -\frac{x}{x^2-1}K(x) + m \\ -\frac{x}{x^2-1}K(1/x) \end{pmatrix}, \quad K(x) \equiv \sqrt{m^2x^2 + \mathcal{J}^2}. \tag{3.292}$$

Notice furthermore that the pole synchronization fixed the total anomalous dimension in terms of the angular momentum $\mathcal{J}$ and the mode number $m$ as

$$\kappa = \sqrt{m^2 + \mathcal{J}^2}\,. \tag{3.293}$$

For now let us put these results aside. In the next chapter we will see that they reappear nicely from a classical string integrability approach which is of course quite comforting.

[4]Although this is true, this is of course a huge distortion of the historical flow which mostly coincides with the most natural logical flow. Quasi-momenta with the properties described in the text were first found from string theory in [83, 85, 86, 87] and the SYM Bethe equations, in particular the BES kernel, were tuned to fit all available data, in particular to match the string classical limit. In this first part of the thesis we are assuming these equations to be derived/guessed without the knowledge of AdS/CFT and string theory.

## 3.10 Families of long-ranged integrable Hamiltonians

In this section we describe a spin chain toy model with long range interactions including wrapping interactions. It is probably not directly relevant to the study of $\mathcal{N}=4$ SYM but it is a nice application of the algebraic Bethe ansatz formalism and simple enough to be worth the detour.

Let us consider the standard $SU(2)$ spin chain transfer matrix $\hat{T}(u)$ whose spectrum is given by (3.76) where the Bethe roots obey the Bethe equations (3.77). Having diagonalized $\hat{T}$ we have automatically diagonalized *all* Hamiltonians obtained from this transfer matrix as explained in section 3.3. A particularly interesting choice is

$$\hat{H}(g) = \frac{1}{4i}\log\frac{\hat{T}(g^2)}{\hat{T}(0)} + h.c. \tag{3.294}$$

If we think of $g^2$ as being an expansion parameter then we have an infinite range Hamiltonian where, at each order $g^{2n}$ in perturbation theory, the interaction range is $n$. In the notations of [26] we have

$$\hat{H}(g) = \frac{g^2}{2}\sum_j \mathcal{H}_{j,j+1} + \frac{ig^4}{4}\sum_j [\mathcal{H}_{j,j+1}, \mathcal{H}_{j+1,j+2}] + \dots \tag{3.295}$$

where $\mathcal{H}_{j,j+1} = 1 - \mathcal{P}_{j,j+1}$. The spectrum of this Hamiltonian is then given by (3.294) where we simply replace the operators $\hat{T}(\cdot)$ by the corresponding eigenvalues $T(\cdot)$ to get

$$\begin{aligned} E &= \frac{1}{4i}\sum_{j=1}^{M}\log\left(\frac{u_j+\frac{i}{2}-g^2}{u_j-\frac{i}{2}-g^2}\frac{u_j-\frac{i}{2}}{u_j+\frac{i}{2}}\right) \\ &+ \frac{1}{4i}\log\left[1+\left(\frac{g^2}{g^2+i}\right)^L\prod_{j=1}^{M}\frac{u_j-\frac{3i}{2}-g^2}{u_j-\frac{i}{2}-g^2}\frac{u_j-\frac{i}{2}-g^2}{u_j+\frac{i}{2}-g^2}\right] + c.c.\,. \end{aligned} \tag{3.296}$$

The first term comes from the first term in (3.76). It gives a contribution to the energy of the form $\sum\epsilon(p_j)$, that is a sum of the dispersion relations of $M$ individual magnons interacting through (3.77). When written in terms of $p$,

$$\epsilon(p) = \frac{1}{2i}\log\left(\frac{1-2g^2e^{-i\frac{p}{2}}\sin\frac{p}{2}}{1-2g^2e^{+i\frac{p}{2}}\sin\frac{p}{2}}\right) = 2g^2\sin^2\frac{p}{2} + \dots + \frac{(2g^2)^n}{n}\sin\frac{np}{2}\sin^n\frac{p}{2} + \dots \tag{3.297}$$

The second term in (3.296), which comes from the second term in (3.76), is identically zero up to order $g^{2L}$ – precisely when wrapping interactions appear! Thus, at order $g^{2L}$ the energy is given by a sum of dispersion relations of the form (3.297) plus this wrapping

term, which entangles all $M$ magnons and is not writable as a sum of individual dispersion relations. In terms of the several momenta we have

$$E = \sum_{j=1}^{M} \epsilon(p_j) + g^{2L} \frac{1}{4i} \left[ i^{-L} \prod_{j=1}^{M} \left( 2e^{-2ip_j} - e^{-ip_j} \right) - c.c. \right] + \mathcal{O}(g^{2L+1}) \ . \tag{3.298}$$

For example, for two magnons we get

$$E(p,k) \ = \ \epsilon(p) + \epsilon(k) + g^{2L} \left( s(p) + s(k) - \frac{s(0)}{2} - 2s(p+k) \right) + \mathcal{O}(g^{2L+2}) \ , \tag{3.299}$$

where $s(x) \equiv \sin(p + k + L\pi/2 + x)$. It is clear that this correction is not of the form $\delta\epsilon(p) + \delta\epsilon(k)$. This was expected since at order $g^{2L}$ the interaction range covers the entire chain and the notion of asymptotic region where one can safely measure the dispersion relation of each magnon is destroyed [38].

More generically we can easily generate (long-ranged) integrable Hamiltonians by considering

$$\hat{H} = \frac{1}{4i} \sum_{n=1}^{\infty} a_n \frac{g^{2n}}{n!} \frac{d^n}{d\lambda^n} \log \hat{T}(\lambda) \Big|_{\lambda=0} + h.c. \tag{3.300}$$

The spectrum of such Hamiltonians is immediately given by this expression with the operator $\hat{T}(\lambda)$ replaced by the corresponding eigenvalue (3.76). At order $g^{2n}$ these Hamiltonians are local with interactions of range $n$. If we truncate the expansion at a given order $m$ by setting $a_{n>m} = 0$, then for chains of length larger than $m$ we have no wrapping interactions and the energy is simply given by a sum of dispersion relations $\sum_j \epsilon(p_j)$, with[5]

$$\epsilon(u) = \frac{1}{2i} \sum_{n=1}^{\infty} \frac{a_n \, g^{2n}}{n} \left( \frac{1}{(u - i/2)^n} - \frac{1}{(u + i/2)^n} \right) \tag{3.301}$$

If, on the other hand, we consider an infinie sum or, alternatively, if we truncate the expansion in $g^2$ at an order $m > L$, the spectrum (starting at wrapping order $g^{2L}$) will no longer be a sum of individual dispersion relations. In particular, precisely at order $g^{2L}$ we obtain

$$E = \sum_{j=1}^{M} \epsilon(u_j) + \frac{g^{2L}}{4i} \left[ \frac{a_L}{i^L} e^{-iP} \prod_{j=1}^{M} \frac{u_j - 3i/2}{u_j + i/2} - c.c. \right] + \mathcal{O}(g^{2L+2}) \tag{3.302}$$

where the second term takes into account the wrapping interactions. It is interesting to notice that for all these families of long ranged Hamiltonians the expression for the wrapping interactions is quite simple and absolutely universal. The example (3.294) we

[5] If the $a_n$ are not real – which from the definition 3.300 is a perfectly reasonable possibility – we should take the real part of this expression.

considered corresponds to $a_n = 1$ but as we see any choice of $a_n$ will lead to a solvable problem. A particularly funny example would be

$$\hat{H} = \frac{1}{2i}\sum_{n=1}^{\infty} C_n \frac{g^{2n}}{(2n-1)!}\frac{d^{2n}}{d\lambda^{2n}} \log \hat{T}(\lambda)\Big|_{\lambda=0} + h.c.\,,$$

with $C_n$ the Catalan numbers, for which we find the curious expression

$$\epsilon(u) = \frac{g}{i}\left(\frac{1}{X^+(u)} - \frac{1}{X^-(u)}\right)\ ,\ X^{\pm}(u) \equiv \frac{u \pm \frac{i}{2} + \sqrt{\left(u \pm \frac{i}{2}\right)^2 - 4g^2}}{2g}$$

for the dispersion relation. As a function of the Bethe roots this is precisely the dispersion relation appearing in the BDS equations [43] and even in the full AdS/CFT Bethe equations [35]. However, unfortunately, as a function of the magnon momenta this is not the same as (3.196) because the relation between $u$ and $p$ in our toy models is always of the form (3.78). In other words, although the desired dispersion relation can be easily obtained, the Bethe roots are always quantized via the usual Heisenberg spin chain Bethe equations.

We can generalize this construction of long ranged Hamiltonians for other symmetry groups as well. A particularly curious example arises when we consider non-compact spin chains. For example, for the $SL(2)$ spin chain we have [88, 36]

$$T_{sl(2)}(\lambda) = \prod_{j=1}^{M}\frac{\lambda - u_j - i/2}{\lambda - u_j + i/2} + \sum_{n=1}^{\infty}\left(\frac{\lambda}{in+\lambda}\right)^L \prod_{j=1}^{M}\frac{(\lambda - u_j - i/2)^2}{\left(\lambda - u_j + \frac{2n-1}{2}i\right)\left(\lambda - u_j + \frac{2n+1}{2}i\right)} \tag{3.303}$$

with the Bethe equations, following from canceling the poles in this expression, reading

$$\left(\frac{u_j + i/2}{u_j - i/2}\right)^L = \prod_{k\neq j}^{M}\frac{u_j - u_k - i}{u_j - u_k + i} \tag{3.304}$$

which differ from (3.77) by a simple sign in the r.h.s. Again, by expanding the log of the transfer matrix around $\lambda = 0$ we see that only the first term contributes until the $L$'th derivative is taken. Thus if we consider an Hamiltonian of the form (3.300) we have, up to order $g^{2L}$, the energy as a sum of the same dispersion relations (3.301). In particular if the constants $a_n$ are algebraic numbers then so will be $\sum_j \epsilon(u_j)$ when truncated to order $g^{2L}$ because the solutions to (3.304) are clearly also algebraic (complex) numbers.

However, precisely at order $g^{2L}$ the second term in (3.303) starts contributing and we find

$$E = \sum_{j=1}^{M}\epsilon(u_j) + \frac{g^{2L}}{4i}\left[\frac{a_L}{i^L}e^{-iP}\sum_{n=1}^{\infty}\frac{1}{n^L}\prod_{j=1}^{M}\frac{(u_j + i/2)^2}{\left(u_j - \frac{2n-1}{2}i\right)\left(u_j - \frac{2n+1}{2}i\right)} - c.c.\right]. \tag{3.305}$$

This new wrapping term differs from the one computed for the compact groups $SU(N)$ by the fact that it is given by an infinite sum of terms. Thus even if $u_j$ and $a_n$ are perfectly algebraic numbers the energy of this state will only be algebraic up to order $g^{2L}$, when this infinite sum will give a transcendental contribution!

Let us consider a few examples. We chose $a_L = 1$ for simplicity. For $L = 4$ the one magnon state with momentum $2\pi/4$ will be corrected to

$$E = \epsilon(p) - g^6 \left(1 - \zeta(3)\right) + \mathcal{O}(g^8)$$

while for example for a two magnon state with $L = 5$ and momenta[6] $p_1 = -p_2 = p = 2\pi/6$ we get

$$E = \epsilon(p) + \epsilon(-p) + \frac{g^{10}}{4}\left(1 - 2\zeta(3) + 2\zeta(5)\right) + \mathcal{O}(g^{12})$$

In (3.306) we listed a couple of additional examples with $a_n = 1$

| $L$ | $u_{1,2}$ | $\epsilon(p_1) + \epsilon(p_2)$ | $E_{wrapping}(p_1, p_2)$ |
|---|---|---|---|
| 3 | $\frac{\sqrt{3}}{5} \pm \frac{\sqrt{7}}{10}$ | $\frac{11g^2}{8} + \frac{13\sqrt{3}g^4}{32} - \frac{5g^6}{6}$ | $\frac{1}{32}\left(-26 + 3\pi^2 - 4\zeta(3)\right) g^6$ |
| 4 | $\frac{1}{3} \pm \frac{\sqrt{7}}{6}$ | $\frac{5g^2}{4} - \frac{g^4}{8} - \frac{19g^6}{24} + \frac{3g^8}{2}$ | $\left(\frac{41}{32} - \frac{5\pi^2}{48} - \frac{\pi^4}{360}\right) g^8$ |
| 6 | $\pm\frac{1}{2} + \frac{\sqrt{2}}{2}$ | $g^2 + \frac{g^4}{\sqrt{2}} - \frac{g^6}{3} - \sqrt{2}g^8 - \frac{4g^{10}}{5} + \frac{5\sqrt{2}g^{12}}{3}$ | $\frac{-1}{2\sqrt{2}}\left(7 - 4\zeta(3) - 2\zeta(5)\right) g^{12}$ |

(3.306)

Although, this model is not immediately related to the non-compact sector of the AdS/CFT Bethe equations which are much more complicated than (3.304), it is still interesting to see that transcendentality very naturally appears due to the non-compact character of the transfer matrix. In particular, if an extra level of hidden degrees of freedom is to be discovered then the transcendental numbers present in the dressing factor could be an important hint. A more fundamental $PSU(2,2|4)$ symmetric transfer matrix in the field strength representation would also be given by an infinite sum of terms since the representation is infinite dimensional. It would be spectacular if a relatively simple extended transfer matrix with some extra degrees of freedom included and only simple algebraic expressions could lead to the intricate structure of the full dressing factor where transcendental numbers abound. Probably the correct place to try to reverse engineer and find this extra level of hidden particles is the transfer matrix rather than the Bethe equations.

[6]For two magnon with opposite momenta the $sl(2)$ equations are trivially solved. The effect of the second magnon is simply to renormalize $L \to L + 1$. Thus we obtain $p_1 = -p_2 = \frac{2\pi n}{L+1}$ for the two magnon state with opposite symmetric momenta.

# Part III

# Algebraic curves and semi-classics

# Chapter 4

# Integrability in superstring theory and algebraic curves

In this chapter we review classical superstring integrability. More precisely, in section 4.2, we explain how classical integrability appears due to the existence of a flat connection $A(x)$ dependent on an arbitrary spectral parameter $x \in \mathbb{C}$ [10]. Flatness of this current will then allow us to build an infinite set of conserved charges encoded in some algebraic curves [83, 85, 86, 87] (see also [89, 55] for more gauge theory oriented works). In section 4.3 we will present a short overview of the general physical picture inherent to the finite gap construction and in section 4.4, we resume our rigorous treatment and describe the algebraic curve construction. All the remaining sections rely heavily on this formalism so it is important to review it in some detail. The last sections are devoted to the study of the $SU(2)$ sector consisting of strings moving in $R \times S^3 \subset AdS_5 \times S^5$. In particular the Giant Magnon solution [90] is discussed in sec. 4.5.2. Before all that, in the next section, we will recall that the appearance of Rieman surfaces as the classical limit of a quantum system is something rather universal and can be seen in the simplest examples.

## 4.1 1D Quantum Mechanics

As a warm-up for the forthcoming sections let us consider a one-dimensional non-relativistic particle in a smooth potential $V(x)$. In terms of the quasi-momenta

$$p(x) \equiv \frac{\hbar}{i}\frac{\psi'(x)}{\psi(x)}\,,$$

the Schrodinger equation for the wave function $\psi$ takes the Riccati form

$$p^2 - i\hbar p' = 2m\,(E - V)\ . \tag{4.1}$$

What do we know about $p(x)$? It is an analytical function which has, by definition, a pole with residue

$$\alpha = \frac{\hbar}{i} \tag{4.2}$$

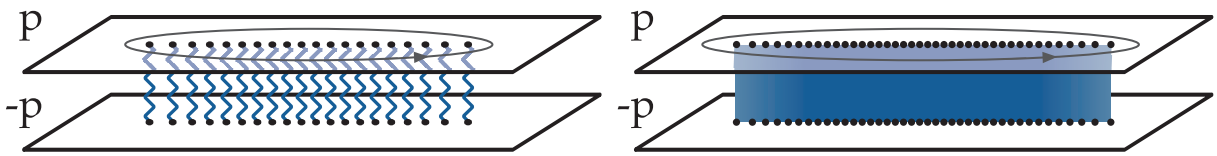


Figure 4.1: Analytical structure of a quasi-momenta $p(x)$ of a one dimensional system. Left: for low lying states $p(x)$ is a collection of poles. Right: for high energy states the poles condense into a square root branch cut.

at each of the zeros of the wave function. For the $N$-th excited state we will have $N$ poles. On the other hand, for very excited states, the right hand side in (4.1) is much larger than $\hbar$ and

$$p \simeq p_{\rm cl} \equiv \sqrt{2m\,(E-V)}$$

describes now a two-sheet Riemann surface. What happened was that, as $N \to \infty$, the poles in $p(x)$ became denser and denser, condensing in a square root cut. Thus, in the semiclassical limit we retrieve the Bohr-Sommerfeld quantization

$$\frac{1}{2\pi\hbar}\oint_{\mathcal{C}} p_{\rm cl}(z)\,dz \simeq \frac{1}{2\pi\hbar}\oint_{\mathcal{C}} p(z)\,dz = N\,, \tag{4.3}$$

where $\mathcal{C}$ encircles the cut. The first integral is precisely the action variable of the classical motion. To anticipate the forthcoming notation we name such integrals *filling fractions*.

Let us now consider the simplest possible potential, namely the harmonic oscillator for which $V = \frac{m\,\omega^2 x^2}{2}$. From (4.1) it follows that $p(x) = im\omega x + \mathcal{O}(1/x)$. Since the quasi-momentum is a meromorphic function with $N$ poles on the real axis, it must be given by

$$p(x) = im\omega x + \frac{\hbar}{i}\sum_{i=1}^{N}\frac{1}{x-x_i}\,.$$

Then, from the large $x$ behavior in (4.1) we read immediately

$$E = \hbar\omega\left(N+\frac{1}{2}\right) \tag{4.4}$$

while from the cancelation of each of the $x_i$ poles in the same equation we get

$$x_i = \frac{\hbar}{\omega m}\sum_{j\neq i}^{N}\frac{1}{x_i - x_j} \tag{4.5}$$

which strongly resembles the equations one finds in the Bethe ansatz context. Its solution is given by the zeros of the Hermite polynomials, $H_N\left(\sqrt{\frac{m\omega}{\hbar}}x_i\right) = 0$, as can be easily derived as in section 3.8.1.

## 4.2 The $AdS_5 \times S^5$ flat connection

In this section we review the work of [10] where integrability first arose for the full $AdS_5 \times S^5$ string. To better understand how non-trivial the emergence of integrability is let us consider a deformation of the Metseav-Tseytlin action (2.4) to

$$S = \frac{\sqrt{\lambda}}{4\pi} \int \text{str} \left( J^{(2)} \wedge *J^{(2)} - \kappa J^{(1)} \wedge J^{(3)} \right) + \Lambda \wedge \text{str}\, J^{(2)} \,, \tag{4.6}$$

where $J^{(n)}$ are the $\mathbb{Z}_4$ components of $J = -g^{-1}dg$ obtained explicitly using (2.2). The equations of motion are still given by (2.7),

$$d * k = 0 \,, \tag{4.7}$$

with $k = g^{-1}Kg$ where now

$$K = J^{(2)} + \frac{\kappa}{2} * J^{(1)} - \frac{\kappa}{2} * J^{(3)} - *\Lambda \,.$$

Since only the capital currents have a neat $\mathbb{Z}_4$ decomposition as described in section (2.2) it is useful to recast (4.7) using the large current $K$,

$$d * K = J \wedge *K + *K \wedge J \,. \tag{4.8}$$

Moreover it will also be important to use the flatness of the $PSU(2,2|4)$ current,

$$dJ = J \wedge J \,, \tag{4.9}$$

which simply follows from the form of the current $J = -g^{-1}dg$. Next we decompose these relations using the $\mathbb{Z}_4$ grading so that (4.9) splits into four equations

$$dJ^{(n)} = \sum_{p+q=n \mod 4} J^{(p)} \wedge J^{(q)} \tag{4.10}$$

while (4.8) gives

$$\begin{aligned}
0 &= J^{(3)} \wedge *J^{(2)} + *J^{(2)} \wedge J^{(3)} - \kappa J^{(3)} \wedge J^{(2)} - \kappa J^{(2)} \wedge J^{(3)} && (4.11)\\
d * J^{(2)} &= J^{(0)} \wedge *J^{(2)} + *J^{(2)} \wedge J^{(0)} + \kappa J^{(1)} \wedge J^{(1)} - \kappa J^{(3)} \wedge J^{(3)} && (4.12)\\
0 &= J^{(1)} \wedge *J^{(2)} + *J^{(2)} \wedge J^{(1)} + \kappa J^{(1)} \wedge J^{(2)} + \kappa J^{(2)} \wedge J^{(1)} && (4.13)
\end{aligned}$$

where we already used (4.10) to eliminate $dJ^{(1)}$ and $dJ^{(3)}$ in (4.11) and (4.13). Using $*A \wedge B = -A \wedge *B$, valid for one-forms, it is easy to see that the projection of (4.8) into the zero-th component yields nothing.

We now want to find a connection $A(x)$ which should be flat on the equations of motion,

$$dA(x) = A(x) \wedge A(x)\,, \tag{4.14}$$

and depend on a generic complex number $x$ which we denote by spectral parameter. Before delving into the technical details let us explain why finding such current is indeed remarkable and indicates the model to be (at least classically) integrable. The key idea is that, using this flat connection, we can define the monodromy matrix

$$\Omega(x) = \mathrm{Pexp} \oint_{\gamma} A(x) \tag{4.15}$$

where $\gamma$ is any path starting and ending at some point $(\sigma, \tau)$ and wrapping the worldsheet cylinder once. Fatness of the connection ensures path independence so we can choose $\gamma$ to be the constant $\tau$ path,

$$\Omega(x) = \mathrm{Pexp} \int_0^{2\pi} d\sigma A_\sigma(x) \tag{4.16}$$

Moreover, placing this loop at some other value of $\tau$ just amounts to a similarity transformation of the monodromy matrix. Thus we conclude that the eigenvalues of $\Omega(x)$ are time independent. Since they depend on a generic complex number $x$, we have obtained in this way an infinite number of conserved charges (by, for example, taylor expanding the eigenvalues around a particular point $x$) thus assuring integrability! For example, as mentioned in section 3.4, if these charges survive quantization – which is by now established beyond reasonable doubt – they imply the $S$-matrix factorization for the worlsheet theory.

To find such current we start by writing down a fairly reasonable general ansatz[1]

$$A(x) = \sum_{n=0}^{3} \alpha_n(x) J^{(n)} + \beta(x)(*J^{(2)} - \Lambda)\,. \tag{4.17}$$

We now want to find $\alpha_i(x)$ and $\beta(x)$ in such a way that (4.14) holds when the e.o.m. (4.7) are satisfied. In the l.h.s. of (4.14) we eliminate the five terms with $dJ^{(n)}$, $d*J^{(2)}$ using the four equations (4.10) and (4.12). Thus the flatness equation becomes now a large linear combination of current bilinears such as $J^{(1)} \wedge J^{(3)}$, $J^{(1)} \wedge *J^{(2)}$ etc. Not all of them are linearly independent since we still did not use (4.11) nor (4.13). Using these relations we

[1] We did not include in our ansatz $*J^{(1)}$, $*J^{(3)}$ or $*J^{(0)}$. The component $J^{(0)}$ was gauged out in our sigma model so there is no equation governing its evolution. The same holds for $J^{(1)}$ and $J^{(3)}$. They are also unfixed because of the ungauged $\kappa$-symmetry. (Actually, for $\kappa \neq 1$ in (4.6) the action is not $\kappa$ symmetric but in any case it still remains true that we do not have equations governing the evolution of the fermionic currents.)

eliminate for example $J^{(1)} \wedge *J^{(3)}$ and $J^{(1)} \wedge *J^{(2)}$. In the process one should keep in mind the identities $*A \wedge B = -A \wedge *B$ and $** = 1$ which hold for 1-forms.

In doing all this one obtains the following expression for $dA(x) - A(x) \wedge A(x)$:

$$\begin{aligned} & (1-\alpha_0)\left[\frac{\alpha_0}{2}\langle J^{(0)}, J^{(0)}\rangle + \sum_{i=1}^{3} \alpha_i \langle J^{(0)}, J^{(i)}\rangle + \beta \langle J^{(0)}, *J^{(2)}\rangle\right] + (\alpha_0 - \alpha_1\alpha_3)\,\langle J^{(1)}, J^{(3)}\rangle \\ + \;& \frac{1}{2}\left(\alpha_2 - \beta\kappa - \alpha_3^2\right)\langle J^{(3)}, J^{(3)}\rangle + \frac{1}{2}\left(\alpha_2 + \beta\kappa - \alpha_1^2\right)\langle J^{(1)}, J^{(1)}\rangle + \frac{1}{2}\left(\alpha_0 + \beta^2 - \alpha_2^2\right)\langle J^{(2)}, J^{(2)}\rangle \\ + \;& \frac{1}{\kappa}\left(\beta\alpha_3\kappa + \alpha_3\alpha_2 - \alpha_1\right)\langle J^{(2)}, *J^{(3)}\rangle + \frac{1}{\kappa}\left(\beta\alpha_1\kappa - \alpha_1\alpha_2 + \alpha_3\right)\langle J^{(2)}, *J^{(1)}\rangle \end{aligned} \tag{4.18}$$

where

$$\langle A, B\rangle \equiv A \wedge B + B \wedge A \tag{4.19}$$

was introduced to shorten the expression. Notice that there are seven coefficients which must set to zero whereas we only have 5 functions $\alpha_i$ and $\beta$ to tune. The first three coefficients in (4.18) yield

$$\alpha_0 = 1\ ,\ \alpha_1 = \frac{1}{\alpha_3}\ ,\ \alpha_2 = \alpha_3^2 + \beta\kappa \tag{4.20}$$

and when plugging these into the fourth coefficient one gets

$$\beta = \frac{1}{2\kappa}\left(\frac{1}{\alpha_3^2} - \alpha_3^2\right)\ . \tag{4.21}$$

So far all functions are expressed in terms of $\alpha_3$ and the last three terms in (4.18) are yet to be set to zero. Remarkably, the last two drop out when we use (4.20) and (4.21). Finally, the remaining term gives

$$\frac{1}{8}\left(\frac{1}{\kappa^2} - 1\right)\left(1 - \frac{1}{\alpha_3^4}\right)^2 \langle J^{(2)}, J^{(2)}\rangle\,. \tag{4.22}$$

We see that if $\kappa = 1$ then $\alpha_3$ is unfixed, $\alpha_3 = f(x)$, and the desired flat connection $A(x)$ is obtained! If on the other hand $\kappa \neq 1$ then $\alpha_3$ is fixed to a number and we simply obtain a trivial flat current rather than a full family parametrized by a continuous parameter. The model is therefore integrable only for $\kappa = 1$ which is precisely the value for the Metseav-Tseytlin action (2.4) [34]! In the derivation of this formula the authors fixed this coefficient by imposing the action to be $\kappa$-symmetric. It would be interesting to further explore the connection between $\kappa$-symmetry and integrability.

Particular choices of $f(x)$ simply amount to redefinitions of the spectral parameter $x$. In the original work [10] $f(x) = e^x$ whereas for us the choice [87] $f(x) = \sqrt{\frac{x-1}{x+1}}$ turns out to be more convient. Hence

$$A(x) = J^{(0)} + \frac{x^2+1}{x^2-1}\,J^{(2)} - \frac{2x}{x^2-1}\left(*J^{(2)} - \Lambda\right) + \sqrt{\frac{x+1}{x-1}}\,J^{(1)} + \sqrt{\frac{x-1}{x+1}}\,J^{(3)} \tag{4.23}$$

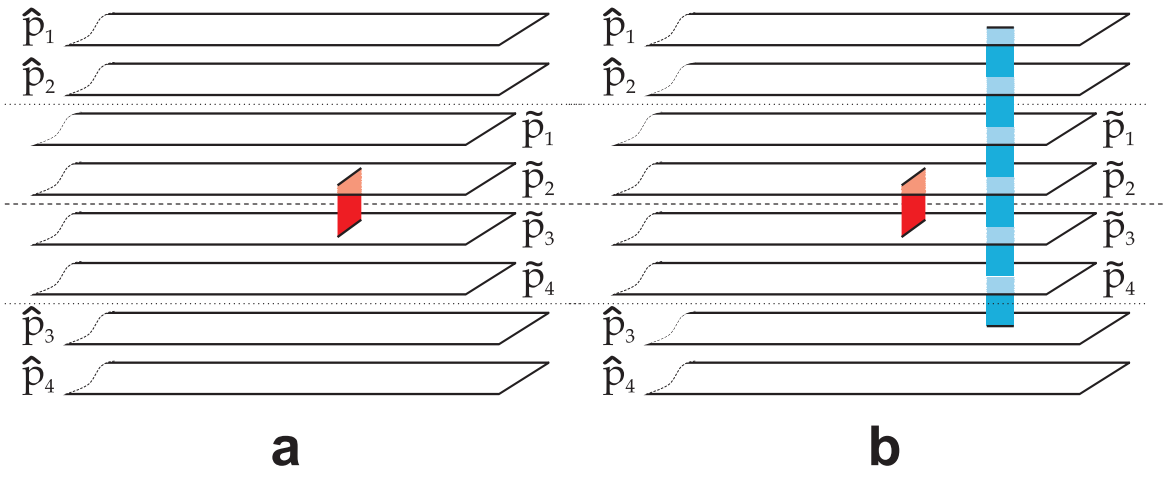


Figure 4.2: Examples of simple Riemann surfaces arising from solving the characteristic polynomial equation appearing when computing the eigenvalues of the string monodromy matrix.

is flat for any complex number $x$ [10]. As mentioned above this is the crucial observation which indicates the model to be (at least classically) integrable with an infinite number of conserved charges encoded in the eigenvalues of the monodromy matrix (4.16). Finally we also notice that under periodic $SP(2,2) \times SP(4)$ gauge transformations we have (2.5) and (2.6) so the monodromy matrix is simply conjugated and thus the eigenvalues are gauge invariant. The same is true for $\kappa$ symmetry transformations.

In the next section let us make a short overview of the general physical picture behind the algebraic construction of [83, 87] described in greater detail in the forthcoming sections.

## 4.3 Algebraic curves – Physical picture

The eigenvalues of the $8 \times 8$ monodromy matrix $\Omega(x)$ will be of upmost important throughout all this monograph. We denote them by

$$\lambda = \{e^{i\hat{p}_1}, e^{i\hat{p}_2}, e^{i\hat{p}_3}, e^{i\hat{p}_4} | e^{i\tilde{p}_1}, e^{i\tilde{p}_2}, e^{i\tilde{p}_3}, e^{i\tilde{p}_4}\}$$

where $\hat{p}_j$ and $\tilde{p}_j$ are called quasi-momenta. We will explain below why some quasi-momenta are hatted while others are tilded. For each classical solution we compute the eigenvalues of the monodromy matrix by solving a polynomial characteristic equation. This defines an eight-sheeted Riemann surface for the eigenvalues $\lambda$ with square root cuts uniting the several sheets as represented in figure 4.2. For example when crossing a cut $\tilde{\mathcal{C}}_{23}$ shared by the eigenvalues $e^{i\tilde{p}_2}$ and $e^{i\tilde{p}_3}$ we simply change Riemann sheet,

$$\left(e^{i\tilde{p}_2}\right)^+ - \left(e^{i\tilde{p}_3}\right)^- = 0 \ , \quad x \in \tilde{\mathcal{C}}_{23} \tag{4.24}$$

where the superscript $\pm$ indicates the function is evaluated immediately above/below the cut. The quasi-momenta on the other hand are not exactly the eigenvalues but rather their logarithms. Thus when crossing the very same cut the quasimomenta will in general also gain an integer multiple of $2\pi$,

$$\tilde{p}_2^+ - \tilde{p}_3^- = 2\pi n \ , \ \ x \in \tilde{\mathcal{C}}_{23} \, . \tag{4.25}$$

In figure 4.2a we have a cut uniting these quasimomenta while in figure 4.2b we also have an additional cut between $\hat{p}_1$ and $\hat{p}_3$.

Notice that if we consider the derivative of the quasimomenta these extra constants drop out so we obtain again a proper algebraic curve,

$$(\tilde{p}_2')^+ - (\tilde{p}_3')^- = 0 \ , \ \ x \in \tilde{\mathcal{C}}_{23} \, . \tag{4.26}$$

All this will become quite clear in the next section when we consider a simple explicit example of these algebraic curves.

Apart from the mode number $n$ each cut will also be described by a filling fraction as in (4.3) obtained by integrating the quasimomenta around each cut. The picture we have in mind is that the cut is indeed the result of a condensation of a large number of quantum poles as we saw in our simple quantum mechanics example in section 4.1 or in the condensation of Bethe roots described in the end of the previous chapter starting from section 3.8.1. That is we expect $p_i(x)$ to be the continuous limit of some discrete sum

$$p \simeq \sum_{k=1}^{S_n} \frac{\alpha(x_k)}{x - x_k} + \dots \, ,$$

as depicted in figure 4.1 or more generally in figure 3.19. The knowledge of the residues $\alpha(x)$ is the most important information required to be able to quasi-classical quantize the solutions. This is so because only by knowing $\alpha(x)$ can we choose the appropriate measure in such a way that when integrating the quasi-momenta around the cut we count the number of quantum excitations out of which the cut is made. In the next two chapters we will explain why the correct choice for the residue is

$$\alpha(x) = \frac{4\pi}{\sqrt{\lambda}} \frac{x^2}{x^2 - 1} \, . \tag{4.27}$$

so that the proper definition of the filling fractions should be

$$S_{ij} = \pm \frac{\sqrt{\lambda}}{8\pi^2 i} \oint\limits_{\mathcal{C}_{ij}} \left(1 - \frac{1}{x^2}\right) p_i(x) dx. \tag{4.28}$$

obtained by integrating the quasi-momenta around the square root cut. The indices run over

$$i = \tilde{1}, \tilde{2}, \hat{1}, \hat{2} \ , \ \ j = \tilde{3}, \tilde{4}, \hat{3}, \hat{4} \tag{4.29}$$

and we denote

$$p_{\tilde{1},\tilde{2},\tilde{3},\tilde{4}} \equiv \tilde{p}_{1,2,3,4} \ , \ p_{\hat{1},\hat{2},\hat{3},\hat{4}} \equiv \hat{p}_{1,2,3,4} \, . \tag{4.30}$$

In (4.28) we should choose the plus sign for $i = \hat{1}, \hat{2}$ and the minus sign for the remaining excitations with $i = \tilde{1}, \tilde{2}$. We should mention that one can rigorously show that the filling fractions defined as in (4.28) are indeed the action variables of the theory thus justifying the choice (4.27) [91, 92]. Finally notice that if we change variable via the Zhukowsky map

$$z = x + \frac{1}{x} \tag{4.31}$$

the filling fraction expression becomes simply

$$S_{ij} = \pm \frac{\sqrt{\lambda}}{8\pi^2 i} \oint\limits_{\mathcal{C}_{ij}} dz \, p_i(z) \tag{4.32}$$

which seems to indicate that the $z$ variables will be more suitable for quantization[2].

So far we have see that, given a classical solution, we can compute and diagonalize the monodromy matrix and its eigenvalues will describe some Riemann surface. Each cut of the algebraic curve is characterized by a discrete label $(i, j)$, corresponding to the two sheets being united, an integer $n$, the multiple of $2\pi$ mention above, and a real filling fraction. These three quantities are the analogues of the polarization, mode number and amplitude of the flat space fourier decomposition of a given classical solution.

Therefore figure 4.2a would describe a string motion with a single polarization excited and the filling fraction of the cut would correspond to the amplitude of the excitation. Figure 4.2b would describe a string motion with two excited modes, each corresponding to a different $AdS_5 \times S^5$ polarization. To be more specific we must explain the significance of the hats and tildes of the quasi-momenta. When we consider a classical string solution we have a bosonic representative of the form (2.11). After all, the motion of the string is obviously described by the (bosonic) embedding coordinates. Thus the currents $J^{(1)}$ and $J^{(3)}$ will vanish and the flat connection will be of the form

$$A_\sigma(x;\sigma,\tau) = \left( \begin{array}{c|c} A_\sigma^{AdS}(x;\sigma,\tau) & 0 \\ \hline 0 & A_\sigma^{S}(x;\sigma,\tau) \end{array} \right) . \tag{4.33}$$

The monodromy matrix will inherit this block diagonal form and therefore there will be two groups of quasi-momenta, those coming from the diagonalization of the $S^5$ part and those stemming from the $AdS_5$ part. The quasimomenta associated to the $S^5$ ($AdS_5$) eigenvalues are denoted by $\tilde{p}_i$ ($\hat{p}_j$).

Notice that we might expect that the algebraic curve obtained from a given classical solution will be in fact decoupled into two four-sheeted algebraic curves, one for the sphere

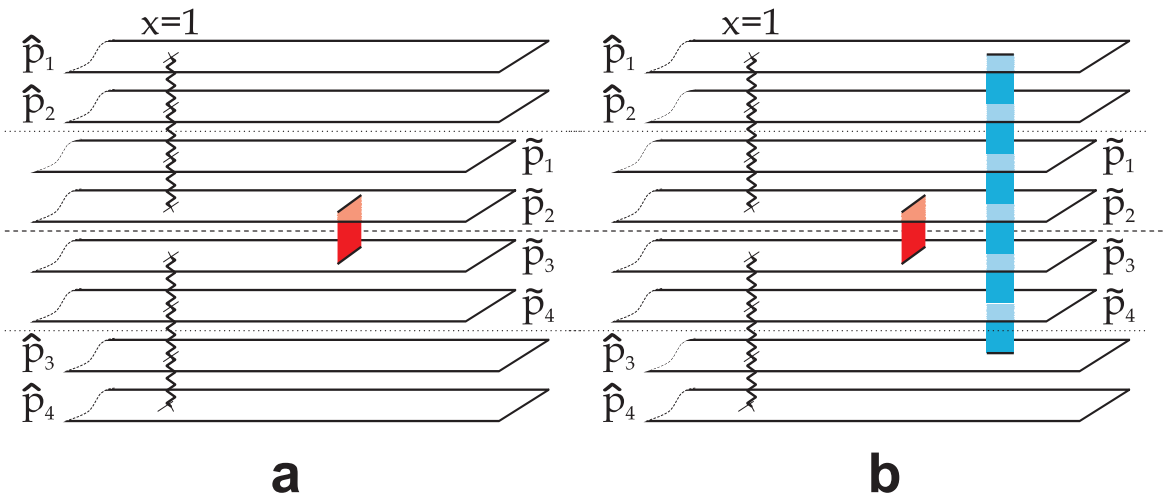


Figure 4.3: Classically the $AdS_5 \times S^5$ algebraic curve factorized into two separate groups of four sheeted curves described by the $S^5$ quasimomenta $\tilde{p}_i$ and the $AdS_5$ quasi-momenta $\hat{p}_i$. These curves are related to one another by the synchronization of the pole singularities at $x = \pm 1$. Physically this synchronization is a translation of the Virasoro constraints.

motion and another for the string movement in anti de-Sitter. This is almost true. However the Virasoro constraints set the total stress energy tensor to zero and couple the $S^5$ and $AdS_5$ evolution. In the algebraic curve language this is manifest in the following way: As we see from the form of the current (4.23) the points $x = \pm 1$ are potentially singular and indeed the quasimomenta will have simple poles at this points. The Virasoro constraints will synchronize the poles of the several quasimomenta and thus couple the two seemingly disconnected curves [87]. This synchronization is schematically depicted in figure 4.3 where we added the $x = \pm 1$ poles to figure 4.2.

Now we can be more precise when describing figure 4.2 or its updated version 4.3. In figure 4.3a we have a string which is point like with respect to the AdS space and has an $S^5$ mode excited. Figure 4.3b corresponds to a solution with two different polarizations excited – one in $S^5$ and the other in $AdS_5$.

What about fermions? Well, classically they don't appear at all. This is simply because their amplitudes are described by fermionic excitations which only admit 0 or 1 as occupation numbers by the Pauli exclusion principle whereas for the bosonic amplitudes the classical limit is attained by condensation of a large number of excitations. A mathematical way of seeing this is as follows. Bosonic branch cuts appear when two eigenvalues with the same grading coincide. However when two eigenvalues with a different grading coincide they do not develop a square root singularity but rather a pole divergency [87].

[2]This was first noticed in [83]. See also [11] for further evidence from this point of view.

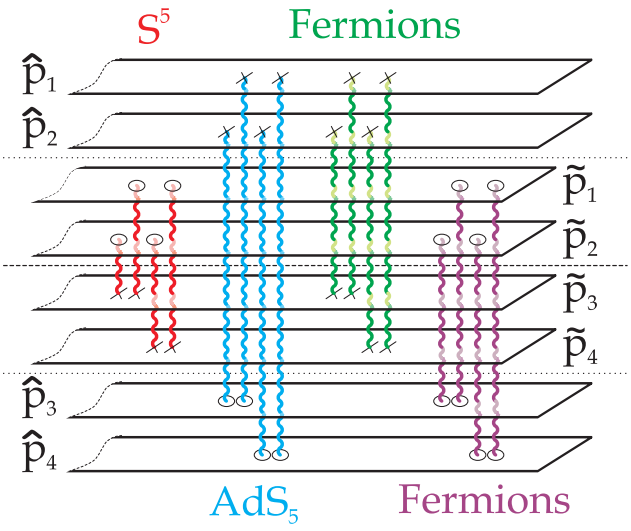


Figure 4.4: The several string polarizations are nothing but the several possible choices of which Riemann sheets to connect. All fluctuations must cross the middle dashed line.

On the other hand fermions do appear very naturally in the algebraic curve when we consider the semi-classical quantization of the theory. This will be described in the next chapters. The idea is that if we want to study quantum fluctuations around a given classical solution we should add extra singularities to the classical algebraic curve corresponding to the classical solution in study [93, 13]. These singularities can be though as either microscopic cuts or poles. The (sixteen) superstring physical polarizations correspond to the pairing of sheets

$$\begin{aligned} S^5: &\quad (\tilde{1},\tilde{3}),(\tilde{1},\tilde{4}),(\tilde{2},\tilde{3}),(\tilde{2},\tilde{4}) \\ AdS_5: &\quad (\hat{1},\hat{3}),(\hat{1},\hat{4}),(\hat{2},\hat{3}),(\hat{2},\hat{4}) \\ \text{Fermions}: &\quad (\tilde{1},\hat{3}),(\tilde{1},\hat{4}),(\tilde{2},\hat{3}),(\tilde{2},\hat{4}) \\ &\quad (\hat{1},\tilde{3}),(\hat{1},\tilde{4}),(\hat{2},\tilde{3}),(\hat{2},\tilde{4}). \end{aligned} \tag{4.34}$$

represented in figure 4.4. The rule – which will be explained in more detail in the following chapters – is the following: We must always connect a sheet with index number 1 or 2 to another sheet with index 3 or 4. Graphically, we must connect one of the four upper sheets in figure 4.4 with one of the bottom four. If we connect $\hat{p}_i$ with $\hat{p}_j$ we describe an $AdS_5$ fluctuation, if the fluctuation is shared by $\tilde{p}_i$ and $\tilde{p}_i$ it corresponds to an $S^5$ mode and finally if it connects quasimomenta $\hat{p}_i$ and $\tilde{p}_j$ it is a fermionic excitation. Figure 4.5, e.g., would correspond to a classical solution with two classical modes excited – one in the sphere and the other in anti de-Sitter – plus three small (semi-classical) fluctuations. Two of those are bosonic and live in $S^5$ and $AdS_5$ whereas the third one is a fermionic

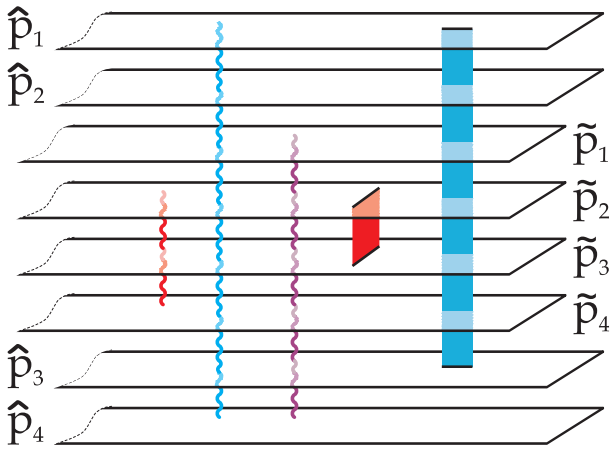


Figure 4.5: Classical solution (the cuts) plus quantum fluctuations (poles) are described in the same unifying formalism.

excitation.

In the next section we resume our rigorous analysis of the algebraic curve.

## 4.4 Classical algebraic curves

In this section we review the algebraic curve of Beisert, Kazakov, Sakai and Zarembo [87]. We will start by considering some particular - and simple - classical solutions which will allow us to easily identify many of the universal features shared by all the algebraic curves associated with the superstring classical motion. The most general curves are studied in section 4.5.

### 4.4.1 Circular string solutions

In this section we consider an important class of rigid circular strings solutions studied in [94]. In terms of the $AdS_5$ and $S^5$ embedding coordinates, we can represent this general class of strings solutions with global charges $E = \sqrt{\lambda}\,\mathcal{E}$, $J_1 = \sqrt{\lambda}\,\mathcal{J}_1$, ..., as [94]

$$\begin{aligned} u_2 + iu_1 &= \sqrt{\frac{\mathcal{J}_3}{w_3}}\, e^{i(w_3\tau + m_3\sigma)} \quad , \quad v_2 + iv_1 = \sqrt{\frac{\mathcal{S}_2}{\mathrm{w}_2}}\, e^{i(\mathrm{w}_2\tau + k_2\sigma)} \,, \\ u_4 + iu_3 &= \sqrt{\frac{\mathcal{J}_2}{w_2}}\, e^{i(w_2\tau + m_2\sigma)} \quad , \quad v_4 + iv_3 = \sqrt{\frac{\mathcal{S}_1}{\mathrm{w}_1}}\, e^{i(\mathrm{w}_1\tau + k_1\sigma)} \,, \\ u_6 + iu_5 &= \sqrt{\frac{\mathcal{J}_1}{w_1}}\, e^{i(w_1\tau + m_1\sigma)} \quad , \quad v_6 + iv_5 = \sqrt{\frac{\mathcal{E}}{\kappa}}\, e^{i\kappa\tau} \,. \end{aligned} \tag{4.35}$$

The condition (2.10) that the embedding coordinates parametrize the sphere and anti-de Sitter fixes

$$1=\sum_{i=1}^{3}\frac{\mathcal{J}_i}{w_i}\ ,\ 1=\frac{\mathcal{E}}{\kappa}-\sum_{j=1}^{2}\frac{\mathcal{S}_j}{\mathrm{w}_j} \tag{4.36}$$

while the equations of motion and Virasoro constraints[3] yield

$$\begin{aligned}\mathrm{w}_j^2&=\kappa^2+k_j^2\ ,\ \kappa^2=\sum_{j=1}^{2}\mathcal{S}_j\frac{2k_j^2}{\mathrm{w}_j}+\sum_{i=1}^{3}\mathcal{J}_i\frac{w_i^2+m_i^2}{w_i}\,,\\ w_i^2&=\nu^2+m_i^2\ ,\ \nu^2\equiv\sum_{i=1}^{3}\mathcal{J}_i\frac{w_i^2-m_i^2}{w_i}\,.\end{aligned} \tag{4.37}$$

To build the corresponding quasi-momenta $p_i(x)$ associated with this class of solutions we should

1. Translate the embedding coordinates into the group element $g(\sigma,\tau)\in PSU(2,2|4)$;
2. Compute the current $J=-g^{-1}dg$ and project it into its $\mathbb{Z}_4$ components $J^{(n)}$;
3. Write the flat connection (4.23) ;
4. Compute the monodromy matrix (4.16);
5. Diagonalize $\Omega(x)$ and read the quasi-momenta.

As for 1) we notice that the embedding coordinates (4.35) are found from the map (2.12) if

$$g=\left(\begin{array}{c|c}\mathcal{Q}&0\\\hline 0&\mathcal{R}\end{array}\right)\,, \tag{4.38}$$

with

$$\mathcal{R}=\prod_{i=1}^{3}e^{\frac{i}{2}(w_i\tau+m_i\sigma)\Phi_i}\cdot\mathcal{R}_0\ \in SU(4)\,, \tag{4.39}$$

and

$$\mathcal{Q}=e^{\frac{i}{2}\kappa\tau\Phi_1}\cdot\prod_{i=1}^{2}e^{-\frac{i}{2}(\mathrm{w}_i\tau+k_i\sigma)\Phi_{i+1}}\cdot\mathcal{Q}_0\ \in SU(2,2)\,, \tag{4.40}$$

[3]The Virasoro conditions are simply $T_{\mu\nu}=0$ where for this purely bosonic setup we can derive the stress energy tensor from (2.9).

where $\Phi_i$ are the Cartan generators,

$$\Phi_1 = \text{diag } (+,+,-,-) \ , \ \Phi_2 = \text{diag } (+,-,+,-) \ , \ \Phi_3 = \text{diag } (-,+,+,-) \ ,$$

and $\mathcal{R}_0 = e^{\Phi_{42}\theta} e^{\Phi_{64}\gamma}$ and $\mathcal{Q}_0 = e^{\Phi'_{42}\psi} e^{\Phi'_{64}\rho}$ are constant matrices with

$$(\cos\gamma, \sin\gamma\cos\theta, \sin\gamma\sin\theta) = \left(\sqrt{\frac{\mathcal{J}_1}{w_1}}, \sqrt{\frac{\mathcal{J}_2}{w_2}}, \sqrt{\frac{\mathcal{J}_3}{w_3}}\right) \ ,$$

$$(\cosh\rho, \sinh\rho\cos\psi, \sinh\rho\sin\psi) = \left(\sqrt{\frac{\mathcal{E}}{\kappa}}, \sqrt{\frac{\mathcal{S}_1}{\mathrm{w}_1}}, \sqrt{\frac{\mathcal{S}_2}{\mathrm{w}_2}}\right) \ ,$$

and $\Phi_{42}, \Phi_{64}, \Phi'_{42}, \Phi'_{64}$ given respectively by

$$\frac{1}{2}\begin{pmatrix} 0 & -1 & 0 & 0 \\ 1 & 0 & 0 & 0 \\ 0 & 0 & 0 & -1 \\ 0 & 0 & 1 & 0 \end{pmatrix}, \begin{pmatrix} 0 & 0 & 0 & 0 \\ 0 & 0 & -1 & 0 \\ 0 & 1 & 0 & 0 \\ 0 & 0 & 0 & 0 \end{pmatrix}, \frac{1}{2}\begin{pmatrix} 0 & -1 & 0 & 0 \\ 1 & 0 & 0 & 0 \\ 0 & 0 & 0 & 1 \\ 0 & 0 & -1 & 0 \end{pmatrix}, \frac{1}{2}\begin{pmatrix} 0 & 0 & 0 & 1 \\ 0 & 0 & -1 & 0 \\ 0 & -1 & 0 & 0 \\ 1 & 0 & 0 & 0 \end{pmatrix}.$$

This finishes point 1). What is remarkable about these solutions is that they are Abelian with respect to the $\tau$ and $\sigma$ evolution whereas the nontrivial nonabelian structure is simply introduced by the constant matrices $\mathcal{R}_0$ and $\mathcal{Q}_0$. This is quite nice because this form of representative immediately implies that

$$J = -g^{-1}dg = -\left(\begin{array}{c|c} \mathcal{Q}^{-1}d\mathcal{Q} & 0 \\ \hline 0 & \mathcal{R}^{-1}d\mathcal{R} \end{array}\right) \tag{4.41}$$

is a constant connection! The $\tau$ and $\sigma$ dependence immediately disappears from the current and therefore the path order exponential in the definition of the monodromy will become a simple exponential and the computation simplifies dramatically.

Next point 2). It requires (almost) no brain activity. We simply pick the group elements above, plug them into the current (4.41) and plug the current into (2.2) to find the several projections. Point 3) is equally straightfoward. Having the projections $J^{(n)}$, we sum them as in (4.23) to build the flat connection $A(x)$. The general output for generic angular momenta, spin and windings is presented in the appendix A.

4) is in general the only nontrivial step but for the solutions we chose this point is also straightforward because, as explained above, the current $A(x)$ – being made out of the components of the constant connection $J$ – does not depend on $\tau$ or $\sigma$. Thus the computation of the path ordered exponential (4.16) is trivial and the quasi-momenta $p(x)$ are simply obtained from the eigenvalues of $\frac{2\pi}{i}A_\sigma(x)$. Thus point 5) is equally immediate.

First let us consider the simplest solution in the family (4.35). It is the BMN string [95] given by

$$u_6 + iu_5 = e^{i\mathcal{J}\tau} \ , \ v_6 + iv_5 = e^{i\mathcal{J}\tau} \tag{4.42}$$

For this solution the flat connection is the diagonal matrix

$$\frac{2\pi}{i}A_\sigma(x) = \frac{2\pi\mathcal{J}x}{x^2-1}\mathrm{diag}\,(1,1,-1,-1;1,1,-1,-1) \tag{4.43}$$

so that the quasi-momenta are simply

$$\tilde{p}_{1,2} = -\tilde{p}_{3,4} = \hat{p}_{1,2} = -\hat{p}_{3,4} = \frac{2\pi\mathcal{J}x}{x^2-1}\,. \tag{4.44}$$

This is the simplest possible algebraic curve. It has no cuts at all!

Let us now consider the next to the simplest circular string solution which corresponds to a string rotating in $S^3$ and point like w.r.t. the $AdS$ space. It will be very useful for illustration purposes. After understanding the analytical properties of the quasi-momenta for this simple case we shall come back to the general solution (4.35). We set

$$\mathcal{J}_1 = \mathcal{J}_2 = \frac{\mathcal{J}}{2}\ ,\ m_1 = -m_2 = m \tag{4.45}$$

with all other spins, angular momenta, mode numbers and frequencies being zero. The classical energy is then given by $\mathcal{E} = \kappa$ with

$$\kappa = \sqrt{\mathcal{J}^2 + m^2}\,. \tag{4.46}$$

For this solution, following the steps described above, we find

$$\frac{2\pi}{i}A_\sigma(x) = \frac{2\pi}{x^2-1}\left(\begin{array}{cccc|cccc} \kappa\,x & & & & & & & \\ & \kappa\,x & & & & & & \\ & & -\kappa\,x & & & & 0 & \\ & & & -\kappa\,x & & & & \\ \hline & & & & \mathcal{J}x & & & -m \\ & & 0 & & & \mathcal{J}x & m\,x^2 & \\ & & & & & m\,x^2 & -\mathcal{J}x & \\ & & & & -m & & & -\mathcal{J}x \end{array}\right) \tag{4.47}$$

so that all eigenvalues corresponding to the $AdS_5$ part of the current are trivial,

$$\left(\begin{array}{c}\hat{p}_1\\ \hat{p}_2\\ \hat{p}_3\\ \hat{p}_4\end{array}\right) = \frac{2\pi\kappa\,x}{x^2-1}\left(\begin{array}{c}+1\\ +1\\ -1\\ -1\end{array}\right) \tag{4.48}$$

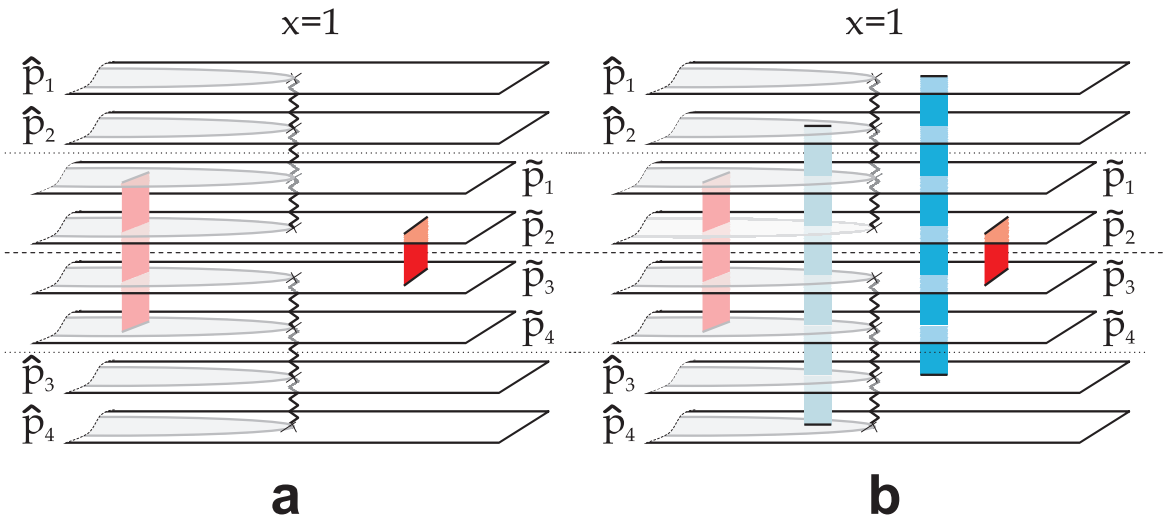


Figure 4.6: Inversion symmetry $x \to 1/x$. To each physical cut outside the unit circle there is a mirror cut inside the unit circle.

while the diagonalization of the $S^5$ part yields[4]

$$\begin{pmatrix} \tilde{p}_1 \\ \tilde{p}_2 \\ \tilde{p}_3 \\ \tilde{p}_4 \end{pmatrix} = 2\pi \begin{pmatrix} +\frac{x}{x^2-1}K(1/x) \\ +\frac{x}{x^2-1}K(x) - m \\ -\frac{x}{x^2-1}K(x) + m \\ -\frac{x}{x^2-1}K(1/x) \end{pmatrix}, \quad K(x) \equiv \sqrt{m^2x^2 + \mathcal{J}^2}. \tag{4.49}$$

Let us now consider the analyticity structure of these quasi-momenta.

First look at $\tilde{p}_2(x)$. It is an analytic function except for the square root cut. If we *enter* the cut we change the sign of the square root, $K(x) \to -K(x)$. But this, apart from a constant $4\pi m$, transforms precisely $\tilde{p}_2(x)$ into $\tilde{p}_3(x)$! That is $\tilde{p}_2$ and $\tilde{p}_3$ are united by a square root cut $\tilde{\mathcal{C}}_{23}$,

$$\tilde{p}_2^+ - \tilde{p}_3^- = 2\pi n \ , \ \ x \in \ \tilde{\mathcal{C}}_{23} \tag{4.50}$$

where the superscript $\pm$ means the function is evaluated immediately above/below the cut. The integer $n$ is in this case $n = 2m$. This is precisely (4.25) anticipated in our physical discussion in the previous section. Notice also that when we exponentiate the quasi-momenta the $2\pi m$ constant drops and we find (4.24). The same holds when we consider the derivative of the quasi-momenta; in this case we obtain (4.26). Thus $\tilde{p}_2'$ and $\tilde{p}_3'$ are the two branches of a single function taken values in a two-sheeted Riemann surface.

[4]We add the constant shifts $\pm 2\pi m$ which 1) clearly does not change $e^{ip_j(x)}$ and 2) yields $p_j \sim 1/x$ at large $x$. We are always free to add such shift and we will always do so to ensure that the quasi-momenta vanish for large $x$.

Computing the filling fraction (4.28) we find

$$-\frac{\sqrt{\lambda}}{8\pi^2 i}\oint\limits_{\mathcal{C}_{23}}\left(1-\frac{1}{x^2}\right)\tilde{p}_2(x)=\frac{\sqrt{\lambda}\mathcal{J}}{2} \tag{4.51}$$

and, therefore, so far the physical picture is precisely as anticipated in the previous section. The solution is excited in the sphere target space and indeed only for the tilded quasi-momenta we obtain square root cuts. The discontinuity of the quasi-momenta is related to mode numbers in (4.35) and the filling fraction is indeed measuring the amplitude of the corresponding mode.

Next let us look at $\tilde{p}_1$ and $\tilde{p}_4$. Again these quasimomenta share a square root cut whose branchpoints are the image under $x \to 1/x$ of the previous cut $\tilde{\mathcal{C}}_{23}$. More than that, we observe that there is a curious inversion symmetry

$$\begin{aligned}\tilde{p}_1(x) &= -2\pi m-\tilde{p}_2(1/x)\\ \tilde{p}_4(x) &= +2\pi m-\tilde{p}_3(1/x),\end{aligned} \tag{4.52}$$

whose origin will be elucidated briefly. This symmetry, is also present, although in a much more trivial incarnation, for the $AdS_5$ quasimomenta,

$$\begin{aligned}\hat{p}_1(x) &= -\hat{p}_2(1/x)\\ \hat{p}_4(x) &= -\hat{p}_3(1/x).\end{aligned} \tag{4.53}$$

Thus, in this more precise analysis we see that figure 4.3a should be replaced by figure 4.6a.

Next let us continue our enumeration of the analytic properties of the quasi-momenta by looking at their asymptotics. Due to the $x \to 1/x$ symmetry it suffices to look at the large $x$ behavior. We notice that the quasimomenta vanish as $1/x$ with the residues being the global charges of the solution,

$$\left(\begin{array}{c}\hat{p}_1\\ \hat{p}_2\\ \hat{p}_3\\ \hat{p}_4\\ \hline \tilde{p}_1\\ \tilde{p}_2\\ \tilde{p}_3\\ \tilde{p}_4\end{array}\right)\simeq\frac{2\pi}{x}\left(\begin{array}{c}+\mathcal{E}\\ +\mathcal{E}\\ -\mathcal{E}\\ -\mathcal{E}\\ \hline +\mathcal{J}\\ 0\\ 0\\ -\mathcal{J}\end{array}\right). \tag{4.54}$$

Finally we consider the only remaining singularities, the poles at $x=\pm 1$. We easily see that the $AdS_5$ and the $S^5$ poles are synchronized and

$$\{\hat{p}_1,\hat{p}_2,\hat{p}_3,\hat{p}_4|\tilde{p}_1,\tilde{p}_2,\tilde{p}_3,\tilde{p}_4\}\simeq\frac{\{\kappa,\kappa,-\kappa,-\kappa|\kappa,\kappa,-\kappa,-\kappa\}}{x\pm 1}\,. \tag{4.55}$$

This is again fairly generic as explained in the next section.

Let us now mention what we would obtain had we considered the generic solution in our family of circular strings (4.35). Now the flat connection, presented in appendix A, is a constant block diagonal matrix with constant entries,

$$A_\sigma(x) = \left(\begin{array}{c|c} A_\sigma^{AdS}(x) & 0 \\ \hline 0 & A_\sigma^{S}(x) \end{array}\right) \tag{4.56}$$

and the diagonalization of this matrix is of course more involved. In particular we will have in general more cuts uniting the $AdS$ quasimomenta,

$$\hat{p}_i^+ - \hat{p}_j^- = 2\pi n_{ij} \ , \ \ x \in \hat{\mathcal{C}}_{ij} \, , \tag{4.57}$$

and cuts shared by the sphere $\tilde{p}_i$,

$$\tilde{p}_i^+ - \tilde{p}_j^- = 2\pi n_{ij} \ , \ \ x \in \tilde{\mathcal{C}}_{ij} \, . \tag{4.58}$$

In figure 4.6 we represented a possible configuration.

To find the analytical properties of the quasimomenta we don't need to completely diagonalize the flat connection. It is easier to study the characteristic equation $\det\left(\frac{2\pi}{i}A_\sigma(x) - \mathbb{I}p\right) = 0$. We find that

1. The inversion symmetry (4.52) and (4.53) holds without any change ($m$ is in this case a simple linear combination of the several windings $m_i$ and $k_i$),

$$\tilde{p}_{1,4}(1/x) = \mp 2\pi m - \tilde{p}_{2,3}(x) \ , \ \ \hat{p}_{1,4}(1/x) = -\hat{p}_{2,3}(x) \, . \tag{4.59}$$

2. From the large $x$ asymptotics we can again read the several global charges, more precisely

$$\left(\begin{array}{c} \hat{p}_1 \\ \hat{p}_2 \\ \hat{p}_3 \\ \hat{p}_4 \\ \hline \tilde{p}_1 \\ \tilde{p}_2 \\ \tilde{p}_3 \\ \tilde{p}_4 \end{array}\right) \simeq \frac{2\pi}{x\sqrt{\lambda}} \left(\begin{array}{c} +E - S_1 + S_2 \\ +E + S_1 - S_2 \\ -E - S_1 - S_2 \\ -E + S_1 + S_2 \\ \hline +J_1 + J_2 - J_3 \\ +J_1 - J_2 + J_3 \\ -J_1 + J_2 + J_3 \\ -J_1 - J_2 - J_3 \end{array}\right) \, . \tag{4.60}$$

3. The quasimomenta have simple poles at $x = \pm 1$ and the residues of the sphere and anti de-Sitter quasimomenta are again synchronized

$$\{\hat{p}_1, \hat{p}_2, \hat{p}_3, \hat{p}_4 | \tilde{p}_1, \tilde{p}_2, \tilde{p}_3, \tilde{p}_4\} \simeq \frac{\{\alpha_\pm, \alpha_\pm, -\alpha_\pm, -\alpha_\pm | \alpha_\pm, \alpha_\pm, -\alpha_\pm, -\alpha_\pm\}}{x \pm 1} \, . \tag{4.61}$$

which is a slightly more general relation than (4.55). We will see that this relation holds for all bosonic solutions whereas if we allow for fermionic excitations this expression still needs to be slightly modified. We also stress that the precise values of the residues are in general not directly related to any physical quantity. The only relevant information to retain is the synchronization between the $AdS_5$ and $S^5$ quasi-momenta. As explained below this follows from the Virasoro constraints that couples string motion in the two spaces.

In the next section we shall explain the origin of each of these analytical properties and what to expect for the most general string solution.

## 4.5 General configurations

In this section we consider the analytical properties of the quasimomenta obtained for a general classical solution. Hopefully, the discussion of the two previous sections will render this general treatment quite digestible. The quasimomenta $\{\hat{p}_1, \hat{p}_2, \hat{p}_3, \hat{p}_4 | \tilde{p}_1, \tilde{p}_2, \tilde{p}_3, \tilde{p}_4\}$ are obtained from the eigenvalues

$$\{e^{i\hat{p}_1}, e^{i\hat{p}_2}, e^{i\hat{p}_3}, e^{i\hat{p}_4} | e^{i\tilde{p}_1}, e^{i\tilde{p}_2}, e^{i\tilde{p}_3}, e^{i\tilde{p}_4}\}$$

of the monodromy matrix (4.16) obtained by integrating the flat connection $A(x)$ (4.23) around the worldsheet cylinder. This connection is made out of the several components of the $psu(2,2|4)$ current $J$. The "p" in $psu(2,2|4)$ means the current $J$ is supertraceless and thus so is $A(x)$. Thus we will always have

$$(\hat{p}_1 + \hat{p}_2 + \hat{p}_3 + \hat{p}_4) - (\tilde{p}_1 + \tilde{p}_2 + \tilde{p}_3 + \tilde{p}_4) = 0\,. \tag{4.62}$$

Moreover for bosonic classical solutions $A(x)$ will be block diagonal as in (4.33) with each block being an element of $su(2,2)$ and $su(4)$. Therefore, for purely bosonic solutions, both terms in the parentheses vanish separately. We can immediately check this property for the quasi-momenta discussed in the previous section.

Next let us consider the inversion symmetry (4.59). It will hold precisely as it is for any classical solution with $m$ being an integer dependent on the classical solution. This symmetry folows from the identity

$$C^{-1}\,\Omega(x)\,C = \Omega^{-ST}(1/x), \qquad C = \left(\begin{array}{c|c} E & 0 \\ \hline 0 & -iE \end{array}\right),$$

where the supertranspose is defined as

$$\left(\begin{array}{c|c} A & B \\ \hline C & D \end{array}\right)^{ST} = \left(\begin{array}{c|c} A^T & C^T \\ \hline -B^T & D^T \end{array}\right) \tag{4.63}$$

To prove it we simply need to understand what happens when we sandwich $A(x)$ between $C$ and $C^{-1}$. Using (2.2) it is easy to see that

$$C^{-1}J^{(n)}C = -i^n \left(J^{(n)}\right)^{ST} . \tag{4.64}$$

Then we notice that each coefficient before $J^{(n)}$ in (4.23) gains such $i$ factors under the map $x \to 1/x$! Thus

$$C^{-1}A(x)C = -A^{ST}(1/x) , \tag{4.65}$$

so that (4.63) follows. Let us simply comment on the integers appearing in the identity (4.59). For $\hat{p}$ there is no $2\pi m$ imposed by requiring absence of time windings [85, 87]. As for $\tilde{p}_i$ there is a single integer $m$ because two integers would not be compatible with the supertraceless condition (4.62).

Let us now revisit the large $x$ asymptotics (4.60). Again this remains valid for the most general solution. These asymptotics follow because at large $x$

$$A_\sigma \simeq -g^{-1}\left(\partial_\sigma + \frac{2}{x}\, k_\tau\right) g \tag{4.66}$$

where $k$, appearing in (2.7), is the Noether current associated with the left global symmetry. Thus, from the behavior at infinity we can read the conserved global charges[5] as in (4.60). In particular the classical energy of the string is obtained from

$$E = \frac{\sqrt{\lambda}}{4\pi} \lim_{x\to\infty} x\left(\hat{p}_1(x) + \hat{p}_2(x)\right) . \tag{4.67}$$

Finally the poles at $x = \pm 1$. The fact that the quasimomenta have poles at these values of the spectral parameter is a simple consequence of the form of the flat connection (4.23) which has these singularities from the beginning. What is nontrivial is the fact that the poles for the several quasimomenta are highly synchronized. Indeed naively one would expect 8 different poles for $x \simeq 1$. However the $x \to 1/x$ symmetry (4.59) immediately reduces this number to 4, the supertraceless condition (4.62) following from

$$\mathrm{str}\, J^{(2)} = 0 ,$$

to 3, and the virasoro contraints

$$\mathrm{str}\, \left(J^{(2)}\right)^2 = 0 ,$$

leave only 2 independent poles. In general we expect therefore

$$\{\hat{p}_1, \hat{p}_2, \hat{p}_3, \hat{p}_4 | \tilde{p}_1, \tilde{p}_2, \tilde{p}_3, \tilde{p}_4\} \simeq \frac{\{\alpha_\pm, \alpha_\pm, \beta_\pm, \beta_\pm | \alpha_\pm, \alpha_\pm, \beta_\pm, \beta_\pm\}}{x \pm 1} . \tag{4.68}$$

[5]These are the bosonic charges, the ones which are present for a classical solution. Latter we shall consider all kind of fluctuations, including the fermionic ones. Then we shall slightly generalize this expression to (5.8).

For bosonic solutions one has not only the supertraceless condition but the tracelessness of both the $S^5$ and $AdS_5$ quasimomenta so that (4.61) holds and $\beta_\pm = -\alpha_\pm$.

An important side comment: All these analytic properties are precisely those of the quasi-momenta obtained in section 3.9 when we considered the scaling limit of the Beisert-Staudacher equations [35]! For example that the quasi-momenta (4.49) computed in this section are precisely the same as (3.292) obtained from the Bethe ansatz computation. This is of course a highly non-trivial test of the strong coupling limit of the BS equations. Actually, historically, when the Bethe equations were conjectured one of the main constraints used to guess their form was the requirement that they would reproduce the string finite-gap equations of [87]. This was also so concerning the AFS Bethe ansatz [66] describing the $SU(2)$ sector of the theory at strong coupling. This ansatz is based on the discretization of the KMMZ integral formulas [83].

So far we understood that given a generic classical solution we can compute the quasi-momenta and are bound to find an eight-sheeted Riemann surface with some precise analytical properties[6]. One can now turn the problem around and use the power of complex analysis to make an exhaustive catalogue of all possible Riemann surfaces given the predicted analytic behavior. In this way, analyticity is turned into a powerful tool to study classical string motion in full generality! We will explain how this works in the next section where we describe strings moving in $R\times S^3 \subset AdS_5\times S^5$, an important (classical) subsector of the full sigma model.

Finally we should also mention that given a set of quasi-momenta it is possible to consider the inverse map and reconstruct the classical motion. This is not surprising since the quasi-momenta encode an infinite quantity of conserved charges. In [91] the inverse map was studied for classical string moving in $R \times S^3$.

To finish this section let us mention a couple of generic features of the algebraic curves corresponding to classical solutions of strings which move in $S^5$ and are point-like in $AdS_5$ with

$$e^{it} \equiv v_6 + iv_5 = e^{i\mathcal{E}\tau}\,.$$

For these solutions the $AdS$ quasi-momenta $\hat{p}_j$ are always given by

$$\hat{p}_{1,2} = -\hat{p}_{3,4} = \frac{2\pi\mathcal{E}x}{x^2-1}\,, \tag{4.69}$$

where $\mathcal{E}$ is the energy of the string with respect to the $AdS$ global time $t$. This can be seen from two ways:

1. First by simply computing the $A_\sigma^{AdS}(x)$ as in (4.33). It is clear that we will always have

[6] In fact, as discussed in section 4.3, due the the mode numbers $2\pi n$ gained by the quasimomenta as they cross a cut, the quasimomenta describe an infinite genus surface. To obtain a good algebraic surface we should consider either the eigenvalues $e^{ip}$ or the derivative of the quasimomenta $p'$.

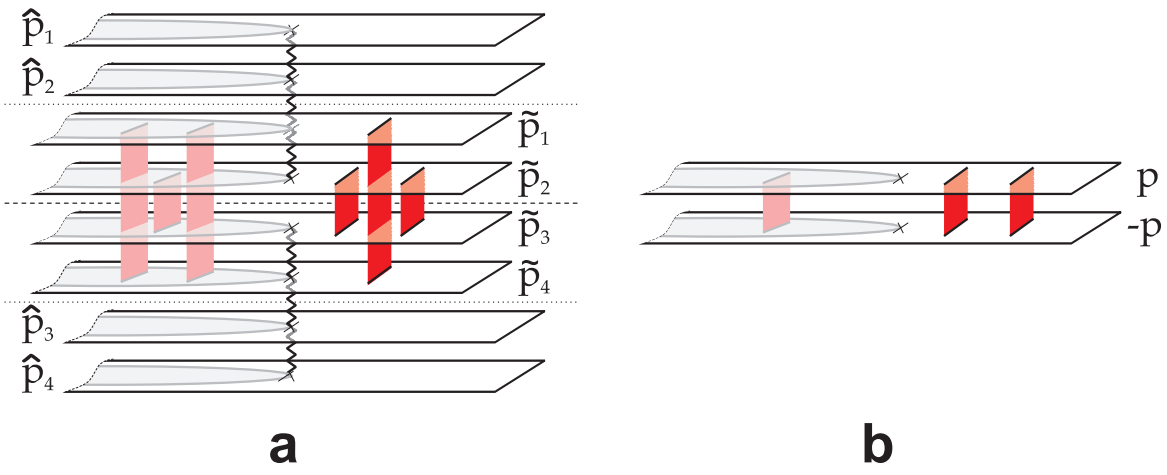


Figure 4.7: For $su(2)$ solutions we have $\{\hat{p}_1, \hat{p}_2, \hat{p}_3, \hat{p}_4\} = \frac{2\pi\mathcal{E}x}{x^2-1}\{1, 1, -1, -1\}$ and $\{\tilde{p}_1, \tilde{p}_2, \tilde{p}_3, \tilde{p}_4\} = \{2\pi m - p(1/x), p(x), -p(x), -2\pi m + p(1/x)\}$ so that all information (in the left figure) is encoded in a single quasi-momentum $p(x)$ (see figure in the right).

$\frac{2\pi}{i} A_\sigma^{AdS}(x) = \frac{2\pi\mathcal{E}x}{x^2-1}\,\mathrm{diag}\,(1, 1, -1, -1)$ as in (4.47). This matrix is already diagonal so the quasi-momenta (4.69) follow trivially.

2. Alternatively we can compute the $AdS$ classical quasi-momenta from its analyticity properties. Since we only excite $S^5$ modes, the $AdS_5$ quasi-momenta must have no cuts and be therefore rational functions with simple poles at $x = \pm 1$, large $x$ asymptotics

$$\hat{p}_{1,2}, -\hat{p}_{3,4} \simeq \frac{2\pi\mathcal{E}}{x}\,, \tag{4.70}$$

and inversion symmetry

$$\hat{p}_{1,4}(1/x) = -\hat{p}_{2,3}(x)\,. \tag{4.71}$$

Clearly this fixes uniquely the quasi-momenta to be of the form (4.69).

### 4.5.1 The $S^3$ subsector – Moduli fixing

In this section we review the construction of the quasi-momenta for generic $su(2)$ solutions corresponding to strings vibrating in $S^3$ and point-like in the remaining space [83]. For these configurations $S_1 = S_2 = J_3 = 0$ and the the two physical modes in the three sphere $S^3$ correspond, in the algebraic curve language, to cuts uniting $\tilde{2}\tilde{3}$ and $\tilde{1}\tilde{4}$ as represented in figure 4.7a.

For these configurations we have (4.69) and

$$\tilde{p}_2(x) = -\tilde{p}_3(x) \equiv p(x) \;\;,\;\; \tilde{p}_1(x) = -\tilde{p}_4(x) = 2\pi m - p(1/x) \tag{4.72}$$

so to completely analyze string solutions moving in $R \times S^3$ we need only to study the two sheeted Rieman surface generated by $\pm p(x)$ as depicted in figure 4.7b.

More precisely, all the other quasi-momenta will only manifest themselves through the several asymptotic properties to be imposed on $p(x)$. For example, the poles at $x = \pm 1$ must be synchronized as in (4.68) and thus, since the AdS quasi-momenta are given by (4.69), $p(x)$ will have two simple poles at $x = \pm 1$ with the same residue corresponding to the energy of the classical string configuration,

$$p(x) \simeq \frac{\pi \mathcal{E}}{x \pm 1} \,. \tag{4.73}$$

At infinity, from (4.60),

$$p(x) = \frac{2\pi(\mathcal{J}_1 - \mathcal{J}_2)}{x} + \mathcal{O}(1/x^2) \tag{4.74}$$

and finally at zero we must also fix its asymptotic behavior to

$$p(x) = 2\pi m - 2\pi(\mathcal{J}_1 + \mathcal{J}_2)x + \mathcal{O}(x^2) \tag{4.75}$$

in order to ensure the proper asymptotics for the quasi-momenta $\tilde{p}_1 = -\tilde{p}_4 = 2\pi m - p(1/x)$.

Having these analytical properties at hand we can forget about all other quasi-momenta and work only with $p(x)$. As explained before its derivative $p'(x)$ will define a $K$-cut two-sheeted Riemann surface with double poles at $x = \pm 1$. Therefore $p'(x)$ must be of the form [83]

$$p'(x) = \frac{g(x)}{(x^2-1)^2\sqrt{f(x)}} \,, \tag{4.76}$$

where $f(x) = \prod_{j=1}^{2K}(x - x_j)$ and $g(x) = \sum_{j=1}^{N} c_j x^{j-1}$. Indeed, notice that close to a branch point $x_k$ we have

$$p'(x) \sim \partial_x \sqrt{x - x_k} \sim \frac{1}{\sqrt{x - x_k}} \,, \tag{4.77}$$

while close to the simple poles of the quasimomenta

$$p'(x) \sim \partial_x \frac{1}{x \pm 1} \sim \frac{1}{(x \pm 1)^2} \,, \tag{4.78}$$

thus our ansatz. To construct the quasimomenta $p(x)$ we should start at $x = \infty$ in the upper sheet and integrate $p'(x)$ up to the point $x$ without entering any cut as depicted in figure 4.8.

Let us now explain how to determine all the unknown constants in (4.76). Since $p(x)$ falls as $1/x$ at large $x$, its derivative must decay as $1/x^2$ which fixes the degree of the polynomial $g(x)$ to be $K + 2$ so that $N = K + 3$. Thus, we have the $K + 3$ constants $c_j$ plus the $2K$ branch-points $x_k$ making a total of

$$3K + 3 \text{ constants to fix.} \tag{4.79}$$

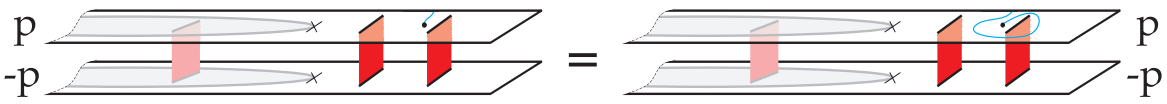


Figure 4.8: To compute $p(x)$ where $x$ is the solid black dot in the figure we should integrate $p'(x)$ from $x=\infty$ in the upper shift to the point $x$ without entering any cut. The two possible paths represented in the figures must yield the same result and this translated into the $A$-cycle integrals $\oint_{\mathcal{C}_j} p'(x)dx = 0$ around each of the cuts of the algebraic curve. For the configuration in the figure this would impose 2 constraints since the integral over the third cut can be blown into the previously computed cycles plus the integral over the fixed singularities at $x=\pm 1$.

We will explain how to reduce this number to zero. When we integrate from infinity to a given point $x$ to find the value of the quasimomenta the choice of path must not matter and therefore the integrals of $p'(x)$ around the several cuts must vanish

$$\oint_{\mathcal{C}_j} p'(x)dx = 0 \tag{4.80}$$

which yields $K-1$ independent constraints. The discontinuity conditions (4.50) which are now simply

$$p(x+i0) - (-p(x-i0)) = 2\pi n_j \ , \ x \in \mathcal{C}_j \tag{4.81}$$

can be written as the $K$ conditions

$$2\pi n_j \ = \ \int_{\infty}^{x+i\epsilon} p'(y)dy + \int_{\infty}^{x-i\epsilon} p'(y)dy \ , \ x \in \mathcal{C}_j \tag{4.82}$$

Moreover, each cut is also characterized by the filling fraction (4.28)

$$S_j \ = \ -\oint_{\mathcal{C}_|} (x+1/x)p'(x)dx \tag{4.83}$$

where we integrated by parts. This imposes $K-1$ constraints. Thus, at this point, one has

$$3K+3-(3K-2) = 5 \text{ constants to fix.} \tag{4.84}$$

Then there are the poles at $x=\pm 1$. From (4.73),

$$p'(x) = -\frac{\pi\mathcal{E}}{(x\pm 1)^2} + \mathcal{O}(1)\,. \tag{4.85}$$

Notice that we must have no $1/(x-1)$ term because this would lead to log singularities for $p(x)$. Thus, at each of the two points $x = \pm 1$, we have two conditions leaving us with a single $(5 - 2 \times 2)$ constant to fix.

Finally the asymptotics at $x = \infty$ and at $x = 0$ given by (4.74) and (4.75) yield (the last) two extra conditions. One of them finishes fixing all constants in terms of the charges, filling fractions and mode numbers of the solution, including the string energy. To solve the last condition we will obtain the string energy as a function of the remaining moduli.

Thus the complete classical spectrum of the string in $S^3$ was mapped to the study of hyperelliptic two-sheeted Riemann surfaces [83]. Let us consider an example to see this at work for a simple 2 cut solution in the next subsection.

### 4.5.2 Two-cut solution and the Giant Magnon

In this section we consider a generic 2 cut solution in the $SU(2)$ sector. The ansatz (4.76) is conveniently re-written as

$$p'(x) = -\frac{\pi}{f(x)}\left(\frac{\mathcal{E}f(1)}{(x-1)^2} + \frac{\mathcal{E}f'(1)}{x-1} + \frac{\mathcal{E}f(-1)}{(x+1)^2} + \frac{\mathcal{E}f'(-1)}{x+1} + 2(\mathcal{J}_1 - \mathcal{J}_2)\right). \tag{4.86}$$

where

$$f(x)\sqrt{(x-a)(x-\bar{a})(x-b)(x-\bar{b})}\,. \tag{4.87}$$

The first four terms inside the paretheses ensure (4.85) whereas the last (constant) term is engineered to ensure the correct large $x$ asymptotics (4.60). Obviously this is just a smarter way to write (4.76) since we now only need to fix the branch-points and the string energy as a function of the charges $\mathcal{J}_1$ and $\mathcal{J}_2$. To find them we should impose the several $A$ and $B$ cycle integrals (4.80,4.82) and the filling fraction conditions (4.83).

Since the solution is a two cut solution we will obtain that the moduli are elliptic functions of the branch-points. Finally to get the quasi-momenta we would have to integrate the meromorphic differential $p'dx$. These last steps will again yield the quasi-momenta as elliptic functions of $x$ and of the branch-points.

In certain instances there can be considerable simplifications due to degenerate choice of moduli of the curve. This is for example the case for the giant magnon [90, 96] solution [97, 98, 99], where the two cuts are very close, $a \sim b$ and $\bar{a} \sim \bar{b}$. We will now consider this singular limit. For that we parametrize the branch-points as

$$a = X^+ + \frac{\delta}{2}\,, \qquad b = X^+ - \frac{\delta}{2}\,. \tag{4.88}$$

$\bar{a}$ and $\bar{b}$ are complex conjugates and we will denote $X^- \equiv (X^+)^*$. We shall always work up to second order in $\delta$.

Away from the branch-points the two-cuts become indistinguishable, $a \simeq b \simeq X^+$ etc., and the quasi-momenta can be obtained from (4.86) as

$$p'(x) \simeq \frac{d}{dx}\left(\frac{2\pi\mathcal{E}x}{x^2-1} + \frac{2\pi(\mathcal{E}-\mathcal{J}+\mathcal{Q})}{X^+-X^-}\log\frac{x-X^+}{x-X^-}\right), \tag{4.89}$$

where we replaced $\mathcal{J}_1 \to \mathcal{J}$ and $\mathcal{J}_2 \to \mathcal{Q}$. We see that $p(x)$ has a log-cut condensate coming from the superposition of the two square root cuts with consecutive mode numbers [97, 98, 99]. Indeed, as we cross the two cuts we have

$$p(x) \overset{\text{first cut}}{\longrightarrow} -p(x)+2\pi(n+1) \overset{\text{second cut}}{\to} -(-p(x)+2\pi n)+2\pi(n+1) = p(x)+2\pi\,, \tag{4.90}$$

so that when the two square roots become coincident we jump directly from $p(x)$ to $p(x)+2\pi$ precisely as when changing log branch. From the algebraic curve construction it is also clear that if two branch-points collide we have $p'(x) \sim \frac{1}{\sqrt{(x-a)(x-b)}} \simeq \frac{1}{x-a}$ which integrated leads to a log cut singularity.

Notice that since we must have a jump of $2\pi$ when we cross the cut the prefactor before the log in (4.89) must be $1/i$. This fixes the leading order expression

$$\mathcal{E}-\mathcal{J}+\mathcal{Q} = \frac{1}{2\pi i}(X^+-X^-)+O(\delta^2) \tag{4.91}$$

for the energy as a function of the log Branch-points. Therefore we have

$$p'(x) \simeq p'_{far}(x) \equiv \frac{d}{dx}\left(\frac{2\pi\mathcal{E}x}{x^2-1} + \frac{1}{i}\log\frac{x-X^+}{x-X^-}\right), \qquad |x-X^+|, |x-X^-| \gg \delta\,. \tag{4.92}$$

Since the quantity inside brackets is already decaying as $x \to 1/x$ one might be tempted to identify it with the quasi-momenta $p_{far}(x)$. Actually we need to be more careful. For solutions with zero worldsheet momentum,

$$0 = \int_0^{2\pi} g^{-1}\partial_\sigma g \;\Rightarrow\; P\exp\left(-\int_0^{2\pi} d\sigma g^{-1}\partial_\sigma g\right) = g(2\pi)g^{-1}(0) = 1\,. \tag{4.93}$$

Hence, from (4.66),

$$\Omega(x) \overset{x\to\infty}{\longrightarrow} 1 \tag{4.94}$$

which means $p_i(x) \to 0$. However the GM solution describes an open string whose end-points lie on the equator of $S^3$, seperated by an angle $p$ [90]. For this non-periodic solution, the quasi-momenta at infinity are related to $p$ and

$$p_{far}(x) = \frac{\Delta}{2g}\frac{x}{x^2-1} + \frac{1}{i}\log\frac{x-X_+}{x-X_-} + \tau \tag{4.95}$$

with [17] $\tau = -p/2 = \frac{i}{2}\log\frac{X^+}{X^-}$. Moreover the inversion symmetry reads

$$\tilde{p}_1(x) = \tilde{p}_2(0) + \tau - \tilde{p}_2(1/x) \tag{4.96}$$

where we recall that $\tilde{p}_2(x) = p(x)$ in this section.

Close to the branch-points $a$ and $b$ given in (4.88), the quasi-momentum (4.86) becomes

$$p'(x) \simeq p'_{close}(x) \equiv \frac{1}{\sqrt{(x - X^+ - \frac{\delta}{2})(X^+ - \frac{\delta}{2} - x)}}\,, \qquad |x - X^+| \ll 1\,, \tag{4.97}$$

where we used again the leading order expression for the energy (4.91). Note that up to an overall constant this expression is obvious, as this is the only function that has the correct branch-cut. Imposing the same asymptotics for the overlap region $\delta \ll x - X^+ \ll 1$ as $p_{\bar{2}}$ in (4.97) fixes the overall factor in this expression. Alternatively we could fix this constant from $p(b) - p(a) = \int_a^b p' dx = \pi$ which is precisely what we used above to find the prefactor of the log.

As we explained below, the classical energy, total filling fraction and momenta of this solution, obtained by integrating the quasi-momenta with suitable measures around the two cuts, will be given by

$$\begin{aligned} \Delta - J &= \frac{g}{i}\left(X_+ - \frac{1}{X_+} - \frac{\delta^2}{8(X_+)^3}\right) + c.c.\,, \\ Q &= \frac{g}{i}\left(X_+ + \frac{1}{X_+} + \frac{\delta^2}{8(X_+)^3}\right) + c.c.\,, \\ P &= \frac{1}{i}\left(\log X_+ - \frac{\delta^2}{16(X_+)^2}\right) + c.c.\,. \end{aligned} \tag{4.98}$$

Finally, $\delta$ is fixed by imposing the B-cycle condition $\int_\infty^a p' = \pi n$, which yields [99][7]

$$\delta^2 = 16(X^+ - X^-)^2 \exp\left(-2i\tau - i\frac{4\pi\Delta}{\sqrt{\lambda}}\frac{X^+}{(X^+)^2 - 1}\right)\,. \tag{4.99}$$

These relations allow to parametrize the branch-points $X^\pm$ in terms of $\mathcal{Q}$ and $P$. In particular, for $\mathcal{Q} = Q/\sqrt{\lambda} \to 0$ we obtain [100]

$$E \simeq 4g\sin\frac{p}{2}\left(1 - 4\sin^2\frac{p}{2}e^{-\frac{\Delta}{2g\sin\frac{p}{2}}} + \ldots\right) \tag{4.100}$$

For general $\mathcal{Q}$ and to leading order we obtain the Dyonic Giant Magnon dispersion relation [96]

$$\epsilon_\infty(p) = \sqrt{Q^2 + \frac{\lambda}{\pi^2}\sin^2\frac{p}{2}}\,. \tag{4.101}$$

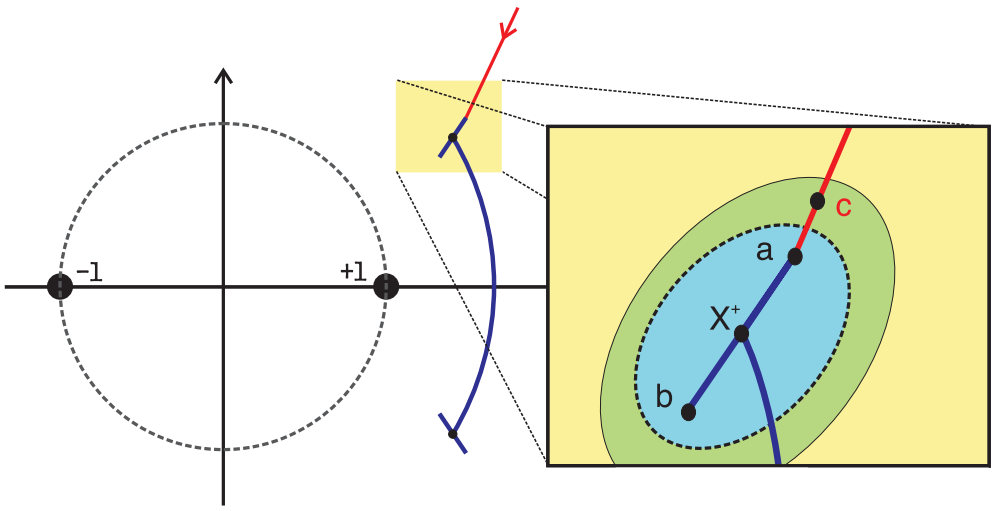


Figure 4.9: Integration regions. In the yellow region (4.95) holds whereas in the blue region the quasi-momenta is given by (4.97). In the overlapping green region both expressions can be used.

### Derivations

We now provide the details for the results in the last subsection. First let us consider $\delta^2$. It is determined by fixing the B-cycle integral. We will compute this integral using different approximations to the quasi-momentum, depending on how far the integration point is from the branch-point

$$\pi n = \int_{\infty}^{a} p' = \int_{\infty}^{c} p'_{far} + \int_{c}^{a} p'_{close} \,, \tag{4.102}$$

where $c = X^+ + \epsilon$ is an arbitrary point in the overlapping region $\delta \ll |x - X^+| \ll 1$, i.e. $\delta \ll \epsilon \ll 1$ as depicted in figure 4.9. Evaluating the integrals yields

$$\pi n \simeq \left[\frac{2\pi\mathcal{E}X^+}{(X^+)^2-1} + \frac{1}{i}\log\frac{\epsilon}{X^+ - X^-} + \tau\right] + \left[\frac{1}{i}\log\frac{\delta}{4\epsilon}\right] . \tag{4.103}$$

Here $\tau$ is the value of the quasi-momenta at infinity. As required, the dependence on $\epsilon$ cancels and we obtain $\delta$ as function of $X^\pm$ in (4.99).

Next we derive the expressions for the charges from the general relations

$$\Delta - J \;=\; \frac{g}{2\pi i}\oint dx\, p'(x)\left(x - \frac{1}{x}\right)$$

[7]The twist $\tau$ is fixed as in the appendix of [17].

$$\begin{aligned} Q &= \frac{g}{2\pi i}\oint dx\, p'(x)\left(x+\frac{1}{x}\right) \\ P &= \frac{1}{2\pi i}\oint dx\, p'(x)\log x\,. \end{aligned} \tag{4.104}$$

For this purpose we write

$$\oint dx\, p'(x)f(x) = \oint dx\, p'_{far}(x)f(x) + \oint dx\, \left(p'(x)-p'_{far}(x)\right) f(x)\,. \tag{4.105}$$

The first term obviously yields the leading order charges (4.98). The second term can be evaluated by deforming the contour to the region where the integrand is singular, i.e. $x \sim X^+$. In this region $p_{\tilde{2}}$ can be approximated by $p_{close}$

$$\oint dx\, \left(p'_{\tilde{2}}(x)-p'_{far}(x)\right) f(x) \simeq \oint \left(\frac{1}{\sqrt{(x-X^+-\frac{\delta}{2})(X^+-\frac{\delta}{2}-x)}} - \frac{i}{x-X^+}\right) f(x) + c.c.\,, \tag{4.106}$$

and the contour integral encircles all the poles of the integrand. The integrals can be easily computed and yield (4.98).

This ends this chapter. We analyzed the general classical algebraic construction and finished with an application of the formalism to the study of the classical Giant Magnon solution including the exponential corrections in the angular momentum $\mathcal{J}$. In the next chapter we move to the study of the string semi-classical quantization. As an example we will come back to the Giant-Magnon solution and quantize the string around this classical motion always keeping track of the exponential corrections. As explained in section 6.3 these exponential corrections can actually be used to check, in a very non-trivial way, the world-sheet scattering $S$-matrix.

# Chapter 5

# Quantum Fluctuations

This chapter is devoted to the study of the semi-classical quantization of type IIB strings in $AdS_5 \times S^5$ around any possible classical motion.

When we expand the superstring action around some classical solution, characterized by some conserved charges, we obtain, for the oscillations, a quadratic lagrangian whose quantization yields the semiclassical spectrum

$$E(\lambda, \{N_{A,n}\}) = E_{cl} + E_0 + \sum_{A,n} N_{A,n}\, \mathcal{E}_{A,n}\,, \tag{5.1}$$

where $N_{A,n}$ is the number of excited quanta with energy $\mathcal{E}_{A,n}$. The subscript $A$ labels the several possible string polarizations we can excite while the mode number $n$ is the Fourier mode of the quantum fluctuation. The classical energy is is $E_{cl}$ and $E_0$ is the ground state energy. The classical energy is of order $\sqrt{\lambda}$ while the last two terms are of order 1 and are the analogues of $\frac{1}{2}\omega$ and $N\omega$ in the Harmonic oscillator example (4.4).

Of course, the ground state and fluctuation energies in any quantum field theory are related, in the same way that if we know the level spacing $\omega$ for the Harmonic oscillator we infer the ground state energy $\frac{1}{2}\omega$. For a field theory we have an infinite number of fluctuation energies and thus the one loop shift is given by a (graded) sum of halved fluctuation energies,

$$E_0 = \frac{1}{2}\sum_{A,n}(-1)^{F_A}\mathcal{E}_{A,n} \tag{5.2}$$

where $(-1)^{F_A} = \pm 1$ for a bosonic/fermionic excitation.

In this chapter we will concentrate on the problem of using the algebraic curve formalism described in the previous chapter to compute the fluctuation energies around any classical solution.

Let us explain the idea behind the computation. There are basically two main steps involved. First we construct the curve associated with the classical trajectory around which we want to consider the quantum fluctuations. This will be some Riemann surface with some cuts uniting some of the eight sheets. The second step consist of considering the small excitations around this classical solution in the spirit of [93]. In terms of the algebraic curve this consists of adding microscopic cuts to this macroscopic background. These small cuts can be treated as a finite number of poles whose residue we know [66, 35, 11], just like in

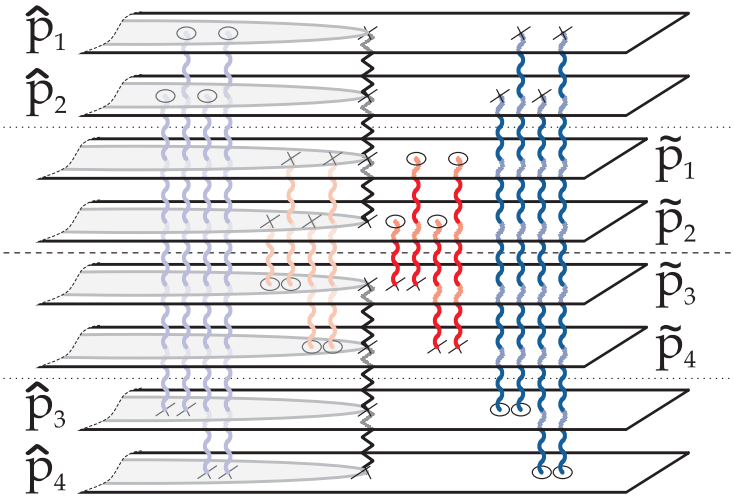


Figure 5.1: Some configuration of poles on the algebraic curve corresponding to the $S^5$ excitations (red) and $AdS_5$ excitations (blue). Black line denotes poles at $\pm 1$, connecting 4 sheets with equal residues. The crosses correspond to the residue $+\alpha(x)$, while circles to residue $-\alpha(x)$. Physical domain of the surface lies outside the unit circle.

the simple example (4.2). Then, by construction, the energy of the perturbed configuration is quantized as in (5.1). We must stress that the knowledge of the residue (4.27), of utmost importance, is the only extra input we needed to compute the quasi-classical spectrum.

The several possible choices of sheets to be connected by these poles correspond to the several possible polarizations of the superstring, i.e. to the different quantum numbers. The 16 physical excitations are the 4+4 modes in $AdS_5$ and $S^5$ (fig 5.1) plus the 8 fermionic fluctuations (fig 5.2).

Let us give a bit more of flavor to this discussion. As anticipated in the previous chapter, the equations describing the eight sheet quasi-momenta can be discretized [66, 35] yielding a set of Bethe ansatz equations for the roots $x_i$ making up the cuts. Roughly speaking, the resulting equations resemble (4.5) with an extra $2\pi n_i$ in the left hand side

$$\sum_{j\neq i} \frac{1}{x_i - x_j} = 2\pi n_i + V(x_i)\,.$$

This means that we can think of $x_i$ as being the position of a particle interacting with many others via a two-dimensional Coulomb interaction, placed in an external potential and feeling an external force $2\pi n_i$. What we are then doing is first considering a large number of particles which will condense in some disjoint supports – the cuts – with each cut being made out of particles with the same mode number $n_i$. Then we add an extra particle with some other mode number $n$. At leading order, two things happen. The particle will seek its equilibrium point in this background and will backreact, shifting the

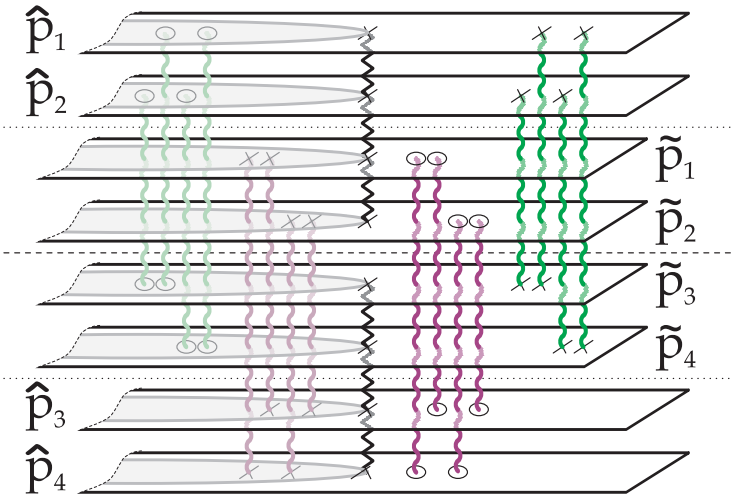


Figure 5.2: Some configuration of poles on the algebraic curve corresponding to the 8 fermionic excitations. Black line denotes poles at $\pm 1$, connecting 4 sheets with equal residues. The crosses correspond to the residue $\alpha(x)$, while circles to residue $-\alpha(x)$. Physical domain of the surface lies outside the unit circle.

background slightly by its presence [78, 93]. The (AdS global time) energy $E$ of the new configuration is then shifted. When adding $N$ particles we get precisely the quantum steps in the spectrum, i.e. (5.1).

Technically the computations can be divided into two main steps. In what follows we will use the notation (4.30) intensively. One must satisfy

$$(p_i + \delta p_i)^+ - (p_j + \delta p_j)^- = 2\pi n \ , \ \ x \in \mathcal{C}_{ij} \tag{5.3}$$

for all cuts of the Riemann surface where $p$ is the quasi-momenta associated with the classical solution, $\delta p$ is the perturbation and, therefore, $p + \delta p$ is the quasi-momenta of the perturbed algebraic curve.

- When applied to the microscopic cut, i.e. pole, equation (5.3) gives us, to leading order, the position $x_n^{ij}$ of the pole,

$$p_i(x_n^{ij}) - p_j(x_n^{ij}) = 2\pi n, \qquad |x_n^{ij}| > 1 \ , \tag{5.4}$$

  where $i < j$ take values $\hat{1}, \hat{2}, \hat{3}, \hat{4}, \tilde{1}, \tilde{2}, \tilde{3}, \tilde{4}$ and indicate which two sheets share the pole. We refer to domain $|x| > 1$ as *physical domain*. The interior of the unit circle is just the mirror image of the physical domain, as we saw in the previous chapter, (4.59).

- Then, to find $\delta p$ and, in particular, the energy shift $\delta E$, we must solve the same equations but now in the macroscopic cuts

$$\delta p_i^+ - \delta p_j^- = 0 \ , \ \ x \in \mathcal{C}_n^{ij} \ . \tag{5.5}$$

This linear problem is to be supplemented with the known analytical properties of $\delta p(x)$ namely the asymptotic behavior presented below and the simple pole singularities with residues (4.27). In this way we are computing the backreaction described above.

Before proceeding it is useful to introduce some simple notation. We shall consider $N_n^{ij}$ excitations with mode number $n$ between sheet $p_i$ and $p_j$ such that

$$N_{ij} \equiv \sum_n N_n^{ij}$$

is the total number of poles connecting these two sheets. Moreover, each fluctuation has its own quantum numbers according to the global symmetry. The $S^5$, $AdS_5$ and fermionic quanta can then be identified as the several possible choices of sheets to be connected, see figs 5.1 and 5.2,

$$\begin{aligned} S^5 \quad &, \quad (i,j) = (\tilde{1},\tilde{3}),(\tilde{1},\tilde{4}),(\tilde{2},\tilde{3}),(\tilde{2},\tilde{4}) \\ AdS_5 \quad &, \quad (i,j) = (\hat{1},\hat{3}),(\hat{1},\hat{4}),(\hat{2},\hat{3}),(\hat{2},\hat{4}) \\ \text{Fermions} \quad &, \quad (i,j) = (\tilde{1},\hat{3}),(\tilde{1},\hat{4}),(\tilde{2},\hat{3}),(\tilde{2},\hat{4}), \\ &\qquad\qquad (\hat{1},\tilde{3}),(\hat{1},\tilde{4}),(\hat{2},\tilde{3}),(\hat{2},\tilde{4}) \end{aligned} \tag{5.6}$$

The 16 physical degrees of freedom of the superstring are precisely these 16 elementary fluctuations, also called *momentum carrying excitations* [55, 87].

When adding extra poles to the classical solutions its energy will be shifted by

$$\delta E = \delta\Delta + \sum_{\text{AdS}^5} N_{ij} + \frac{1}{2}\sum_{\text{Ferm}} N_{ij}\,, \tag{5.7}$$

where we isolated the anomalous part $\delta\Delta$ of the energy shift from the trivial bare part. Then, it is convenient to recast (4.60), for the quantum perturbations, as

$$\delta \left(\begin{array}{c} \hat{p}_1 \\ \hat{p}_2 \\ \hat{p}_3 \\ \hat{p}_4 \\ \hline \tilde{p}_1 \\ \tilde{p}_2 \\ \tilde{p}_3 \\ \tilde{p}_4 \end{array}\right) \simeq \frac{4\pi}{x\sqrt{\lambda}} \left(\begin{array}{ccc} +\delta\Delta/2 & +N_{\hat{1}\tilde{4}} + N_{\hat{1}\tilde{3}} & +N_{\hat{1}\tilde{3}} + N_{\hat{1}\tilde{4}} \\ +\delta\Delta/2 & +N_{\hat{2}\tilde{3}} + N_{\hat{2}\tilde{4}} & +N_{\hat{2}\tilde{4}} + N_{\hat{2}\tilde{3}} \\ -\delta\Delta/2 & -N_{\hat{2}\tilde{3}} - N_{\hat{1}\tilde{3}} & -N_{\tilde{1}\hat{3}} - N_{\tilde{2}\hat{3}} \\ -\delta\Delta/2 & -N_{\hat{1}\tilde{4}} - N_{\hat{2}\tilde{4}} & -N_{\tilde{2}\hat{4}} - N_{\tilde{1}\hat{4}} \\ \hline & -N_{\tilde{1}\hat{4}} - N_{\tilde{1}\tilde{3}} & -N_{\tilde{1}\hat{3}} - N_{\tilde{1}\hat{4}} \\ & -N_{\tilde{2}\tilde{3}} - N_{\tilde{2}\tilde{4}} & -N_{\tilde{2}\hat{4}} - N_{\tilde{2}\hat{3}} \\ & +N_{\tilde{2}\tilde{3}} + N_{\tilde{1}\tilde{3}} & +N_{\hat{1}\tilde{3}} + N_{\hat{2}\tilde{3}} \\ & +N_{\tilde{1}\tilde{4}} + N_{\tilde{2}\tilde{4}} & +N_{\hat{2}\tilde{4}} + N_{\hat{1}\tilde{4}} \end{array}\right) \tag{5.8}$$

These filling fractions $N_{ij}^n$ are not independent. Any algebraic curve must obey the Riemann bilinear identity (see eqs. 3.38 and 3.44 in [87]). Since this was already the case for the

classical solution around which we are expanding, the new filling fractions are constrained by

$$\sum_n n \sum_{\text{All ij}} N_n^{ij} = 0\,, \tag{5.9}$$

which is nothing but the string level matching condition in the algebraic curve language.

It is also important to note that the sign of the residues can be summarized by the following formula

$$\operatorname*{res}_{x=x_n^{ij}} \hat{p}_k = \left(\delta_{i\hat{k}} - \delta_{j\hat{k}}\right) \alpha(x_n^{ij}) N_n^{ij}, \qquad \operatorname*{res}_{x=x_n^{ij}} \tilde{p}_k = \left(\delta_{j\tilde{k}} - \delta_{i\tilde{k}}\right) \alpha(x_n^{ij}) N_n^{ij}\,, \tag{5.10}$$

with $k = 1, 2, 3, 4$ and $i < j$ taking values $\hat{1}, \hat{2}, \hat{3}, \hat{4}, \tilde{1}, \tilde{2}, \tilde{3}, \tilde{4}$, as summarized in figs 5.1 and 5.2.

The poles of the shifted quasi-momenta must still be synchronized as in (4.68) which means

$$\{\delta\hat{p}_1, \delta\hat{p}_2, \delta\hat{p}_3, \delta\hat{p}_4 | \delta\tilde{p}_1, \delta\tilde{p}_2, \delta\tilde{p}_3, \delta\tilde{p}_4\} \simeq \frac{\{\delta\alpha_\pm, \delta\alpha_\pm, \delta\beta_\pm, \delta\beta_\pm | \delta\alpha_\pm, \delta\alpha_\pm, \delta\beta_\pm, \delta\beta_\pm\}}{x \pm 1}\,, \tag{5.11}$$

and the inversion symmetry (4.59) must hold for the perturbed curve so that

$$\{\delta\hat{p}_1(1/x), \delta\hat{p}_4(1/x) | \delta\tilde{p}_1(1/x), \delta\tilde{p}_4(1/x)\} = -\{\delta\hat{p}_2(x), \delta\hat{p}_3(x) | \delta\tilde{p}_2(x), \delta\tilde{p}_3(x)\}\,. \tag{5.12}$$

We must stress again than when we add a quantum fluctuation to the curve only two quasi-momenta get a pole (in the physical region) but in general, *all* the quasi-momenta will be shifted because of the back-reaction. This shift must be such that the analytical properties just enumerated are satisfied.

We can already notice that, using this procedure, one relies uniquely on considerations of analyticity and *need not* introduce any particular parametrization of the group element $g(\sigma, \tau)$ for the fluctuations around the classical solution, contrary to what is usually done in this type of analysis [101, 102, 94, 103]. It is also nice to see that the fermionic and bosonic frequencies appear, in our approach, on a completely equal footing, both corresponding to simple poles which differ only by the sheets they unite - see figs 5.1 and 5.2. Finally, in principle, we can apply our method to any classical solution whereas the same generalization seems to be highly non-trivial to do directly from the string action since we no longer have a simple field redefinition to make it time and space independent as in [102, 103]. Instead, from the action point of view, we must consider the generalization of the fluctuation energies to what is called the stability angles and the treatment quickly becomes highly involved.

In the next sections we will compute the fluctuations energies around the BMN point like string and around the simple circular string described in section 4.4. This will illustrate the kind of analyticity arguments involved in this sort of computations. In section 5.5

we present a more powerful (complementary) method based on the notion of *off-shell fluctations energies*. We will explain that for most classical solutions of interest – including in particular all $SU(2)$ solutions – we can obtain the full semi-classical spectrum with all the sixteen excitations from the knowledge of two fluctuation energies alone (for example one in $S^5$ and another in $AdS_5$). In the last section we apply this efficient method to the study of the $SU(2)$ two cut solution considered before in section 4.5.2.

## 5.1 The BMN string

In this section we shall consider the simplest possible solution amongst the family of circular strings presented in section 4.4.1 – the rotating point like BMN string [104] moving around a big circle of $S^5$. For this solution the quasi-momenta are given by (4.44). This is indeed the simplest 8 sheet algebraic curve we could have built – it has neither poles nor cuts connecting its sheets other than the trivial ones at $x = \pm 1$ (4.68).

We shall now study the quantum fluctuations around this solution. We will do it using a few different methods which will be useful for latter discussions of the string quantization around more complicated classical configurations.

To consider the 16 types of physical excitations we add all types of poles on the fig 5.1 and 5.2. From (5.4) we find that the poles in the physical domain with $|x| > 1$, for this simple case, are all located at the same position

$$x_n^{ij} = x_n = \frac{1}{n}\left(\mathcal{J} + \sqrt{\mathcal{J}^2 + n^2}\right) , \tag{5.13}$$

which follows from

$$\frac{4\pi\mathcal{J}x_n}{x_n^2 - 1} = 2\pi n \, . \tag{5.14}$$

Now we must find the quasi-momenta $p(x) + \delta p(x)$. About $\delta p(x)$ we know that

- it has poles located at (5.13) with residues (5.10) connecting the several sheets,
- must obey the $x \to 1/x$ inversion symmetry property (5.12),
- must have simple poles at $x = \pm 1$ with residues grouped as in (5.11),
- decays as $1/x$ at large $x$ as prescribed in (5.8).

Notice that for this simple solution there are no singularities other than poles so the $\delta p_i$ are simple rational functions which (as any rational function) are uniquely fixed by their asymptotics and singularities.

We will first do this computation considering only the $S^3$ fluctuations corresponding to the polarization $\tilde{2}\tilde{3}$. Next we will study the $AdS_3$ ones with polarization $\hat{2}\hat{3}$ and finally we will consider the general case.

### 5.1.1 $S^3$ excitations

Here we consider only excitations between $\tilde{p}_2$ and $\tilde{p}_3$. To render the expressions simpler we can now drop the polarization index in $N_n^{ij}$ and $x_n^{ij}$ because they are always $ij = \tilde{2}\tilde{3}$. The quasi-momenta can have poles at $x = \pm 1$, and $x = x_n$ and must decay as $1/x$ at infinity. The most general expression we can write is

$$\begin{aligned}
\delta\tilde{p}_2(x) &= \frac{\delta\alpha_+}{x-1} + \frac{\delta\alpha_-}{x+1} - \sum_n \frac{\alpha(x_n)N_n}{x-x_n} \\
\delta\tilde{p}_3(x) &= \frac{\delta\beta_+}{x-1} + \frac{\delta\beta_-}{x+1} + \sum_n \frac{\alpha(x_n)N_n}{x-x_n} \\
\delta\hat{p}_2(x) &= \frac{\delta\alpha_+}{x-1} + \frac{\delta\alpha_-}{x+1} \\
\delta\hat{p}_3(x) &= \frac{\delta\beta_+}{x-1} + \frac{\delta\beta_-}{x+1}
\end{aligned}$$

where the residues at $x = \pm 1$ were already synchronized as in (5.11). The remaining quasi-momenta are not free but given by the inversion symmetry (5.12). Now we will fix all these constants from the several asymptotics. From (5.8) we see that

$$\delta\hat{p}_2(x), -\delta\hat{p}_3(x) \simeq \frac{2\pi\delta\mathcal{E}}{x} \tag{5.15}$$

which means

$$\delta\alpha_+ + \delta\alpha_- = -\delta\beta_+ - \delta\beta_- = 2\pi\delta\mathcal{E}\,. \tag{5.16}$$

The same asymptotics must hold for $\delta p_1(x) = -\delta p_2(1/x)$ and for $\delta p_4(x) = -\delta p_3(1/x)$ and this yields $\delta\alpha_+ = \delta\alpha_-$ and $\delta\beta_+ = \delta\beta_-$ so that[1]

$$\delta\tilde{p}_2(x) = -\delta\tilde{p}_3(x) = \frac{2\pi\delta\mathcal{E}x}{x^2-1} - \sum_n \frac{\alpha(x_n)N_n}{x-x_n}\,, \tag{5.17}$$

$$\delta\hat{p}_2(x) = -\delta\hat{p}_3(x) = \frac{2\pi\delta\mathcal{E}x}{x^2-1}\,. \tag{5.18}$$

Now we consider the large $x$ asymptotics of the sphere quasi-momenta. From (5.8), one has

$$\delta\tilde{p}_2(x), -\delta\tilde{p}_3(x) \simeq \sum_n \frac{4\pi N_n}{\sqrt{\lambda}}\frac{1}{x} \tag{5.19}$$

[1]When we only add $S^3$ quantum fluctuations to the BMN string we are simply studying a solution in the $S^3$ sector and therefore the hatted quasi-momenta ought to be as in (4.69) and $\tilde{p}_2 = -\tilde{p}_3$ as explained in section 4.5.1. Thus (5.17) and (5.18) could have well been our starting point. We chose to do some unnecessary and repeated work in order to provide us with some training concerning the kind of manipulations involved in the study of algebraic curves.

which leads to

$$2\pi\delta\mathcal{E} = \sum_n N_n \left(\alpha(x_n) - \frac{4\pi}{\sqrt{\lambda}}\right) \tag{5.20}$$

so we could be tempted stop here and move to the $AdS_3$ fluctuations. This would be premature since, as we will soon see, the remaining conditions still have some juice to extract. For example notice that we already anticipated in (4.27) what the function $\alpha(x)$ is but we will see that this can actually be derived.

Let us check the asymptotics of $\delta\tilde{p}_1(x) = -\delta\hat{p}_2(1/x)$ and $\delta\tilde{p}_4(x) = -\delta\hat{p}_3(1/x)$. For the former one finds

$$\delta\tilde{p}_1(x) \simeq -\sum_n N_n \frac{\alpha(x_n)}{x_n} + \left(2\pi\delta E - \sum_n N_n \frac{\alpha(x_n)}{x_n^2}\right)\frac{1}{x} \tag{5.21}$$

but from (5.8) we see that $\delta p_1$ should decay as $1/x^2$! From the cancelation of the $1/x$ term, combined with (5.20), we get

$$\sum_n N_n \frac{\alpha(x_n)}{x_n^2} = \sum_n N_n \left(\alpha(x_n) - \frac{4\pi}{\sqrt{\lambda}}\right) \tag{5.22}$$

from which we derive

$$\alpha(x) = \frac{4\pi}{\sqrt{\lambda}} \frac{x^2}{x^2-1} \tag{5.23}$$

which is precisely the residue condition (4.27). The algebraic curve knows about how to quantize itself! The cancelation of the constant term in (5.21) can be written as

$$\sum_n N_n \frac{x_n}{x_n^2 - 1} = 0 \tag{5.24}$$

but, from (5.14), this is nothing but the string level matching condition

$$\sum_n N_n n = 0\,. \tag{5.25}$$

Thus we get

$$\delta\Delta = \sum_n N_n \Omega_{BMN}(x_n) \tag{5.26}$$

where

$$\Omega_{BMN}(x) = \frac{2}{x^2-1} \tag{5.27}$$

Using (5.13) one finds

$$\delta\Delta = \sum_n N_n \left(\sqrt{1 + \frac{n^2}{\mathcal{J}^2}} - 1\right) \tag{5.28}$$

where we recognize the famous BMN frequencies [104] in the anomalous part of the energy shift.

### 5.1.2 $AdS_3$ excitations

Let us now consider excitations connecting $\hat{p}_2$ and $\hat{p}_3$. Again we omit the polarization index and write the ansatz

$$\delta\tilde{p}_2(x) = \frac{\delta\alpha_+}{x-1} + \frac{\delta\alpha_-}{x+1} \tag{5.29}$$

$$\delta\tilde{p}_3(x) = \frac{\delta\beta_+}{x-1} + \frac{\delta\beta_-}{x+1} \tag{5.30}$$

$$\delta\hat{p}_2(x) = \frac{\delta\alpha_+}{x-1} + \frac{\delta\alpha_-}{x+1} + \sum_n \frac{\alpha(x_n)N_n}{x-x_n} \tag{5.31}$$

$$\delta\hat{p}_3(x) = \frac{\delta\beta_+}{x-1} + \frac{\delta\beta_-}{x+1} - \sum_n \frac{\alpha(x_n)N_n}{x-x_n} \tag{5.32}$$

The computation of the $AdS$ fluctuations is actually much more trivial than the one in the previous section and

$$\delta\alpha_\pm = \delta\beta_\pm = 0$$

because we need $\delta\tilde{p}_j$ for $j = 1, 2, 3, 4$ to decay as $1/x^2$ at infinity. Physically this is quite clear. We add a fluctuation inside $AdS_5$ so there is no shift for the $S^5$ quasi-momenta, $\delta\tilde{p}_j = 0$. Notice that the reverse is not true because of the Virasoro constraints. There are physical fluctuations which live purely in the $AdS$ space but not in the sphere due to the signatures of both spaces.

As before, from the asymptotics of the hatted quasi-momenta we would derive again the value of $\alpha(x)$, the level matching condition and, for the spectrum, we would get exactly the same expressions (5.26) and (5.28).

### 5.1.3 Full spectrum

From the requirements listed in the beginning of this section, one can easily write the form of $\delta p_j$ for a general perturbation of the BMN quasi-momenta. For example

$$\delta\hat{p}_2 = \hat{a} + \frac{\delta\alpha_+}{x-1} + \frac{\delta\alpha_-}{x+1} + \sum_{i=\hat{3},\hat{4},\bar{3},\bar{4}} \sum_n \frac{\alpha(x_n^{\hat{2}i})N_n^{\hat{2}i}}{x-x_n^{\hat{2}i}} - \sum_{i=\hat{3},\hat{4},\bar{3},\bar{4}} \sum_n \frac{\alpha(x_n^{\hat{1}i})N_n^{\hat{1}i}}{1/x-x_n^{\hat{1}i}} \tag{5.33}$$

$$\delta\hat{p}_3 = \hat{b} + \frac{\delta\beta_+}{x-1} + \frac{\delta\beta_-}{x+1} - \sum_{i=\hat{1},\hat{2},\bar{1},\bar{2}} \sum_n \frac{\alpha(x_n^{\hat{3}i})N_n^{\hat{3}i}}{x-x_n^{\hat{3}i}} + \sum_{i=\hat{1},\hat{2},\bar{1},\bar{2}} \sum_n \frac{\alpha(x_n^{\hat{4}i})N_n^{\hat{4}i}}{1/x-x_n^{\hat{4}i}} \tag{5.34}$$

where $\hat{a}, \hat{b}$ and $\delta\alpha_\pm, \delta\beta_\pm$ are constants to be fixed and the last terms ensure the right poles in physical domain for $\delta\hat{p}_{1,4}(x) = -\delta\hat{p}_{2,3}(1/x)$. Notice that it is no longer true that the quasi-momenta automatically decay as $1/x$ at large $x$ and that is why constant terms need

to be included. Similar expressions can be immediately written down for $\delta\hat{p}_{2,3}$ with the introduction of two new constants $\tilde{a}$ and $\tilde{b}$,

$$\delta\tilde{p}_2 = \tilde{a} + \frac{\delta\alpha_+}{x-1} + \frac{\delta\alpha_-}{x+1} - \sum_{i=\hat{3},\hat{4},\tilde{3},\tilde{4}} \sum_n \frac{\alpha(x_n^{\tilde{2}i}) N_n^{\tilde{2}i}}{x - x_n^{\tilde{2}i}} + \sum_{i=\hat{3},\hat{4},\tilde{3},\tilde{4}} \sum_n \frac{\alpha(x_n^{\tilde{1}i}) N_n^{\tilde{1}i}}{1/x - x_n^{\tilde{1}i}} \tag{5.35}$$

$$\delta\tilde{p}_3 = \tilde{b} + \frac{\delta\beta_+}{x-1} + \frac{\delta\beta_-}{x+1} + \sum_{i=\hat{1},\hat{2},\tilde{1},\tilde{2}} \sum_n \frac{\alpha(x_n^{\tilde{3}i}) N_n^{\tilde{3}i}}{x - x_n^{\tilde{3}i}} - \sum_{i=\hat{1},\hat{2},\tilde{1},\tilde{2}} \sum_n \frac{\alpha(x_n^{\tilde{4}i}) N_n^{\tilde{4}i}}{1/x - x_n^{\tilde{4}i}} \tag{5.36}$$

and $\delta\tilde{p}_{1,4}(x) = -\delta\tilde{p}_{2,3}(1/x)$.

At this point we are left with the problem of fixing the eight constants

$$\hat{a}, \hat{b}, \tilde{a}, \tilde{b}, \delta\alpha_+, \delta\alpha_-, \delta\beta_+, \delta\beta_- \,.$$

This is precisely the number of conditions one obtains by imposing the $1/x$ behavior at large $x$ for the quasi-momenta (5.8) . The asymptotic of $\hat{p}_2, \hat{p}_3, \tilde{p}_2, \tilde{p}_3$ fix the first four constants,

$$\begin{aligned} \hat{a} &= -\sum_n \frac{2\pi n}{\sqrt{\lambda}\mathcal{J}} \sum_{i=\hat{3},\hat{4},\tilde{3},\tilde{4}} N_n^{\hat{1}i}, \qquad \hat{b} = +\sum_n \frac{2\pi n}{\sqrt{\lambda}\mathcal{J}} \sum_{i=\hat{1},\hat{2},\tilde{1},\tilde{2}} N_n^{\hat{4}i}\,, \\ \tilde{a} &= +\sum_n \frac{2\pi n}{\sqrt{\lambda}\mathcal{J}} \sum_{i=\hat{3},\hat{4},\tilde{3},\tilde{4}} N_n^{\tilde{1}i}, \qquad \tilde{b} = -\sum_n \frac{2\pi n}{\sqrt{\lambda}\mathcal{J}} \sum_{i=\hat{1},\hat{2},\tilde{1},\tilde{2}} N_n^{\tilde{4}i}\,, \end{aligned}$$

while the remaining four equations, solvable only if the level matching condition (5.9) is satisfied, fix the remaining coefficients,

$$\begin{aligned} \delta\alpha^+ - \delta\alpha^- &= -\sum_n \frac{2\pi n}{\sqrt{\lambda}\mathcal{J}} \sum_{i=\hat{3},\hat{4},\tilde{3},\tilde{4}} \sum_{j=\hat{1},\hat{2}} N_n^{ij}\,, \\ \delta\beta^+ - \delta\beta^- &= -\sum_n \frac{2\pi n}{\sqrt{\lambda}\mathcal{J}} \sum_{i=\hat{3},\hat{4},\tilde{3},\tilde{4}} \sum_{j=\tilde{3},\tilde{4}} N_n^{ij}\,. \end{aligned}$$

yielding

$$\delta\Delta = \sum_{\text{All ij}} \sum_n N_n^{ij} \Omega_{BMN}(x_n^{ij}) \tag{5.37}$$

which using (5.13) gives

$$\delta E = \sum_{\text{All ij}} \sum_n \frac{\sqrt{n^2+\mathcal{J}^2} - \mathcal{J}}{\mathcal{J}} N_n^{ij} + \sum_{\text{AdS}^5} N^{ij} + \frac{1}{2} \sum_{\text{Ferm}} N^{ij}\,. \tag{5.38}$$

### 5.1.4 BMN string fluctuation energies and analyticity

It is possible to derive the fluctuation energies from simple analyticity arguments and that is what we shall now do. This method can be generalized to more complicated solutions and we will exemplify it on the circular string studied in the next section.

The idea is that we should think of the fluctuation energies as

$$\mathcal{E}_n^{ij} = \Omega^{ij}(y)_{y=x_n^{ij}} \,. \tag{5.39}$$

In other words, we first compute the energy shift when we perturb the algebraic curve by adding an extra pole at $x = y$ shared between the quasi-momenta $p_i$ and $p_j$ to find

$$\Omega^{ij}(y) \tag{5.40}$$

which depends only on the choice of sheets $(i, j)$. We denote these quantities by off-shell fluctuation energies. Then we fix the position of the fluctuation $y$ by the map (5.13)

$$p_i(y) - p_j(y) = 2\pi n \tag{5.41}$$

which gives

$$y = x_n^{ij} \,, \tag{5.42}$$

and thus (5.39).

From the definition of $\Omega^{ij}(y)$ it is clear that this quantity will have no singularity as a function of $y$ unless $y$ approaches some dangerous points like $\pm 1$ or some of the branch-points of the classical algebraic curve. Thus, the singularities in $\mathcal{E}_n^{ij}$ as a function of $n$ must come from the map (5.41). For example the loci $n^*$ where

$$p_i(y^*) - p_j(y^*) = 2\pi n^*$$

with

$$p_i'(y^*) - p_j'(y^*) = 0 \tag{5.43}$$

are examples of such singular points of the map $n \to x_n^{ij}$. For $n \simeq n^*$ one has

$$n - n^* \sim (y - y^*)^2 \tag{5.44}$$

while in the $y$ plane nothing special happens when we pass this point so that

$$\Omega^{ij}(y) \simeq \Omega^{ij}(y^*) + \frac{d\Omega^{ij}}{dy}(y^*)(y - y^*) \tag{5.45}$$

which means that

$$\mathcal{E}_n^{ij} \simeq A + B\sqrt{n - n^*} \,, \tag{5.46}$$

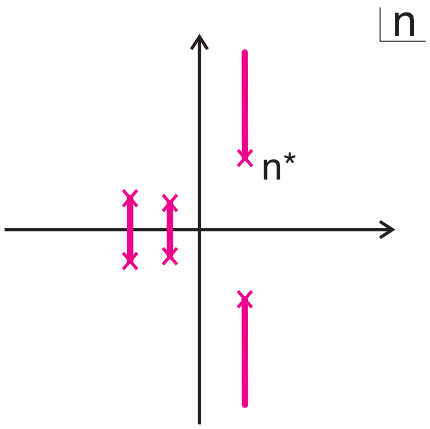


Figure 5.3: Typical analytical structure of the excitation energies as a function of the mode number $n$. The branchpoints associated to the cuts going to infinity are large if some charge of the classical solution is large. There could also be extra cuts in the $n$ plane.

as $n$ approaches $n^*$.

Let us apply these considerations to the BMN string described by the quasi-momenta (4.44). Here there are no cuts at all so the singularities must come from the points where (5.43) holds which in this case means

$$\frac{d}{dx}\left(\frac{x}{x^2-1}\right) = 0 \;\Rightarrow\; x = \pm i \tag{5.47}$$

which for the quasi-momenta yields

$$p_i(\pm i) - p_j(\pm i) = \pm 2\pi i \mathcal{J} \tag{5.48}$$

so that $n^* = \pm i\mathcal{J}$.

If the world-sheet time $\tau$ and the target-space global time $t$ are related by $t = \kappa\tau$ then, for large $n$, all fluctuation energies must behave like $\frac{1}{\kappa}\sqrt{n^2}$. For solutions moving in the sphere only we have moreover $\kappa = \mathcal{E}$, the energy of the string. For the BMN string we have $\kappa = \mathcal{E} = \mathcal{J}$. This large $n$ behavior means that there should always exist two branch-points somewhere in the complex $n$ plane. Adding to these there could in general exist more branch cuts as depicted in figure 5.3.

For the BMN string we found no extra singularities apart from the two branch points at $n^* = i\mathcal{J}$ and thus we conclude that

$$\mathcal{E}_n^{ij} = \sqrt{1 + \frac{n^2}{\mathcal{J}^2}} - 1 \tag{5.49}$$

where the constant term was added to have $\mathcal{E}_0^{ij} = 0$ – a property we expect for the fluctuation energies since for $n = 0$ they should correspond to the zero modes associated with the $PSU(2,2|4)$ global symmetries of the theory. Expression (5.49) yields precisely the BMN spectrum we found in the previous section.

### 5.1.5 BMN $SU(2)$ frequencies from quasi-energy.

So far we explained how the quasi-momenta can be used to compute the fluctuation energies. In [105] Vicedo explained how the quasi-energy can be used to find the $S^3$ fluctuation energies for string solutions moving in the three-sphere and point-like w.r.t the $AdS$ space. In this case we have $\tilde{p}_2 = -\tilde{p}_3 = p$ as explained in section (4.5.1). This is of course the case for the BMN string. The formalism in [105] is based on an extra function, the quasi-energy $q(x)$. This function is characterized by having the same cuts as the classical quasi-momenta $p(x)$ and also two simple poles at $x = \pm 1$. The key difference is that the residues at these points should be given by

$$q(x) \simeq \mp \frac{\alpha}{x \pm 1} \text{ if } p(x) \simeq \frac{\alpha}{x \pm 1}\,. \tag{5.50}$$

Then, according to [105], the fluctuation energies are simply

$$\mathcal{E}_n^{S^3} = \frac{1}{2\pi\mathcal{E}}\, q(x_n) \tag{5.51}$$

where the position $x_n$ is fixed by the usual relation

$$p(x_n) = \pi n\,. \tag{5.52}$$

For the BMN string we have

$$p(x) = \frac{2\pi\mathcal{J}x}{x^2 - 1} \tag{5.53}$$

and to find the quasi-energy we simply take out the $x$ in the numerator so that the residues at $x = \pm 1$ become of opposite signs,

$$q(x) = \frac{2\pi\mathcal{J}}{x^2 - 1}\,. \tag{5.54}$$

Then, from (5.51) and (5.52),

$$E_n^{S^3} = \frac{1}{x_n^2 - 1} = \sqrt{1 + \frac{n^2}{\mathcal{J}^2}} - 1 \tag{5.55}$$

as found in the previous sections.

## 5.2 Physical polarizations

In this section we will explain why (5.6) corresponds to the proper choice of physical polarizations. This section can be skipped in a first reading but it might be useful as a companion to section 6.2.2 in the last chapter.

In the previous section we computed the full set of sixteen physical fluctuations around the BMN point-like string. Each physical fluctuation is obtained by adding a pole at position $x_n$ found from

$$p_i(x_n) - p_j(x_n) = 2\pi n \tag{5.56}$$

to a given pair of quasi-momenta $p_i$ and $p_j$. Physical polarizations are obtained when $p_i$ belongs to the set $\{\tilde{p}_1, \tilde{p}_2, \hat{p}_1, \hat{p}_2\}$ whereas $p_j$ is a quasi-momenta in the list $\{\tilde{p}_3, \tilde{p}_4, \hat{p}_3, \hat{p}_4\}$, see table (5.6).

A simple reason for choosing these pairing of quasi-momenta is because no other choice is possible as we will now explain. First of all, if the quasi-momenta $p_i$ and $p_j$ belong to the sets we just mentioned, one has

$$p_i(x_n) - p_j(x_n) = \frac{4\pi \mathcal{J} x_n}{x_n^2 - 1} \tag{5.57}$$

and $p_i(x_n) - p_j(x_n) = 2\pi n$ can be solved for any $n$. On the other hand, if the two quasi-momenta belong to the same set, for example $\{\tilde{p}_1, \tilde{p}_2, \hat{p}_1, \hat{p}_2\}$, we obtain

$$p_i(x_n) - p_j(x_n) = 0\,, \tag{5.58}$$

and there is no background potential to fix the position of the particle. Thus the only possible choices are indeed those listed in (5.6).

An alternative way to see that other polarizations are not compatible with the algebraic curve is to try to compute $\delta p_i$ for unphysical polarizations and obtain some impossible conditions. For example, if we try to repeat the computation in section 5.1.2 for fluctuations connecting $\hat{p}_1$ and $\hat{p}_2$. For such fluctuations we expect

$$\delta \begin{pmatrix} \hat{p}_1 \\ \hat{p}_2 \\ \hat{p}_3 \\ \hat{p}_4 \\ \hline \tilde{p}_1 \\ \tilde{p}_2 \\ \tilde{p}_3 \\ \tilde{p}_4 \end{pmatrix} \simeq \frac{4\pi}{x\sqrt{\lambda}} \begin{pmatrix} +\delta\Delta/2 + N_{\hat{1}\hat{2}} \\ +\delta\Delta/2 - N_{\hat{1}\hat{2}} \\ -\delta\Delta/2 \\ -\delta\Delta/2 \\ \hline 0 \\ 0 \\ 0 \\ 0 \end{pmatrix}$$

which is impossible to satisfy: Since we do not want to perturb the tilded sphere quasi-momenta $\delta\tilde{p}_j$, we should not have poles at $x = \pm 1$ for the anti-de-Sitter hatted $\delta\hat{p}_j$'s

because this would induce a perturbation in the former through (5.11). Moreover, since there are no fluctuation poles connecting $\hat{p}_3$ or $\hat{p}_4$, they should have no poles at all. But rational functions with no pole singularities and $1/x$ behavior at infinity do not exist and we arrive at the above mentioned inconsistency.

All this discussion concerns the BMN point-like string corresponding to the vacuum algebraic curve with no cuts at all. When we start exciting some cuts we will no longer have (5.58) for unphysical polarizations. Still, by continuity, this difference will be bounded around zero and we will still find no solutions to $p_i(x_n) - p_j(x_n) = 2\pi n$ if we chose an unphysical polarization $(i, j)$. On the other hand, if the cuts are big enough, it might well be that the unphysical difference $p_i(x) - p_j(x)$ will touch $2\pi$ or $-2\pi$ for some $x$. In this case a physical fluctuation connecting this pair of sheets would exist at this point $x$. What happens is that as we increase the filling fraction of the cuts, a physical fluctuation which was connecting a pair of physical momenta can enter the cut and become what we would normally call an unphysical polarization as depicted in figure 6.2, see also [15]. Note that going through a cut is an absolutely smooth procedure and therefore no non-analyticity arises at all.

Anyway, in the worst case scenario we will have a finite number of fluctuations connecting such unphysical pairs of sheets. Most fluctuation energies will still be obtained when considering the physical polarizations (5.6). For each choice in this list we will always find an infinite number of physical fluctuations obtained by adding extra poles to the algebraic curve at the positions found from (5.56). In particular, in principle we can use this infinite set of fluctuation energies to compute $\mathcal{E}_n^{ij}$ as an analytic function of $n$. Thus, do we need to care if, for a finite number of mode numbers $n$, the fluctuations actually went through some of the cuts and now connect unphysical pairs of quasi-momenta? No. If we already have $\mathcal{E}_n^{ij}$ we simply evaluate this function at those values of $n$.

So, when do we need to take into account these unphysical fluctuations? For example, if we are using the algebraic curve to sum all fluctuation energies to compute the one-loop shift (5.2). As explained in the next chapter this sum can be transformed into the computation of some contour integrals in the algebraic curve encircling the positions of all fluctuations. These integrals can then be deformed and in doing so we compute the one-loop shift in a very efficient way. In this setup we must start off with the correct integration contour and thus we should be careful about the possible existence of these unphysical fluctuations, see section 6.2.2.

## 5.3 *AdS* fluctuations around strings moving in $S^5$.

In this section we want to point out that for any solution with energy $\mathcal{E}$ moving in $S^5$ and point-like in *AdS* with $t = \mathcal{E}\tau$ (or in terms of the *AdS* embedding coordinates $v_6 + iv_5 =$

$e^{i\mathcal{E}\tau}$) the $AdS$ fluctuation energies are always trivial to compute and simply given by

$$\mathcal{E}_n^{AdS} = \sqrt{1 + \frac{n^2}{\mathcal{E}^2}} - 1\,. \tag{5.59}$$

Let us explain why this is so from several equivalent arguments, one of them relying on the direct expansion of the string action and the other two using the algebraic curve language:

- First of all (5.59) is clear from the expansion of $v_j \to v_j + \delta v_j$ in the action (2.9). From the Virasoro coupling of the $AdS_5$ and $S^5$ motion it is easy to see that the Lagrange multiplier before the $v \cdot v - 1$ constraint is given by $\mathcal{E}^2$ and therefore the expansion gives $\sqrt{n^2 + \mathcal{E}^2}$ for the world-sheet energies in static gauge. Since $t = \mathcal{E}\tau$ we obtain the announced expression for the target space energy.

- From the point of view of the algebraic curve this is equally manifest. Since the $AdS$ coordinates are simply $v_6 + iv_5 = e^{i\mathcal{E}\tau}$, the $AdS$ quasi-momenta read (4.69) as explained in the end of section 4.5. To compute $AdS$ fluctuation energies we add a pole shared by two of the hatted quasi-momenta. We do not want $\delta\hat{p}_j$ to have poles at $x = \pm 1$ because due to the Virasoro contrains (5.11) this would lead to $\delta\tilde{p}_j \neq 0$. Moreover (4.69) have no cuts at all. Thus, for example for a $\hat{2}\hat{3}$ excitation we can only have poles at $x = x_n$ and therefore we are lead to

  $$\delta\hat{p}_2(x) = -\delta\hat{p}_3(x) = \sum_n \frac{\alpha(x_n)N_n}{x - x_n} \tag{5.60}$$

  as for the BMN string. Hence, as before,

  $$\delta\Delta = \sum_n N_n \Omega_{BMN}(x_n) \tag{5.61}$$

  where

  $$\Omega_{BMN}(x) = \frac{2}{x^2 - 1}\,. \tag{5.62}$$

  The only difference is that when computing $x_n$ we now have (5.14) with $\mathcal{J}$ replaced by $\mathcal{E}$ and therefore (5.59) follows.

- Finally we could use the analyticity reasoning described for the BMN string in section 5.1.4. The singularities of the $AdS$ frequencies

  $$\mathcal{E}_n^{ij} = \Omega^{ij}(y)_{y=x_n^{ij}} \tag{5.63}$$

  will follow from the singularities of the map $n \to x_n^{ij}$ which for the AdS quasi-momenta is the same as for the BMN string with $\mathcal{J} \to \mathcal{E}$. Thus, as in section 5.1.4, we conclude that the fluctuation energies have no singularities apart from two branch-points at $n^* = \pm i\mathcal{E}$ and together with the known large $n$ asymptotics this fixes (5.59).

## 5.4 $SU(2)$ Circular string

The next less trivial example is the simple $su(2)$ rigid circular string [101] already encountered in the previous chapter. The quasi-momenta associated with this classical solution are given by (4.48) and (4.49),

$$\begin{pmatrix} \hat{p}_1 \\ \hat{p}_2 \\ \hat{p}_3 \\ \hat{p}_4 \\ \hline \tilde{p}_1 \\ \tilde{p}_2 \\ \tilde{p}_3 \\ \tilde{p}_4 \end{pmatrix} = \frac{2\pi x}{x^2-1} \begin{pmatrix} +K(1) \\ +K(1) \\ -K(1) \\ -K(1) \\ \hline +K(1/x) \\ +K(x) \\ -K(x) \\ -K(1/x) \end{pmatrix} + \begin{pmatrix} 0 \\ 0 \\ 0 \\ 0 \\ \hline 0 \\ -2\pi m \\ +2\pi m \\ 0 \end{pmatrix}, \quad K(x) \equiv \sqrt{m^2x^2 + \mathcal{J}^2}. \tag{5.64}$$

In this section we will compute two fluctuation energies associated with the $S^3$ and the $AdS_3$ excitations. We will not compute the remaining fourteen $(16-2)$ polarizations for two reasons. On the one hand because after the computation of the two fluctuation energies the remaining excitations are easily found with only some very minor differences in the actual computations. On the other hand, and more importantly, because as we will explain in the next section it is possible to obtain all other fourteen fluctuation energies – including the fermionic ones – from the knowledge of the $S^3$ and $AdS_3$ excitations alone.

### 5.4.1 Standard Computation Method

Suppose we want to compute the variation of the quasi-momenta $\delta p(x)$ when a small pole is added to a generic finite gap solution with some square root cuts. Since the branch points will be slightly displaced we conclude that $\delta p(x)$ behaves like $\partial_{x_0}\sqrt{x-x_0} \sim 1/\sqrt{x-x_0}$ near each such point.

Here we are dealing with a 1-cut finite gap solution. Then, for $\delta\tilde{p}_2$, we can assume the most general analytical function with one branch cut, namely $f(x) + g(x)/K(x)$ where $f$ and $g$ are some rational functions and $K(x)$ is the square root in (5.64). To obtain $\delta\tilde{p}_3$ it suffices to notice that (5.5) is simply telling us that $\delta\tilde{p}_3$ is the analytical continuation of $\delta\tilde{p}_2$ through the cut. This is a fancy way of saying that $K(x) \to -K(x)$. The remaining quasi-momenta $\delta\tilde{p}_{1,4}$ can then be obtained from these ones by the inversion symmetry (5.12). We conclude that

$$\begin{pmatrix} \delta\tilde{p}_1 \\ \delta\tilde{p}_2 \\ \delta\tilde{p}_3 \\ \delta\tilde{p}_4 \end{pmatrix} = \begin{pmatrix} -f(1/x) - \frac{g(1/x)}{K(1/x)} \\ f(x) + \frac{g(x)}{K(x)} \\ f(x) - \frac{g(x)}{K(x)} \\ -f(1/x) + \frac{g(1/x)}{K(1/x)} \end{pmatrix}. \tag{5.65}$$

The only singularities of $\delta\tilde{p}_2$ apart from the branch cut are eventual simple poles at $\pm 1$ and $x_n$ and so the same must be true for $f(x)$ and $g(x)$. Then, just like in the previous example, these functions are uniquely fixed by the large $x$ asymptotics (5.8) and by the residues at $x_n$ (5.10) of the quasi-momenta.

Finally, since the $AdS_5$ part of the quasi-momenta of the non-perturbed finite gap solution has no branch-cuts, their variations $\delta\hat{p}_i$ have the same form (5.33),(5.34) as for the simplest BMN string.

The $AdS_5$ fluctuations were already treated in a much more general setup in the previous section. We find

$$\mathcal{E}_n^{AdS} = \Omega_{BMN}(x_n^{ij}) \ , \ \ \Omega_{BMN}(y) = \frac{2}{y^2-1} \tag{5.66}$$

or (5.59).

Next we consider the $S^5$ fluctuations. We must now analyze the shift in quasi-momenta due to the excitation of the algebraic curve by the four type of poles $(\tilde{1}\tilde{3}, \tilde{2}\tilde{4}, \tilde{2}\tilde{3}, \tilde{1}\tilde{4})$. We will only study the excitation $\tilde{2}\tilde{3}$ in detail. As mentioned above we will be able to reproduce all these fluctuations together with the fermionic ones from the knowledge of the single $AdS$ fluctuation energy determined above plus the $S^3$ excitation $\tilde{2}\tilde{3}$ which we will now compute.

As for the BMN string we omit the polarization superscript $\tilde{2}\tilde{3}$ from the occupation numbers $N_n^{\tilde{2}\tilde{3}}$ and from the pole positions $x_n^{\tilde{2}\tilde{3}}$.

Since the $AdS$ quasi-momenta are trivial, with no cuts, we obtain for $\delta\hat{p}$ the same kind of expression we had for the BMN string (4.44), that is

$$\delta\hat{p}_{1,2} = -\delta\hat{p}_{3,4} = \frac{2\pi\delta E}{\sqrt{\lambda}}\frac{x}{x^2-1}\,. \tag{5.67}$$

Due to the Virasoro constraints, the poles at $x = \pm 1$ in the $AdS_5$ and $S^5$ sectors are synchronized as in (4.68). Thus, we merely need to fix $f(x)$ and $g(x)$ from the large $x$ asymptotics (5.8) and the residue condition (5.10) and then extract, from these two functions, the residues at $x = \pm 1$.

For fluctuations connecting $\tilde{p}_2$ to $\tilde{p}_3$ the symmetry of the problem constrains $\delta\tilde{p}_2 = -\delta\tilde{p}_3$ and therefore $f(x) = 0$ as mentioned in section (4.5.1). Alternatively we can derive this from the following simple reasoning:

$$f(x) = \frac{1}{2}\left(\delta\tilde{p}_2(x) + \delta\tilde{p}_3(x)\right)$$

which means $f(x)$ has no pole at $x = x_n$. Moreover since the residues of $\delta\tilde{p}_{2,3}$ at $x = \pm 1$ are synchronized to those of $\delta\hat{p}_{2,3}$ as in (5.11) we see that $f(x)$ has no poles at $x = \pm 1$ either. Thus $f(x)$ has no poles at all. Since it must vanish at infinity we conclude $f(x) = 0$.

The remaining function $g(x)$ will then be given by

$$g(x) = -\frac{4\pi m}{\sqrt{\lambda}}\sum_n N_n + \frac{\pi\mathcal{E}K(1)}{x-1} + \frac{\pi\mathcal{E}K(-1)}{x+1} - \sum_n N_n\frac{\alpha(x_n)K(x_n)}{x-x_n} \tag{5.68}$$

All prefactors were fixed so that the residues at $x = \pm 1$ for $\delta\tilde{p}_{2,3}$ are synchronized with the AdS quasi-momenta as in (5.11) and in order to have the proper residues $\mp\alpha(x_n)$ at $x = x_n$ as required from (5.10). Finally, the first constant term was fixed by the large $x$ asymptotics for $\delta\tilde{p}_2(x)$.

Next we impose the large $x$ asymptotics for $\delta\tilde{p}_1(x) = -\delta\tilde{p}_2(1/x)$. This quasi-momentum must decay at least at $1/x^2$. The cancelation of the $1/x$ term fixes the fluctuation energies to be

$$\mathcal{E}_n^{\tilde{2}\tilde{3}} = \tilde{\Omega}(y)_{y=x^n} \quad , \quad \tilde{\Omega}(y) = \frac{\sqrt{m^2y^2 + \mathcal{J}^2}}{\sqrt{m^2 + \mathcal{J}^2}} \frac{2}{y^2 - 1} \tag{5.69}$$

and setting the constant term to zero yields the level matching condition $\sum_n N_n n = 0$.

To find $\mathcal{E}_n^{\tilde{2}\tilde{3}}$ as a function of the mode number $n$ we simply need to solve $\tilde{p}_2(x_n) - \tilde{p}_3(x_n) = 2\pi n$ and plug $x_n$ into the off-shell fluctuation energies to obtain

$$\mathcal{E}_n^{\tilde{2}\tilde{3}} = \sqrt{2\mathcal{J}^2 + (n+2m)^2 - 2\sqrt{\mathcal{J}^4 + (n+2m)^2(\mathcal{J}^2 + m^2)}} \tag{5.70}$$

reproducing the result of [106].

In a similar way we could compute all the other fluctuation energies. Let us just provide a glimpse of the reasonings involved. Take for example the fluctuations $\tilde{1}\tilde{3}$. Since the difference

$$\delta\tilde{p}_3 = f(x) - g(x)/K(x)$$

must have a single pole at $x_n^{\tilde{1}\tilde{3}}$ with residue $\alpha(x_n^{\tilde{1}\tilde{3}})$, whereas the sum

$$\delta\tilde{p}_2 = f(x) + g(x)/K(x)$$

must be analytical, we infer the value of the residues of both $f$ and $g$ at this point. This line of thought should be carried over for all the other excitations and for the points $x = \pm 1$. Knowing the positions and residues of all possible poles we would write a similar ansatz as in (5.68) for both $f(x)$ and $g(x)$ and the large $x$ asymptotics would fix the energy as above.

In similar lines we could study fermionic fluctuations. We would find the full spectrum as

$$\begin{aligned}
\kappa\, \delta E \;=\; & \sum_n \left(N_n^{\tilde{1}\tilde{3}} + N_n^{\tilde{2}\tilde{4}}\right)\left(\omega_{n+m}^{S} - \mathcal{J}\right) + N_n^{\tilde{2}\tilde{3}}\omega_{n+2m}^{S_-} + N_n^{\tilde{1}\tilde{4}}\left(\omega_n^{S_+} - 2\mathcal{J}\right) \\
+ \; & \sum_n \left(N_n^{\hat{1}\tilde{4}} + N_n^{\hat{2}\tilde{4}} + N_n^{\hat{3}\tilde{1}} + N_n^{\hat{4}\tilde{1}}\right)\left(\omega_n^{F} - \mathcal{J} + \frac{\kappa}{2}\right) \\
+ \; & \sum_n \left(N_n^{\hat{1}\tilde{3}} + N_n^{\hat{2}\tilde{3}} + N_n^{\hat{3}\tilde{2}} + N_n^{\hat{4}\tilde{2}}\right)\left(\omega_{n+m}^{F} - \frac{\kappa}{2}\right) \\
+ \; & \sum_n \left(N_n^{\hat{1}\hat{3}} + N_n^{\hat{1}\hat{4}} + N_n^{\hat{2}\hat{3}} + N_n^{\hat{2}\hat{4}}\right)\omega_n^{A}\,,
\end{aligned} \tag{5.71}$$

Table 5.1: *Simple $su(2)$ frequencies computed in [101]*

| | **eigenmodes** | **notation** |
|---|---|---|
| $\mathbf{S^5}$ | $\sqrt{2\mathcal{J}^2+n^2\pm 2\sqrt{\mathcal{J}^4+n^2\mathcal{J}^2+m^2n^2}}$ | $\omega_n^{S_\pm}$ |
| | $\sqrt{\mathcal{J}^2+n^2-m^2}$ | $\omega_n^{S}$ |
| **Fermions** | $\sqrt{\mathcal{J}^2+n^2}$ | $\omega_n^{F}$ |
| $\mathbf{AdS_5}$ | $\sqrt{\mathcal{J}^2+n^2+m^2}$ | $\omega_n^{A}$ |

with the notation introduced in the table. We notice the appearance of some minor constant shifts and relabeling of the frequencies when compared to those in table 5.1. This point is briefly discussed in appendix C.

### 5.4.2 Analytical power

In this section let us revisit the arguments in section (5.1.4) applied to this $SU(2)$ circular string. Again, we can find the singularities of the map $p_i(x)-p_j(x)=2\pi n$ by computing the values of $x^*$ (and corresponding $n^*$) so that $p_i'(x^*)-p_j'(x^*)=0$. We obtain

| $x^*$ | $n^*$ | $(i,j)$ |
|---|---|---|
| $\pm i$ | $\pm\sqrt{\mathcal{J}^2+m^2}$ | $(\hat{1},\hat{3}),(\hat{1},\hat{4}),(\hat{2},\hat{3}),(\hat{2},\hat{4})$ |
| $\pm i\mathcal{J}/\sqrt{m^2+\mathcal{J}^2}$ | $m\pm i\mathcal{J}$ | $(\hat{1},\tilde{3}),(\hat{2},\tilde{3}),(\tilde{2},\hat{3}),(\tilde{2},\hat{4})$ |
| $\pm i\sqrt{m^2+\mathcal{J}^2}/\mathcal{J}$ | $2m\pm i\mathcal{J}$ | $(\hat{1},\tilde{4}),(\hat{2},\tilde{4}),(\tilde{1},\hat{3}),(\tilde{1},\hat{4})$ |
| $\pm i$ | $m\pm i\sqrt{\mathcal{J}^2-m^2}$ | $(\tilde{1},\tilde{3}),(\tilde{2},\tilde{4})$ |

(5.72)

which covers fourteen out of sixteen fluctuation energies. It is easy to see that for those fluctuations no more singularities arise. Thus, for example, from the last two lines we conclude that there are two $S^5$ fluctuation energies given by

$$\frac{1}{\sqrt{m^2+\mathcal{J}^2}}\sqrt{(n-m)^2+\mathcal{J}^2-m^2}-\frac{\mathcal{J}}{\sqrt{m^2+\mathcal{J}^2}}\,. \tag{5.73}$$

Which is precisely the value in (5.71). In this way we can derive fourteen fluctuations energies with almost no work at all! As for the BMN string there are two constants in this expressions which we had to fix: the one multiplying the square-root and the constant outside the square root. They are fixed so that $E_0^{ij}=0$ (zero mode condition) and $E_n^{ij}\simeq|n|/\kappa$ for large $n$.

The remaining two fluctuation energies corresponding to the polarizations $\tilde{2}\tilde{3}$ and $\tilde{1}\tilde{4}$ would require some more gymnastics. From (5.71) we see that these last two fluctuation

energies are given by

$$\mathcal{E}_n^{\tilde{2}\tilde{3}} = \frac{1}{\mathcal{E}}\sqrt{2\mathcal{J}^2 + (n+2m)^2 - 2\sqrt{\mathcal{J}^4 + (n+2m)^2(\mathcal{J}^2+m^2)}}\,. \tag{5.74}$$

and

$$\mathcal{E}_n^{\tilde{1}\tilde{4}} = \frac{1}{\mathcal{E}}\left(\sqrt{2\mathcal{J}^2 + n^2 + 2\sqrt{\mathcal{J}^4 + n^2(\mathcal{J}^2+m^2)}} - 2\mathcal{J}\right)\,. \tag{5.75}$$

We can check that the small square root inside the large square in each of these expressions has branch-points for $n^*$ which precisely correspond to the loci where $\tilde{p}_i' - \tilde{p}_j' = 0$.

Additional singularities should be expected for $x$ approaching the branch-points of the classical quasi-momenta. Close to these points $\tilde{p}_i - \tilde{p}_j \sim \sqrt{x - x^*}$ so that $x - x^* \sim (n - n^*)^2$. Thus if the fluctuation energies are a regular function of $x$ close to $x = x^*$ we will have

$$\Omega^{ij}(x_n^{ij}) \simeq A + B(n - n^*)^2 \tag{5.76}$$

which means

$$\frac{d}{dn}\Omega^{ij}(x_n^{ij})\bigg|_{n=n^*} = 0 \tag{5.77}$$

which can be easily checked. For example for $\tilde{2}\tilde{3}$ the branch point is at $x = \pm iJ/m$ and corresponds to $n = -2m$. Indeed

$$\frac{d}{dn}\mathcal{E}_n^{\tilde{2}\tilde{3}}\bigg|_{n=-2m} = 0\,. \tag{5.78}$$

It is curious that the analytical properties of the classical quasi-momenta can tell us much about the analytical structure of the fluctuation energies without the need to preform any explicit perturbation analysis. It would be interesting to try to completely constrain $\mathcal{E}_n^{ij}$ from the several asymptotics of the classical quasi-momenta and thus to formulate some sort of finite gap problem for the fluctuation energies.

### 5.4.3 Quasi-energy

In this section we repeat the analysis of section 5.1.5 applied to the circular string. The quasi-momenta $\tilde{p}_2 = -\tilde{p}_3 \equiv p$ is in this case

$$p(x) = \frac{2\pi x K(x)}{x^2 - 1} - 2\pi m \tag{5.79}$$

and to obtain the quasi-energy we must find a function with almost the same analytical properties as $p(x)$ but with opposite residues at $x = \pm 1$ [105]. As in section (5.1.5) this is simply obtained by taking out the $x$ from the numerator in the quasi-momentum,

$$q(x) = \frac{2\pi K(x)}{x^2 - 1}\,. \tag{5.80}$$

We also eliminated the constant $2\pi m$ because without the $x$ in the numerator the quasi-energy automatically decays as $1/x$ at large $x$. Thus, the $S^3$ fluctuation energies are simply given from (5.51) which yields precisely (5.69) found before,

$$\mathcal{E}_n^{\tilde{2}\tilde{3}} = \tilde{\Omega}(y)_{y=x^n} \quad , \quad \tilde{\Omega}(y) = \frac{\sqrt{m^2y^2+\mathcal{J}^2}}{\sqrt{m^2+\mathcal{J}^2}}\frac{2}{y^2-1} \tag{5.81}$$

or, using the explicit expression for the pole position,

$$\mathcal{E}_n^{\tilde{2}\tilde{3}} = \sqrt{2\mathcal{J}^2+(n+2m)^2-2\sqrt{\mathcal{J}^4+(n+2m)^2(\mathcal{J}^2+m^2)}}\,. \tag{5.82}$$

This end our discussion of the single cut solution.

## 5.5 Off-shell method

In this section we describe an efficient quantization method which allows us to determine the several fluctuation energies from the knowledge of two excitations alone. Since we will work with relations connecting the several fluctuations energies for different polarizations $(i,j)$ it is important to be more rigorous with the indices than in the previous sections. For example when adding a fluctuation with polarization $(i,j)$ and mode number $n$ to the algebraic curve we shift the quasi-momenta as

$$p_k(x) \to p_k(x) + \delta_n^{ij} p_k(x)$$

where $\delta_n^{ij} p_k(x)$ is constrained by the analytical properties mentioned in the beginning of the chapter. Let us stress again that even though we are considering a polarization $(i,j)$, in general all quasi-momenta $p_k$ are shifted because of the back-reaction of the curve upon the addition of the extra pole. The quasi-momenta $\delta_n^{ij} p_i$ and $\delta_n^{ij} p_j$ which are the quasi-momenta connected by the fluctuation at stake must behave as

$$\delta_n^{ij} p_i(x) \simeq \pm \frac{\alpha(x_n^{ij})}{x - x_n^{ij}}$$

close to the pole position $x_n^{ij}$ which is determined by (5.4),

$$p_i(x_n^{ij}) - p_j(x_n^{ij}) = 2\pi n\,. \tag{5.83}$$

The physical poles correspond to solutions of this equation with $|x_n^{ij}| > 1$. The precise choice of signs above as well as $\alpha(y)$ is given in (5.10) and (4.27), see also figures 5.1 and 5.2. Having found $\delta_n^{ij} p_k$ we read off the fluctuation energy with mode number $n$ and polarization $(i,j)$ from the large $x$ asymptotics

$$\mathcal{E}_n^{ij} = -2\,\delta_{i,\hat{1}} + \frac{\sqrt{\lambda}}{2\pi}\lim_{x\to\infty} x\,\delta_n^{ij}\hat{p}_1(x)\,. \tag{5.84}$$

We will now explain that in fact we need not compute separately each of the sixteen physical fluctuations corresponding to the various string polarizations (4.34) but that it suffices to compute two of them, at least for a huge number of interesting solutions. In particular we shall see that the fermionic fluctuations can be obtained from the $S^3$ and $AdS_3$ fluctuation energies.

Notice that the dependence in $n$ for the shift in the quasi-momenta $\delta_n^{ij}p_k$ only appears through $x_n^{ij}$ determined in (5.83). In other words the shift in the quasi-momenta is actually a function of the position of the pole,

$$\delta_n^{ij}p_k(x) = \delta^{ij}p_k(x;y)\big|_{y=x_n^{ij}} \ . \tag{5.85}$$

Moreover the *off-shell* quantity $\delta^{ij}p_k(x;y)$ is a well defined function of $y$. It is determined by the same asymptotics as for the *on-shell* shift of quasi-momenta $\delta_n^{ij}p_k(x)$ except that the position of the pole is left unfixed. An obvious consequence is that the fluctuation energies read from (5.84) are, by construction, of the form

$$\mathcal{E}_n^{ij} = \Omega^{ij}(y)\big|_{y=x_n^{ij}} \tag{5.86}$$

where the function $\Omega^{ij}(y)$ is independent of the mode number $n$. We call $\Omega^{ij}(y)$ the *off-shell* fluctuation energies, see section (5.1.4).

Given an on-shell fluctuation energy $\mathcal{E}_n^{ij}$ as a function of the mode number $n$ we can always reconstruct the off-shell frequencies by first computing the quasi-momenta $p_i(x)$ for the underlying classical solution and then simply replace $n$ using (5.83), that is

$$\Omega^{ij}(y) = \Omega_n^{ij}\big|_{n\to\frac{p_i(y)-p_j(y)}{2\pi}} \ . \tag{5.87}$$

We will now explain how, using the inversion symmetry (5.12), we can relate the several off-shell fluctuation energies.

### Frequencies from inversion symmetry

An important property of the quasi-momenta, which follows from the $\mathbb{Z}_4$-grading of the $\mathfrak{su}(2,2|4)$ superalgebra, is the inversion symmetry (4.59) under $x \to 1/x$, which exchanges the quasi-momenta $p_{\tilde{1},\tilde{4}} \leftrightarrow p_{\tilde{2},\tilde{3}}$ and likewise for the AdS hatted quasi-momenta. Thereby, a pole connecting the sheets $(\tilde{2},\tilde{3})$ at position $y$, always comes with an image pole at position $1/y$ connecting the sheets $(\tilde{1},\tilde{4})$. We can obtain a physical frequency $\Omega^{\tilde{1}\tilde{4}}(y)$, by analytically continuing the off-shell frequency $\Omega^{\tilde{2},\tilde{3}}(y)$, inside the unit circle. This is because when we cross the unit-circle, the physical pole for $(\tilde{2}\tilde{3})$ becomes unphysical, thereby rendering its image, which lies now outside the unit-circle, a physical pole for $(\tilde{1},\tilde{4})$ as depicted in figure 5.4.

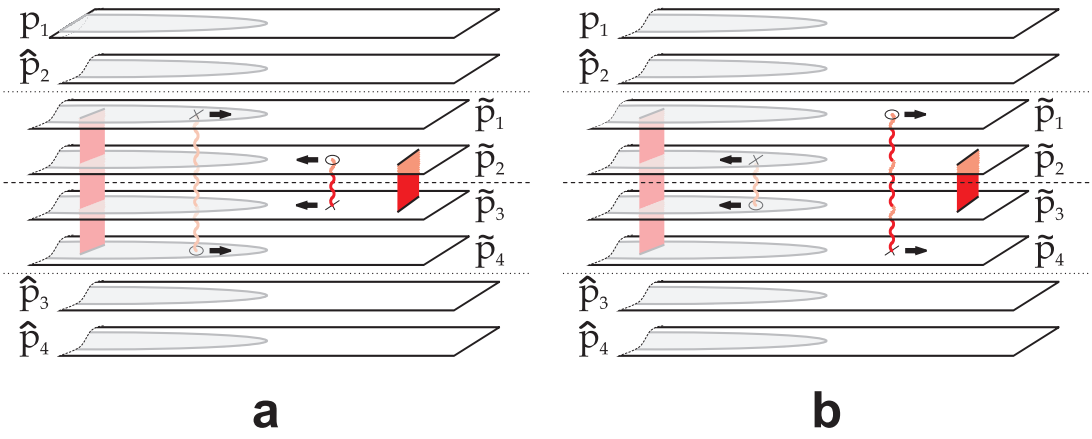


Figure 5.4: As we analytically continue a fluctuation energy $\Omega^{\hat{2}\tilde{3}}(y)$ from a point $|y| > 1$ to the interior of the unit circle we see that its mirror image becomes physical.

Let us consider in detail how this works for the $AdS$ fluctuations. As we will now demonstrate

$$\Omega^{\hat{1}\hat{4}}(y) = -\Omega^{\hat{2}\hat{3}}(1/y) - 2\,. \tag{5.88}$$

Thus, suppose we know $\Omega^{\hat{2}\hat{3}}(y)$. This fluctuation energy appears in the asymptotics of the shifted quasi-momenta $\delta^{\hat{2}\hat{3}}p_k(x;y)$ defined by the analytic properties listed in Appendix $B$. Consider now $-\delta^{\hat{2}\hat{3}}p_k(x;1/y)$. From the analytic properties of $\delta^{\hat{2}\hat{3}}p_k(x;y)$ we conclude that

- Close to $x = y$ we have

$$-\delta^{\hat{2}\hat{3}}p_{\hat{1}}(x;1/y) \simeq \frac{\alpha(y)}{x-y} \quad , \quad -\delta^{\hat{2}\hat{3}}p_{\hat{4}}(x;1/y) \simeq -\frac{\alpha(y)}{x-y} \tag{5.89}$$

- The poles at $x = \pm 1$ for these functions $-\delta^{\hat{2}\hat{3}}p_k(x;1/y)$ are also synchronized as in equation (5.11).

- Close to the branch points of the original solution these functions exhibit inverse square root singularities.

These are precisely the required properties for $\delta^{\hat{1}\hat{4}}p_k(x;y)$! Therefore

$$\delta^{\hat{1}\hat{4}}p_k(x;y) = -\delta^{\hat{2}\hat{3}}p_k(x;1/y)\,. \tag{5.90}$$

From the large $x$ asymptotics we have

$$-\frac{\sqrt{\lambda}}{4\pi}\lim_{x\to\infty} x\,\delta^{\hat{2}\hat{3}}\hat{p}_{\hat{1}}(x;1/y) \;=\; -\frac{\Omega^{\hat{2}\hat{3}}(1/y)}{2} \tag{5.91}$$

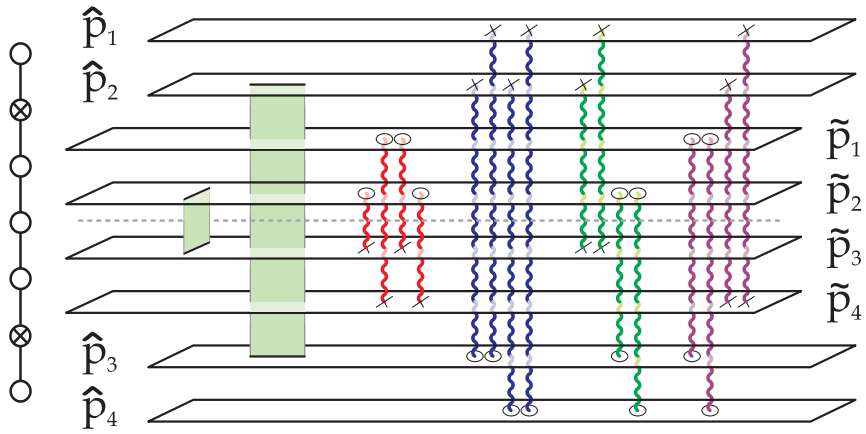


Figure 5.5: Algebraic curve for classical superstrings on $AdS_5 \times S^5$. If the configuration is symmetric under reflection w.r.t to horizontal dashed line then we can obtain the full spectrum of all excitations from the knowledge of two fluctuation energies alone.

while by definition $\Omega^{\hat{1}\hat{4}}(y)$ can be read off from

$$\frac{\sqrt{\lambda}}{4\pi} \lim_{x\to\infty} x\, \delta^{\hat{1}\hat{4}} \hat{p}_{\hat{1}}(x;y) \;=\; \frac{\Omega^{\hat{1}\hat{4}}(y)}{2} + 1 \tag{5.92}$$

From the identification (5.90) we thus conclude (5.88).

Similarly we can proceed for the $S^5$ frequencies and relate $\Omega^{\tilde{2}\tilde{3}}(y)$ with $\Omega^{\tilde{1}\tilde{4}}(y)$. It is clear that $\Omega^{\tilde{1}\tilde{4}}(y) = -\Omega^{\tilde{2}\tilde{3}}(1/y) + \textit{constant}$ and to find these constant we can either repeat the analysis we just did applied to the sphere fluctuations or we can be smarter and fix it from $\Omega^{\tilde{1}\tilde{4}}(\infty) = 0$. This must of course hold since the energy shift when we add an extra root at infinity is obviously zero, in other words, roots at infinity are zero modes. Thus, the relation we find is similar to (5.88), except that the constant term differs:

$$\Omega^{\tilde{1}\tilde{4}}(y) = -\Omega^{\tilde{2}\tilde{3}}(1/y) + \Omega^{\tilde{2}\tilde{3}}(0)\,. \tag{5.93}$$

Obviously for the purpose of computing the one-loop shift these constants are irrelevant as they will cancel in the sum.

So far we have obtained the frequencies $(1,4)$ from $(2,3)$. In the next subsection we will show how to derive all remaining frequencies. For a very large class of classical solutions we will be able to extract all fluctuation energies, including the fermionic ones, from the knowledge of a single $S^3$ and a single $AdS_3$ fluctuation energy.

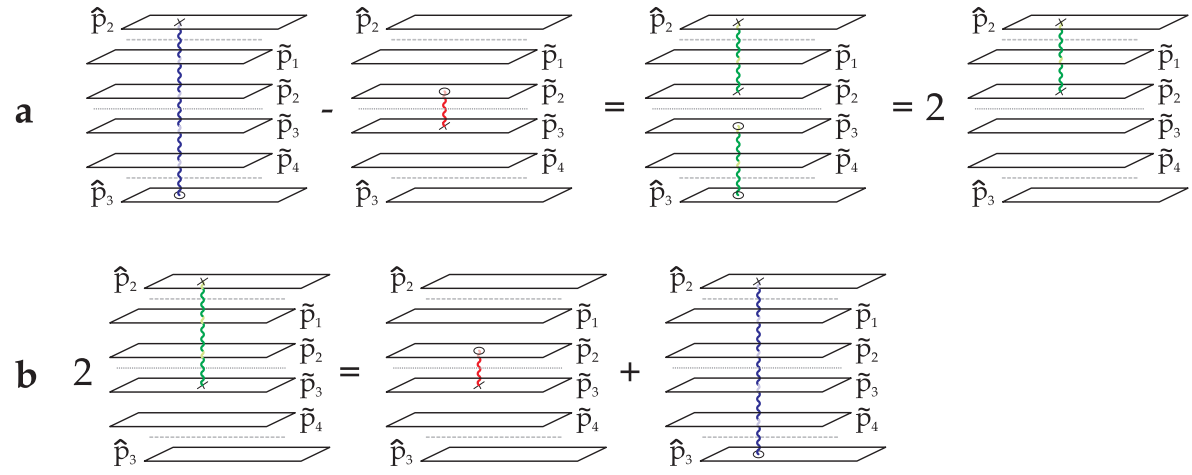


Figure 5.6: Depiction of equation (5.98). On top: we see that for symmetric configurations we can obtain the off-shell fluctuation frequency $\Omega^{\hat{2}\tilde{2}} = \Omega^{\tilde{3}\hat{3}}$ from the knowledge of the two $S^5$ and $AdS_5$ frequencies. On bottom: With this unphysical excitation at hand we can compute the fermionic fluctuation frequency $\Omega^{\hat{2}\tilde{3}} = \Omega^{\tilde{2}\tilde{3}} + \Omega^{\hat{2}\tilde{2}}$ in terms of the two bosonic fluctuations.

### Basis of fluctuation energies

For simplicity let us consider only symmetric classical configurations that have pairwise symmetric quasi-momenta

$$p_{\hat{1},\hat{2},\tilde{1},\tilde{2}} = -p_{\hat{4},\hat{3},\tilde{4},\tilde{3}}\,, \tag{5.94}$$

as depicted in figure 5.5. This is in particular the case for all rank one solutions, i.e. for the $su(2)$ and $sl(2)$ sectors.

Consider e.g. the fermionic frequency $\Omega^{\hat{2}\tilde{3}}(y)$. This energy can be thought of as a linear combination of the physical fluctuation $\Omega^{\tilde{2}\tilde{3}}(y)$ and an unphysical fluctuation $\Omega^{\hat{2}\tilde{2}}(y)$, which in particular does not appear in the table (4.34) of physical, momentum-carrying polarisations:

$$\Omega^{\hat{2}\tilde{3}}(y) = \Omega^{\tilde{2}\tilde{3}}(y) + \Omega^{\hat{2}\tilde{2}}(y)\,. \tag{5.95}$$

Since we are considering symmetric configurations, this unphysical fluctuation energy is identical to $\Omega^{\tilde{3}\hat{3}}(y)$, i.e.

$$\Omega^{\hat{2}\tilde{2}}(y) = \Omega^{\tilde{3}\hat{3}}(y)\,. \tag{5.96}$$

As in (5.95), these unphysical fluctuations can be linearly combined in terms of physical fluctuations

$$\Omega^{\hat{2}\hat{3}}(y) = \Omega^{\hat{2}\tilde{2}}(y) + \Omega^{\tilde{2}\tilde{3}}(y) + \Omega^{\tilde{3}\hat{3}}(y)\,. \tag{5.97}$$

Combining all these relations we obtain

$$\Omega^{\hat{2}\tilde{3}}(y) = \frac{1}{2}\left(\Omega^{\tilde{2}\tilde{3}}(y) + \Omega^{\hat{2}\hat{3}}(y)\right) , \tag{5.98}$$

as depicted in figure 5.6.

Proceeding in a similar fashion we can derive all frequencies as linear combinations of $\Omega^{\tilde{2}\tilde{3}}(y)$ and $\Omega^{\hat{2}\hat{3}}(y)$. (5.101) summarizes all these relations.

### Final result

The physical frequencies are labeled by the eight bosonic and eight fermionic polarizations (5.6), so we can write them as

$$\Omega^{ij} , \qquad \text{where} \quad i = (\hat{1}, \hat{2}, \tilde{1}, \tilde{2}) \qquad j = (\hat{3}, \hat{4}, \tilde{3}, \tilde{4}) . \tag{5.99}$$

To construct the complete set of off-shell frequencies for a symmetric solution (5.94) in terms of the two fundamental $S^3$ and $AdS_3$ ones $\Omega^{\tilde{2}\tilde{3}}(y)$ and $\Omega^{\hat{2}\hat{3}}(y)$ and their images under $y \to 1/y$, we first construct by inversion

$$\begin{aligned} \Omega^{\tilde{1}\tilde{4}}(y) &= -\Omega^{\tilde{2}\tilde{3}}(1/y) + \Omega^{\tilde{2}\tilde{3}}(0) \\ \Omega^{\hat{1}\hat{4}}(y) &= -\Omega^{\hat{2}\hat{3}}(1/y) - 2 . \end{aligned} \tag{5.100}$$

The remaining frequencies are then obtained by linear combination of these four fluctuation frequencies. In this way we obtain the following concise form for all off-shell frequencies

$$\Omega^{ij}(y) = \frac{1}{2}\left(\Omega^{ii'}(y) + \Omega^{j'j}(y)\right) , \tag{5.101}$$

where

$$(\hat{1}, \hat{2}, \tilde{1}, \tilde{2}, \hat{3}, \hat{4}, \tilde{3}, \tilde{4})' = (\hat{4}, \hat{3}, \tilde{4}, \tilde{3}, \hat{2}, \hat{1}, \tilde{2}, \tilde{1}) . \tag{5.102}$$

This generalizes (5.98).

For the general case of non symmetric solutions, we can repeat the above analysis, however the minimal set of required off-shell fluctuation frequencies will generically be larger than two.

In the rest of the chapter we consider only $SU(2)$ solutions as described in section (4.5.1), see figure 4.7. From the symmetry of the problem it is clear that we generically have 6 different frequencies, namely

1. One internal fluctuation corresponding to a pole shared by $\tilde{p}_2$ and $\tilde{p}_3$ which we denote by

$$\Omega_S(y) = \Omega^{\tilde{2}\tilde{3}}(y) \tag{5.103}$$

2. Another $S^3$ fluctuation connecting $\tilde{p}_1$ and $\tilde{p}_4$

$$\Omega_{\bar{S}}(y) = \Omega^{\tilde{1}\tilde{4}}(y) \tag{5.104}$$

3. Two fluctuations which live in $S^5$ but are orthogonal to the ones in $S^3$,

$$\Omega_{S_\perp}(y) = \Omega^{\tilde{1}\tilde{3}}(y) = \Omega^{\tilde{2}\tilde{4}}(y) \tag{5.105}$$

4. Four $AdS_5$ fluctuations

$$\Omega_A(y) = \Omega^{\hat{1}\hat{3}}(y) = \Omega^{\hat{1}\hat{4}}(y) = \Omega^{\hat{2}\hat{3}}(y) = \Omega^{\hat{2}\hat{4}}(y) \tag{5.106}$$

5. Four fermionic excitations which end on either $p_{\tilde{2}}$ or $p_{\tilde{3}}$ (which are the sheets where there are cuts outside the unit circle),

$$\Omega_F(y) = \Omega^{\hat{1}\tilde{3}}(y) = \Omega^{\hat{2}\tilde{3}}(y) = \Omega^{\tilde{2}\hat{3}}(y) = \Omega^{\tilde{2}\hat{4}}(y) \tag{5.107}$$

6. Four fermionic poles which end on either $p_{\tilde{1}}$ or $p_{\tilde{4}}$ (which are the sheets where there are cuts inside the unit circle)

$$\Omega_{\bar{F}}(y) = \Omega^{\hat{1}\tilde{4}}(y) = \Omega^{\hat{2}\tilde{4}}(y) = \Omega^{\tilde{1}\hat{3}}(y) = \Omega^{\tilde{1}\hat{4}}(y)\,. \tag{5.108}$$

These fluctuations are depicted in figure 5.5 from left to right.

## 5.6 Quantization of the two-cut solution

In this section we explain how to compute the fluctuation energies around a general 2-cut $su(2)$ solution (4.86) with branch points $a, \bar{a}, b, \bar{b}$. We will find out that the fluctuation energies can be obtained by the surprisingly simple expressions

$$\begin{aligned} \Omega_A(y) &= \frac{2}{y^2-1}\left(1 + y\frac{f(1)-f(-1)}{f(1)+f(-1)}\right) \\ \Omega_S(y) &= \frac{4}{f(1)+f(-1)}\left(\frac{f(y)}{y^2-1} - 1\right)\,. \end{aligned} \tag{5.109}$$

with the remaining fluctuation energies obtained through table 5.100. Note that this is a very simple elegant expression for the off-shell fluctuation energies. All the intricate structure that appears for the on-shell frequencies is hidden in the equation for the pole positions $x_n^{ij}$ (5.83).

The computation is very similar to the one in section 5.4.1 so we can be brief and omit the details. To find the fluctuation frequencies we perturb the quasi-momenta (4.86) and

fix $\delta p$ by the required asymptotics (5.8). We consider only the $(\hat{2},\hat{3})$ and $(\tilde{2},\tilde{3})$ fluctuations with $N_{\hat{2}\hat{3}} = N_{\tilde{2}\tilde{3}} = 1$, located at $x = z$ and $x = y$ respectively. The most general ansatz for the shift in quasi-momenta is then

$$\begin{aligned}\delta p_{\tilde{2}}(x;y,z) &= \frac{\alpha(z)}{x-z} + \frac{\delta\alpha_-}{x-1} + \frac{\delta\alpha_+}{x+1} \\ \delta p_{\tilde{3}}(x;y,z) &= \frac{1}{f(x)}\left(-\frac{f(y)\,\alpha(y)}{x-y} + \frac{\delta\alpha_- f(1)}{x-1} + \frac{\delta\alpha_+ f(-1)}{x+1} - \frac{4\pi}{\sqrt{\lambda}}\,x + A\right)\end{aligned} \tag{5.110}$$

where the asymptotics at large $x$ for $\delta p_{\hat{2}}$, $\delta p_{\tilde{2}}$, and also $\delta p_{\hat{1}}$, $\delta p_{\tilde{1}}$ obtained by inversion symmetry (5.12) fix the constants $\delta\alpha_\pm$, $A$ and $\delta\Delta$. The result is

$$\delta\Delta = \Omega_S(y) + \Omega_A(z)\,, \tag{5.111}$$

with (5.109).

Now that we have found the two off-shell frequencies $\Omega_S$ and $\Omega_A$ we can construct the remaining frequencies from (5.101). In this way we obtain the complete set of fluctuation energies around the generic two cut solution. As an application we consider in the next section the Giant Magnon solution which corresponds to a particular (singular) limit of the general treatment we considered so far.

Notice also that our simple treatment can be trivially generalized for $K \geq 3$ cuts.

## 5.7 Quantum wrapped giant magnon

In the previsous section we have determined the off-shell frequencies for the most general two-cut solution. In this section we consider the singular limit discussed in section 4.5.2 where the two cuts collide and we obtain a condensate curve describing the giant magnon solution.

To obtain the on-shell frequencies $\mathcal{E}_n^{ij}$ we simply need to compute the positions of the poles $x_n^{ij}$ from (5.83) and plug them in (5.86). There are two case we have to consider. Mainly $x_n^{ij}$ are situated relatively far from the branch points of the two cuts and we can expand the off-shell frequencies

$$\begin{aligned}\Omega_A(y) &= \Omega^{(0)}(y) - \left(\frac{y}{y^2-1}\frac{X_+(X_-^2-1)}{2\,(X_+^2-1)(X_+X_-+1)^2}\,\delta^2 + c.c.\right) \\ \Omega_S(y) &= \Omega_A(y) - \left(\frac{1}{y-X_+}\frac{X_+-X_-}{4(X_+^2-1)(X_-X_++1)}\delta^2 + c.c.\right).\end{aligned} \tag{5.112}$$

The first term is the leading order frequency, as determined in [17],

$$\Omega^{(0)}(y) = \frac{2}{y^2-1}\left(1 - y\,\frac{X_+ + X_-}{X_+X_- + 1}\right). \tag{5.113}$$

The remaining frequencies are of course determined as in (5.101).

However there are fluctuations corresponding to the variations of the filling fractions of the two cuts. These are situated right at the branch points. To compute their contributions to the 1-loop energy shift we have to expand $\delta E^{\rm BP} \equiv \frac{1}{2}\Omega^{\tilde{2}\tilde{3}}(a) + \frac{1}{2}\Omega^{\tilde{2}\tilde{3}}(b)$. That leads to

$$\delta E^{\rm BP} \simeq \Omega^{(0)}(X_+) + \left( \frac{1 - X_- X_+}{4(X_- X_+ + 1)^2 (X_+^2 - 1)} \delta^2 + c.c. \right) . \tag{5.114}$$

Except for these two fluctuations the positions of the excitations are along the real axis.

We found all fluctuation energies around the general two-cut configuration and in particular around the GM solution. In the next chapter we will focus on a very important quantity in the semi-classical quantization of a physical system – the one-loop shift (5.2). Notice that even though we have the fluctuation energies at hand it is by no means trivial to sum them as in (5.2). For that we need to find the position of each fluctuation which will depend on the mode number $n$ and the polarization $A = (i, j)$ through (5.4), plug the position into the off-sheel fluctuation energies $\Omega^{ij}(y)$ and sum the result over $n$ and $ij$ with some minus signs for the fermionic fluctuations. We will explain in the next chapter how the algebraic curve formalism can be of great help to preform this complicated task.

# Chapter 6

# One–loop shift

This chapter is devoted to the study of the one-loop shift (5.2) around generic classical solutions. We start with a general discussion in section 6.1. In section 6.2 we consider a very illustrative example where we will compute this quantity for the giant magnon two-cut solution studied before. Finally, in section 6.4, we will come back to the general discussion and consider an application of our method to derive the semi-classical Hernandez-Lopez dressing factor in the Beisert-Staudacher equations. This is the universal dressing factor which renders the correct semi-classical quantization around any classical solution.

## 6.1 Splitting of one loop shift into two contributions

So far we computed the semi-classical spectrum around generic classical solutions, that is we computed the level spacing $\mathcal{E}_n^{ij}$ for excitations with mode number $n$ and polarization $ij$ in terms of which

$$E(\{N_n^{ij}\}) - E(\{\}) = \sum_{n,ij} N_n^{ij} \mathcal{E}_n^{ij} + \mathcal{O}(1/\sqrt{\lambda}) \tag{6.1}$$

As mentioned in the beginning of the chapter, another quantity of main interest is the 1-loop shift

$$E_0 = \frac{1}{2} \sum_{ij,n} (-1)^{F_{ij}} \mathcal{E}_n^{ij} \ , \tag{6.2}$$

appearing in the expansion of the energy of the string state,

$$E(\{\}) = E_{cl} + E_0 + \mathcal{O}(1/\sqrt{\lambda}) \tag{6.3}$$

where $E_{cl} = \mathcal{O}(\sqrt{\lambda})$ is the energy of the classical string around which we quantize.

It is important to understand a trivial point. We can use the algebraic curve to find the ground state energy because we can compute all fluctuation energies by perturbing the algebraic curve and then sum them by hand. *But*, if we take the algebraic curve corresponding to some classical solution and compute its energy we will obviously only get $E_{cl}$. It would be nice if we could upgrade the algebraic curve equations so that the energy of a given configuration would automatically yield (6.3). After all, the proper quantum

equations must capture the full $1/\sqrt{\lambda}$ expansion. This is what we will consider in the last section 6.4.

In this section we will continue our general description of the one-loop shift. First of all to operate with the sum (6.2) we write it as

$$E_0 = \frac{1}{2}\sum_{ij}(-1)^{F_{ij}} \oint \mathcal{E}_n^{ij} \cot \pi n \frac{dn}{2i} \ , \tag{6.4}$$

where the integration path encircles all integers $n$. This is true because the function $\cot \pi n$ has poles precisely at the integers,

$$\frac{\cot \pi n}{2i} = \frac{1}{\pi i}\sum_{n=-\infty}^{\infty} \frac{x}{x^2 - n^2} \, . \tag{6.5}$$

Next let us change variables in this integral. For each polarization $ij$ we change from the mode number variable $n$ to the position of the corresponding fluctuation $x_n^{ij}$ found from

$$p_i(x_n^{ij}) - p_j(x_n^{ij}) = 2\pi n \tag{6.6}$$

which means that

$$E_0 = \sum_{ij}(-1)^{F_{ij}} \oint\limits_{\cup x_n^{ij}} \Omega^{ij}(y) \cot\left(\frac{p_i(y) - p_j(y)}{2}\right) \frac{p_i'(y) - p_j'(y)}{2\pi} \frac{dy}{4i} \ , \tag{6.7}$$

where we used

$$\mathcal{E}_n^{ij} = \Omega^{ij}(x_n^{ij}) \tag{6.8}$$

as explained in the previous sections.

The contour integral in the $x$ plane encircles now all the excitation points $x_n^{ij}$. Then we do the most obvious thing – we blow up the contours. We choose to keep the integration contour always outside the unit circle. Thus we are left with two type of contour integrals:

1. The obvious contribution is an integral over the unit circle for each polarization $ij$. We denote this contribution to the one-loop shift by $I_{phase}$.

2. The less obvious part is everything else. What do we mean by *everything else*? Suppose we consider a generic non-singular classical configuration whose algebraic curve contains some square root cuts uniting some of the sheets. Then, if we consider the contribution of a polarization $ij$ for which the classical solution has cuts ending on either $p_i$ or $p_j$ (or both), we will also get additional integrals around the corresponding classical cuts. If we are considering some singular configuration such as the Giant-Magnon then *everything else* stands for the integral over all possible singularities we might encounter when deforming the contour. This contribution to the one-loop shift from all integrals other than that over the unit circle is denoted by $I_{anomaly}$.

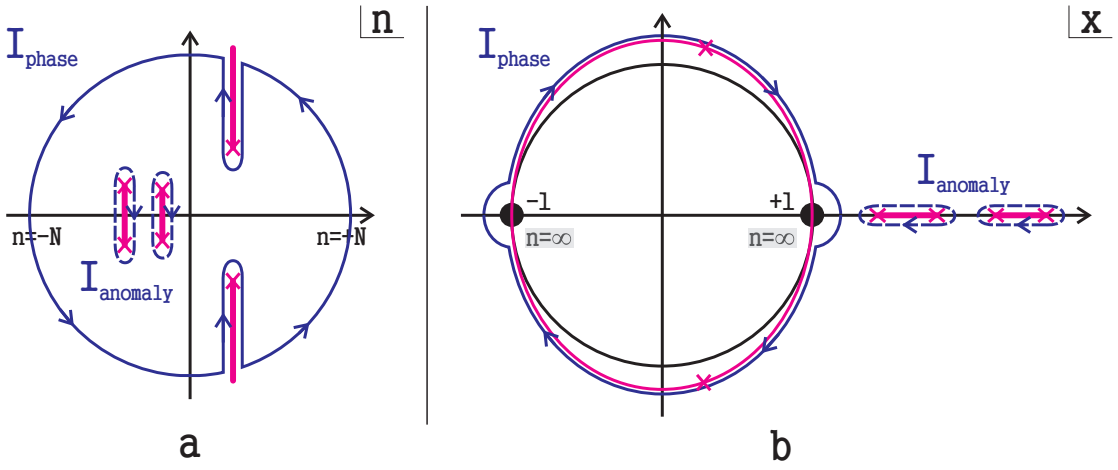


Figure 6.1: Splitting in the $n$ plane. a) Typical analytical structure of the excitation energies as a function of the mode number $n$, see section 5.1.4. The branchpoints associated to the cuts going to infinity are large if some charge of the classical solution is large. There could also be extra cuts in the $n$ plane. The integral (6.4) can then be split into two contributions $I_{phase}$ and $I_{anomaly}$ as depicted in the figure. b) The contour $I_{phase}$ going along the large cuts in the $n$ plane is mapped into some ellipsoidal form in the $x$ plane. The contours around the extra cuts in the $n$ plane are mapped to the cycles around the cuts of the classical solution which we are quantizing.

If the classical solution contains some large charge, say $\mathcal{J}$, then

$$\cot\left(\frac{p_i(y)-p_j(y)}{2}\right) \simeq \pm i \tag{6.9}$$

on the upper/lower half of the unit circle. This is valid with exponential precision in the large charge we consider. Thus, the constribution $I_{phase}$ can be approximated with exponential precision by

$$I_{phase} \simeq I_{HL} \equiv \sum_{ij}(-1)^{F_{ij}} \oint_{U^+} \Omega^{ij}(y)\frac{p_i'(y)-p_j'(y)}{2\pi}\frac{dy}{2} \tag{6.10}$$

where the contour is over the upper half of the unit circle from $x=-1$ to $x=+1$.

As explained in the last section, from the Bethe ansatz point of view, what happens is that the contribution $I_{anomaly}$ is reproduced exactly (no exponential errors) by the finite size corrections – called anomalies – present in these equations [15]. The contribution $I_{phase}$ is not obtained but instead the Hernandez-Lopez phase [77] reproduces precisely the integral $I_{HL}$ [14]. In other words, the Beisert-Staudacher equations yield

$$E_0^{BS} = I_{HL} + I_{anomaly} \tag{6.11}$$

which approximates with exponential precision the correct 1-loop shift

$$E_0 = I_{phase} + I_{anomaly}\,. \tag{6.12}$$

In the next section we take (6.4) as our starting point and compute the one-loop shift around the Giant-Magnon classical solution. In the last section we focus on the derivation of the Hernandez-Lopez phase.

## 6.2 One-loop shift around the Giant Magnon solution

In this section we shall compute the ground state energy $E_0$ around the Giant-Magnon solution studied in sections 4.5.2 and 5.7. In doing so we will keep track of the leading and subleading exponential corrections in the large angular momentum $\mathcal{J}$. The one-loop energy shift is obtained by the weighted sum over all fluctuation frequencies

$$E_0 = \frac{1}{2}\sum_{n,ij}(-1)^{F_{ij}}\Omega_{ij}\left(x_n^{ij}\right) . \tag{6.13}$$

To deal with this sum we first split it into the fluctuation energies $\delta E^{\rm BP}$ corresponding to a variation of the filling fractions of the two cuts (5.114) and the remaining fluctuations. To deal with the latter we transform the sum over $n$ into an integral with $\cot \pi n$ and then pass from the $n$ to the $x$ plane using the map (5.83) as explained in the previous section. Actually, as explained later there is an additional third contribution coming from fluctuations which got trapped between the two cuts when these collapsed into the log cut. This contribution, denoted by $\delta E^{UP}$ is considered in section 6.2.2 (see also section 5.2). Thus we have

$$E_0 = \frac{1}{2}\sum_{ij}(-1)^F \oint_{\mathcal{C}_{\mathbb{R}}} \Omega^{ij}(y)\cot_{ij}\frac{dy}{2\pi i} + \delta E^{\rm BP} + \delta E^{\rm UP} , \tag{6.14}$$

where

$$\cot_{ij} \equiv \partial_y \log\sin\left(\frac{p_i - p_j}{2}\right) , \tag{6.15}$$

and the contour $\mathcal{C}_{\mathbb{R}}$ encircles all the fluctuations on the real axis. Our goal will be to deform this contour to the unit circle, where the argument of the cot has a large imaginary component and the integral can be computed by standard saddle point method.

However, when deforming the contour we will obtain several poles from $\cot_{ij}$ located close to the points $x = X_+, X_-$ and $x = 1/X_+, 1/X_-$. The contribution from these poles is computed in the next section and is denoted by $\delta E^{\rm PL}$. We find therefore

$$E_0 = \delta E^{\rm INT} + \delta E^{\rm PL} + \delta E^{\rm BP} + \delta E^{\rm UP} , \tag{6.16}$$

where

$$\delta E^{\rm INT} = \oint_{\mathcal{C}_{\mathbb{U}}}\left(\frac{1}{2}\sum_{ij}(-1)^F\Omega^{ij}(x)\cot_{ij}\right)\frac{dx}{2\pi i} . \tag{6.17}$$

Notice that since we have already dealt with the zero mode contribution $\delta E^{BP}$ separately we can (and will) now use the far away quasi-momenta (4.95) in the rest of the paper. In the following four sections we will consider each of these four contributions in detail.

In the language of the previous section

$$I_{phase} \simeq \delta E^{INT} \ , \ I_{anomaly} \simeq \delta E^{\rm PL} + \delta E^{\rm BP} + \delta E^{\rm UP} \ . \tag{6.18}$$

The difference is that in what follows we will always drop any contributions much smaller than $\mathcal{O}(\delta^2)$ with (4.99). The notation $\delta E^{\cdots}$ is used to stress that we are working in this singular limit.

### 6.2.1 Extracting poles

We now determine the positions of the poles mentioned above. Consider first the polarization $(\tilde{2}, \tilde{3})$. We have

$$\exp(-i\tilde{p}_2 + i\tilde{p}_3) = \exp\left(-i\frac{x\Delta}{g(x^2-1)} - 2i\tau\right)\frac{(x-X_-)^2}{(x-X_+)^2}\,,$$

so there is an obvious pole from (6.15) at $x = X^+$. However there are also some less obvious poles if the denominator in (6.15) vanishes, i.e. for $\exp(-i\tilde{p}_2 + i\tilde{p}_3) = 1$,

$$\exp\left(-i\frac{x\Delta}{g(x^2-1)} - 2i\tau\right)\frac{(x-X_-)^2}{(x-X_+)^2} = 1\,.$$

The first factor is exponentially small. When $x \sim X_+$ the exponent is of order $\delta^2$ as one can see from (4.99). However we can compensate that if the second factor diverges. To do so look for $x - X_+ \sim \delta$. One then finds poles at $x - X_+ = \epsilon_1^{\pm}$, where

$$\begin{aligned}\epsilon_1^{\pm} &= \pm\frac{\delta}{4} + \frac{\delta^2}{16}\left(\frac{1}{X_+ - X_-} + i\frac{\Delta}{2g}\frac{X_+^2+1}{(X_+^2-1)^2}\right)\\ &\pm \frac{\delta^3}{64}\left(\frac{1}{(X_- - X_+)^2} - \frac{3\Delta^2(X_+^2+1)^2}{8g^2(X_+^2-1)^4} + \frac{i\Delta}{2g}\frac{2X_+^4 + X_-X_+^3 - 3X_+^2 + 3X_-X_+ - 3}{(X_+ - X_-)(X_+^2-1)^3}\right) + \mathcal{O}\left(\delta^4\right)\end{aligned}$$

Proceeding in the same way for the different polarizations we find the position of all existing poles. We have summarized all poles, and whether they are physical or unphysical (around $X_+$ or $1/X_+$, respectively), in table 6.1. In Appendix E we listed the explicit values of the small deviations $\epsilon_j$.

In summary, the contribution to the contour integral from these singularities is

$$\delta E^{\rm PL} = \left(\frac{e^{i\tau}}{(X_-X_+ + 1)(X_+^2-1)} + \frac{2 - X_+(X_- + X_+)}{(X_-X_+ + 1)(X_+^2-1)^2} + \frac{i\Delta}{4g}\frac{(X_- - X_+)(X_+^2+1)}{(X_-X_+ + 1)(X_+^2-1)^3}\right)\frac{\delta^2}{4} + c.c.\,. \tag{6.19}$$

which for small $Q$ values becomes

$$\delta E^{\rm PL} \simeq 8e^{-\frac{J}{2g\sin\frac{p}{2}}-2}\sin^2\frac{p}{2}\,. \tag{6.20}$$

| **Polarization** | **Poles around $X_+$** | **Poles around $1/X_+$** |
|---|---|---|
| $A \times 4$ | | |
| $F \times 4$ | $x - X_+ = 0, \epsilon_3$ | |
| $\bar{F} \times 4$ | | $1/x - X_+ = 0, \epsilon_3$ |
| $S$ | $x - X_+ = \epsilon_1^-, 0, \epsilon_1^+$ | |
| $\bar{S}$ | | $1/x - X_+ = \epsilon_1^-, 0, \epsilon_1^+$ |
| $S_\perp \times 2$ | $x - X_+ = 0, \epsilon_2$ | $1/x - X_+ = 0, \epsilon_2$ |

Table 6.1: Poles of different $\cot_{ij}$ in the upper half plane close to the logarithm branch points

### 6.2.2 Unphysical fluctuations

Next we consider the contribution from the unphysical frequencies discussed in section 5.2. As explained in section 5.2, if we consider a general finite gap solution with small enough filling fractions, we know that the equation

$$p_i(x_n^{ij}) - p_j(x_n^{ij}) = 2\pi n \tag{6.21}$$

for a physical pair $(ij)$ in (5.6) is always solvable[1]. When we gradually start increasing the filling fractions, the cuts become bigger and, at some point, a cut could collide with some $x_n$. After this point we will not be able to find solutions to (6.21) for some values of $n$. This however does not imply any non-analyticity of the fluctuation energies $\Omega^{ij}(x_n^{ij})$ as a function of the filling fractions and we can analytically continue the fluctuation energies below this point. What happens is that the fluctuation $x_n$ passes through a cut and afterwards is connecting two different sheets. This will generically yield unphysical fluctuations. We have depited this process in figure 6.2.

Indeed for each missing solution of (6.21) one could find the corresponding unphysical fluctuation. We conclude that we also have to consider all possible solutions of (6.21) for unphysical pairs $(ij)$.

There are $2 + 4$ unphysical fluctuations $(\tilde{1}, \tilde{2}), (\tilde{3}, \tilde{4})$ and $(\hat{1}\tilde{2}), (\hat{2}\tilde{2}), (\hat{3}\tilde{3}), (\hat{4}\tilde{3})$, which by the above reasoning we also need to take into account. We denote these fluctuations by $S_u$ and $F_u$

$$\Omega_{S_u}(x) = \frac{\Omega_{\bar{S}}(x) - \Omega_S(x)}{2} + c \tag{6.22}$$

$$\Omega_{F_u}(x) = \frac{\Omega_A(x) - \Omega_S(x)}{2} + c\,, \tag{6.23}$$

[1] In fact one should add twists to properly ensure this statement.

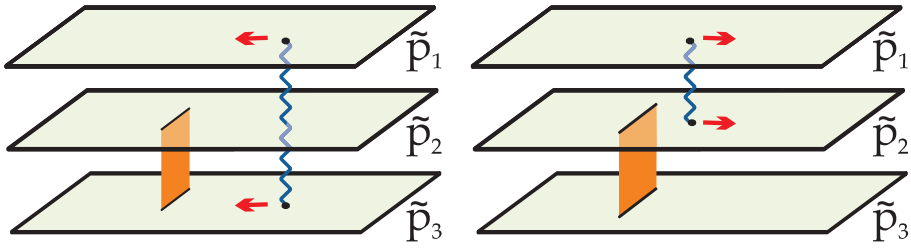


Figure 6.2: When increasing the filling fraction of a cut, the fluctuation could pass through the cut and reappear uniting different sheets. The physical fluctuation $\tilde{2}\tilde{3}$ could become the unphysical one $\tilde{1}\tilde{2}$.

where the specific values of the constant $c$ and of the position of the fluctuations $x^{S_u}$ and $x^{F_u}$ are collected in Appendix E.

Combining this together with the branch-point contribution (5.114) one obtains

$$\delta E^{\rm UP} + \delta E^{\rm BP} = \delta E^{BP} + \frac{2\Omega_{S_u}(0) - 4\Omega_{F_u}(x^{F_u})}{2} = \frac{1-\sqrt{X_-/X_+}}{4(X_-X_+ + 1)(X_+^2 - 1)}\delta^2 + c.c.\,, \quad (6.24)$$

where in particular the leading order term correctly cancels! In the $\mathcal{Q} \to 0$ limit we obtain for this combined contribution

$$\delta E^{\rm UP} + \delta E^{\rm BP} \simeq -8e^{-\frac{J}{2g\sin\frac{p}{2}}-2}\sin^2\frac{p}{2}\,, \quad (6.25)$$

which precisely cancels the contribution of $\delta E^{\rm PL}$ in (6.20). Thus, *for the simple giant-magnon solution* the only contribution is given by the integral over the unit circle (6.17) which we will consider in the next section.

### 6.2.3 Unit circle and final result

In the two previous sections we took into account the extra poles in the complex $x$ plane, the branch-point fluctuations and the unphysical excitations. For a general dyonic magnon these contributions are given by (6.19) added to (6.24) while for a simple giant-magnon this sum vanishes.

In this section we consider the remaining contribution given by the integral (6.17) over the unit circle. There are three contributions into which this integral is naturally split. On the upper/lower half of the unit circle we have

$$\cot\left(\frac{p_i - p_j}{2}\right) = \pm i\left(1 + 2e^{\mp i(p_i - p_j)} + \ldots\right)\,, \quad (6.26)$$

while the fluctuation energies are given by

$$\Omega_{ij}(y) = \Omega^{(0)}(y) + \delta\Omega_{ij}(y)\,. \quad (6.27)$$

- Thus the we can pick the leading term in (6.26) times the leading term in (6.27) to get

$$\delta E^{INT,(0)} = \oint_{\mathcal{C}_{\mathbb{U}}^+} \frac{dy}{2i}(-1)^{F_{ij}}\partial_y\Omega^{(0)}(y)\frac{p_i'-p_j'}{2\pi}\,,$$

where the integral goes over the upper half of the unit circle from $x=-1$ to $x=+1$. Since $\sum_{i=1}^4 \tilde{p}_i - \hat{p}_i = 0$ this contribution vanishes and therefore the one-loop shift around the infinite volume giant magnon is zero [107, 108]. This is precisely what we expect from the infinite volume dispersion relation

$$\epsilon_\infty(p) = \sqrt{Q^2 + \frac{\lambda}{\pi^2}\sin^2\frac{p}{2}} = \frac{\sqrt{\lambda}}{\pi}\sin\frac{p}{2} + 0 + \mathcal{O}(1/\sqrt{\lambda})\,.$$

We are therefore left with the exponentially suppressed contributions.

- The second contribution comes from picking the subleading term in (6.27) and the leading value in (6.26). This gives

$$\delta E^{\text{INT},(1)} \simeq 2\oint_{\mathcal{C}_{\mathbb{U}}^+} \frac{h(x)-h(1/x)/x^2+g(x)}{(X_+^2-1)(X_+X_-+1)}\frac{dx}{2\pi i} + c.c.$$

where

$$\begin{aligned} h(x) &= \frac{\delta^2}{16}\left[\frac{X_- - X_+}{(x-X_+)^2} + \frac{X_- - 2X_+ + X_-X_+^2}{X_+(X_-X_+-1)}\left(\frac{1}{x-X_+}-\frac{1}{x-X_-}\right)\right] \\ g(x) &= \frac{\delta^2}{8}\frac{(X_+-X_-)^2}{(xX_+-1)(xX_--1)X_+}\,. \end{aligned}$$

This integral can be computed yielding

$$\delta E^{\text{INT},(1)} \simeq \frac{i\delta^2}{4\pi}\left[\frac{X_+-X_-}{(X_+X_-+1)(X_+^2-1)^2} + \frac{(X_-^2-1)(\operatorname{arccoth}X_+ - \operatorname{arccoth}X_-)}{(X_+^2-1)(X_+^2X_-^2-1)}\right] + c.c. \quad (6.28)$$

Expanding this result in the $\mathcal{Q}\to 0$ limit we obtain

$$\delta E^{\text{INT},(1)} \simeq 16 e^{-\frac{J}{2g\sin\frac{p}{2}}-2}\left(\frac{g\sin^3\frac{p}{2}}{Q} - \frac{\sin\frac{p}{2}}{\pi}\right)\,. \quad (6.29)$$

Notice that this contribution is singular in the $\mathcal{Q}\to 0$ limit. This singularity will cancel however with the third contribution we will now analyze.

- Finally we have the contribution coming from picking the leading term in (6.27) multiplied by the subleading term in (6.26). This was the contribution analyzed in [17] and [109]. It gives

$$\delta E^{\text{INT},(2)} = \oint_{U^+}\frac{dx}{2\pi i}\partial_x\Omega^{(0)}\left(\frac{x-X_-}{x-X_+}+\frac{x-1/X_+}{x-1/X_-}-2e^{i\tau}\right)^2 e^{-\frac{ix\Delta}{g(x^2-1)}-2i\tau} \quad (6.30)$$

which in the small $\mathcal{Q}$ limit is divergent and becomes

$$\begin{aligned}\delta E^{\text{INT},(2)} &\simeq V.P. \oint_{U^+} \frac{dx}{2\pi i}\partial_x\Omega^{(0)}\left(2\frac{xX_+-1}{x-X_+}-2\right)^2 e^{-ix\frac{J+4g\sin\frac{p}{2}}{g(x^2-1)}} \\ &+ e^{-\frac{J}{2g\sin\frac{p}{2}}-2}\left(-\frac{16g\sin^3\frac{p}{2}}{Q}+\frac{4iJ\cos\frac{p}{2}}{g}-8i\sin\frac{p}{2}+8i\sin p\right),\end{aligned} \tag{6.31}$$

where *V.P.* stands for the principal value of the integral.

Finally, we can combine (6.29) and (6.31) to obtain the final result

$$\begin{aligned}E_0 &\simeq V.P. \oint_{U^+} \frac{dx}{2\pi i}\partial_x\Omega^{(0)}\left(2\frac{xX_+-1}{x-X_+}-2\right)^2 e^{-ix\frac{J+4g\sin\frac{p}{2}}{g(x^2-1)}} \\ &+ e^{-\frac{J}{2g\sin\frac{p}{2}}-2}\left(-\frac{16\sin\frac{p}{2}}{\pi}+\frac{4iJ\cos\frac{p}{2}}{g}-8i\sin\frac{p}{2}+8i\sin p\right).\end{aligned} \tag{6.32}$$

We will show in the next section that this is in precise agreement with the $F$ and $\mu$ terms of the Lüscher-Klassen-Melzer formulas! Note that the expression above is real by construction and the divergences at $\mathcal{Q}=0$ cancelled among the various contributions.

Notice that the two exponentially suppressed contributions clearly have distinct physical meaning. The first one comes from taking into account the fine-structure of the condensate cut. That is it steams from the finite size corrections to the giant magnon we are quantizing. The latter is obtained by properly summing the leading frequencies as opposed to approximating them by an integral over their momenta as done in infinite volume $\mathcal{J}$ [17, 110]. In particular the integral in (6.32) comes from this last contribution. It can be trivially evaluated by saddle point at $x=i$ yielding

$$\begin{aligned}&V.P. \oint_{U^+} \frac{dx}{2\pi i}\partial_x\Omega^{(0)}\left(2\frac{xX_+-1}{x-X_+}-2\right)^2 = \\ &= \frac{8\sin^2\frac{p}{4}\,e^{-\frac{2\pi\Delta}{\sqrt{\lambda}}}}{\pi\left(\sin\frac{p}{2}-1\right)\left(\frac{\Delta}{\sqrt{\lambda}}\right)^{1/2}}\left[1-\frac{7+4\sin p-4\cos p+\sin\frac{p}{2}}{16\pi\left(\sin\frac{p}{2}-1\right)\frac{\Delta}{\sqrt{\lambda}}}+\mathcal{O}\left(\frac{1}{\left(\frac{\Delta}{\sqrt{\lambda}}\right)^2}\right)\right]+\ldots,\end{aligned}$$

which is clearly leading compared to the second line in (6.32).

More generally, as explained in [17], the correction to the dispersion relation of the magnon in infinite volume is given by an expansion of the form

$$\delta E^{1-loop} = \sum_{n,m} a_{n,m}(P,\mathcal{J},\sqrt{\lambda})\left(e^{-2\pi\mathcal{J}}\right)^n\left(e^{-\frac{2\pi\mathcal{J}}{\sin\frac{p}{2}}}\right)^m. \tag{6.33}$$

Classically we only obtain corrections of the form $\left(e^{-\frac{2\pi\mathcal{J}}{\sin\frac{p}{2}}}\right)^m$ [100], i.e.

$$a_{n,m} = \delta_{n,0}\sqrt{\lambda}\, a_n^{cl}(P,\mathcal{J}) + a_{n,m}^{1-loop}(P,\mathcal{J}) + \mathcal{O}(1/\sqrt{\lambda})\,.$$

In [17] we determined the complete set of $a_{n,0}^{1-loop}$ coefficients (see also [109]), which correct the one-loop shift of the giant magnon in finite volume, by properly summing the leading frequencies as opposed to approximating them by an integral over their momenta. They simply come from keeping the next terms in the expansion (6.26) multiplied by the leading order frequencies $\Omega^{(0)}(y)$ in (6.27) so they read

$$a_{n,0}^{1-loop}\left(e^{-\frac{2\pi\Delta}{\sqrt{\lambda}}}\right)^n = V.P.\oint\limits_{\mathbb{U}^+}\frac{dx}{2\pi i n}\partial_x\Omega^{(0)}(x)\sum_{(ij)}(-1)^{F_{ij}}e^{-in(p_i-p_j)}\,. \tag{6.34}$$

From the second line in (6.32) we read $a_{1,1}^{1-loop}$, which is the leading correction to the one-loop shift due to the fine-structure of the condensate cut. Obviously, we have all ingredients needed to compute $a_{1,n}$. It could be interesting to do so to see if some simple structure is found.

### 6.2.4 Combined energy shift for a generic dyonic magnon

Notice that we are by no means obliged to take the simple magnon and our previous formulas are absolutely general and also yield the finite size 1-loop shift around a generic dyonic magnon. Combining all the contributions computed in the previous sections we get

$$\begin{aligned} E_0 \;\simeq\; & \oint\limits_{U^+}\frac{dx}{2\pi i}\partial_x\Omega_0\left(e^{-i\tau}\frac{x-X_-}{x-X_+}+e^{-i\tau}\frac{x-1/X_+}{x-1/X_-}-2\right)^2 e^{-\frac{ix\Delta}{g(x^2-1)}} \\ & + \left(\frac{\delta^2}{4(X_-X_++1)(X_+^2-1)^2}\left[1-X_-X_++i\frac{X_+-X_-}{\pi}-i\,\frac{\Delta}{4g}\frac{(X_+^2+1)(X_+-X_-)}{X_+^2-1}\right.\right. \\ & \left.\left. + \; i\frac{(X_-^2-1)(X_+^2-1)}{2\pi(X_-X_+-1)}\log\left(\frac{(X_++1)(X_--1)}{(X_+-1)(X_-+1)}\right)\right]+c.c.\right)\,. \end{aligned} \tag{6.35}$$

## 6.3 Lüscher-Klassen-Melzer formulas

Finally we compute the finite-size correction (6.32) using the Lüscher-Klassen-Melzer formulas [111, 112, 113, 114, 109, 17, 110]. There are two contributions, the $F$- and the $\mu$-term

$$\delta\epsilon_a^F = -V.P.\int\limits_{\mathbb{R}}\frac{dq}{2\pi}\left(1-\frac{\epsilon'(p)}{\epsilon'(q^*(q))}\right)e^{-iq^*(q)L}\sum_b(-1)^{F_b}S_{ba}^{ba}(q^*(q),p) \tag{6.36}$$

$$\delta\epsilon_a^\mu = -i\left(1-\frac{\epsilon'(p)}{\epsilon'(\tilde{q}^*)}\right)e^{-i\tilde{q}^*L}\mathrm{Res}_{q=\tilde{q}}\left(\sum_b(-1)^{F_b}S_{ba}^{ba}(q_*(q),p)\right)\,, \tag{6.37}$$

which describe the corrections to the dispersion relation of a single magnon with momentum $p$ due to virtual particles running in the loop, and bound state formation, respectively. We have used the notation for the on-shell momentum

$$q^2 + \epsilon(q_*)^2 = 0\,,$$

and $\tilde{q}$ denotes the Euclidean energy of the bound state. Inserting the all-loop AdS/CFT S-matrix [51, 52, 68, 75, 24], one can expand to arbitrary order and obtain the leading-volume correction.

Through a trivial change of variables, the F-term can be written as [17]

$$\delta\epsilon^F = V.P.\oint\limits_{\mathbb{U}^+} \frac{dx}{2\pi i}\,\partial_x\Omega_0(x)\,e^{-4\pi\frac{iJ}{\sqrt{\lambda}}\frac{x}{x^2-1}}e^{-4\pi\frac{i(\Delta-J)}{\sqrt{\lambda}}\frac{x}{x^2-1}}\left(2\,\frac{x-X_-}{x-X_+}\sqrt{\frac{X_+}{X_-}}-2\right)^2\,, \tag{6.38}$$

where

$$\Delta = J + \frac{\sqrt{\lambda}}{\pi}\sin\frac{p}{2}\,. \tag{6.39}$$

In the limit of $\mathcal{Q}\to 0$, $X_+\sim 1/X_-$ and thus the F-term agrees precisely with the first line in (6.32)!

For the $\mu$-term we have to evaluate the residue at the bound states, as done in [109], to subleading order. Since the computation is exactly as done in this paper we omit the details. There are three contributions: The contribution of the classical S-matrix, the effect from the one-loop dressing factor and the higher-loop contributions. In summary we obtain

$$\delta\epsilon^\mu = e^{-\frac{2\pi J}{\sqrt{\lambda}\sin\frac{p}{2}}}\delta_1\delta_2\delta_3\,, \tag{6.40}$$

where

$$\delta_1 = -4g\sin^3\frac{p}{2} + i\left(\frac{J}{g}\cos\frac{p}{2} - 2\sin\frac{p}{2} + \sin p\right) + \mathcal{O}\left(\frac{1}{g}\right) \tag{6.41}$$

$$\delta_2 = \frac{1}{2} + \frac{1}{g}\left(\frac{1}{2\pi\sin^2\frac{p}{2}} - \frac{i\cos\frac{p}{2}}{4\sin^2\frac{p}{2}}\right) + \mathcal{O}\left(\frac{1}{g^2}\right) \tag{6.42}$$

$$\delta_3 = \frac{8}{e^2} + \mathcal{O}\left(\frac{1}{g^2}\right)\,, \tag{6.43}$$

so that the $\mu$-term up to this order is

$$\delta\epsilon_\mu = -e^{-\frac{2\pi J}{\sqrt{\lambda}\sin\frac{p}{2}}-2}\left(16g\sin^3\frac{p}{2} + \frac{16}{\pi}\sin\frac{p}{2} - 4i\left(\mathcal{J}\cos\frac{p}{2} - 2\sin\frac{p}{2} + 2\sin p\right)\right) + \mathcal{O}\left(\frac{1}{g}\right)\,. \tag{6.44}$$

The leading $\mathcal{O}(g)$ contribution to the $\mu$-term yields the classical correction (4.100) [109]. The subleading terms are in complete agreement with the corrections appearing in the second line of our result (6.32).

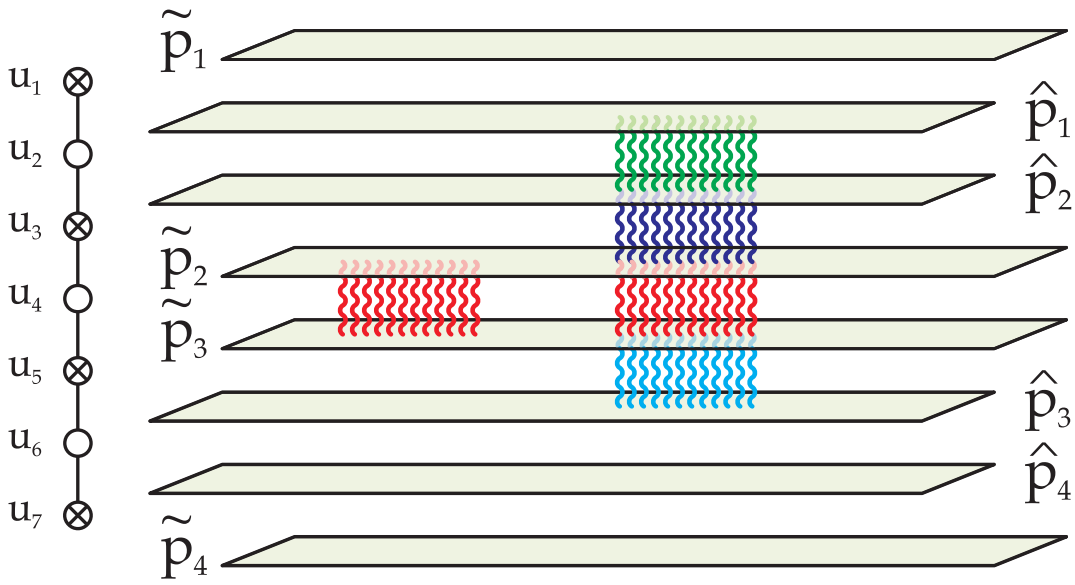


Figure 6.3: Discretization of the algebraic curve. Only the exterior of the unit circle is represented.

Thus we have successfully demonstrated the agreement of our result (6.32) with the Lüscher-Klassen-Melzer approach of computing finite-size effects. It would be interesting to reproduce from a Luscher like approach the full result (6.35) for the finite size corrections to the Dyonic magnon.

## 6.4 Semi-classical dressing phase

In this section we consider a last application of our formalism. We will understand how to modify the finite gap equations in such a way that the universal contribution $I_{HL}$ (6.10) to the one-loop shift around any classical solution is reproduced. The remaining contributions, discussed in section 6.1, are reproduced by the finite size corrections to the scaling limit of the BS equations and were analyzed in [15].

To proceed we need to discretize the algebraic curve. We will do it in several steps, gradually moving towards the final discretization. Of course we already know the result. It is given by (3.282) as already checked in section 4.5 (see discussion after equation (4.68)). However it is instructive to re-derive this result because in section 3.9 the quasi-momenta (3.282) were computed in order to reproduce the Bethe equations whereas here we want to explain how they can be naturally found from the algebraic curve alone.

The picture we have in mind is figure 6.3 (except that in this figure we are representing

only the exterior of the unit circle). Cuts uniting $\hat{p}_1$ to $\hat{p}_3$ as depicted in this figure are cuts of stacks made out of roots $u_2$, $u_3$, $u_4$ and $u_5$ as described in section 3.9. Let us then consider $\tilde{p}_1$, the quasi-momentum on top of figure 6.3. It contains poles at the positions of the roots of type $u_1$. These can then condense into cuts as explained in chapter 3. Thus we start discretizing as

$$\tilde{p}_1(x) = -G_1(x) + \dots \tag{6.45}$$

or

$$\tilde{p}_1(x) = -H_1(x) + \dots \tag{6.46}$$

where

$$G_a(x) = \sum_{j=1}^{K_a} \frac{\alpha(y_{a,j})}{x - y_{a,j}} \,, \;\; H_a(x) = \sum_{j=1}^{K_a} \frac{\alpha(x)}{x - y_{a,j}} \,. \tag{6.47}$$

with

$$\alpha(x) \equiv \frac{4\pi}{\sqrt{\lambda}} \frac{x^2}{x^2 - 1} \,,$$

are the resolvents introduced before. We chose these resolvents because as explained in the previous chapters we want the residues to be $-\alpha(y_{a,j})$. Notice that $H(x)$ has also poles at $x = \pm 1$ but this is perfectly consistent with the algebraic curve so (6.45) and (6.46) are equally good starting points. We will choose to work with (6.46). The dots in this expression mean it is still *under construction*.

Let us now give a sneak peak at $\tilde{p}_2(x)$. It should have poles at $x = x_{3,j}$ with residue $+\alpha(x_{3,j})$ and poles at $x = x_{4,j}$ with residue $-\alpha(x_{3,j})$. Therefore

$$\tilde{p}_2(x) = H_3(x) - H_4(x) + \dots \,. \tag{6.48}$$

Now we recall that the algebraic curve should obey the inversion symmetry $\tilde{p}_1(1/x) = 2\pi m - \tilde{p}_2(x)$. For the moment we ignore the momentum $P \equiv 2\pi m$ – we will restore it latter. The $x \to 1/x$ symmetry leads us to upgrade (6.46) and (6.48) to

$$\tilde{p}_1(x) = -H_1(x) - \bar{H}_3(x) + \bar{H}_4(x) + \dots \,, \tag{6.49}$$

$$\tilde{p}_2(x) = +H_3(x) - H_4(x) + \bar{H}_1(x) + \dots \,, \tag{6.50}$$

where $\bar{H}_a(x) = H_a(1/x)$. When we consider no roots at all these expressions would be zero. However we know that the vacuum algebraic curve corresponds to the BMN quasi-momenta and thus we have

$$\tilde{p}_1(x) = \frac{2\pi\mathcal{J}x - P}{x^2 - 1} - H_1(x) - \bar{H}_3(x) + \bar{H}_4(x) \,, \tag{6.51}$$

$$\tilde{p}_2(x) = \frac{2\pi\mathcal{J}x - P}{x^2 - 1} + H_3(x) - H_4(x) + \bar{H}_1(x) \,, \tag{6.52}$$

where we now took into account the $P = 2\pi m$ in a way consistent with the large $x$ asymptotics. Notice that we no longer put any dots in this expressions because as we explain below they already yield the proper curve discretization. Similarly we would write

$$\begin{aligned}\hat{p}_1(x) &= \frac{2\pi\mathcal{J}x}{x^2-1} - H_1(x) + H_2(x) + \bar{H}_2(x) - \bar{H}_3(x) + \dots \\ \hat{p}_2(x) &= \frac{2\pi\mathcal{J}x}{x^2-1} - H_2(x) + H_3(x) + \bar{H}_1(x) - \bar{H}_2(x) + \dots ,\end{aligned}$$

but since we need to have (4.60) for large $x$ we slightly improve this expressions to

$$\hat{p}_1(x) = \frac{2\pi\mathcal{J}x + 2\pi\mathcal{D}x}{x^2-1} - H_1(x) + H_2(x) + \bar{H}_2(x) - \bar{H}_3(x) \tag{6.53}$$

$$\hat{p}_2(x) = \frac{2\pi\mathcal{J}x + 2\pi\mathcal{D}x}{x^2-1} - H_2(x) + H_3(x) + \bar{H}_1(x) - \bar{H}_2(x) , \tag{6.54}$$

Expressions (6.51),(6.52), (6.53), (6.54) are almost perfect but there are still things to be understood. To check that this descritization works nicely we should check that the residues at $x = \pm 1$ are the same for $\tilde{p}_1$ and $\hat{p}_1$ for example, see (4.68). In other words

$$\hat{p}_1(x) - \tilde{p}_1(x) = \frac{2\pi\mathcal{D}x + P}{x^2-1} - \bar{H}_4 + H_2 + \bar{H}_2 \tag{6.55}$$

should be regular for $x = \pm 1$. It is easy to see that the last two terms $H_2 + \bar{H}_2 = G_2 + \bar{G}_2$ and have therefore no poles at $x = \pm 1$. If we impose that the remaining terms are also regular we obtain a relation between the total momenta $P$ and the anomalous dimensions $\mathcal{D}$ appearing in the quasi-momenta and the momentum carrying roots $x_{4,j}$. More precisely we find

$$P = \sum_{j=1}^{K_4} \frac{\alpha(x_{4,j})}{x_{4,j}} \ , \ 2\pi\mathcal{D} = \sum_{j=1}^{K_4} \frac{\alpha(x_{4,j})}{x_{4,j}^2} \tag{6.56}$$

which is exactly the same as

$$P = Q_1 \ , \ \Delta = 2gQ_2 \tag{6.57}$$

where

$$G_4(x) \equiv -\sum_{n=0}^{\infty} Q_{n+1} x^n . \tag{6.58}$$

Using these relations we can follow the exact same reasonings as above and write all quasi-

momenta as

$$\begin{array}{l|l}
\hat{p}_1 = +\dfrac{2\pi\mathcal{J}x - G_4'(0)x}{x^2-1} - H_1 + H_2 + \bar{H}_2 - \bar{H}_3 & \tilde{p}_1 = +\dfrac{2\pi\mathcal{J}x + G_4(0)}{x^2-1} - H_1 - \bar{H}_3 + \bar{H}_4 \\
\hat{p}_2 = +\dfrac{2\pi\mathcal{J}x - G_4'(0)x}{x^2-1} - H_2 + H_3 + \bar{H}_1 - \bar{H}_2 & \tilde{p}_2 = +\dfrac{2\pi\mathcal{J}x + G_4(0)}{x^2-1} + H_3 - H_4 + \bar{H}_1 \\
\hat{p}_3 = -\dfrac{2\pi\mathcal{J}x - G_4'(0)x}{x^2-1} - H_5 + H_6 + \bar{H}_6 - \bar{H}_7 & \tilde{p}_3 = -\dfrac{2\pi\mathcal{J}x + G_4(0)}{x^2-1} - H_5 + H_4 - \bar{H}_7 \\
\hat{p}_4 = -\dfrac{2\pi\mathcal{J}x - G_4'(0)x}{x^2-1} - H_6 + H_7 + \bar{H}_5 - \bar{H}_6 & \tilde{p}_4 = -\dfrac{2\pi\mathcal{J}x + G_4(0)}{x^2-1} + H_7 + \bar{H}_5 - \bar{H}_4
\end{array} \tag{6.59}$$

which are precisely the quasi-momenta (3.282) following from the scaling limit of the Beisert-Staudacher equations with the AFS phase! This very simple sequence of steps can be used to discretize other integrable models and are a precious help in guessing the form of the full quantum equations. See for example [20] where the algebraic curve in [19] together with the weak coupling results of [115] allowed for a conjecture for the all-loop Bethe equations yielding the asymptotic spectrum of the ABJM theory [116] in the planar limit.

The Bethe equations in the scaling limit coincide with the finite gap equations

$$p_i^+ - p_j^- = 2\pi n_{ij} \tag{6.60}$$

on a cut shared by the quasi-momenta $p_i$ and $p_j$.

We now arrive at the most interesting part. We want to understand how to modify these equations in such a way that the semi-classical effects are automatically included. In particular we want to be able to compute the energy around a general classical solution and obtain the correct semi-classical result (6.3).

If we add a stack connecting sheets $i$ and $j$ to some configuration of Bethe roots with all roots condensed into some cuts as described above, the position of the new stack will be given by (2.12) and all the other roots will be slightly shifted $u_j \to \tilde{u}_j$. Then the energy of the new configuration will be given by the energy of the original configuration plus the fluctuation energy with mode number $n$ associated to the corresponding string polarization

$$\tilde{\Delta} = \Delta + \mathcal{E}_n^{ij}\,. \tag{6.61}$$

Let us now perform a simple rewriting exercise and treat each of the roots of this new stack separately in $p_k$. That is, if the stack contains a root associated with the Dynkin node $a$ we write

$$G_a(x) \to G_a(x) + \frac{\alpha(x_n)}{x - x_n}\ ,\ H_a(x) \to H_a(x) + \frac{\alpha(x)}{x - x_n}$$

where $G_a$ and $H_a$ are now defined with the sum over roots going only over $j = 1, \ldots, K_a$ where $K_a$ is the *original* number of roots of type $u_{a,j}$ before adding the extra fluctuation.

Then, with this new stack, each quasi-momentum $p_k$ can be written as before but using the new resolvents $G_a$ and $H_a$ containing only the $K_a$ original roots plus an extra term $V_k^{ij}$ which we call potential and read [2]

$$\begin{pmatrix} V_{\hat{1}}(x) \\ V_{\hat{2}}(x) \\ V_{\hat{3}}(x) \\ V_{\hat{4}}(x) \end{pmatrix}^{ij} = \begin{pmatrix} +1 \\ +1 \\ -1 \\ -1 \end{pmatrix} \frac{x}{x^2-1} \frac{\alpha(x_n^{ij})}{(x_n^{ij})^2} + \begin{pmatrix} +\delta_{\hat{1}i} \\ +\delta_{\hat{2}i} \\ -\delta_{\hat{3}j} \\ -\delta_{\hat{4}j} \end{pmatrix} \frac{\alpha(x)}{x - x_n^{ij}} - \begin{pmatrix} +\delta_{\hat{2}i} \\ +\delta_{\hat{1}i} \\ -\delta_{\hat{4}j} \\ -\delta_{\hat{3}j} \end{pmatrix} \frac{\alpha(1/x)}{1/x - x_n^{ij}}, \tag{6.62}$$

and

$$\begin{pmatrix} V_{\tilde{1}}(x) \\ V_{\tilde{2}}(x) \\ V_{\tilde{3}}(x) \\ V_{\tilde{4}}(x) \end{pmatrix}^{ij} = \begin{pmatrix} -1 \\ -1 \\ +1 \\ +1 \end{pmatrix} \frac{1}{x^2-1} \frac{\alpha(x_n^{ij})}{x_n^{ij}} - \begin{pmatrix} +\delta_{\tilde{1}i} \\ +\delta_{\tilde{2}i} \\ -\delta_{\tilde{3}j} \\ -\delta_{\tilde{4}j} \end{pmatrix} \frac{\alpha(x)}{x - x_n^{ij}} + \begin{pmatrix} +\delta_{\tilde{2}i} \\ +\delta_{\tilde{1}i} \\ -\delta_{\tilde{4}j} \\ -\delta_{\tilde{3}j} \end{pmatrix} \frac{\alpha(1/x)}{1/x - x_n^{ij}}, \tag{6.63}$$

Two trivial observations: First, even though we are treating the roots of the fluctuation stack separately by hiding them into the potentials, they also contribute to the charges (because every stack contains a $u_4$ root)

$$Q_m = \oint \frac{dx}{2\pi i} \frac{G_4(x)}{x^m} + \frac{\alpha(x_n)}{x_n^m}. \tag{6.64}$$

Second, the potentials $V_k^{ij}$ are different for different quasi-momenta.

Now suppose that instead of (6.61) we want

$$\tilde{\Delta} = \Delta + I_{HL} \tag{6.65}$$

with $I_{HL}$ given in (6.10). By linearity, we need only to replace $V_k^{ij}$ by

$$V_k(x) = \frac{1}{2} \sum_{ij} (-1)^{F_{ij}} \oint_{U^+} V_k^{ij}(x,y) \frac{p_i'(y) - p_j'(y)}{2\pi} \frac{dy}{2} \quad . \tag{6.66}$$

That is we add the appropriate sea of virtual particles. Let us now show that all the potentials $V_k$ are the same up to a sign and are equal to

$$\mathcal{V}(x) \equiv \int_{-1}^{1} \partial_y \left[ G_4(y) - G_4(1/y) \right] \left( \frac{\alpha(x)}{x-y} - \frac{\alpha(1/x)}{1/x - y} \right) \frac{dy}{2\pi}. \tag{6.67}$$

Indeed

[2] For example, consider a fermionic stack $i,j = \tilde{2}, \hat{3}$ connecting $\tilde{p}_2$ and $\hat{p}_3$. As we see from figure 3.18 this stack is made of two almost coincident $u_4$ and $u_5$ roots. The first term in the potentials comes from the resolvent of the middle node though the $G_4(0)$ and $G_4'(0)$ terms present in all quasimomenta (3.282). The new terms in $\tilde{p}_1, \tilde{p}_2, \hat{p}_3, \hat{p}_4$ come from the resolvents $H_4$ and $H_5$ which, for the other quasimomenta, are either not present or appear with opposite signs.

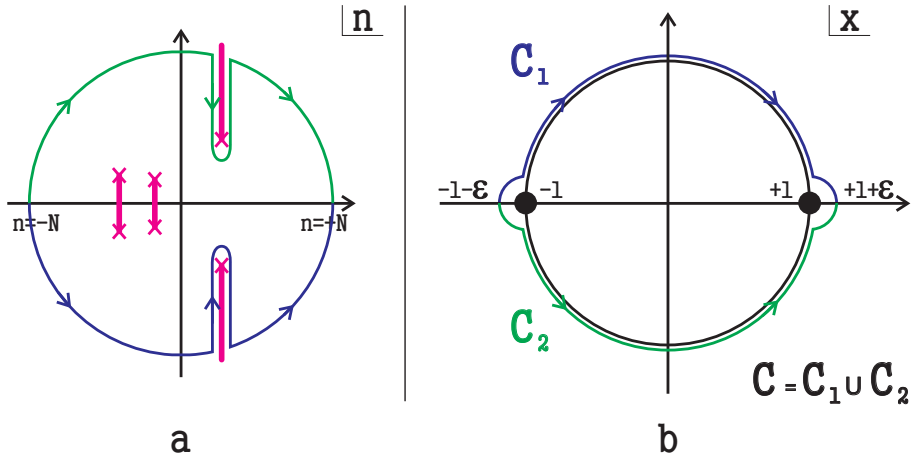


Figure 6.4: a) The "non-analytic" contribution $I_{HL}$ is given by the integral (6.28) whose integration path goes along the large cuts discussed in section 2. The difference in orientations with respect to figure 6.1a is due to the absence of cot in expression (6.10) compared to (6.7). b) In the $x$ plane the integral can be safely deformed to go over the upper and lower halves of the unit circle. In the main text we use the shorthand $\int_{-1}^{+1}$ to denote $\frac{1}{2}\int_{C_1}+\frac{1}{2}\int_{C_2}$. The relation between the large $N$ regularization in the $n$ plane and the $\epsilon$ regularization in the $x$ plane is discussed in [14, 15].

1. The first terms in (6.62) and (6.63) do not contribute to $V_k$. The reason being that, if we integrate some function of $x_n^{ij}$ summed over the 16 possible excitations listed in figure 3.18 with a $(-1)^F$ weight

$$\sum_{ij}(-1)^F\int_{-N}^{N} f(x_n^{ij})dn\,,$$

we obtain[3],

$$\int_{-1-\epsilon}^{+1+\epsilon} f(y)\left[\sum_{i=1,2\,,j=3,4}(\tilde{p}_i'-\tilde{p}_j')+(\hat{p}_i'-\hat{p}_j')-(\tilde{p}_i'-\hat{p}_j')-(\hat{p}_i'-\tilde{p}_j')\right]\frac{dy}{2\pi}=0\,. \qquad (6.68)$$

[3]We can as well use the quasi-momenta with the resolvents $G_a$ and $H_a$ summed only over the original roots because the inclusion of the potentials in (5.4) is an higher order effect.

2. Finally, consider for example $V_{\hat{1}}$. We have

$$\begin{aligned} V_{\hat{1}}(x) &= \frac{1}{2}\int_{-1-\epsilon}^{1+\epsilon}[(\hat{p}'_1-\hat{p}'_3)+(\hat{p}'_1-\hat{p}'_4)-(\hat{p}'_1-\tilde{p}'_3)-(\hat{p}'_1-\tilde{p}'_4)]\,\frac{\alpha(x)}{x-y}\frac{dy}{2\pi} \\ &- \frac{1}{2}\int_{-1-\epsilon}^{1+\epsilon}[(\hat{p}'_2-\hat{p}'_3)+(\hat{p}'_2-\hat{p}'_4)-(\hat{p}'_2-\tilde{p}'_3)-(\hat{p}'_2-\tilde{p}'_4)]\,\frac{\alpha(1/x)}{1/x-y}\frac{dy}{2\pi}\,. \end{aligned}$$

We see that $\hat{p}_1$ and $\hat{p}_2$ drop out so that the expression simplifies considerably. The same happens for the other $V_i$ and moreover, due to the super-tracelessness of the monodromy matrix, $\tilde{p}_1+\tilde{p}_1+\tilde{p}_1+\tilde{p}_4=\hat{p}_1+\hat{p}_1+\hat{p}_1+\hat{p}_4$, and all the potentials are equal. Using (6.59) we have

$$V_{\hat{1},\hat{2},\tilde{1},\tilde{2}}(x)=-V_{\hat{3},\hat{4},\tilde{3},\tilde{4}}(x)\equiv\mathcal{V}(x)=\int_{-1}^{1}\partial_y\left[G_4(y)-G_4(1/y)\right]\left(\frac{\alpha(x)}{x-y}-\frac{\alpha(1/x)}{1/x-y}\right)\frac{dy}{2\pi} \tag{6.69}$$

Notice also that due to 1) the extra terms in the charges (6.64) give no contribution! This is a huge difference compared with the usual addition of a single stack and has remarkable consequences. If we re-define the quasi-momenta in (6.59) by adding these new potentials

$$\begin{aligned} \tilde{p}_1 &= +\frac{2\pi\mathcal{J}x+G_4(0)}{x^2-1}-H_1-\bar{H}_3+\bar{H}_4 \quad +\mathcal{V} \\ &\cdots \\ \tilde{p}_2 &= +\frac{2\pi\mathcal{J}x+G_4(0)}{x^2-1}+H_3-H_4+\bar{H}_1 \quad +\mathcal{V} \\ \tilde{p}_3 &= -\frac{2\pi\mathcal{J}x+G_4(0)}{x^2-1}-H_5+H_4-\bar{H}_7 \quad -\mathcal{V} \\ &\cdots \\ \tilde{p}_4 &= -\frac{2\pi\mathcal{J}x+G_4(0)}{x^2-1}+H_7+\bar{H}_5-\bar{H}_4 \quad -\mathcal{V} \end{aligned}$$

and solve (6.60) as usual but for the new quasi-momenta, then, by construction, the energy as obtained from the *physical* charges (6.58) will automatically reproduce the contribution (6.10). Let us stress out once again the importance of the fact that the contribution of the virtual particles to the physical charges vanishes. Only because of this can we think of the potential as a mere deformation of the quasi-momenta and simply use the original roots to compute the energy from (6.58). The seven Beisert-Staudacher equations correspond to considering the difference of the several consecutive quasi-momenta $(\tilde{p}_1,\hat{p}_1)$, $(\hat{p}_1,\hat{p}_2)$, $(\hat{p}_2,\tilde{p}_2)$, etc. We see that the addition of these potentials only changes the middle mode equations obtained from

$$\tilde{p}_2^{+}-\tilde{p}_3^{-}=2\pi n\,, \tag{6.70}$$

when written in terms of the resolvents of the several Bethe roots. In all other differences the potentials cancel out! Thus this potential corresponds precisely to a correction to the $AFS$ dressing factor,

$$\prod_{j\neq k}\sigma_{AFS}(x_{4,k},x_{4,j})\to e^{i\mathcal{V}(x_{4,k})}\prod_{j\neq k}\sigma_{AFS}(x_{4,k},x_{4,j})\,. \tag{6.71}$$

Since

$$G_4(y)=-\sum_{n=0}^{\infty}Q_{n+1}y^n\,, \tag{6.72}$$

we can also write

$$\mathcal{V}(x)=\alpha(x)\sum_{\substack{r,\,s=2\\ r+s\,\in\,Odd}}^{\infty}\frac{1}{\pi}\frac{(r-1)(s-1)}{(s-r)(r+s-2)}\left(\frac{Q_r}{x^s}-\frac{Q_s}{x^r}\right) \tag{6.73}$$

where we recognize precisely the Hernandez-Lopez coefficients [77]! To obtain the values of the potential for $|x|<1$ we can simply use the exact symmetry

$$\mathcal{V}(1/x)=-\mathcal{V}(x) \tag{6.74}$$

which is obvious from (6.69) but not manifest in the form (6.73).

If we want, on the other hand, to write

$$e^{i\mathcal{V}(y_{4,k})}=\prod_{j\neq k}^{K_4}e^{i\theta(y_{4,k},y_{4,j})}$$

where the factorized scattering property is manifest we just need to use the definition (6.47) and integrate over $y$ to get[4]

$$\theta(x,y)=-\frac{\alpha(x)\,\alpha(y)}{\pi}\left[\left(\frac{1}{(x-y)^2}+\frac{1}{(xy-1)^2}\right)\log\left(\frac{x+1}{x-1}\frac{y-1}{y+1}\right)+\frac{2}{(x-y)(xy-1)}\right] \tag{6.75}$$

The *real* scattering phase, the phase that describes the scattering between two magnons in the Bethe ansatz equation, must inherit the explicit $x$ to $1/x$ oddness (6.74) of the potential. To obtain the values of the phase for $|x|<1$ we use $\theta(1/x,y)=-\theta(x,y)$. Alternatively, we recall that the contour in figure 6.4b tells us that to be completely rigorous we should replace the log in (6.75) by $\frac{1}{2}\left(\log_+(\dots)+\log_-(\dots)\right)$ where $\log_\pm$ has a branchcut in the upper/lower half of the unit circle – see figure 6.4b. Then the expression for $\theta(x,y)$ becomes explicitly $x$ to $1/x$ odd and is discontinuous on the unit circle. If, on the other hand, we

[4]By resuming the Hernandez-Lopez coefficients the phase $\theta(x,y)$ was written down in [117], see also the appendix B in [118].

analytically continue the expression (6.75) from some point $x$ outside the unit circle up to some point $1/x$ inside the unit circle we get $2\pi i$ from one of the $\log_\pm$ so that we trivially find

$$i\theta(x,y) + i\tilde{\theta}(1/x,y) = -\alpha(x)\,\alpha(y)\left(\frac{1}{(x-y)^2} + \frac{1}{(xy-1)^2}\right),$$

which is precisely Janik's crossing relation [74] for the dressing factor at $1/\sqrt{\lambda}$ order [117].

# Part IV

# Conclusion

# Chapter 7

# Conclusions, State of the Art and Future Directions

No non-trivial field theory in $d \geq 3$ space-time dimensions was ever solved. Optimistically, one might expect that if we solve one we will open a Pandora box in the same way that Lars Onsager solution of the two dimension Ising model did.

We seem to be approaching such remarkable point. It is now clear that the techniques of Integrability, normally used in the two dimensional realm, can sometime play a key role in the study of higher dimensional super-conformal gauge theories [9, 115]. $\mathcal{N} = 4$ SYM, studied in this thesis, is probably just the most well known example out of many which can be attacked by Bethe ansatz techniques. More examples known to date are deformations of $\mathcal{N} = 4$ and three dimensional super Chern-Simons conformal theories [116, 119, 115, 120]. All these share some common freatures:

They are super-conformal gauge theories with a gravity dual.

Integrability arises for these conformal theories when we try to compute the spectrum of single trace gauge invariant operators. The dilatation operator turns out to be equivalent to an integrable spin chain Hamiltonian. The planar limit is crucial to be able to interpret the single trace operators as spin chains.

These theories admit simple gravity duals. For $\mathcal{N} = 4$ we have type IIB superstrings on $AdS_5 \times S^5$ while for ABJM we have type IIA on $AdS_4 \times CP^3$. These dual two dimensional theories are quite simple and symmetric and thus, not surprisingly, they are classically integrable. Moreover they are super-symmetric. The rule of thumb is that two dimensional super-symmetric classically integrable theories are quantum mechanically integrable. This is often not the case for purely bosonic models though [121, 122, 123]. This means we will probably find many more examples of integrable gauge theories from the duals of superstring theory on simple $AdS_d \times X$ backgrounds. It is crucial to search for these theories and corresponding gravity duals.

The Gauge symmetry was another important feature in these recent advances. The reason is that when we have a supersymmetric gauge theory the supersymmetry transformations are usually non-linearly realized. Often the commutator of two supersymmetry

transformations yields something of the form

$$[\delta_\epsilon, \delta_{\epsilon'}]\, Field = \partial_\mu\, Field + [\Phi, Field] \tag{7.1}$$

which means that the fermionic transformations commute to the momentum generator up to somehow unusual gauge transformations where the gauge parameter is one of the fields $\Phi$. This will imply that the symmetry algebra transforming the elementary fields into one another should be thought as some centrally extended (super)algebra. In particular, in all examples we mentioned there exists a subset of fields which transform under $SU(2|2)$ extended. Theories based on such extensions are highly constrained [51, 52] and this was quite important to help understand the finite coupling regime interpolating between the $CFT$ and the dual $AdS$ theories [51, 68, 115, 124, 20, 125].

On the other hand we can also play the devil's advocate. First of all we are always working in the strict planar limit with $N = \infty$ and moreover we are computing *only* the spectrum of the conformal theory. To completely solve it we would also need the three point couplings. Integrability should play a important role to tackle this problem. It would be vital to understand how.

Furthermore, so far only the spectrum of large operators is properly understood. This limitation will probably be surpassed in the short term. More precisely, Bethe equations are valid when we consider single trace operators made out of a large enough number of fields [38]. When we start considering small operators (or string states with small angular momentum in the light-cone gauge), wrapping effects corresponding to virtual particles winding around the spin chain (or world-sheet) become relevant [111, 114]. The effects were studied at strong coupling [109, 126, 99, 17, 110, 21] with great success in reproducing the finite size corrections to the so called Giant Magnon [90]. The Giant magnon is the dual string state corresponding to a single spin flip in the dual gauge theory. These computations are quite interesting for two reasons. On the one hand they give us the leading finite size corrections and are therefore a first window towards the finite size spectrum of the theory. On the other hand these computations can be used to check the validity of the $AdS/CFT$ S-matrix [51, 68, 75, 24]. In particular, in [109, 21], the all loop dressing kernel of [24] was probed.

In [127] Bajnok and Janik performed an impressive computation. They generalized the Luscher formulas for many particle states and applied this to the computation of the finite size corrections to a two magnon state in string theory. When the length of the state (angular momentum of the string) is taken to be 4 and small t'Hooft coupling is considered (highly quantum string) we are, by the $AdS/CFT$ duality, studying the Konishi operator,

$$\mathrm{Tr}(ZXZX) - \mathrm{Tr}(ZZXX)\,, \tag{7.2}$$

in the perturbative SYM regime. Remarkably, the string computation in this very rough

limit – highly quantum string and very small angular momentum – reproduces precisely the weak coupling direct Feynman diagramatic computation of [128, 129]!

All these advances indicate that the finite size limitation will be overcome. More precisely all the above mentioned works are based on the Luscher formulas which only yield the leading finite size corrections to the anomalous dimensions. Such Luscher formulas are usually (or at least often) the large volume limit of some exact Thermodynamical Bethe Ansatz equations. To write down such equations, and to be able to plot the anomalous dimensions of simple operators such (7.2) as a function of the t'Hooft coupling, is of utmost importance. Some first steps of this very non-trivial program were made in [130, 131].

Finally, optimistically, if we find the full spectrum of these gauge theories and, even more optimistically, manage to compute the three point couplings and thus obtain all the correlation functions, fundamental questions still remain. Why are these theories integrable? What is the landscape of integrable theories? Can one turn the problem around and build the field theories starting from the integrable structures? How close to QCD can we get? Are all integrable theories dual to some string theory? If so, what can we learn about quantum gravity? Is the planar limit an absolute limitation or will we be able to overcome this obstacle for some theories?

A probably more pragmatic approach would be to try to merge the very developed field of Integrability in AdS/CFT with the computation of Scattering Amplitudes and Wilson Loops, which has also developed enormously in the last few years (see [132] for a very nice review and references). Such symbiosis would probably greatly expand our understanding of the subject and most likely shed light over some of the just posed questions.

Certainly, the days to come will be at least as exciting as the last few years in theoretical physics. This thesis ends here.

# Part V

# Appendices

# Appendix A

# Bosonic duality

In this Appendix we discuss in detail the bosonic duality (3.278) mentioned in section 3.8.2. There are two main steps to be considered.

On the one hand we have to prove that for a set of $K_2$ generic complex numbers $u_2$ and $K_1$ roots $u_1$ obeying the auxiliary Bethe equations (3.270) it is possible to write ($\tau = \phi_1 - \phi_2$)

$$2i \sin(\tau/2)\, Q_2(u) = e^{i\tau/2} Q_1(u - i/2)\tilde{Q}_1(u + i/2) - e^{-i\tau/2} Q_1(u + i/2)\tilde{Q}_1(u - i/2)\,, \quad \text{(A.1)}$$

and that, in doing so, we define the position of a new set of numbers $\tilde{u}_1$. A priori this is not at all a trivial statement because we have a polynomial of degree $K_2$ on the left whereas on the right hand side we have only $K_2 - K_1$ parameters to fix. However, as we will see, if $K_1$ equations (3.270) are satisfied it is possible to write $Q_2(u)$ in this form. This will be the subject of the section A.1.

The second step is the trivial one. Assuming (A.1) to be proved we can use this relation to show that in the original Bethe equations we can replace the roots $u_1$ by the new roots $\tilde{u}_1$ with the simultaneous exchange $\phi_1 \leftrightarrow \phi_2$. Indeed if we evaluate the duality at $u = u_{2,j}$ we find

$$\frac{Q_1(u_{2,j} - i/2)}{Q_1(u_{2,j} + i/2)} = e^{i(\phi_2 - \phi_1)} \frac{\tilde{Q}_1(u_{2,j} - i/2)}{\tilde{Q}_1(u_{2,j} + i/2)}\,,$$

meaning that in the equation (3.271) for the $u_2$ roots we can replace the roots $u_1$ by the dual roots $\tilde{u}_1$ provided we replace $\phi_1 \leftrightarrow \phi_2$. Moreover if we take $u = \tilde{u}_{1,j} \pm i/2$ we will get

$$e^{i\phi_2 - i\phi_1} = -\frac{\tilde{Q}_1(\tilde{u}_1 + i)}{\tilde{Q}_1(\tilde{u}_1 - i)} \frac{Q_2(\tilde{u}_1 - i/2)}{Q_2(\tilde{u}_1 + i/2)}\,,$$

which we recognize as equation (3.270) with $K_2 - K_1$ roots $\tilde{u}_1$ in place of the $K_1$ original roots $u_1$ and with $\phi_1 \leftrightarrow \phi_2$. Finally evaluating (A.1) at $u = u_{1,j} \pm i/2$ we will get the original equation (3.270) so that we see that it must be satisfied in order to equation (A.1) to be valid.

## A.1 Decomposition proof

In this section we shall prove that one can always decompose $Q_2(u)$ as in (A.1) and that this decomposition uniquely fixes the position of the new set of roots $\tilde{u}_1$. In other words, let us show that we can set the polynomial

$$P(u) \equiv e^{+i\frac{\tau}{2}} Q_1(u-i/2)\tilde{Q}_1(u+i/2) - e^{-i\frac{\tau}{2}} Q_1(u+i/2)\tilde{Q}_1(u-i/2) - 2i\sin\frac{\tau}{2} Q_2(u)$$

to zero through a unique choice of the dual roots $\tilde{u}_1$.

- Consider first the case $K_1 = 0$. Then it is trivial to see that we can always find unique polynomial $\tilde{Q}_1 = u^{K_2} + \sum_{n=1}^{K_2} a_n u^{n-1}$ such that

  $$e^{+i\frac{\tau}{2}} \tilde{Q}_1(u+i/2) - e^{-i\frac{\tau}{2}} \tilde{Q}_1(u-i/2) = 2i\sin\frac{\tau}{2} Q_2(u)\,.$$

  because this amounts to solving $K_2$ linear equations for $K_2$ coefficients $a_n$ with non-degenerate triangular matrix.

- Next let us consider $K_1 \leq K_2/2$. First we choose $\tilde{Q}_1$ to satisfy $K_1$ equations

  $$\tilde{Q}_1(u_p^1) = 2ie^{-i\frac{\tau}{2}} \sin\frac{\tau}{2} \frac{Q_2(u_p^1 - i/2)}{Q_1(u_p^1 - i)} \equiv c_p \quad , \quad p = 1, \ldots, K_1$$

  these conditions will define $\tilde{Q}_1(u)$ up to a homogeneous solution proportional to $Q_1(u)$,

  $$\tilde{Q}_1(u) = Q_1(u)\tilde{q}_1(u) + \sum_{p=1}^{K_1} \frac{Q_1(u)}{Q_1'(u_p^1)(u-u_p^1)}\, c_p$$

  where $\tilde{q}_1(u)$ is some polynomial of the degree $K_2 - 2K_1$. Now from (3.270) we notice that with this choice of $\tilde{Q}_1$ we have

  $$\frac{P(u_p^1 + i/2)}{Q_2(u_p^1 + i/2)} = \frac{P(u_p^1 - i/2)}{Q_2(u_p^1 - i/2)} = 0 \quad , \quad p = 1, \ldots, K_3$$

  and thus

  $$P(u) = Q_1(u+i/2)Q_1(u-i/2)p(u)$$

  where

  $$p(u) = e^{i\frac{\tau}{2}} \tilde{q}_1(u+i/2) - e^{-i\frac{\tau}{2}} \tilde{q}_1(u-i/2) - 2i\sin\frac{\tau}{2}\, q_2(u)$$

  and $q_2$ is a polynomial. Thus we are left to the same problem as above where $K_1 = 0$. For completeness let us note that we can write $q_2(u)$ explicitly in terms of the original roots $u_1$ and $u_2$,

  $$q_2(u) = \frac{Q_2(u)}{Q_1(u+i/2)Q_1(u-i/2)} - \text{poles}$$

  where the last term is a simple collection of poles at $u = u_p^1 \pm i/2$ whose residues are such that $q_2(u)$ is indeed a polynomial.

- We can see that the number of the solutions of (3.270) with $K_1 = K$ and $K_1 = K_2 - K$ is the same (see [36] for examples of states counting). Thus for each solution with $K_1 \geq K_2/2$ we can always find one dual solution with $K_1 \leq K_2/2$ and in this way we prove our statement for $K_1 \geq K_2/2$

- Finally let us stress the uniqueness of the $\tilde{Q}_1$. If $K_1 > \tilde{K}_1$ we have nothing to show since we saw explicitly above how the bosonic duality constrains uniquely the dual polynomial $\tilde{Q}_1$. Let us then consider $K_1 < \tilde{K}_1$ and assume we have two different solutions $\tilde{Q}_1^1$ and $\tilde{Q}_1^2$. Then from the duality relation (A.1) for either solution we find

$$e^{i\frac{\tau}{2}} Q_1(u - i/2) \left( \tilde{Q}_1^1(u + i/2) - \tilde{Q}_1^2(u + i/2) \right) =$$
$$e^{-i\frac{\tau}{2}} Q_1(u + i/2) \left( \tilde{Q}_1^1(u - i/2) - \tilde{Q}_1^2(u - i/2) \right) .$$

  Evaluating this expression at $u = u_{1,j} + i/2$ we find that $\tilde{Q}_1^1(u_{1,j}) - \tilde{Q}_1^2(u_{1,j}) = 0$ so that $\tilde{Q}_1^1(u_1) - \tilde{Q}_1^2(u_1) = Q_1(u)h(u)$ and therefore

$$e^{i\frac{\tau}{2}} h(u + i/2) = e^{-i\frac{\tau}{2}} h(u - i/2)$$

  which is clearly impossible for polynomial $h(u)$ – for large $u$ we can neglect the $i/2$'s to obtain $e^{i\tau} = 1$ thus leading to a contradiction.

## A.2 Transfer matrix invariance and the bosonic duality for $SU(K|M)$

In this section we review the formalism of [53] which allows one to derive the transfer matrices of usual (super) spin chains in any representation. In this work Kazakov, Sorin and Zabrodin reduce the Bethe ansatz quantum problem to the study of classical discrete dynamics in the space $(a, s, K, M)$ where $(a, s)$ are labels of the representation of the supergroup $SU(K|M)$. To derive such dynamics – which will in particular yield the main formula (A.2) considered below – the starting point is the conjectured Bazhanov-Reshitikhin determinant relation [133] recently derived in [16]. We will the general formalism of [53] to prove the invariance of all possible transfer matrices under the bosonic dualities.

For the standard $SU(K|M)$ super spin chains (based on the standard $R$–matrix $R(u) = u + i\mathcal{P}$ with $\mathcal{P}$ the super permutation) we can find the (twisted) transfer matrix eigenvalues for the single column young tableau with $a$ boxes through the *non-commutative generating functions* [53, 84]

$$\sum_{a=0}^{\infty} (-1)^a e^{ia\partial_u} \frac{T_a(u)}{Q_{K,M}(u + (a - K + M + 1)\, i/2)} e^{ia\partial_u} = \overrightarrow{\prod}_{(x,n)\in\gamma} \hat{V}_{x,n}^{-1}(u) \tag{A.2}$$

where $\gamma$ is a path starting from $(M,K)$ and finishing at $(0,0)$ (always approaching this point with each step) in a rectangular lattice of size $M\times K$ as in figure 3.10[1], $x=(m,k)$ is point in this path and $n=(0,-1)$ or $(-1,0)$ is the unit vector looking along the next step of the path. Each path describes in this way a possible Dynkin diagram of the $SU(K|M)$ super group with corners denoting fermionic nodes and straight lines bosonic ones, see figure 3.10. Finally,

$$\begin{aligned}\hat{V}^{-1}_{(m,k),(0,-1)}(u) &= e^{i\phi_k}\frac{Q_{k,m}(u+i(m-k-1)/2)}{Q_{k,m}(u+i(m-k+1)/2)}\frac{Q_{k-1,m}(u+i(m-k+2)/2)}{Q_{k-1,m}(u+i(m-k+0)/2)}-e^{i\partial_u}\\ \hat{V}^{-1}_{(m,k),(-1,0)}(u) &= \left(e^{i\varphi_m}\frac{Q_{k,m-1}(u+i(m-k-2)/2)}{Q_{k,m-1}(u+i(m-k+0)/2)}\frac{Q_{k,m}(u+i(m-k+1)/2)}{Q_{k,m}(u+i(m-k-1)/2)}-e^{i\partial_u}\right)^{-1}\end{aligned}$$

where $Q_{k,m}$ is the Baxter polynomial for the roots of the corresponding node[2] and $\{\phi_k,\varphi_m\}$ are twists introduced in the transfer matrix [84].

Let us then consider a bosonic node like the one in the middle of figure 3.10 (the *vertical* bosonic node is treated in the same fashion). If the position of this node on the $M\times K$ lattice is given by $(m,k)$ then it is obvious that the only combination containing $Q_{m,k}$ in the right hand side of (A.2) comes from the product of $\hat{V}^{-1}_{(m,k),(-1,0)}(u)\hat{V}^{-1}_{(m+1,k),(-1,0)}(u)$ which reads

$$\begin{aligned}&\left[e^{i\varphi_m+\varphi_{m+1}}\frac{Q_{k,m+1}(u+i(m-k+2)/2)}{Q_{k,m+1}(u+i(m-k+0)/2)}\frac{Q_{k,m-1}(u+i(m-k-2)/2)}{Q_{k,m-1}(u+i(m-k+0)/2)}+e^{2i\partial_u}-\right.\\ &-\left(e^{i\varphi_{m+1}}\frac{Q_{k,m}(u+i(m-k-1)/2)}{Q_{k,m}(u+i(m-k+1)/2)}\frac{Q_{k,m+1}(u+i(m-k+2)/2)}{Q_{k,m+1}(u+i(m-k+0)/2)}+\right.\\ &\left.\left.+e^{i\varphi_m}\frac{Q_{k,m-1}(u+i(m-k+0)/2)}{Q_{k,m-1}(u+i(m-k+2)/2)}\frac{Q_{k,m}(u+i(m-k+3)/2)}{Q_{k,m}(u+i(m-k+1)/2)}\right)e^{i\partial_u}\right]^{-1}\end{aligned}\tag{A.3}$$

So, if we want to study the bosonic duality on the node $(k,m)$ and its relation with the invariance of several transfer matrices we need to study the last two lines of this expression. For simplicity let us shift $u$, omit the subscript $k$ in the Baxter polynomials $Q_{k,m-1},Q_{k,m},Q_{k,m+1}$ and define the reduced transfer matrix as

$$t(u,\varphi_m,\varphi_{m+1})\equiv e^{i\varphi_{m+1}}\frac{Q_m(u-i)}{Q_m(u)}\frac{Q_{m+1}(u+i/2)}{Q_{m+1}(u-i/2)}+e^{i\varphi_m}\frac{Q_{m-1}(u-i/2)}{Q_{m-1}(u+i/2)}\frac{Q_m(u+i)}{Q_m(u)}\,.\tag{A.4}$$

Notice that the absence of poles at the zeros of $Q_m$ yields precisely the Bethe equations for this auxiliary node.

[1] Notice that the path goes in opposite direction compared to the labelling $a$ of the Baxter polynomial $Q_a$ used before. In the notation of this section $Q_{k,m}$ corresponds to the node is at position (m,k) in this lattice.

[2] $\hat{Q}_{0,0}$ is normalized to 1. If we are considering a spin in the representation where the first Dynkin node has a nonzero Dynkin label then $Q_{M,K}$ will play the role of the potential term. In general the situation is more complicated, see [53]. In any case we are mainly interested in the dualization of roots which are not momentum carrying thus we need not care about such matters.

**Bosonic duality ⇒ Transfer matrices invariance**

Thus, to check the invariance of the transfer matrices in all representations it suffices to verify that the reduced transfer matrix $t(u,\varphi_m,\varphi_{m+1})$ is invariant under $\varphi_m \leftrightarrow \varphi_{m+1}$ and $Q_m \to \tilde{Q}_m$ where

$$2i\sin\left(\frac{\varphi_{m+1}-\varphi_m}{2}\right) Q_{m-1}(u)Q_{m+1}(u) = \tag{A.5}$$
$$e^{i\frac{\varphi_{m+1}-\varphi_m}{2}} Q_m(u-i/2)\tilde{Q}_m(u+i/2) - e^{-i\frac{\varphi_{m+1}-\varphi_m}{2}} Q_m(u+i/2)\tilde{Q}_m(u-i/2)\,.$$

which can be easily verified. If suffices to replace, in $t(u,\varphi_m,\varphi_{m+1})$ in (A.4),

$$\begin{aligned}
\frac{Q_m(u-i)}{Q_m(u)} \;\to\; & e^{-i(\varphi_{m+1}-\varphi_m)}\frac{\tilde{Q}_m(u-i)}{\tilde{Q}_m(u)} \\
& +2ie^{-i\frac{\varphi_{m+1}-\varphi_m}{2}}\sin\left(\frac{\varphi_{m+1}-\varphi_m}{2}\right)\frac{Q_{m-1}(u+i/2)Q_{m+1}(u+i/2)}{Q_m(u)\tilde{Q}_m(u)}\,, \\
\frac{Q_m(u+i)}{Q_m(u)} \;\to\; & e^{+i(\varphi_{m+1}-\varphi_m)}\frac{\tilde{Q}_m(u+i)}{\tilde{Q}_m(u)} \\
& -2ie^{-i\frac{\varphi_{m+1}-\varphi_m}{2}}\sin\left(\frac{\varphi_{m+1}-\varphi_m}{2}\right)\frac{Q_{m-1}(u-i/2)Q_{m+1}(u-i/2)}{Q_m(u)\tilde{Q}_m(u)}\,,
\end{aligned}$$

which are obvious consequences of the bosonic duality.

**Transfer matrix invariance ⇒ Bosonic duality**

On the other hand suppose we have two solutions of Bethe equations, one of them characterized by the Baxter polynomials $\{\dots,Q_{m-1},Q_m,Q_{m+1},\dots\}$ with twists $\{\dots,\varphi_m,\varphi_{m+1},\dots$ and another with $\{\dots,Q_{m-1},\tilde{Q}_m,Q_{m+1},\dots\}$ with twists $\{\dots,\varphi_{m+1},\varphi_m,\dots\}$ for which the transfer matrices are the same, that is

$$t(u,\varphi_m,\varphi_{m+1}) = \tilde{t}(u,\varphi_{m+1},\varphi_m)\,. \tag{A.6}$$

Then we can show that these two solutions are related by the bosonic duality (A.5). Indeed if we build the Wronskian like object

$$W(u) \equiv e^{i\frac{\varphi_{m+1}-\varphi_m}{2}}\frac{Q_m(u-i/2)\tilde{Q}_m(u+i/2)}{Q_{m-1}(u)Q_{m+1}(u)} - e^{-i\frac{\varphi_{m+1}-\varphi_m}{2}}\frac{Q_m(u+i/2)\tilde{Q}_m(u-i/2)}{Q_{m-1}(u)Q_{m+1}(u)}\,.$$

we can easily check that

$$\begin{aligned}
& W(u+i/2)-W(u-i/2) = \\
& -e^{-i\frac{\varphi_{m+1}+\varphi_m}{2}}\frac{Q_m(u)\tilde{Q}_m(u)}{Q_{m-1}(u-i/2)Q_{m+1}(u+i/2)}\left(t(u,\varphi_m,\varphi_{m+1})-\tilde{t}(u,\varphi_{m+1},\varphi_m)\right)=0
\end{aligned}$$

Since by definition $W(u)$ is a rational function this means it must be a constant. Thus if $\varphi_m \neq \varphi_{m+1}$ we must have $K_m + \tilde{K}_m = K_m + K_{m+1}$ and the value of $W$ can be read from the large $u$ behavior. In this way we obtain precisely the bosonic duality (A.5). If $\varphi_m = \varphi_{m+1}$ then we see that $K_m + \tilde{K}_m = K_m + K_{m+1} + 1$ and we will obtain a different value for the constant $W$ which will correspond to the untwisted bosonic duality described in [15].

# Appendix B

# Explicit expressions for the flat connection for circular strings

In this appendix we present the general expressions obtained for the constant flat connections associated with the circular string solutions (4.35) discussed in section 4.4.1. The $S^5$ components $\tilde{p}_i$ are given in terms of the eigenvalues of the symmetric matrix

$$\frac{2\pi}{i}A_\sigma^S(x) = \pi \begin{pmatrix} -\tilde{a}_+(1/x) & \tilde{b}_+ & -\tilde{c}(1/x) & \tilde{d}(x) \\ \tilde{b}_+ & \tilde{a}_+(x) & \tilde{d}(1/x) & \tilde{c}(x) \\ -\tilde{c}(1/x) & \tilde{d}(1/x) & \tilde{a}_-(x) & \tilde{b}_- \\ \tilde{d}(x) & \tilde{c}(x) & \tilde{b}_- & -\tilde{a}_-(1/x) \end{pmatrix} \tag{B.1}$$

with

$$\begin{aligned}
\tilde{a}_\pm(x) &= \pm\tilde{a}(x) - m_3\cos\theta \\
\tilde{a}(x) &= -\frac{m_1 - w_1 x + (m_2 - w_2 x)\cos\theta + x\cos 2\gamma(-w_1 + m_1 x + (w_2 - m_2 x)\cos\theta)}{x^2-1} \\
\tilde{b}_\pm &= (m_2 \mp m_3)\cos\gamma\sin\theta \\
\tilde{c}(x) &= \frac{(m_2+m_3)x^2 - (m_2 - m_3) - 2w_3 x}{x^2-1}\sin\gamma\sin\theta \\
\tilde{d}(x) &= \frac{-m_1 + w_1 x + (m_2 - w_2\, x)\cos\theta}{x^2-1}\sin 2\gamma
\end{aligned}$$

while the $AdS$ quasi-momenta $\hat{p}_i$ are the eigenvalues of

$$\frac{2\pi}{i}A_\sigma^{AdS}(x) = \pi \begin{pmatrix} -\hat{a}_+(1/x) & \hat{b}_+ & -\hat{c}(x) & \hat{d}(x) \\ \hat{b}_+ & \hat{a}_+(x) & \hat{d}(x) & \hat{c}(x) \\ \hat{c}(x) & -\hat{d}(x) & \hat{a}_-(x) & \hat{b}_- \\ -\hat{d}(x) & -\hat{c}(x) & \hat{b}_- & -\hat{a}_-(1/x) \end{pmatrix} \tag{B.2}$$

with

$$\begin{aligned}
\hat{a}_{\pm}(x) &= \pm\frac{2\pi\kappa - k_1\,(x^2-1)\cos\theta}{x^2-1}\cosh\rho + k_2\cos\psi \\
\hat{b}_{\pm} &= (k_2\cosh\rho \mp k_1)\sin\psi \\
\hat{c}(x) &= \frac{k_2\,(x^2+1) - 2\mathrm{w}_2 x}{x^2-1}\sin\psi\sinh\rho \\
\hat{d}(x) &= \frac{k_1\,(x^2+1) - 2\mathrm{w}_1 x}{x^2-1}\cos\psi\sinh\rho
\end{aligned}$$

For the simple $su(2)$ or $sl(2)$ solutions we have, amongst other conditions, $\theta = \psi = 0$ which simplifies the computation drastically.

Finally, let us comment on a subtle point ignored up to now– the periodicity of the rotation matrices $\mathcal{R}$ (and $\mathcal{Q}$) in (4.39). For some integers $m_i$ we see that this matrix could become anti-periodic. This means that in principle we should use another representative, $\mathcal{R}^{periodic}$, for which we should still have (2.12) but which should be periodic. However, if both $\mathcal{R}$ and $\mathcal{R}^{periodic}$ yield the same embedding coordinated under (2.12) this means that they are related by an anti-periodic $SP(4)$ gauge transformation. This means that for the purpose of computing the quasi-momenta $p(x)$ we can indeed always use the element (4.38) provided we keep in mind that if $\mathcal{R}$ is antiperiodic we can recover the real quasi-momenta through

$$\begin{aligned}
&\{e^{i\hat{p}_1}, e^{i\hat{p}_2}, e^{i\hat{p}_3}, e^{i\hat{p}_4} | e^{i\tilde{p}_1}, e^{i\tilde{p}_2}, e^{i\tilde{p}_3}, e^{i\tilde{p}_4}\} && \text{For the true representative } \mathcal{R}^{periodic} \\
&= \{e^{i\hat{p}_1}, e^{i\hat{p}_2}, e^{i\hat{p}_3}, e^{i\hat{p}_4} | -e^{i\tilde{p}_1}, -e^{i\tilde{p}_2}, -e^{i\tilde{p}_3}, -e^{i\tilde{p}_4}\} && \text{Using the anti–periodic } \mathcal{R} \text{ instead}
\end{aligned} .$$

The same kind of statement hold for the $AdS$ element $\mathcal{Q}$. Also, to each eigenvalues we choose to add a multiple of $\pi$ in such a way that the quasimomenta vanish at $x = \infty$. If $\mathcal{R}$ is periodic this multiple should contain an even number of $\pi$'s whereas if it is anti-periodic, we should add $\pi n$ with $n$ odd to each quasi-momenta. Notice that since the eigenvalues are $e^{ip}$ and not $p$ we are always free to perform these shifts.

# Appendix C

# Shifts in fluctuation energies

In this section we discuss the origin of the constant shifts in the fluctuation energies appearing in section 5.4.1. Let us first look at the $su(2)$ result (5.71) and pick one if the frequencies, say the first one

$$\omega^S_{n+m} - \mathcal{J}\,. \tag{C.1}$$

We find two kinds of shifts relatively to the frequencies listed in the table 5.1, namely the constant shift $\mathcal{J}$ and the shift in the fourier mode $n \to n+m$.

Let us understand the origin of this shifts. For that purpose consider a system of two harmonic oscillators,

$$L_x = \frac{\dot{x}_1^2 + \dot{x}_2^2}{2} - \frac{\omega^2}{2}\left(x_1^2 + x_2^2\right)\,,$$

and suppose that, instead of quantizing this system, we chose to quantize the system obtained by rotating $x_1, x_2$ with angular velocity $\mathcal{J}$, i.e. we move to the $y$ frame

$$x_1 + i x_2 = (y_1 + i y_2)\, e^{i\mathcal{J}t}\,.$$

Then, we obtain[1]

$$H_y = H_x + \mathcal{J} L_z\,,$$

where $L_z$ is the usual angular momentum, so that

$$E^y_{n_1,n_2} = \omega + (\omega - \mathcal{J})\, n_1 + (\omega + \mathcal{J})\, n_2\,.$$

Thus for the radially symmetric wave function, for which $n_1 = n_2$ (and in particular for the ground state energy), the constant shifts cancel and we obtain the same energies as for the first system. That, in general, the two results are different is obvious since the energy depends on the observer.

The constant shifts mentioned above have exactly this origin. In fact, when expanding the Metsaev-Tseytlin string action around the classical $su(2)$ circular string one obtains

[1] In the $y$ frame the Lagrangian takes the form $2L_y = \dot{y}_1^2 + \dot{y}_2^2 - (\omega^2 - \mathcal{J}^2)\left(x_1^2 + x_2^2\right) + 2\mathcal{J} y_1 \dot{y}_2 - 2\mathcal{J}\dot{y}_1 y_2\,.$

an effective *time and space dependent* Lagrangian whose $\sigma, \tau$ dependence can be killed by a change of frame

$$\delta X = R(\sigma, \tau)\delta Y$$

where $\delta X$ are the (bosonic) components of the fluctuations and $R$ is a time and space dependent rotation matrix – see for instance expression (2.14) in [102]. The same kind of field redefinitions are also present for the fermion fields. The time dependence of the rotation matrix gives the constant shifts as in the simple example we just considered while the space dependence in this change of frame is responsible for the relabeling of the mode numbers.

To make contact with the algebraic curve let us return to the frequency (C.1) we picked as illustration. It corresponds to a pole from sheet $\tilde{p}_1$ to $\tilde{p}_3$ (or from $\tilde{p}_2$ to $\tilde{p}_4$) whose position is fixed by (5.4). The result in the rotated frame, $\omega_n^S$, would correspond to a pole with mode number $n + m$ whose position is given by

$$\tilde{p}_1(x_n^{\tilde{1}\tilde{3}}) - \tilde{p}_3(x_n^{\tilde{1}\tilde{3}}) = 2\pi n + 2\pi m\,.$$

When plugging the actual expressions (4.49) for $\tilde{p}_1$ and $\tilde{p}_3$ in this equation we see that the $2\pi m$ disappears and the equation looks simpler than (5.4). However, for several cut solutions there is no such obvious choice of mode numbers (or field redefinition which kills the time dependence in the Lagrangian).

# Appendix D
# Details of the one-loop shift computation

In this appendix we collect some intermediate formulas related to the computations of section 6.2.

## D.1 Extra poles

Solving $\exp(i\tilde{p}_1 - i\tilde{p}_3) = 1$ we get

$$\begin{aligned}
\epsilon_2 &= \delta^2 \frac{X_-(X_+^2-1)}{16X_+(X_+-X_-)(X_+X_--1)} && \text{(D.1)}\\
&+ \frac{\delta^4}{256}\left(\frac{(X_+^2-1)(X_-X_+^3-2X_+^2+X_-X_+-X_-{}^2+1)X_-{}^2}{X_+^2(X_+-X_-)^3(X_+X_--1)^3}\right. && \text{(D.2)}\\
&+ \left. i\frac{\Delta}{g}\frac{(X_+^2+1)X_-{}^2}{X_+^2(X_+-X_-)^2(X_+X_--1)^2}\right) + \mathcal{O}(\delta^5)\,, && \text{(D.3)}
\end{aligned}$$

while from $\exp(i\hat{p}_1 - i\tilde{p}_3) = 1$ we get

$$\epsilon_3 = \delta^2\frac{e^{i\tau}}{16(X_+-X_-)} + \frac{\delta^4}{256}\left(\frac{e^{2i\tau}}{(X_+-X_-)^3} + \frac{i\Delta}{g}\frac{(X_+^2+1)e^{2i\tau}}{(X_+^2-1)^2(X_+-X_-)^2}\right) + \mathcal{O}(\delta^5)\,. \quad \text{(D.4)}$$

## D.2 Unphysical fluctuations

We have

$$c = -\frac{2}{X_-X_++1} + \left(\frac{(1-X_+X_-)}{4(X_+X_-+1)^2(X_+^2-1)}\delta + c.c.\right)\,, \quad \text{(D.5)}$$

and

$$x^{S_u} = 0\,, \qquad x^{F_u} = \frac{X_+X_-^{1/2} - X_-X_+^{1/2}}{X_-^{1/2} - X_+^{1/2}}\,. \quad \text{(D.6)}$$

The weighted sum of the unphysical fluctuations becomes therefore

$$\frac{2\Omega_{S_u}(0) - 4\Omega_{F_u}(x^{F_u})}{2} = \frac{2}{X_-X_++1} - \left(\frac{X_+^{1/2}X_-^{3/2} - 2X_+X_- + X_+^{-1/2}X_-^{1/2}}{4(X_+^2-1)(X_+X_-+1)^2}\delta^2 + c.c.\right)\,. \quad \text{(D.7)}$$

# Bibliography


[1] J. M. Maldacena, "The large N limit of superconformal field theories and supergravity," *Adv. Theor. Math. Phys.* **2** (1998) 231–252, arXiv:hep-th/9711200.

[2] E. Witten, "Anti-de Sitter space and holography," *Adv. Theor. Math. Phys.* **2** (1998) 253–291, arXiv:hep-th/9802150.

[3] S. S. Gubser, I. R. Klebanov, and A. M. Polyakov, "Gauge theory correlators from non-critical string theory," *Phys. Lett.* **B428** (1998) 105–114, arXiv:hep-th/9802109.

[4] O. Aharony, S. S. Gubser, J. M. Maldacena, H. Ooguri, and Y. Oz, "Large N field theories, string theory and gravity," *Phys. Rept.* **323** (2000) 183–386, arXiv:hep-th/9905111.

[5] E. D'Hoker and D. Z. Freedman, "Supersymmetric gauge theories and the AdS/CFT correspondence," arXiv:hep-th/0201253.

[6] R. Gopakumar and C. Vafa, "On the gauge theory/geometry correspondence," *Adv. Theor. Math. Phys.* **3** (1999) 1415–1443, arXiv:hep-th/9811131.

[7] H. Ooguri and C. Vafa, "Worldsheet derivation of a large N duality," *Nucl. Phys.* **B641** (2002) 3–34, arXiv:hep-th/0205297.

[8] D. Gaiotto and L. Rastelli, "A paradigm of open/closed duality: Liouville D-branes and the Kontsevich model," *JHEP* **07** (2005) 053, arXiv:hep-th/0312196.

[9] J. A. Minahan and K. Zarembo, "The Bethe-ansatz for N = 4 super Yang-Mills," *JHEP* **03** (2003) 013, arXiv:hep-th/0212208.

[10] I. Bena, J. Polchinski, and R. Roiban, "Hidden symmetries of the AdS(5) x S**5 superstring," *Phys. Rev.* **D69** (2004) 046002, arXiv:hep-th/0305116.

[11] N. Gromov, V. Kazakov, K. Sakai, and P. Vieira, "Strings as multi-particle states of quantum sigma- models," *Nucl. Phys.* **B764** (2007) 15–61, arXiv:hep-th/0603043.

[12] L. Cornalba, M. S. Costa, J. Penedones, and P. Vieira, "From fundamental strings to small black holes," *JHEP* **12** (2006) 023, arXiv:hep-th/0607083.

[13] N. Gromov and P. Vieira, "The AdS(5) x S**5 superstring quantum spectrum from the algebraic curve," *Nucl. Phys.* **B789** (2008) 175–208, arXiv:hep-th/0703191.

[14] N. Gromov and P. Vieira, "Constructing the AdS/CFT dressing factor," *Nucl. Phys.* **B790** (2008) 72–88, arXiv:hep-th/0703266.

[15] N. Gromov and P. Vieira, "Complete 1-loop test of AdS/CFT," *JHEP* **04** (2008) 046, arXiv:0709.3487 [hep-th].

[16] V. Kazakov and P. Vieira, "From Characters to Quantum (Super)Spin Chains via Fusion," arXiv:0711.2470 [hep-th].

[17] N. Gromov, S. Schafer-Nameki, and P. Vieira, "Quantum Wrapped Giant Magnon," arXiv:0801.3671 [hep-th].

[18] J. Penedones and P. Vieira, "Toy models for wrapping effects," arXiv:0806.1047 [hep-th].

[19] N. Gromov and P. Vieira, "The AdS4/CFT3 algebraic curve," arXiv:0807.0437 [hep-th].

[20] N. Gromov and P. Vieira, "The all loop AdS4/CFT3 Bethe ansatz," arXiv:0807.0777 [hep-th].

[21] N. Gromov, S. Schafer-Nameki, and P. Vieira, "Efficient precision quantization in AdS/CFT," arXiv:0807.4752 [hep-th].

[22] N. Gromov, V. Kazakov, and P. Vieira, "Classical limit of quantum sigma-models from Bethe ansatz," *PoS* **SOLVAY** (2006) 005, arXiv:hep-th/0703137.

[23] L. Cornalba, M. S. Costa, J. Penedones, and P. Vieira, "From fundamental strings to small black holes," *Nucl. Phys. Proc. Suppl.* **171** (2007) 306–307.

[24] N. Beisert, B. Eden, and M. Staudacher, "Transcendentality and crossing," *J. Stat. Mech.* **0701** (2007) P021, arXiv:hep-th/0610251.

[25] K. Zarembo, "Semiclassical Bethe ansatz and AdS/CFT," *Comptes Rendus Physique* **5** (2004) 1081–1090, arXiv:hep-th/0411191.

[26] N. Beisert, "The dilatation operator of N = 4 super Yang-Mills theory and integrability," *Phys. Rept.* **405** (2005) 1–202, arXiv:hep-th/0407277.

[27] J. Plefka, "Spinning strings and integrable spin chains in the AdS/CFT correspondence," *Living Rev. Rel.* **8** (2005) 9, arXiv:hep-th/0507136.

[28] T. McLoughlin, "The near-Penrose limit of AdS/CFT,". UMI-31-97357.

[29] I. Swanson, "Superstring holography and integrability in AdS(5) x S**5," arXiv:hep-th/0505028.

[30] J. A. Minahan, "A brief introduction to the Bethe ansatz in N=4 super-Yang-Mills," *J. Phys.* **A39** (2006) 12657–12677.

[31] K. Okamura, "Aspects of Integrability in AdS/CFT Duality," arXiv:0803.3999 [hep-th].

[32] F. Gliozzi, J. Scherk, and D. I. Olive, "Supersymmetry, Supergravity Theories and the Dual Spinor Model," *Nucl. Phys.* **B122** (1977) 253–290.

[33] L. Brink, J. H. Schwarz, and J. Scherk, "Supersymmetric Yang-Mills Theories," *Nucl. Phys.* **B121** (1977) 77.

[34] R. R. Metsaev and A. A. Tseytlin, "Type IIB superstring action in AdS(5) x S(5) background," *Nucl. Phys.* **B533** (1998) 109–126, arXiv:hep-th/9805028.

[35] N. Beisert and M. Staudacher, "Long-range PSU(2,2—4) Bethe ansaetze for gauge theory and strings," *Nucl. Phys.* **B727** (2005) 1–62, arXiv:hep-th/0504190.

[36] L. D. Faddeev, "How Algebraic Bethe Ansatz works for integrable model," arXiv:hep-th/9605187.

[37] R. Shankar and E. Witten, "The S Matrix of the Supersymmetric Nonlinear Sigma Model," *Phys. Rev.* **D17** (1978) 2134.

[38] M. Staudacher, "The factorized S-matrix of CFT/AdS," *JHEP* **05** (2005) 054, arXiv:hep-th/0412188.

[39] H. Bethe, "On the theory of metals. 1. Eigenvalues and eigenfunctions for the linear atomic chain," *Z. Phys.* **71** (1931) 205–226.

[40] I. G. Gochev, "Two-magnon states in a one-dimensional Heisenberg model with second-neighbor interaction,"
*Theoretical and Mathematical Physics* **15** (1973) 402–406.

[41] I. G. Gochev, "Bound magnon-exciton states,"
*Theoretical and Mathematical Physics* **22** (1975) 290–293.

[42] N. Beisert, C. Kristjansen, and M. Staudacher, "The dilatation operator of N = 4 super Yang-Mills theory," *Nucl. Phys.* **B664** (2003) 131–184, arXiv:hep-th/0303060.

[43] N. Beisert, V. Dippel, and M. Staudacher, "A novel long range spin chain and planar N = 4 super Yang- Mills," *JHEP* **07** (2004) 075, arXiv:hep-th/0405001.

[44] M. Karowski, "ON THE BOUND STATE PROBLEM IN (1+1)-DIMENSIONAL FIELD THEORIES," *Nucl. Phys.* **B153** (1979) 244.

[45] E. Ogievetsky, N. Reshetikhin, and P. Wiegmann, "THE PRINCIPAL CHIRAL FIELD IN TWO-DIMENSION AND CLASSICAL LIE ALGEBRA,". NORDITA-84/38.

[46] A. B. Zamolodchikov and A. B. Zamolodchikov, "Relativistic Factorized S Matrix in Two-Dimensions Having O(N) Isotopic Symmetry," *Nucl. Phys.* **B133** (1978) 525.

[47] B. Berg, M. Karowski, V. Kurak, and P. Weisz, "SCATTERING AMPLITUDES OF THE GROSS-NEVEU AND NONLINEAR sigma MODELS IN HIGHER ORDERS OF THE 1/N EXPANSION," *Phys. Lett.* **B76** (1978) 502.

[48] A. B. Zamolodchikov and A. B. Zamolodchikov, "Massless factorized scattering and sigma models with topological terms," *Nucl. Phys.* **B379** (1992) 602–623.

[49] N. Beisert, "The complete one-loop dilatation operator of N = 4 super Yang-Mills theory," *Nucl. Phys.* **B676** (2004) 3–42, arXiv:hep-th/0307015.

[50] B. Sriram Shastry, "Decorated star-triangle relations and exact integrability of the one-dimensional Hubbard model," *Journal of Statistical Physics* **50** (1988) 57–79.

[51] N. Beisert, "The su(2—2) dynamic S-matrix," arXiv:hep-th/0511082.

[52] N. Beisert, "The Analytic Bethe Ansatz for a Chain with Centrally Extended su(2—2) Symmetry," *J. Stat. Mech.* **0701** (2007) P017, arXiv:nlin/0610017.

[53] V. Kazakov, A. Sorin, and A. Zabrodin, "Supersymmetric Bethe ansatz and Baxter equations from discrete Hirota dynamics," *Nucl. Phys.* **B790** (2008) 345–413, arXiv:hep-th/0703147.

[54] Z. Tsuboi, "Analytic Bethe Ansatz And Functional Equations Associated With Any Simple Root Systems Of The Lie Superalgebra SL(r+1—s+1)," *Physica* **A252** (1998) 565–585.

[55] N. Beisert, V. A. Kazakov, K. Sakai, and K. Zarembo, "Complete spectrum of long operators in N = 4 SYM at one loop," *JHEP* **07** (2005) 030, arXiv:hep-th/0503200.

[56] N. y. Reshetikhin, "A METHOD OF FUNCTIONAL EQUATIONS IN THE THEORY OF EXACTLY SOLVABLE QUANTUM SYSTEMS," *Lett. Math. Phys.* **7** (1983) 205–213.

[57] N. Y. Reshetikhin, "INTEGRABLE MODELS OF QUANTUM ONE-DIMENSIONAL MAGNETS WITH O(N) AND SP(2K) SYMMETRY," *Theor. Math. Phys.* **63** (1985) 555–569.

[58] N. Beisert and M. Staudacher, "The N = 4 SYM integrable super spin chain," *Nucl. Phys.* **B670** (2003) 439–463, arXiv:hep-th/0307042.

[59] N. Beisert, T. McLoughlin, and R. Roiban, "The Four-Loop Dressing Phase of N=4 SYM," *Phys. Rev.* **D76** (2007) 046002, arXiv:0705.0321 [hep-th].

[60] B. I. Zwiebel, "N = 4 SYM to two loops: Compact expressions for the non-compact symmetry algebra of the su(1,1—2) sector," *JHEP* **02** (2006) 055, arXiv:hep-th/0511109.

[61] B. I. Zwiebel, "Iterative Structure of the N=4 SYM Spin Chain," *JHEP* **07** (2008) 114, arXiv:0806.1786 [hep-th].

[62] N. Mann and J. Polchinski, "Bethe ansatz for a quantum supercoset sigma model," *Phys. Rev.* **D72** (2005) 086002, arXiv:hep-th/0508232.

[63] N. Gromov and V. Kazakov, "Asymptotic Bethe ansatz from string sigma model on S**3 x R," *Nucl. Phys.* **B780** (2007) 143–160, arXiv:hep-th/0605026.

[64] A. Rej, D. Serban, and M. Staudacher, "Planar N = 4 gauge theory and the Hubbard model," *JHEP* **03** (2006) 018, arXiv:hep-th/0512077.

[65] A. Rej, M. Staudacher, and S. Zieme, "Nesting and dressing," *J. Stat. Mech.* **0708** (2007) P08006, arXiv:hep-th/0702151.

[66] G. Arutyunov, S. Frolov, and M. Staudacher, "Bethe ansatz for quantum strings," *JHEP* **10** (2004) 016, arXiv:hep-th/0406256.

[67] G. Arutyunov, S. Frolov, J. Plefka, and M. Zamaklar, "The off-shell symmetry algebra of the light-cone AdS(5) x S**5 superstring," *J. Phys.* **A40** (2007) 3583–3606, arXiv:hep-th/0609157.

[68] G. Arutyunov, S. Frolov, and M. Zamaklar, "The Zamolodchikov-Faddeev algebra for AdS(5) x S**5 superstring," *JHEP* **04** (2007) 002, arXiv:hep-th/0612229.

[69] T. Klose, T. McLoughlin, R. Roiban, and K. Zarembo, "Worldsheet scattering in AdS(5) x S**5," *JHEP* **03** (2007) 094, arXiv:hep-th/0611169.

[70] T. Klose and K. Zarembo, "Reduced sigma-model on AdS(5) x S(5): one-loop scattering amplitudes," *JHEP* **02** (2007) 071, arXiv:hep-th/0701240.

[71] T. Klose, T. McLoughlin, J. A. Minahan, and K. Zarembo, "World-sheet scattering in AdS(5) x S**5 at two loops," *JHEP* **08** (2007) 051, arXiv:0704.3891 [hep-th].

[72] J. M. Maldacena and I. Swanson, "Connecting giant magnons to the pp-wave: An interpolating limit of $AdS_5 \times S^5$," *Phys. Rev.* **D76** (2007) 026002, arXiv:hep-th/0612079.

[73] V. Giangreco Marotta Puletti, T. Klose, and O. Ohlsson Sax, "Factorized world-sheet scattering in near-flat $AdS_5 x S^5$," *Nucl. Phys.* **B792** (2008) 228–256, arXiv:0707.2082 [hep-th].

[74] R. A. Janik, "The AdS(5) x S**5 superstring worldsheet S-matrix and crossing symmetry," *Phys. Rev.* **D73** (2006) 086006, arXiv:hep-th/0603038.

[75] N. Beisert, R. Hernandez, and E. Lopez, "A crossing-symmetric phase for AdS(5) x S**5 strings," *JHEP* **11** (2006) 070, arXiv:hep-th/0609044.

[76] N. Dorey, D. M. Hofman, and J. M. Maldacena, "On the singularities of the magnon S-matrix," *Phys. Rev.* **D76** (2007) 025011, arXiv:hep-th/0703104.

[77] R. Hernandez and E. Lopez, "Quantum corrections to the string Bethe ansatz," *JHEP* **07** (2006) 004, arXiv:hep-th/0603204.

[78] N. Beisert, J. A. Minahan, M. Staudacher, and K. Zarembo, "Stringing spins and spinning strings," *JHEP* **09** (2003) 010, arXiv:hep-th/0306139.

[79] B. Sutherland, "Low-Lying Eigenstates of the One-Dimensional Heisenberg Ferromagnet for any Magnetization and Momentum," *Physical Review Letters* **74** (1995) 816–819.

[80] S. Randjbar-Daemi, A. Salam, and J. A. Strathdee, "Generalized spin systems and sigma models," *Phys. Rev.* **B48** (1993) 3190–3205, arXiv:hep-th/9210145.

[81] M. Kruczenski, "Spin chains and string theory," *Phys. Rev. Lett.* **93** (2004) 161602, arXiv:hep-th/0311203.

[82] M. Kruczenski, A. V. Ryzhov, and A. A. Tseytlin, "Large spin limit of AdS(5) x S**5 string theory and low energy expansion of ferromagnetic spin chains," *Nucl. Phys.* **B692** (2004) 3–49, arXiv:hep-th/0403120.

[83] V. A. Kazakov, A. Marshakov, J. A. Minahan, and K. Zarembo, "Classical / quantum integrability in AdS/CFT," *JHEP* **05** (2004) 024, arXiv:hep-th/0402207.

[84] A. Zabrodin, "Backlund transformations for difference Hirota equation and supersymmetric Bethe ansatz," arXiv:0705.4006 [hep-th].

[85] V. A. Kazakov and K. Zarembo, "Classical / quantum integrability in non-compact sector of AdS/CFT," *JHEP* **10** (2004) 060, arXiv:hep-th/0410105.

[86] N. Beisert, V. A. Kazakov, and K. Sakai, "Algebraic curve for the SO(6) sector of AdS/CFT," *Commun. Math. Phys.* **263** (2006) 611–657, arXiv:hep-th/0410253.

[87] N. Beisert, V. A. Kazakov, K. Sakai, and K. Zarembo, "The algebraic curve of classical superstrings on AdS(5) x S**5," *Commun. Math. Phys.* **263** (2006) 659–710, arXiv:hep-th/0502226.

[88] P. P. Kulish, N. Y. Reshetikhin, and E. K. Sklyanin, "Yang-Baxter Equation and Representation Theory. 1," *Lett. Math. Phys.* **5** (1981) 393–403.

[89] S. Schafer-Nameki, "The algebraic curve of 1-loop planar N = 4 SYM," *Nucl. Phys.* **B714** (2005) 3–29, arXiv:hep-th/0412254.

[90] D. M. Hofman and J. M. Maldacena, "Giant magnons," *J. Phys.* **A39** (2006) 13095–13118, arXiv:hep-th/0604135.

[91] N. Dorey and B. Vicedo, "On the dynamics of finite-gap solutions in classical string theory," *JHEP* **07** (2006) 014, arXiv:hep-th/0601194.

[92] N. Dorey and B. Vicedo, "A symplectic structure for string theory on integrable backgrounds," *JHEP* **03** (2007) 045, arXiv:hep-th/0606287.

[93] N. Beisert and L. Freyhult, "Fluctuations and energy shifts in the Bethe ansatz," *Phys. Lett.* **B622** (2005) 343–348, arXiv:hep-th/0506243.

[94] G. Arutyunov, J. Russo, and A. A. Tseytlin, "Spinning strings in AdS(5) x S**5: New integrable system relations," *Phys. Rev.* **D69** (2004) 086009, arXiv:hep-th/0311004.

[95] D. E. Berenstein, J. M. Maldacena, and H. S. Nastase, "Strings in flat space and pp waves from N = 4 super Yang Mills," *JHEP* **04** (2002) 013, arXiv:hep-th/0202021.

[96] N. Dorey, "Magnon bound states and the AdS/CFT correspondence," *J. Phys.* **A39** (2006) 13119–13128, arXiv:hep-th/0604175.

[97] J. A. Minahan, A. Tirziu, and A. A. Tseytlin, "Infinite spin limit of semiclassical string states," *JHEP* **08** (2006) 049, arXiv:hep-th/0606145.

[98] B. Vicedo, "Giant magnons and singular curves," *JHEP* **12** (2007) 078, arXiv:hep-th/0703180.

[99] J. A. Minahan and O. Ohlsson Sax, "Finite size effects for giant magnons on physical strings," arXiv:0801.2064 [hep-th].

[100] G. Arutyunov, S. Frolov, and M. Zamaklar, "Finite-size effects from giant magnons," *Nucl. Phys.* **B778** (2007) 1–35, arXiv:hep-th/0606126.

[101] S. Frolov and A. A. Tseytlin, "Multi-spin string solutions in AdS(5) x S**5," *Nucl. Phys.* **B668** (2003) 77–110, arXiv:hep-th/0304255.

[102] S. Frolov and A. A. Tseytlin, "Quantizing three-spin string solution in AdS(5) x S**5," *JHEP* **07** (2003) 016, arXiv:hep-th/0306130.

[103] I. Y. Park, A. Tirziu, and A. A. Tseytlin, "Spinning strings in AdS(5) x S**5: One-loop correction to energy in SL(2) sector," *JHEP* **03** (2005) 013, arXiv:hep-th/0501203.

[104] D. E. Berenstein, J. M. Maldacena, and H. S. Nastase, "Strings in flat space and pp waves from N=4 Super Yang Mills," *AIP Conf. Proc.* **646** (2003) 3–14.

[105] B. Vicedo, "Semiclassical Quantisation of Finite-Gap Strings," *JHEP* **06** (2008) 086, arXiv:0803.1605 [hep-th].

[106] S. Frolov and A. A. Tseytlin, "Semiclassical quantization of rotating superstring in AdS(5) x S(5)," *JHEP* **06** (2002) 007, arXiv:hep-th/0204226.

[107] G. Papathanasiou and M. Spradlin, "Semiclassical Quantization of the Giant Magnon," *JHEP* **06** (2007) 032, arXiv:0704.2389 [hep-th].

[108] H.-Y. Chen, N. Dorey, and R. F. Lima Matos, "Quantum Scattering of Giant Magnons," *JHEP* **09** (2007) 106, arXiv:0707.0668 [hep-th].

[109] R. A. Janik and T. Lukowski, "Wrapping interactions at strong coupling – the giant magnon," *Phys. Rev.* **D76** (2007) 126008, arXiv:0708.2208 [hep-th].

[110] M. P. Heller, R. A. Janik, and T. Lukowski, "A new derivation of Luscher F-term and fluctuations around the giant magnon," *JHEP* **06** (2008) 036, arXiv:0801.4463 [hep-th].

[111] M. Luscher, "Volume Dependence of the Energy Spectrum in Massive Quantum Field Theories. 1. Stable Particle States," *Commun. Math. Phys.* **104** (1986) 177.

[112] M. Luscher, "Volume Dependence of the Energy Spectrum in Massive Quantum Field Theories. 2. Scattering States," *Commun. Math. Phys.* **105** (1986) 153–188.

[113] T. R. Klassen and E. Melzer, "On the relation between scattering amplitudes and finite size mass corrections in QFT," *Nucl. Phys.* **B362** (1991) 329–388.

[114] J. Ambjorn, R. A. Janik, and C. Kristjansen, "Wrapping interactions and a new source of corrections to the spin-chain / string duality," *Nucl. Phys.* **B736** (2006) 288–301, arXiv:hep-th/0510171.

[115] J. A. Minahan and K. Zarembo, "The Bethe ansatz for superconformal Chern-Simons," arXiv:0806.3951 [hep-th].

[116] O. Aharony, O. Bergman, D. L. Jafferis, and J. Maldacena, "N=6 superconformal Chern-Simons-matter theories, M2-branes and their gravity duals," arXiv:0806.1218 [hep-th].

[117] G. Arutyunov and S. Frolov, "On AdS(5) x S**5 string S-matrix," *Phys. Lett.* **B639** (2006) 378–382, arXiv:hep-th/0604043.

[118] S. Schafer-Nameki, M. Zamaklar, and K. Zarembo, "How accurate is the quantum string Bethe ansatz?," *JHEP* **12** (2006) 020, arXiv:hep-th/0610250.

[119] O. Aharony, O. Bergman, and D. L. Jafferis, "Fractional M2-branes," arXiv:0807.4924 [hep-th].

[120] D. Bak, D. Gang, and S.-J. Rey, "Integrable Spin Chain of Superconformal U(M)xU(N) Chern- Simons Theory," arXiv:0808.0170 [hep-th].

[121] E. Abdalla, M. Forger, and A. Lima Santos, "NONLOCAL CHARGES FOR NONLINEAR SIGMA MODELS ON GRASSMANN MANIFOLDS," *Nucl. Phys.* **B256** (1985) 145.

[122] E. Abdalla, M. Forger, and M. Gomes, "ON THE ORIGIN OF ANOMALIES IN THE QUANTUM NONLOCAL CHARGE FOR THE GENERALIZED NONLINEAR SIGMA MODELS," *Nucl. Phys.* **B210** (1982) 181.

[123] J. M. Evans, D. Kagan, and C. A. S. Young, "Non-local charges and quantum integrability of sigma models on the symmetric spaces SO(2n)/SO(n) x SO(n) and Sp(2n)/Sp(n) x Sp(n)," *Phys. Lett.* **B597** (2004) 112–118, arXiv:hep-th/0404003.

[124] D. Gaiotto and E. Witten, "Janus Configurations, Chern-Simons Couplings, And The Theta-Angle in N=4 Super Yang-Mills Theory," arXiv:0804.2907 [hep-th].

[125] C. Ahn and R. I. Nepomechie, "N=6 super Chern-Simons theory S-matrix and all-loop Bethe ansatz equations," arXiv:0807.1924 [hep-th].

[126] Y. Hatsuda and R. Suzuki, "Finite-Size Effects for Dyonic Giant Magnons," arXiv:0801.0747 [hep-th].

[127] Z. Bajnok and R. A. Janik, "Four-loop perturbative Konishi from strings and finite size effects for multiparticle states," arXiv:0807.0399 [hep-th].

[128] F. Fiamberti, A. Santambrogio, C. Sieg, and D. Zanon, "Wrapping at four loops in N=4 SYM," *Phys. Lett.* **B666** (2008) 100–105, arXiv:0712.3522 [hep-th].

[129] F. Fiamberti, A. Santambrogio, C. Sieg, and D. Zanon, "Anomalous dimension with wrapping at four loops in N=4 SYM," arXiv:0806.2095 [hep-th].

[130] G. Arutyunov and S. Frolov, "On String S-matrix, Bound States and TBA," *JHEP* **12** (2007) 024, arXiv:0710.1568 [hep-th].

[131] G. Arutyunov and S. Frolov, "The S-matrix of String Bound States," arXiv:0803.4323 [hep-th].

[132] L. F. Alday and R. Roiban, "Scattering Amplitudes, Wilson Loops and the String/Gauge Theory Correspondence," arXiv:0807.1889 [hep-th].

[133] V. Bazhanov and N. Reshetikhin, "RESTRICTED SOLID ON SOLID MODELS CONNECTED WITH SIMPLY BASED ALGEBRAS AND CONFORMAL FIELD THEORY," *J. Phys.* **A23** (1990) 1477.